The epigenetic network mediated by Ehmt1 and its role in neurodevelopment disorders

A thesis submitted for the degree of

Doctor of Philosophy (PhD)

Jamie Wood

2024

School of Bioscience

Acknowledgements

First, I would like to thank my supervisor Professor Adrian Harwood for his consistent support and guidance throughout the project. Professor Harwood's enthusiastic and helpful advice has made the research a truly rewarding experience.

My thanks also to my funding body the GW4 BioMed MRC Doctoral Training Partnership, who beyond enabling my research, have taken genuine interest in my personal development throughout.

Next, I would like to thank the members of the Neuroscience and Mental Health Innovation Institute who have helped and supported me during my work. Thanks to the members of the Harwood lab team, including Gemma Wilkinson, Karolina Dec and Shane Wainwright, who have always been available to discuss results and troubleshoot issues. I am also grateful to past member Mouhamed Alsaqati, who's work not only laid the foundation of my project, but also provided advice and guidance. Thanks also to Emma and the lab technicians Toni and Olena, who enabled smooth running of my work throughout. I would like to express my particular thanks to Josephine Haddon, who consistently leant her ear and extensive experience to help at every point of the project. Her support throughout has been invaluable.

Finally, I am extremely grateful to my family and my wonderful partner Ceris, for whom this endeavour would not have been possible without. Your consistent belief and tremendous understanding have always elevated me over the past few years.

Abstract

Euchromatic Histone Methyltransferase 1 (*EHMT1*) is an epigenetic regulator, for which mutations are known to cause the neurodevelopmental disorder (NDD), Kleefstra Syndrome (KS). Despite this, the understanding around the etiology of KS, the role of *EHMT1* in neurodevelopment and its overlap with other phenotypically similar NDDs remains poor. The work in this project describes the role of *EHMT1* in human neuronal development, alongside the implications of its loss in the establishment of KS. The project utilises CRISPR edited induced pluripotent stem cells (iPSCs) to derive human neurons, investigating epigenetic networks, which underscore proper timing and development.

Chapter 3 describes the computational analysis of *EHMT1* depleted neurons, focusing on the transcriptional implications and underlying epigenetic changes. Computational modelling revealed significant changes in the genetic architecture of derived neurons which were validated in various cell models.

Chapter 4 studies the changes in microRNA expression profiles in *EHMT1* depleted cells at both pluripotent and neuronal timepoints. Novel prediction pipelines and manipulation tools were developed to predict these changes. Differing microRNAs were affected at each timepoint, impacting on the expression of other epigenetic modifiers central to neurodevelopment.

Chapter 5 describes the implications of *EHMT1* loss on the timing of neuronal development and maturation. Changes in epigenetic modifiers and brain specific microRNAs significantly altered the timing and progression of neuronal cells, with changes in various maturation markers.

Chapter 6 investigates the epigenetic crosstalk that exists between *EHMT1* and other epigenetic modifiers. Global changes were identified in neuronal cells, whilst intricate *EHMT1* regulated crosstalk was seen at loci specific regions in pluripotent cells.

The project presents novel computational and molecular tools, using them to demonstrate the function of *EHMT1* in neurodevelopmental timing and progression. The work elucidates the core mechanisms involved in the establishment of Kleefstra syndrome with broader implications for similar neurodevelopmental disorders.

Contents

List of figures

List of tables

List of abbreviations

AD	*Alzheimer's disease*
AGO	*Agronaute*
ASD	*Autism spectrum disorder*
ceRNA	*Competing endogenous RNA*
ChIP	*Chromatin immunoprecipitation*
CLB	*Cell lysis buffer*
CoIP	*Co-immunoprecipitation*
CRR	*Cystine rich region*
CTDSP	*C-terminal domain small phosphatases*
DEG	*Differentially expressed genes*
DGE	*Differential gene expression*
DMEM	*Dulbecco's modified eagle medium*
DMSO	*Dimethyl sulfoxide*
EDTA	*Ethylenediaminetetraacetic acid*
EHMT1	*Euchromatic histone methyltransferase 1*
EHMT2	*Euchromatic histone methyltransferase 2*
EV	*Empty vector*
EXP5	*Exportin 5*
EZH2	*Enhancer of zeste homolog 2*
FC	*Fold change*
FDR	*False discovery rate*
GEO	*Gene expression omnibus*
GO	*Gene ontology*
GSEA	*Gene set enrichment analysis*
GWAS	*Genome wide association study*
HAT	*Histone acetyltransferase*
HCl	*Hydrogen chloride*
HDAC	*Histone deacetylase*
HDM	*Histone demethylase*
HMT	*Histone methyltransferase*

IGEPAL	*Octylphenoxypolyethoxyethanol*
iPSC	*Induced pluripotent stem cell*
KLEFS2	*Kleefstra syndrome 2*
KS	*Kleefstra syndrome*
LDN	*LDN193189*
LiCl	*Lithium chloride*
LSD1	*Lysine specific histone demethylase 1*
LTP	*Long term potentiation*
MBVS	*MicroRNA binding site*
MCS	*Multiple cloning site*
MEA	*Multi electrode array*
MECP2	*Methyl-CPG-binding-protein 2*
miRNA	*Micro RNA*
mRNA	*Messenger RNA*
mRSIC	*MiRNA induced silencing complex*
NaCl	*Sodium chloride*
NaHCO3	*Sodium bicarbonate*
ncRNA	*Non coding RNAs*
NDD	*Neurodevelopmental disorder*
NEC	*Neuroepithelial cells*
NFR	*Nucleosome free regions*
NGS	*Next generation sequencing*
NLB	*Nuclear lysis buffer*
NRSF	*Neuron restrictive silencing factor*
NSC	*Neural stem cell*
PBS	*Phosphate buffered saline*
PFA	*Paraformaldehyde*
PMSF	*Phenylmethylsulphonyl fluoride*
PRC2	*Polycomb repressive complex 2*
Pre-miRNA	*Precursor miRNA*
Pri-miRNA	*Primary miRNA*

PSG	*Penicillin-streptomycin glutamine*
PTM	*Post translational modification*
qPCR	*Quantitative polymerase chain reaction*
RA	*Retinoic acid*
RE1	*Response element 1*
REST	*RE1-silencing transcription factor*
RGC	*Radial glial cell*
RISC	*RNA induced silencing complex*
RT	*Room temperature*
SCZ	*Schizophrenia*
SDS	*Sodium dodecyl sulfate*
SEM	*Standard error of the mean*
SNP	*Single nucleotide polymorphism*
TBS	*Tris buffered saline*
TF	*Transcription factor*
TSS	*Transcription start site*
UTR	*Untranslated region*
β-ME	*2 mercaptoethanol*

1 General Introduction

1.1 Overview

Currently almost 15% of the global population lives with a mental disorder, often with little to no treatment. This includes common conditions such as autism spectrum disorder and schizophrenia, alongside a plethora of other rare developmental diseases. Despite a robust occurrence and steadily increasing prevalence (Cainelli and Bisiacchi, 2022), the cause of these mental disorders remains unknown.

A fascinating clue lies in the frequent co-occurrence of seemingly distinct disorders. Patients are commonly co-diagnosed with multiple conditions such as Schizophrenia and psychosis. A massive study in 2019 investigating this concurrence revealed a staggering link: that diagnosis of any mental disorder increased the risk of developing others, no matter how distinct (Plana-Ripoll et al., 2019). Genetics plays a fundamental role, with evidence of significant overlap between seemingly separate disorders such as schizophrenia and autism. Despite this, studies reveal that many genes with small effects, not single genes, influence mental illness risk.

The development and differentiation of the human brain is a highly protracted process, spanning decades (Sydnor et al., 2021), predisposing humans to a unique risk for the occurrence of mental disorders. Central to understanding how these disorders occur is the detailed mapping of how genes guide brain development, ensuring the right cells form in the right place at the right time. Recent advancements in next generation sequencing techniques have empowered a range of large-scale genetic studies, revealing the complex genetic and epigenetic networks underling mental health disorders. In particular, in-silico modelling has drastically accelerated our understanding of how these networks relate to each other in a biological setting. Together with the advancement of induced pluripotent stem cells (iPSCs), we are now able to generate patient specific neurons, modelling the various stages of neuronal development.

In spite of this, we still lack a complete understanding of the human neurodevelopmental process and the flaws that lead to phenotypically similar mental disorders. This chapter provides an overview of mammalian neurogenesis and neurodevelopmental disorders, considering the key role of epigenetic modifiers in these processes.

1.2 Vertebrate neurogenesis

The human nervous system is comprised of two significant cell types, neurons, responsible for transducing electrical signals within the brain, and supporting glial cells, including Oligodendrocytes and Astrocytes. During neurodevelopment these cell types are generated from multipotent neural stem cells (NSCs) and the process of generating neurons is referred to as neurogenesis.

Human cortical neurogenesis begins with the symmetric division of neuroepithelial cells (NECs), producing progeny cells of identical cell fate. These NECs will also divide asymmetrically generating both a progeny NEC as well as an intermediate progenitor cell, referred to as a radial glial cell (RGC). RGCs are fate restricted to a single cell type including, astrocytes, oligodendrocytes or primarily neurons (Götz and Huttner, 2005). Like NSCs, RGCs will divide asymmetrically, generating a new RGC alongside a post-mitotic neuron. Eventually RGCs undergo terminal differentiation, generating two post-mitotic neurons (Rowitch and Kriegstein, 2010). The spatiotemporal balance between NSC self-renewal and the generation of neurons is a tightly controlled process crucial to proper brain development, structure, and function.

During embryonic development, several signalling pathways are central to regulating neural induction and patterning, through their control of cellular transcription. The Notch signalling pathway plays a key role in neuronal development by facilitating direct cell-cell interactions. Its activity serves to impede neuronal differentiation by suppressing proneuronal genes like *ASCL1* and *NGN* while simultaneously enhancing the proliferative capacity of neural stem cells (NSCs) (Paridaen and Huttner, 2014). In contrast Wnt signalling is required throughout neurogenesis, serving differing roles. During early neurogenesis Wnt signalling works to increase the number of neuronal precursor cells, promoting symmetric RGC division and proliferation (Mutch et al., 2010). However as neurogenesis continues, Wnt signalling shifts to increase neuronal differentiation though transcriptional of N-myc and in turn proneuronal factors Ngn1/2 (Kuwahara et al., 2010). As with Notch, the FGF and Shh signalling pathways are essential for the maintenance of the NSC state and proliferation (Sahara and O'Leary, 2009). Premature ablation of FGF receptors leads to precocious neural differentiation and the depletion of RGCs (Kang et al., 2009). Moreover, these pathways show significant cross talk, implicated by compensation between the Notch, FGF and Shh pathways (Kang et al., 2009,

Brodski et al., 2019). Together these pathways shape the complex spatiotemporal transcriptional landscape that ensure the correct expression of proneuronal genes that leads the cells through the correct cell types underscoring neurodevelopment.

1.2.1 Neurodevelopmental timing

To generate a complex range of cell types and structures in the brain, NPCs must go through distinct multi-stage transitions. Findings have demonstrated that progression through each of these cell stages are crucial to proper neurodevelopment, with signals provided by previous cells dictating temporal regulation (Koo et al., 2023). Neurodevelopmental timings vary significantly between species and in humans this is a highly protracted process. For example, human neurons show up to 3-fold slower development during early embryogenesis, with later developmental stages rising from 10-100-fold longer in humans (Miller et al., 2012, Van den Ameele et al., 2014, Matsuda et al., 2020).

Already, there is strong evidence that the timing of early human neurogenesis is governed by cell-intrinsic factors. Human NPCs derived from iPSCs, recapitulate a prolonged differentiation timeline compared to their primate counterparts (Kanton et al., 2019). This is also true when human NPCs are co-cultured with primate cells, suggesting a level of centralised control in species specific (Otani et al., 2016). In-vivo experiments further support this idea, as human NPCs transplanted into the developing mouse cortex retained the human tempo of differentiation and maturation (Espuny-Camacho et al., 2013, Linaro et al., 2019). Together this evidence suggests cell-intrinsic factors are central to determining the pace and subsequent successful development of neurogenesis.

Within each cell temporal changes in neurogenesis are dictated by tightly controlled transcription profiles. This is best demonstrated by transcriptomics studies demonstrating human neuronal transcription shows distinct stage specific differences compared to primate and mouse (Telley et al., 2016, Kanton et al., 2019, Telley et al., 2019, Brown et al., 2021). Early in neurodevelopment the expression of proneural genes is repressed and only upregulated as cells begin neurogenesis. For example, transcription factors such as *NEUROD1* and *ASCL1* are dominant regulators of neuronal differentiation and display distinct developmental profiles (Kim et al., 2007, Boutin et al., 2010). Regulating the expression of these neuronal specific genes and at the heart of neurogenesis is the master regulator,

Repressor Element 1 Silencing Transcription factor, *REST* (also known as Neuron-Restrictive Silencing Factor, NRSF).

1.2.2 The REST/NRSF complex

The REST protein is one of several proteins that combine to form the REST complex, that is widely expressed during embryogenesis and plays a huge role in neural differentiation. The complex binds to a specific 21 base pair motif termed Response Element 1 (RE1), found most commonly in the regulatory region of neuron-specific genes (Bruce et al., 2004). Species studies have shown that nearly one third of RE1 sites are primate specific, whilst a subset of sites are human specific (Johnson et al., 2009, McGann et al., 2021).

The REST protein is capable of binding directly to RE1 sites, where it recruits a number of other proteins, forming a complex acting as a negative regulator of neurogenesis (Figure 1.1). REST recruits the CoREST protein at the C terminus and mSin3 at its N terminus (Naruse et al., 1999, Ueda et al., 2017, Andrés et al., 1999). In turn these two corepressors recruit histone deacetylases 1/2 (HDAC-1/2), which catalyse the deacetylation of lysine residues, tightening the chromatin structure leading to transcriptional repression of the target genes (Ballas et al., 2001, Robey et al., 2011). CoREST also recruits other histone modifiers, including the histone methyltransferase G9a (also known as EHMT2), which catalyses methylation of histone 3 at lysine 9 (H3K9me3), along with the lysine specific histone demethylase 1 (LSD1), which demethylates histone 3 at lysine 4 (H3k4) (Ding et al., 2008, Yokoyama et al., 2008, Roopra et al., 2004). Furthermore, the CoREST complex also contains MECP2, a methyl CpG binding protein, recruited to methylated CpGs. Finally in addition to recruiting repressive proteins, REST has also been shown to be promote gene activation through the recruitment of the chromatin remodelling proteins Tet1/3 (Perera et al., 2015).

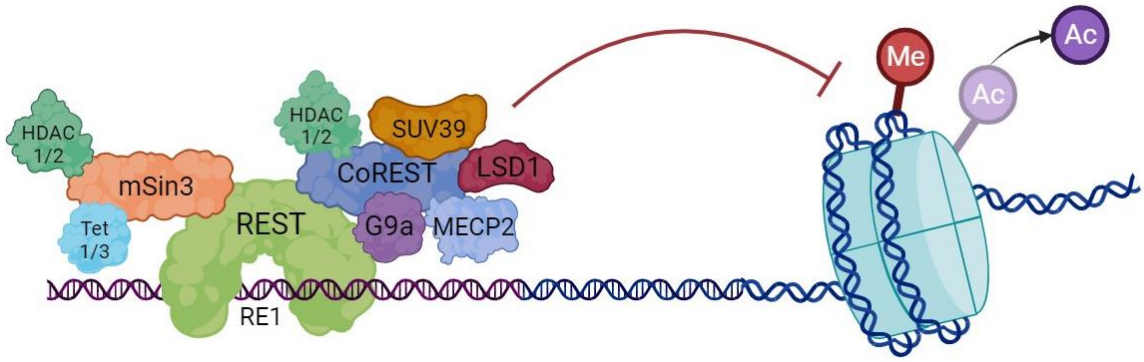

Figure 1.1 The REST/NRSF complex and its components.
The complex binds to RE1 sites in the genome via the REST protein, to repress target genes through either histone methylation or deacetylation. Various accessory proteins bind to either the rest protein or co-bound proteins to form the complex.

1.2.3 The role of REST in neurogenesis

Knock out experiments have demonstrated that REST is required for embryogenesis, with embryonic lethality occurring at day 11.5 (Chen et al., 1998). Moreover, the upregulation of neuron specific genes in non-neuronal tissue demonstrated the proteins importance in supressing neuronal transcripts (Jones and Meech, 1999). Genes containing conserved REST binding sites not only exhibit enrichment for neural functions but are also more likely to be upregulated when REST is depleted (Rockowitz and Zheng, 2015). Interestingly, human stem cells harbour nearly double the number of REST gene targets compared to mice. Additionally, human targets display a higher density of REST binding peaks. These enriched genes in humans are significantly associated with learning and memory functions, further emphasizing the crucial role of REST in human neurodevelopment. Early in-vitro studies highlighted that during neural differentiation, REST protein is gradually decreased leading to the increased expression of pro-neural genes such as *MASH1* and *NGN1* (Ballas et al., 2005, Sun et al., 2008). The gradual loss of REST appears to be phasic, where although REST is initially lost from RE1 sites, the CoREST protein remains bound and capable of inducing repression of target genes. In fact although REST expression decreases, a level of expression remains in adult neurons and has been shown to be necessary for their proper function (Gao et al., 2011). Despite its central role in neurogenesis, the overexpression and prolonged expression of REST does not prevent the formation of neurons, but rather shifts the timeline for neuronal fate commitment (Mandel et al., 2011). In line with this idea of REST having a temporal role in

neurogenesis, its conditional knockdown during NPCs leads to an accelerated increase in pro-neuronal gene expression, exit from the cell cycle and reduced proliferation culminating in fewer neurons (Aoki et al., 2012, Gao et al., 2011).

1.2.4 Regulation of REST expression and function

The mechanistic control of REST is vital to ensuring a gradual precise reduction of the pathway during neural development. The signalling pathway Wnt has been shown to directly induce REST expression in embryonic neurodevelopment (Nishihara et al., 2003), however the primary mechanism of action in the reduction of REST lies within post-transcriptional modifications (PTM). The PTM regulation of REST is highly complex and a variety of controls at different stages have been reported. The splicing factor Ser/Arg Repetitive Matrix 4 (SRRM4) is specifically expressed in neuronal tissue and leads to exon inclusion within REST, resulting in a truncated form of the protein (Ohnishi et al., 2017, Shimojo et al., 2001). The truncated form of REST, termed REST4, retains the ability to bind to RE1 sites but not repress the genes, ultimately leading to increases in REST targets.

Well-established feedback loops between microRNAs (miRNAs) and the REST complex have also been shown to contribute to the continued decrease of REST function. These include brain specific miRNAs, such as miR-9-5p and miR-124-3p, which target both the REST and CoREST proteins (Packer et al., 2008, Wohl and Reh, 2016). Furthermore, post-translational modifications such as the ubiquitination, phosphorylation and methylation of the REST protein have been shown to control its function (Westbrook et al., 2008, Gervasi et al., 2021). Despite these numerous controls, the initial switch that destabilises the REST pathway and initiates neuronal differentiation is poorly defined. Several recent studies have pointed toward miRNAs and histone modifiers as potential master regulators of REST/NRSF (Alsaqati et al., 2022, Lee et al., 2018, Sauer et al., 2021).

1.3 miRNAs

Non-coding RNAs have been identified as key regulators of various biological processes and within this family, miRNAs have been the most widely researched since their discovery. miRNAs are short single stranded RNAs, approximately 22nt in length, which regulate gene expression at the post-transcriptional level through the inhibition and degradation of messenger RNA (mRNA) (Gebert and MacRae, 2019).

1.3.1 miRNA biogenesis

The biogenesis of miRNAs is a multistep process involving a number of proteins (Figure 1.3), hence dysregulation results in a number of human diseases. Mature miRNAs arise from intergenic miRNA genes or from intragenic miRNA genes located within host genes (Ha and Kim, 2014). The latter of these is often under the transcriptional regulation of their host genes, although not all and some intronic miRNAs are independently transcribed (Ramalingam et al., 2014). MicroRNAs can also be found in clusters of two or more miRNAs that are transcribed together as a single polycistronic transcript and processed to individual miRNAs.

Transcription of miRNAs is achieved by either RNA-polymerase II or RNA-polymerase III, although typically the former, before acquiring a 7-methylguanosine cap and a poly A tail (Ha and Kim, 2014). The subsequently transcribed primary miRNA (pri-miRNA) typically presents as a stem loop structure, whilst miR clusters form more complex structures (Figure 1.2). The lower stem contains 11 bp region, flanked by nine unstructured nucleotides, important for microprocessor cleavage (Auyeung et al., 2013). At the 5’ and 3’ ends, there are UG and CNCC motifs respectively, and a third UGUG motif is found in the loop of human miRNAs (Nguyen et al., 2015). These structures have been shown to facilitate the binding of microprocessors during processing (Auyeung et al., 2013).

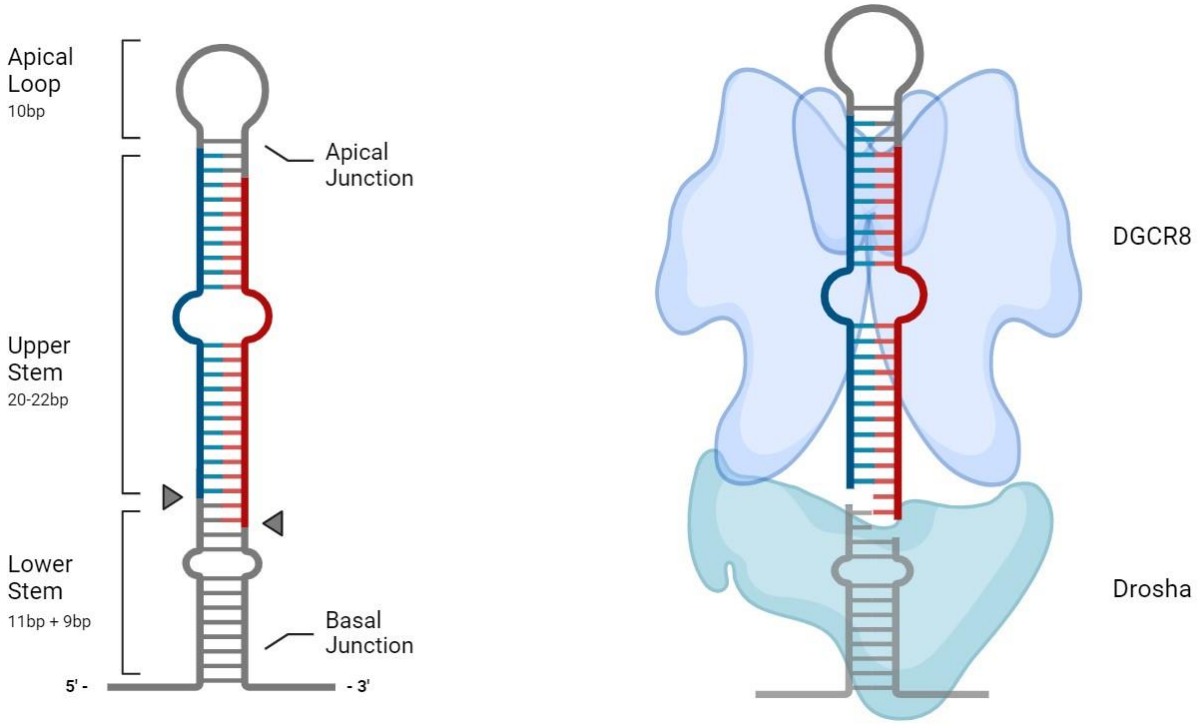

Figure 1.2 Processing of miRNA

LEFT: pri-miRNA structure composed of lower stem, upper stem and apical loop, arrows denote DROSHA cute site. RIGHT: pre-miRNA binding to DROSHA/DGCR8 complex, DGCR8 forms a dimer that binds to the apical loop of the pri-miRNA.

The subsequently transcribed primary miRNA (pri-miRNA) is then cleaved by a microprocessor complex consisting of one DROSHA protein and two DiGeorge syndrome Critical Region 8 (DGCR8) proteins, leaving the pre-miRNA, approximately 70nt in length (Gregory et al., 2004). Interestingly both the DROSHA and DGCR8 proteins have been shown to be post-transcriptionally regulated by the DROSHA/DGCR8 complex itself, demonstrating that miRNA biogenesis is a finely balance and highly regulated process (Han et al., 2009). DGCR8 binds to the stem and apical loop of the pri-miRNA, two RNA binding haem domains are required for dimerization and recruitment of DROSHA (Senturia et al., 2010, Weitz et al., 2014, Partin et al., 2017). DROSHA is an RNAse III endonuclease and cleaves the pri-miR approximately 22bp from the apical junction or 11bp from the basal junction (Han et al., 2006, Zeng et al., 2005). The ablation of DROSHA causes embryonic lethality at E7.5 in mice (Bernstein et al., 2003), however despite a significant reduction in global miRNA expression, a number of miRNAs are still expressed (Kim et al., 2016). In addition to canonical DROSHA dependent processing, a non-canonical pathway also exists, which relies on splicing to form miRNAs. Termed miRtrons,

these spliced RNAs fold to form typical stem loop structures, similar to processed pri-miRs (Miyoshi et al., 2010).

Following pri-miRNA processing the pre-miRNA is then transported out of the nucleus by the exportin-V (EXP5) protein into the cytoplasm. EXP5 binds to a 14bp dsDNA region of the pre-miRNA stem and the 3' overhang (Okada et al., 2009), whilst differences in this overhang and the apical loop are the main factors determining EXP5 binding efficiency (Zhang et al., 2021b). Interestingly, the knockout of EXP5 only modestly impacted global miRNA biogenesis, suggesting alternative export pathways are significant to miRNA production (Kim et al., 2016).

Once exported to the cytoplasm the pre-miRNA is further processed by the DICER1 protein into a 21-22nt miRNA duplex pair. The structure of the pre-miRNA is important to its processing and the double stranded stem-loop structure significantly helps with binding to the Dicer1 protein for cleavage (Tsutsumi et al., 2011). Once cleaved a guide strand of the miRNA duplex binds to the AGO (Argonaute) protein, forming the miRNA-induced silencing complex (miRISC/RISC). Typically the guide strand that binds to the AGO is that with the lower thermodynamic stability (Medley et al., 2021).

1.3.2 miRNA mode of function

Various cellular process have been shown to be regulated by miRNAs, including differentiation, metabolism, and embryonic development (Tay et al., 2008, Rottiers and Näär, 2012, Inui et al., 2010). MicroRNAs as part of the RISC complex are guided to specific mRNAs which are recognised by binding with the miRNA sequence, whilst AGO proteins act to recruit factors inducing target repression. The binding sites for miRNAs are typically found in the 3' untranslated region (UTR) of target genes and crucial to their binding is nucleotides 2-8 of the miRNA, termed as the 'seed' region (Bartel, 2018). AGO proteins use nucleotides 2-4 of the miRNA to rapidly scan RNA, diffusing laterally and pausing at complementary sites (Chandradoss et al., 2015). Pausing enables the transition to a stable binding state of the seed region, nucleotides 2-8. Initial by the seed region is extended to the 5' end of the miRNA increasing binding efficacy (Broughton et al., 2016).

Gene silencing by miRNAs is thought to happen by either translational repression or mRNA degradation. Translational inhibition is generally thought to occur at the initiation stage and caused by the disruption of EIF4 complex (comprised of the eIF4E, eIF4G and eIF4A proteins)

binding (Jonas and Izaurralde, 2015, Fukaya et al., 2014, Fukao et al., 2014, Zdanowicz et al., 2009). There is good evidence for translational inhibition, as identified by hundreds of miRNA targets that show significant decreases in protein levels but not in their levels of mRNA (Selbach et al., 2008). This was supported by studies that showed increases in eIF4F lead to decreased miRNA mediated gene repression (Mathonnet et al., 2007). Importantly it was demonstrated that miRNA mediated translational inhibition is reversable, and in response to stress inactivated genes were reactivated (Bhattacharyya et al., 2006).

In contrast mRNA degradation by miRNAs is non-reversable and is thought to be the main driver of miRNA activity, accounting for up to 90% of miRNA silencing (Guo et al., 2010). The AGO protein of the mRISC complex, interacts with a GW182 trinucleotide-repeat-containing protein, and this in turn interacts with the cytoplasmic poly(A)-binding protein (PABPC) bound to the mRNA poly(A) tail (Huntzinger and Izaurralde, 2011). Upon binding the mRNA is deadenylated by the CAF1–CCR4–NOT deadenylase complex, before being de-capped by the DCP2 enzyme (Rehwinkel et al., 2005, Behm-Ansmant et al., 2006). These de-capped mRNAs are subsequently degraded by XRN1 exonuclease (Zangari et al., 2017, Nagarajan et al., 2013). Numerous studies have demonstrated that the significance of this miRNA induced degradation pathway by demonstrating an increase in target expression when the various components are inhibited (Piao et al., 2010, Chu and Rana, 2006, Rehwinkel et al., 2005).

Both the exact mechanisms behind miRNA repression and the balance between the two are highly contentious areas of research that are still poorly understood. However, several studies investigating the temporal kinetics of miRNA repression have provided strong evidence that translational repression precedes mRNA decay (Djuranovic et al., 2012, Bazzini et al., 2012). Moreover, it is generally accepted that translation inhibition is an important step in mRNA degradation and that the two are intrinsically linked (Jonas and Izaurralde, 2015).

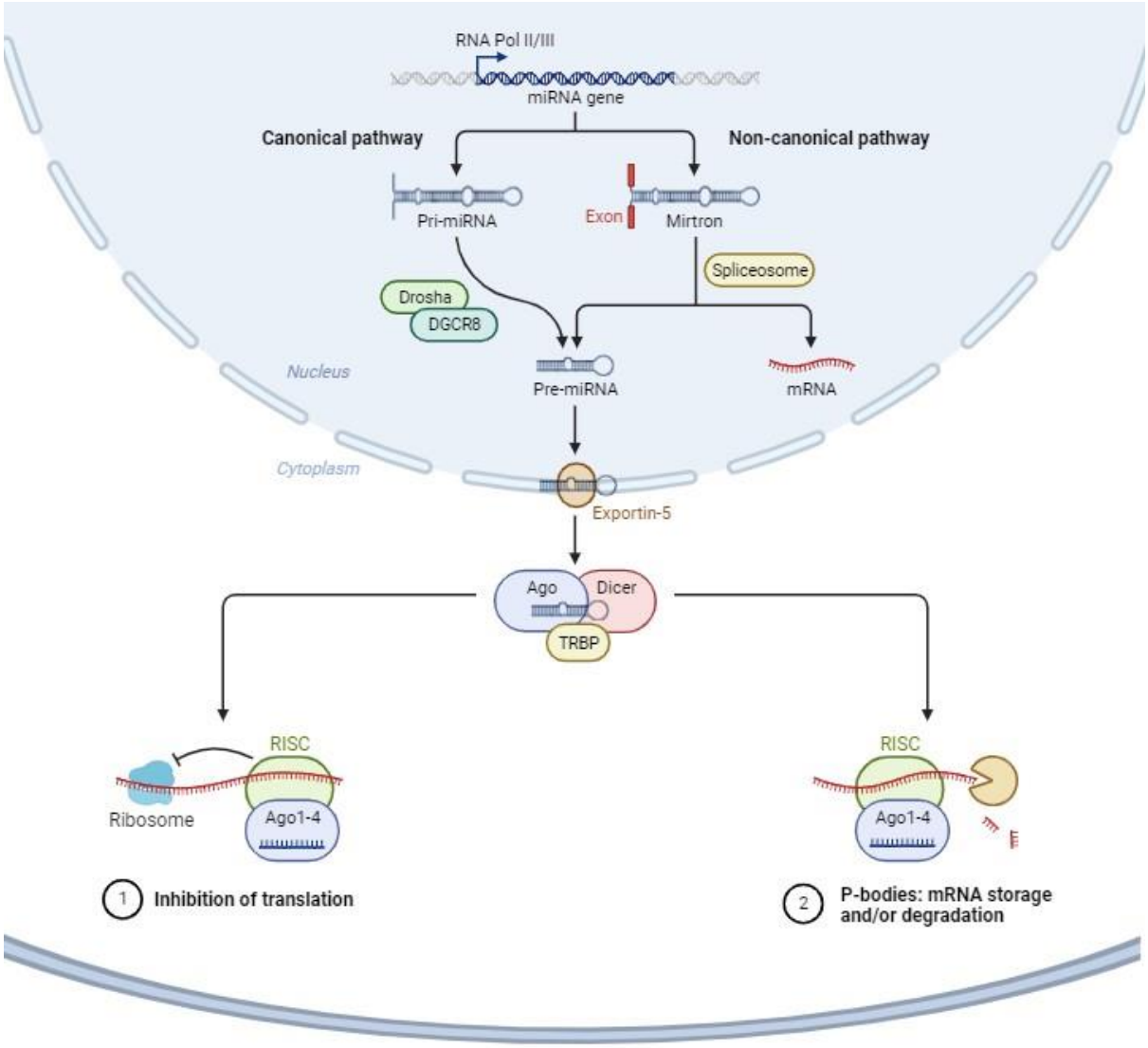

Figure 1.3 Vertebrae miRNA biosynthesis pathway

Pri-miRNA is transcribed before being processed by the DGCR8/DROSHA complex and exported into the cytoplasm by Exportin-5. The pre-miRNA is further processed by DICER, before a single miRNA strand is preferentially loaded onto an Argonaute (AGO)protein, to form a RNA-induced silencing complex (RISC.) The loaded miRNA subsequently represses gene expression through either translational inhibition or mRNA degradation.

1.3.3 miRNA kinetics

Until recently the bulk of miRNA research was focused on one-to-one interactions between a miRNA and a target gene, despite it being well known that each miRNA is capable of targeting hundreds of genes (Friedman et al., 2009). Initial work demonstrated that it was possible for two miRNAs to repress synthetic mRNA simultaneously (Doench and Sharp, 2004), giving credence to the idea that miRNAs could act in together in-vivo. It was then shown that several

miRNAs could target the *CDKN1A* mRNA simultaneously, primarily at the translational level (Wu et al., 2010). Embracing the complexity of miRNA binding, it has been possible to elucidate the many-to-many relationships of miRNAs, whereby multiple miRNAs act in concert to target and regulate the expression of multiple mRNAs (Hashimoto et al., 2013).

An important finding from this work was that rather than simply binding multiple miRNA to a target mRNA, the mRISCs could act cooperatively to impart a cumulative effect on target expression (Broderick et al., 2011). Interestingly, the distance between two miRNA binding sites determines if the miRNAs will have a combinatorial effect, with sites within 40bp of one another showing an additive effect (Diener et al., 2023, Briskin et al., 2020). Studies demonstrated two closely bound mRISCs are bridged by the GW182 protein, allowing for stabilisation of bound miRNAs and an increase in their efficacy (Briskin et al., 2020, Flamand et al., 2017). This is supported by studies demonstrating miRNAs that have no target effect on their own are still capable of compounding the effects of locally bound miRNAs (Flamand et al., 2017). Screening of the human transcriptome also highlighted significant enrichment for these cooperative miRNA binding sites, suggesting evolutionary importance (Rinck et al., 2013).

In addition to cooperative binding, miRNAs can also act competitively when their binding sites overlap. This is most often the case in families of miRNAs which share the same or similar binding sites and in these instances the miRNA with the greater free energy will preferentially bind to the mRNA (Aisina et al., 2019). Competitive binding is also seen when two or more miRNAs target the same RNA, termed competing endogenous RNA (ceRNA). By titrating away one miRNA, ceRNAs have been shown to increase the number of other unbound miRNAs, modulating their activity (Gao et al., 2021, Chen et al., 2022).

Taken together, these results highlight the complexity of miRNA binding and its implications on the collective activity of miRNAs. This has presented particular problems in computational modelling of miRNA target prediction, where the failure to consider this biological complexity leads to high rates of false positives.

1.3.4 miRNAs and REST

As previously discussed in chapter 1.1.4, the controlled release of the REST pathway is essential for accurate neurogenesis. Alongside suppressing a range of pro-neural genes, the

REST pathway has been shown to also repress various miRNAs. Indeed, screening studies of RE1 sites throughout the human transcriptome identified colocalization with brain-enriched miRNAs such as miR-124-3p, miR-9-5p, miR-132-3p, miR-153-3p and let-7-5p (Wu and Xie, 2006, Otto et al., 2007). Further work experimentally validated the REST mediated regulation of specific miRNAs (Johnson et al., 2006, Bruce et al., 2006). These miRNAs are known to be important at various stages of neurodevelopment. For example, let-7-5p expression is highly expressed in early neurogenesis and is a requirement for lineage commitment (Smirnova et al., 2005). The expression of miR-124-3p, miR-9-5p and mIR-153-3p are brain-specific (Lagos-Quintana et al., 2002) and each play significant roles in neuronal lineage commitment. Upregulation of miR-124 alone is sufficient to shift gene expression in cells to that seen in the brain (Lim et al., 2005), whilst miR-9-5p is a strong regulator of proliferation during neurodevelopment, through its regulation of the FoxG1, Hes1 and Tlx genes (Zhao et al., 2009, Shibata et al., 2008, Bonev et al., 2012). Moreover, miR-132-3p is an important regulator of *BDNF* and *MECP2* expression during neural differentiation and inhibition of the miRNA led to increases in the genes, accompanied by neurodevelopmental defects (Klein et al., 2007). As neurodevelopment progresses the level of these miRNAs increase, where REST acts in a temporal manner allowing for their dynamic release (Gao et al., 2012). This gives further credence to the idea that REST is acting as an inducer of neurogenesis, but also an important temporal regulator.

Within the discovery that REST regulates miRNAs during neurodevelopment, a specific set of REST dependent miRNAs were predicted to target the REST protein and members of the REST complex (Wu and Xie, 2006). Subsequent work confirmed that miRNAs directly target various elements of the REST complex, resulting in a stabilised double negative feedback loop (Figure 1.4) (Chen et al., 2021a, Packer et al., 2008, He et al., 2018, Duan et al., 2014). Destabilization of this feedback loop at the NPC stage, through overexpression of either miR-9-5p (Zhao et al., 2009), or miR-124 (Cheng et al., 2009, Åkerblom et al., 2012) leads to accelerated neuronal differentiation, further implicating REST as a temporal regulator of neuronal differentiation. In fibroblasts, the endogenous overexpression of miR-9-5p and miR-124-3p is sufficient to generate induced neurons through the repression of REST (Lee et al., 2018).

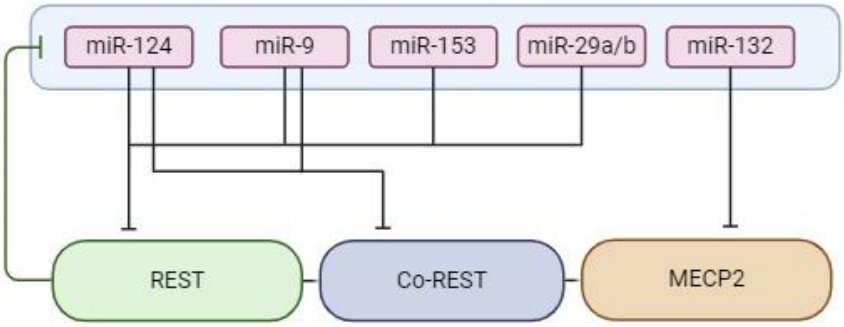

Figure 1.4 REST-miRNA feedback loop

Diagram of the miRNAs directly repressed by the REST protein, which in turn target one or more of the REST complex genes. In this manner a feedback loop exists, whereby destabilisation of the REST complex leads to increased repression via regulated miRNAs.

However, given that these miRNAs are repressed themselves by the REST complex, an external trigger must first destabilise this feedback loop. A recent paper demonstrated that one possible trigger is the miR-26 family (miR-26a/b) acting upstream of the REST pathway (Sauer et al., 2021). Knock-out of the miR-26 family did not prevent differentiation to NPC, however cells were unable to form mature neurons, instead arrested at the progenitor stage. Interestingly the miR-26 family are intronic miRNAs, encoded within the C-terminal domain small phosphatases (*CTDSPs*) (Han et al., 2012). Moreover, the *CTDSPs* all contain binding sites for the miR-26 family, providing a short negative feedback loop that is only activated during neuronal differentiation (Sauer et al., 2021). Therefore, a critical question remains as to how the REST-miRNA feedback loop is initially destabilized. Recent work from our laboratory has demonstrated that there are other miRNAs that appear to be upstream of the REST pathway and capable of targeting the protein (Alsaqati et al., 2022).

1.4 Epigenetics

The classical definition of epigenetics is the study of heritable changes in gene activity states, acting independently of DNA sequence modification (Bollati and Baccarelli, 2010). Epigenetic mechanisms including histone modifications, act rapidly to repress or de-repress target genes, often acting simultaneously or subsequently, to generate the complex gene architecture required for proper human development. Importantly epigenetic modifications are

reversible, enabling a dynamic state that strongly underlies cellular plasticity and the transcriptional landscape (Glaros et al., 2007). Epigenetic dysregulation has already been directly linked to a variety of diseases, including cancers, immune disorders, and neurodevelopmental disorders (NDDs) (Jin et al., 2007, Mittal and Roberts, 2020, Kleefstra et al., 2006a).

1.4.1 Nucleosome structure

Epigenetic modifications occur at the level of DNA or chromatin, for which the most basic molecule is the nucleosome (Figure 1.5). The nucleosome consists of a DNA stand wrapped around an octamer comprised of 4 pairs of histone proteins H2A, H2B H3 and H4, each with a histone tail (Arents et al., 1991). Each of these histones contains a tail to which covalent modifications can change the chemical structure and confirmation of the chromatin.

The distribution and organisation of nucleosomes across the genome has significant implications for cell fate (Lam et al., 2008, Shivaswamy et al., 2008). Nucleosome occupancy determines the probability that a specific genomic sequence is occupied by nucleosomes, with functional regions such as promoters and enhancers typically having lower occupancy, often termed as nucleosome free regions (NFR) (He et al., 2010). Another consideration in chromatin organization is the level of nucleosome positioning. This is a measure of the nucleosome position in relation to the DNA and how aligned these positions are between cells (Chereji and Clark, 2018). Studies into nucleosome positioning within the human genome have demonstrated that only a very small percentage of nucleosomes display strong positioning (Valouev et al., 2011). Despite this, positioning is crucial to neurodevelopment and the number of positioned nucleosome increases greater than 8-fold from the ESC state when compared to NPCs (Harwood et al., 2019).

Chromatin is found in two states, heterochromatin, where the DNA is tightly coiled, less accessible, and conducive to transcriptional silencing, and euchromatin, an open DNA structure which is associated with actively transcribed genes. These confirmations in chromatin can be induced by chemical modifications including methylation, acetylation, phosphorylation, ubiquitination and sumoylation (Walker et al., 2013, Shvedunova and Akhtar, 2022, Roidl and Hacker, 2014, Ryu and Hochstrasser, 2021, Li et al., 2020). These modifications occur on distinct amino acid residues of the histone tails are determined by

complex epigenetic readers, writers and erasers, which can recognise and remove the PTM marks (Kong et al., 2022). Typically, the addition of methyl marks by histone methyl transferases (HMTs) is associated with transcriptional silencing, whilst their removal by histone demethylases (HDM) induces activation. Likewise, the acetylation by histone acetyltransferases (HAT) is required for transcriptional activation and removal by histone deacetylases confirms a silent state.

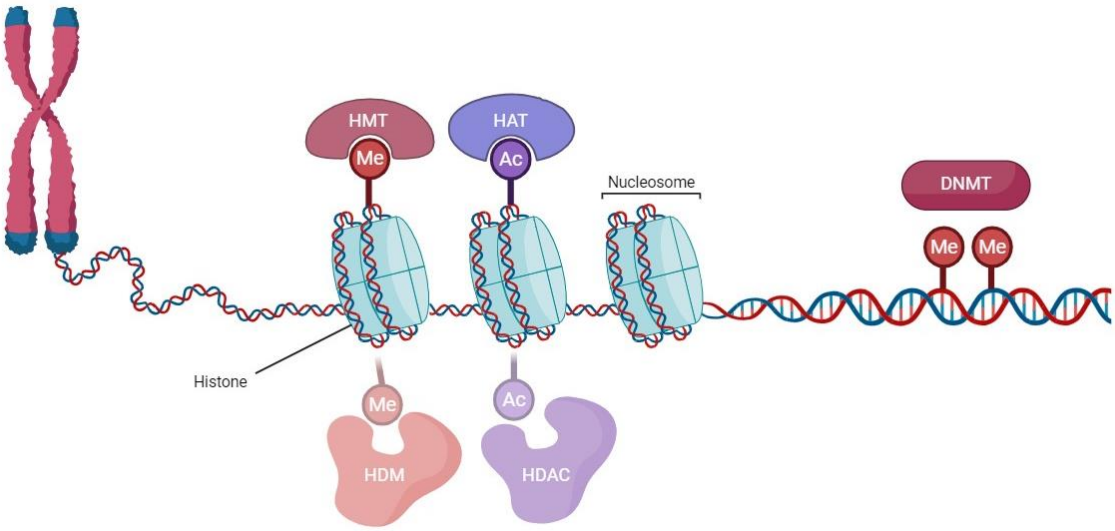

Figure 1.5 Epigenetic summary

Chromatin is formed when DNA strands loop around histones to form repeating nucleosomes. Chemical changes to the tails of these histones, including methylation and acetylation by epigenetic modifiers can induce changes in gene expression levels. Additionally, methylation patterns on the DNA can also change gene expression.

1.4.2 EHMT1

The gene Euchromatic Histone Methyltransferase 1 (*EHMT1*) encodes the HMT protein also known as G9a-like protein (GLP) or KMT1D, belonging to the broader SET domain-containing family (Kleefstra et al., 2006a). The primary role of *EHMT1* is the methylation of lysine residue 9 on histone H3, specifically the mono-methylation (H3K9me1) and di-methylation (H3K9me2) (Tachibana et al., 2007).

1.4.2.1 EHMT1 structure and dimers

Despite being able to form homodimers, *EHMT1* most commonly forms a stoichiometric heterodimer with its paralogue EHMT2, also known as G9a (Tachibana et al., 2005). Both the H3K9me reading and writing capabilities are significantly higher *in-vivo* when the proteins are in the heterodimer configuration (Sanchez et al., 2021). Together the dimer interacts with

other proteins including WIZ (Ueda et al., 2006), DNMT1 (Estève et al., 2006) and JARID1A (Chaturvedi et al., 2012). The structure of both the *EHMT1* and EHMT2 proteins are highly comparable (76.5%), containing a cystine rich region (CRR), ankyrin repeat, ring domain, and SET domain. The pre-/post-and SET domains are responsible for the enzymatic lysine methyltransferase activity of the proteins (Chang et al., 2009). The CRR enables protein binding to a number of auxiliary complexes, including cyclinD1 (Kerchner et al., 2021) and REST (Roopra et al., 2004) in the case of EHMT2. Both also contain multiple ankyrin repeats that have been shown to be responsible for binding to H3k9me1 and H3k9me2 marks (Tachibana et al., 2001, Collins et al., 2008).

1.4.2.2 EHMT1-EHMT2 H3K9me2 repression

The canonical role for the *EHMT1/2* is the establishment of H3K9me1 and H3K9me2 marks, with knockouts of either gene leading to global reductions in H3K9me2 levels (Tachibana et al., 2005). Despite a significant amount of structural similarity between *EHMT1* and EHMT2 and heterodimer binding, the two proteins appear to retain functionally independent roles. For example, whilst mutations in the EHMT2 SET domain convey embryonic lethality (Tachibana et al., 2002b), this is not the case in *EHMT1* where embryos remain viable (Inagawa et al., 2013, Kleefstra et al., 2006a). Furthermore, mutations of the ankyrin repeat within *EHMT1*, but not EHMT2 conferred a loss of *EHMT1/2* dimer binding to H3K9me1 (Liu et al., 2015). This was supported by further work that demonstrated *EHMT1* has a higher affinity for mono-methylated H3K9 compared to EHMT2 (Benevento et al., 2016). This indicates that *EHMT1* is required for the binding to H3K9me1 and recruitment of EHMT2, which acts as the primary driver in establishing H3K9me2 marks.

Traditionally *EHMT1/2* has been associated with depositing large blocks of repressive H3K9me2 marks, typically thought to be constitutive heterochromatin, persisting throughout the cell cycle and development (Wen et al., 2009). The H3K9me2 modification of peripheral heterochromatin has been shown to dictate its inherited spatial positioning (Poleshko et al., 2019). However, this idea has been challenged by others that suggest H3K9me2 is not deposited in large segments during cell differentiation (Filion and van Steensel, 2010, Lienert et al., 2011). Instead, it is suggested that *EHMT1/2* also has a secondary function, acting to establish facultative heterochromatin that is supressed in a cell-specific manner during development (Adam and Isles, 2017). Depletion of either *EHMT1* or EHMT2 postnatally in

neurons was shown to lead to significant reductions in H3K9me2 and an increase in a number of lineage specific genes (Schaefer et al., 2009). Many of these genes were not normally expressed in neurons and a significant fraction were involved in development. This was supported by further work that has demonstrated depletion of *EHMT1* in the forebrain leads to a significant upregulation of genes associated with skeletal development, posing a role for *EHMT1* in the direct repression of non-neuronal genes (Balemans et al., 2014).

1.4.3 EZH2

Another methyltransferase that plays a key role in epigenetic regulation is Enhancer of Zeste Homolog 2 (*EZH2*). The EZH2 protein is a catalytic unit responsible for trimethylating lysine 27 of histone 3 (H3K27me3), a modification that is associated with transcriptional repression. This histone modification is strongly associated with facultative heterochromatin and EZH2 has been shown to be involved in regulating a number of processes in early development (Wiles and Selker, 2017).

1.4.3.1 PRC2 complex

EZH2 is a catalytic subunit of the Polycomb Repressive Complex 2 (PRC2), a highly conserved chromatin modifier that is conserved across both plants and animals (O'Meara and Simon, 2012). In addition to EZH2, the PRC2 complex contains four other proteins, SUZ12, EED, RbAP46/48 and AEBP2. Although EZH2 is the main catalytic unit of the PRC2 complex, it is dependent on its association with both SUZ12 and EED for its enzymatic activity (Simon and Lange, 2008). The EED protein is involved in the reading of established H3K27me3 marks and inducing a conformational shift in the structure of the EZH2's SET domain, allowing the PRC2 complex the same read/write attributes as *EHMT1/2* (Poepsel et al., 2018). Disruption of the EED-EZH2 protein interaction prevents H3K27me3 methylation by the PRC2 complex (Tomassi et al., 2021). Additionally multiple isoforms of the EED protein exist, with several altering both the structure of PRC2 and its enzymatic specificity for H3K27me3 (Kuzmichev et al., 2004). Likewise, SUZ12 interacts directly with both EZH2 and EED, and is required for the PRC2 H3K27me3 establishment (Pasini et al., 2004). SUZ12 is involved in the stabilisation of the PRC2 complex, through the VEFS domain, enabling EZH2's catalytic activity (Højfeldt et al., 2018). Another suggested role for SUZ12 has been the recognition and mediation of existing

methylation marks. The presence of H3K4me3, H3K36me2, and H3K36me3 marks on target PRC2 sites leads to inhibition of the complexes enzymatic activity, a process that is mediated by SUZ12 (Schmitges et al., 2011). This demonstrates the ability of chromatin environment to modulate repressor activity at target sites.

1.4.3.2 EZH2 mediated H3K27me3 repression

The PRC2 complex is a vital regulator of pluripotency and despite a loss of EZH2 leading to embryonic lethality before embryo preimplantation (Huang et al., 2014), the core protein has been shown to be dispensable for stem cell maintenance. Studies have demonstrated that despite being expressed at high levels in stem cells, loss of the protein does not cause cells to lose their pluripotent state (Chamberlain et al., 2008, Walker et al., 2011). This is supported by reprogramming of EZH2-/- mutants, where despite a global loss of H3K27me3, the cells are still capable of successful reprogramming (Fragola et al., 2013). Instead, was postulated EZH2 repression plays a significant role in regulating early developmental targets. EZH2, via PRC2, mediates a range of developmental genes, including the *HOX* and *SIX* clusters, homeodomain-containing transcriptional factors including the Dlx, Irx, Lhx and Pou families, and other key regulators such as *SALL3* (Jarred et al., 2022, Boyer et al., 2006, Kanduri et al., 2013, Bracken et al., 2006). Indeed, mutations of EZH2 lead to significant developmental disorders, with issues of overgrowth, skeletal formation, and cognitive deficits (Gibson et al., 2012, Imagawa et al., 2017, Tatton-Brown et al., 2011, Tatton-Brown et al., 2017).

As demonstrated by the neural deficits caused by a lack of EZH2, the protein also plays a significant role in neurodevelopment. Interestingly, EZH2 appears to be regulated in a temporal manner during cortical neuron differentiation, with differing requirements at developmental stages. As previously mentioned, levels of EZH2 in SCs are high and deletion of the gene at this stage culminates in a loss of neurogenic capacity (Pasini et al., 2007). Levels of EZH2 in NPCs remain high, acting to repress a number of neuronal targets; restraining neuronal commitment and allowing the cells to proliferate (Zhang et al., 2014a). As part of the PRC2 complex, EZH2 has been shown to target many of the key master regulators including NEUROG1, NEUROG2 and ASCL1 (Ezhkova et al., 2009, Li et al., 2019). As cells progress to the neuronal state, levels of EZH2 and H3K27me3 decrease which is accompanied by an increase in transcription and a shift toward a differentiated state (Pereira et al., 2010). In this manner, EZH2 regulates the balance of NPCs and post-mitotic neurons, demonstrating

its role it temporal control of neurodevelopment. Indeed, conditional knockdown of EZH2 at the NPC stage leads to an accelerated neuronal differentiation programme, ultimately culminating in a reduced number of neurons (Pereira et al., 2010).

1.4.4 Bivalent chromatin

An essential trait of the epigenome is the presence of bivalent chromatin, DNA that is characterised simultaneously by both activating and repressing histone marks. First discovered in ESCs, a number of promoters were identified containing repressive EZH2 mediated H3K27me3 marks, alongside KMT2B mediated active H3K4me3 marks (Azuara et al., 2006, Bernstein et al., 2006). Mass spectrometry has been used to demonstrate conclusively that these opposing marks can exist on the same histone tail (Voigt et al., 2012), and it has been further shown that H3K4me3 and H3K27me3 marks can inhibit the activity of one another's writers (Schmitges et al., 2011, Laugesen et al., 2019). Moreover, these bivalent states are cell specific, rather than a heterogenous population of chromatin states in a cell population (Matlik et al., 2023). Importantly transcription of these genes is repressed but not blocked and accessible chromatin means they can be quickly activated in response to developmental cues in a state that is often termed 'poised' (Voigt et al., 2013). As cells differentiate, they will resolve to either a silent or active state, rapidly losing one of their epigenetic marks. Recent studies utilizing high throughput techniques have identified 3,868 '*bona-fide*' bivalent genes within mESCs, with the majority of these genes associated with development, and specifically neurodevelopment (Mas et al., 2018). Indeed, upon ES differentiation these bivalent developmental genes lose their H3K27me3 marks (Pan et al., 2007, Zhao et al., 2007). Interestingly, the loss of H3K27me3 on bivalent promoters does not appear to correlate with an immediate increase in gene expression (Banaszynski et al., 2013), leading to the question as to why this bivalent state exists.

For some time, it was hypothesised that this bivalent state enabled early developmental genes to be rapidly activated or repressed as cells left the pluripotent state. This was supported by the presence of paused polymerases on many of these bivalent genes, a marker that signifies the rapid onset of gene activation (Stock et al., 2007). However, a recent study looking at the transcriptional speed of these bivalent promoters determined they were activated no more quickly than canonically H3K27me3 repressed genes (Kumar et al., 2021). Instead, it was suggested the presence of H3K4 methylation blocked the de-novo DNA

methylation of these genes which would result in permeant silencing. This idea was supported by evidence that these genes became DNA methylated following treatment with H3K4me3 inhibitors. Despite this another recent study has demonstrated that a loss of H3K27me3 at bivalent promoters leads to their premature activation upon differentiation (Zhang et al., 2022). Others have suggested that bivalent genes act to fine-tune gene expression levels (Liu et al., 2017a), a mechanism that has already been demonstrated in H3K27me3 dependent genes (Rajan et al., 2023). It is clear the exact purpose and mechanisms underlying bivalent genes remains poorly understood.

Despite this the involvement of bivalent genes in neurodevelopment is significant. Knockout of the bivalent activator, *MLL2*, leads to the downregulation of numerous genes, but with particular enrichment for neurodevelopmental targets (Mas et al., 2018). This downregulation of early neuronal targets has significant effects on neuronal differentiation, resulting in a reduced neural differentiation capacity. Analysis of bivalent genes within NPCs and neurons determined that clusters of these genes were closely associated with cell-specific functions (Liu et al., 2017a). For example, genes specific to NPCs appeared to be involved in supporting a proliferative state within the NPCs, whilst neuron-specific genes were centred around DNA damage and cellular stress response. This finding was replicated in-vivo where during development, bivalent genes that lost there H3K27me3 marks and increased expression were associated with neuronal differentiation and maturation (Matlik et al., 2023). Moreover, this bivalent regulation appears to be instrumental in the timing of neural differentiation, as ablation of H3K27me3 marks on these genes led to their premature expression, premature terminal differentiation, and precocious maturation (Matlik et al., 2023). In this manner it appears histone modifications regulate the fine-tuned sequential progression of cells through neural differentiation.

1.4.5 Epigenetic crosstalk

Chromatin modifiers are capable of both dynamic activation and repression of gene expression; therefore, it is not wholly unsurprising that these modifiers are capable of regulating each other's activity. The idea of epigenetic crosstalk was only recently proposed, when it was discovered that H3K27me3 marks rarely coexisted with H3K36me2/3 marks and it was demonstrated this was caused by the inhibition of PRC2 mediated H3K27me3 deposition by preexisting H3K36 (Yuan et al., 2011). Already I have touched on the idea of

epigenetic crosstalk in the first chapter, through the ability of H3K4me3 to inhibit EZH2 mediated H3K27me3 deposition and vice versa (Schmitges et al., 2011, Laugesen et al., 2019).

1.4.5.1 EHMT1/2 and EZH2

Not all epigenetic crosstalk is inhibitory, and two epigenetic regulators for which there is increasing evidence of functional crosstalk are the aforementioned *EHMT1/2* and EZH2. As previously discussed, the two enzymes both hold similar roles in development regulation, and the H3K9me and H3K27me marks they deposit, display significant target overlap (Bilodeau et al., 2009, Yuan et al., 2009, Ringrose et al., 2004). Intriguingly, in addition to its principle role of di-methylating H3K9, EHMT2 is also capable of monomethylating H3K27 (H3K27me1), whilst depletion of EHMT2 leads to a reduction in H3K27me1 levels (Tachibana et al., 2001, Tachibana et al., 2002a, Lin et al., 2016). In a seminal paper a functional cooperation was demonstrated between *EHMT1/2* and PRC2, with direct interaction and binding between EHMT2 and EZH2 (Mozzetta et al., 2014). Loss of the EZH2 protein in mESCs had no effect on EHMT1/2 protein levels, whilst the loss of *EHMT1/2* had no effect on global H3K27me3 levels. However, the loss of *EHMT1* or EHMT2 led to the ablation of both H3K9me2 and H3K27me3 marks on a subset of developmentally critical genes (Mozzetta et al., 2014). Moreover, the EHMT catalytic activity was found to be essential for this functional crosstalk. This functional crosstalk mechanism is also shown in-vivo, where the two enzymes target and regulate a set of developmental genes during early development (Zylicz et al., 2015). This role is further supported in cancer studies that show overexpression of EHMT2 and EZH2 proteins preferentially target and repress developmental genes, inducing a state of de-differentiation (Fong et al., 2022).

The dual recruiting of *EHMT1/2* and EZH2 appears to only occur at specific genomic targets, which may in part be due to the binding proteins associated with these modifiers. Neither EHTM1/2 nor the core members of the PRC2 complex, including EZH2, are capable of binding to DNA, making them reliant on other proteins or mechanisms for chromosomal targeting. In this manner several proteins have been suggested to co-recruit the two epigenetic proteins. One of the most frequently reported factors is the transcriptional repressor JARID2, that is not only capable of binding to both *EHMT1/2* and EZH2 (Adhikari et al., 2019, Shirato et al., 2009, Pereira et al., 2014), but also demonstrates significant target overlap (Mozzetta et al., 2014). Other proteins have been shown to simultaneously recruit both *EHMT1/2* and EZH2

including, PHF19 (Pan et al., 2015), PALI1 (Fong et al., 2022), MEF2C (Papait et al., 2017) and ZNF518B (Maier et al., 2015). Interestingly, each of these complexes appear to target unique, if not overlapping, subsets of genes, implying that binding proteins may dictate the pattern of gene repression. This is perhaps best demonstrated by the co-binding of the EZH2, *EHMT1/2* and REST proteins, which appear to selectively target a number of neuronal genes key to neurodevelopment (Mozzetta et al., 2014). Indeed, analysis of target overlap between *EHMT1/2* and EZH2 show the greatest enrichment for pathways specific to neuronal development, suggesting this crosstalk plays a key role in the timing and regulation of neuronal differentiation.

1.4.5.2 Chromatin modifiers and miRNAs

The idea of epigenetic crosstalk is one that is not merely limited to chromatin modifiers and the establishment of feedback loops with microRNAs has been repeatedly reported. I have briefly discussed the crosstalk between wider epigenetic modifiers, such as the REST complex and miRNAs (Wu and Xie, 2006, Conaco et al., 2006). It is now well demonstrated that the REST complex is responsible for repressing a number of miRNAs responsible for promoting neuronal identity. In turn the targeting of the REST protein by several of these miRNAs such as miR-124-3p and miR-9-5p, culminates in a double feedback loop that once destabilised, propagates the acceleration of neuronal differentiation (Packer et al., 2008).

Chromatin modifiers including histone methyltransferases have also been shown to be capable of regulating specific microRNAs in neuronal cells. It has been shown levels of the H3K9me2 and H3K27me3 marks coded by *EHMT1/2* and EZH2 respectively, increase significantly around the *MIR32* host gene in injured trigeminal ganglion neurons (Qi et al., 2022). The result is a significant reduction in miR-32-5p expression, culminating in increased Cav3.2 protein expression and associated neuropathic pain. In lung cancers too, EHMT2 has been shown to target various miRNAs, including miR-151a-3p and miR-106b-3p, leading to significant reductions in the expression of the miRNAs (Pang et al., 2014).

Conversely, miRNAs are also capable of negatively regulating various chromatin modifiers. For instance, *EZH2* is a validated target of miR-101-3p, where overexpression of the miRNA leads to significant protein reduction, reduced H3K27me3 marks and increased anxiety like behaviour in mice (Cohen et al., 2017).

1.5 *EHMT1* in neurodevelopmental disorders

Given the broad expression distribution of epigenetic modifiers, their instrumental role in development and the extensive window of human neurodevelopment, mutations in epigenes often lead to significant multisystem, developmental, and neurodevelopmental disorders. Termed chromatinopathies, these are genetic disorders are caused by mutations in genes capable of modifying the chromatin state (Di Fede et al., 2022). The number of known causative mutations has risen from 20 in 2014 to the most recent estimates identifying 179 disorders associated with 148 epigenes, with over 20% of all 720 epigenes causative for at least one chromatinopathy (Figure 1.6) (Nava and Arboleda, 2023, Harris et al., 2023).

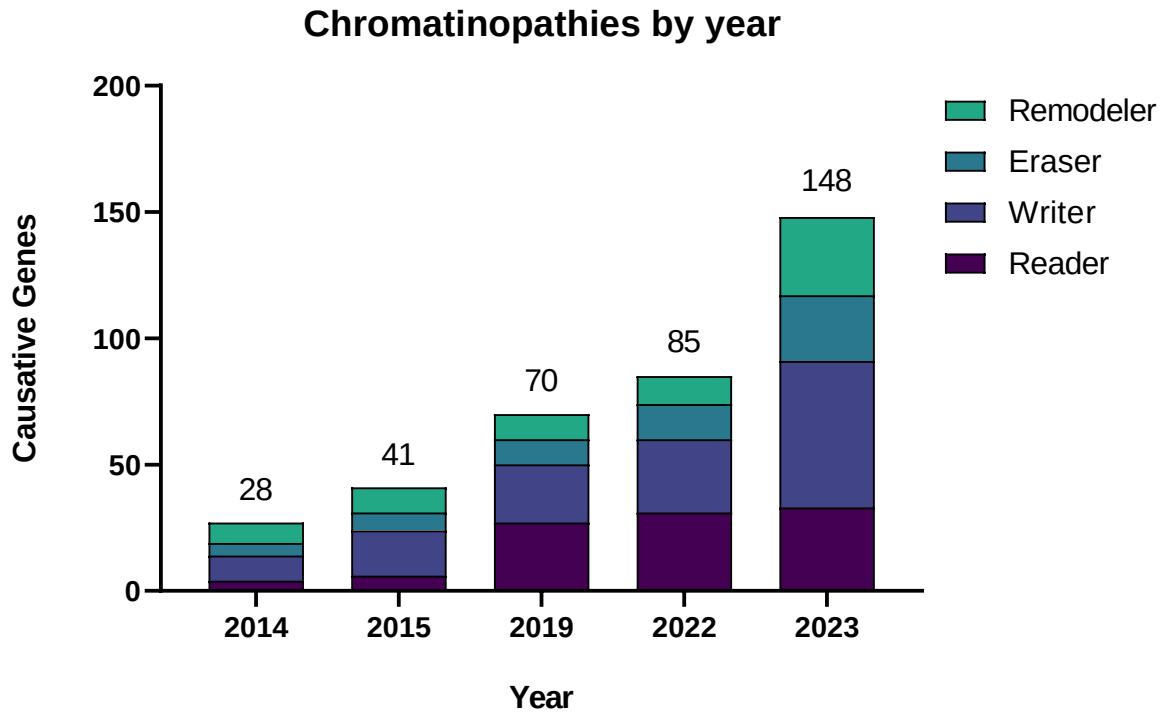

Figure 1.6 Instances of chromatinopathies

Graph summarising the rates of chromatinopathies over the last 10 years. Chromatinopathies are caused by mutations in epigenetic machinery, including reader, writer, eraser, and remodelling proteins. Causative genes have risen from 28 in 2014 to 148 as of 2023.

Furthermore, it's estimated almost all chromatinopathies display some degree of neurological involvement, with 85-93% displaying symptoms of intellectual disability (Kaur et al., 2022, Harris et al., 2023). Typically, these disorders are monogenic and highly penetrant, however they display significant symptomatic overlap, both with one another and more common NDDs

such as Autism or ADHD. Studies have demonstrated that is may in part be due to the genetic and transcriptional convergence of these disorders, implicating commonalities such as WNT signalling and the balance of progenitor and neuronal cells (Ciptasari and van Bokhoven, 2020).

Interestingly, chromatinopathies displaying strong neurological involvement are known to be caused by a broad range of varying epigenes. For example, Kabuki syndrome is a chromatinopathy presenting as multisystem intellectual disability, caused by mutations in the histone methyltransferase gene *KMT2D* (Carosso et al., 2019). However, another form of the disorder termed Kabuki syndrome 2, accounting for less than 10% of cases, is caused by mutations in the histone demethylase *KDM6A*, and similarly shows significant intellectual disability (Lederer et al., 2012). Likewise, mutations in the methyltransferase *KMT2A* are causative for the chromatinopathy Wiedemann-Steiner syndrome, again characterised by sever intellectual disability (Jones et al., 2012). Importantly, these disorders are highly rare, for example only 31 cases of Wiedemann-Steiner syndrome identified within 8 years of its discovery in 2012 (Baer et al., 2018). However, our understanding of causative epigenes and chromatinopathies continues to grow, with recent studies identifying mutations in a range of Histone deacetylases (HDACs) leading to neurodevelopmental disorders (Di Fede et al., 2024). Ultimately as access to high throughput sequencing becomes more readily available, the number of causative epigenes will continue to grow, emphasising the importance of understanding the molecular basis and commonality behind these disorders.

1.5.1 Kleefstra syndrome

One such chromatinopathy is the disorder Kleefstra syndrome (KS), with incidence rates around 1:200,000, it is typically characterised by severe intellectual disability, microencephaly, seizures, behavioural disorders, autism spectrum disorder and hypotonia (Stewart and Kleefstra, 2007, Haseley et al., 2021). The disorder is generally caused by microdeletions of around 700kb in the 9q34 region, which contains the *ZMYND19*, *ARRDC1*, *C9ORF37*, *EHMT1* and *CACNA1B* genes (Kleefstra et al., 2006a). However, loss of the *EHMT1* gene has been shown to be causative of the core KS phenotypes. This is demonstrated by missense mutations of the *EHMT1* gene that lead to improper folding of the protein and culminate in conventional KS symptoms (Blackburn et al., 2017, Yamada et al., 2018). Similarly, intragenic duplications of the *EHMT1* gene also cause a loss of protein function and

lead to the KS phenotype (Schwaibold et al., 2014). *EHMT1* knockout mice reproduce many of the core symptoms seen in patients, including cranial abnormalities, developmental delay, increased anxiety, and autistic like features (Balemans et al., 2010, Balemans et al., 2014). At the cellular level, neurons display abnormal firing, reduced synaptic scaling, reduced dendritic arborization and reduced spines (Benevento et al., 2016, Balemans et al., 2013, Frega et al., 2019).

Highlighting the overlap associated with chromatinopathies, mutations in four similar epigenetic regulators, *MBD5* (Kleefstra et al., 2012), *MLL3* (Siano et al., 2022), *SMARCB1* (Diets et al., 2019) and *NR1I3* (Kleefstra et al., 2012) have been associated with the KS phenotype. These collective disorders are often referred to as Kleefstra-2 (KLEFS2) and each has been demonstrated to directly interact with one another, acting as a highly conserved epigenetic network (Kleefstra et al., 2012). Collective analysis of these mutations at the cellular level revealed these mutant lines show significantly increased neuronal excitability, accompanied by an imbalance in excitatory-inhibitory neurons (Frega et al., 2020). Moreover, each of the knockdown lines showed molecular convergence on 34 commonly dysregulated genes, however loss of *EHMT1* led to increased expression, whilst the KLEFS2 genes led to decreases in gene expression. Interestingly a number of these targets are associated with epilepsy and ASD, further underscoring the overlap seen between neurodevelopmental disorders.

1.5.2 EHMT1 in schizophrenia

Schizophrenia (SCZ) is a neuropsychiatric disorder thought to affect approximately 1% of the world's population (Insel, 2010). Symptoms of SCZ vary significantly and can be split into positive symptoms (delusions, hallucinations, and behavioural traits) or negative symptoms (avolition, asociality and alogia) (Correll and Schooler, 2020). Genetics are thought to play a significant role in SCZ susceptibility, with an estimated heritability rate of 70-80% (Sullivan et al., 2003). In-spite of this, a large number of risk genes have been associated with SCZ and even between monozygotic twins the risk of developing the disorder is 48% (McDonald and Murphy, 2003), leading many to speculate that environmental factors also play a significant role. Moreover, there is mounting evidence that genetic, epigenetic and environmental risk factors converge at early brain development, poising SCZ as a NDD (Birnbaum and Weinberger, 2017).

More recently chromatin regulators have been implicated in the progression and development of SCZ. This has included H3 methyltransferases such as *SETD1A* and *EZH2*, suggesting a temporal role both in development and the adult brain (Billingsley et al., 2018, Singh et al., 2016). *EHMT1* has also been associated to SCZ, with a wide scale CNV analysis of SCZ patients identifying 2 *de-novo* and three exonic CNVs (Kirov et al., 2012). In this analysis *EHMT1* was identified as one of the highest risk genes, converging with other risk genes on synaptic complexes. Interestingly, global levels of EHMT1 protein were found to be significantly increased in the forebrain of SCZ patients (Chase et al., 2013). Furthermore, it was shown that in a sex-specific manner, male SCZ patients had significantly elevated levels of H3K9me2 methylation driven by increases in EHMT2 protein levels (Chase et al., 2015). This increase in H3K9me2 had practical implications for patients, translating to higher levels of symptom presentation and a poorer quality of life. Analysis of H3K9me2 targets in SCZ patients found levels of the methylation mark were dysregulated on several genes closely associated with SCZ (Rizavi et al., 2022). This elevation in *EHMT1/2* driven methylation does not appear to be limited to the brain, with significant increases of both proteins and H3K9me2 methylation also detected in the peripheral blood cells of SCZ patients (Sharma et al., 2015). Moreover levels of H3K9me2 in SCZ patients peripheral blood appear to be inversely correlated to the age of disease onset (Gavin et al., 2009). Collectively, *EHMT1* dysregulation appears to play a significant role in the establishment and progression of SCZ, establishing a repressive chromatin state central to the disorder. Despite this, further work required to determine the mechanistic cause of the phenotypic overlap between SCZ and similar NDDs.

1.5.3 EHMT1 in autism spectrum disorder

Autism spectrum disorder (ASD) is categorised as a range of developmental disorders often displaying widely varying symptoms (Constantino and Marrus, 2017). Incidence rates are significantly higher in males and although diagnostic approaches in female patients have improved, rates remain greater than 3.2 times lower (Solmi et al., 2022). The core symptoms of ASD include social deficits, restrictive repetitive behaviours, and behavioural impairments (McPartland et al., 2012). As with SCZ, ASD is a heritable disorder with co-occurrence observed in monozygotic twins, highlighting genetic significance (Tick et al., 2016). Greater than 50% of risk is predicted to come from common polygenic genes (Gaugler et al., 2014),

however around 5% of cases are thought to be caused by rare CNVs and SNVs (Eyring and Geschwind, 2021).

ASD is known to be comorbid alongside a range of NDDs, including ADHD and Fragile X syndrome (Kaufmann et al., 2017, Hours et al., 2022) and has been previously co-diagnosed alongside Kleefstra Syndrome (Yoshida et al., 2023, Nagy et al., 2017). Sequencing of ASD patient CNVs identified a *de-novo* mutation in the *EHMT1* gene (O'Roak et al., 2012), whilst microdeletions in *EHMT1* have also been identified in autism patients (Talkowski et al., 2012). Additionally, *EHMT1* mosaicism in three separate patients appeared to significantly increase the risk of developing ASD and mood disorders (de Boer et al., 2018). In all three cases, the patients were initially asymptomatic and only referred for investigation following a diagnosis of KS for their child.

Despite a link between *EHMT1* mutations and ASD development, the exact mechanism underlying the interaction is not clear. In mice, the post-natal reduction of *EHMT1/2* was shown to reduce anxiety and ASD like symptoms (Wang et al., 2018a). However, in the same study the pre-natal reduction of *EHMT1/2* from E9.5 to birth increased anxiety and presented autistic like features. In line with this finding levels of *EHMT1/2* were found to be significantly higher in the prefrontal cortex of *SHANK3* autism mouse models (Wang et al., 2020). Furthermore, the reduction of *EHMT1/2* in this model was sufficient to elicit a robust rescue of the ASD like social deficits. Together this data implicates that the potential role of *EHMT1* in ASD may vary depending on the developmental stage of the brain.

1.5.4 EHMT1 environmental interaction

The idea of environmentally induced epigenetic changes has existed for some time, however more recently there is building evidence that EHMT1/2 proteins are receptive to environmental cues. In-vivo administration of nicotine have been shown to significantly reduce global levels of H3K9me2, caused by reductions in *EHMT1*, *EHMT2* and *SETDB1* mRNA (Chase and Sharma, 2013, Castino et al., 2018). This reduction correlates with dysregulation of SCZ and developmentally associated genes, whilst a withdrawal of nicotine led to the restoration of H3K9me2 marks. Similarly, peripheral mononuclear cells from SCZ patients showed elevated levels of H3K9me2 accompanied by increased *EHMT1/2* expression. Importantly SCZ associated genes in these cells were hypermethylated, however treatment

with *EHMT1/2* inhibitors rescued they're expression, whilst treatment in mouse models also rescued expression (Chase et al., 2019). Together this data suggests epigenetic factors of SCZ aetiology may be influenced by environmental factors and reversible.

Another well reported drug dependent regulation of *EHMT1/2* is the self-administration of cocaine. Levels of H3K9me2 were significantly reduced in both mice exposed to cocaine (Maze et al., 2010), and human addicts (Sheng et al., 2011), in response to reduced *EHMT1/2* mRNA levels. This reduction in H3K9me2 in post-mitotic neurons resulted in a significant increase in synaptic plasticity. Interestingly this cocaine induced reduction of H3K9me2 appears to be cell type specific, with opposing effects of cocaine on *EHMT2* in Drd1 vs Drd2 neurons (Jordi et al., 2013). Likewise, treatment and subsequent withdrawal of ethanol in adult cortical neurons leads to a significant reduction of H3K9me2 (Qiang et al., 2011), whilst *EHMT2* has been implicated in direct links between ethanol during development and long term potentiation (LTP) deficits and neurobehavioral abnormalities in mice (Subbanna et al., 2014).

Perhaps the most important finding was the discovery of that *EHMT1* deficits associated with Kleefstra syndrome in mice could be reversed with the post-natal supply of *EHMT1* (Yamada et al., 2021). Crucially ubiquitous supply of *EHMT1* in deficient mice was required in the whole brain to reverse neurological phenotypes. Moreover, this work identified a specific juvenile window, which once passed prevented rescue of KS associated behavioural or cognitive phenotypes. Together, it is clear that *EHMT1/2* are vital in both developmental and adult neurons, where their function is highly amenable to changes in environmental factors.

1.6 Thesis Aims

As outlined above epigenetic modulation has been shown to be a fundamental regulator of both the timing and progression of mammalian neurodevelopment, with mutations in these regulators underlying a spectrum of phenotypically overlapping disorders. Among genes associated with neurodevelopmental disorders (NDDs), mutations in the histone methyltransferase *EHMT1* stand out for their high penetrance and dominant role in causing the NDD Kleefstra Syndrome. Similarly, miRNAs, another class of epigenetic regulators, are increasingly linked to neurodevelopment, suggesting potential connections between these two mechanisms in shaping brain health.

By dissecting the roles of *EHMT1* and miRNA regulation in neurodevelopment, the overall aim of this project is to shed light on the mechanisms underlying brain function and contribute to the development of novel therapeutic targets. To this end the project has the following aims:

- Using bioinformatic analysis to analyse the implications of *EHMT1* heterozygous loss on gene architecture during neurodevelopment. This will be achieved using publicly available RNA sequencing data sets from *EHMT1*$^{+/-}$ cell lines, differentiated to the early neuronal stage (*Chapter 3*).
- Novel predictive analysis and validation of miRNAs in *EHMT1* deficient cell models. This will be done by analysing changes from previous RNA sequencing data and confirming miRNA predictions in *EHMT1* depleted cell models at various stages of neurodevelopment. The work will also aim to validate miRNA induced expression changes (*Chapter 4*).
- Generation of a miRNA modulation system with the aim of rescuing miRNA dysregulation. Once key targets have been identified, the work then aims to modulate these *EHMT1* regulated miRNAs with the intention of reversing *EHMT1* induced changes (*Chapter 5*).
- Identification of epigenetic cross talk between *EHMT1* and similar histone methyltransferases. Utilising findings from the bioinformatic analysis, this work will aim to identify the role of epigenetic crosstalk between *EHMT1* and other histone methyltransferases in a stage specific manner (*Chapter 6*).

2 General Methods

2.1 Cell Culture

2.1.1 Cell lines and maintenance

The cell lines used in this work were the IBJ4, *EHMT1*$^{+/-}$ mutant and two Kleefstra syndrome patient induced Pluripotent Stem Cell (iPSC) lines. The IBJ4 iPSC line was a gift from Josh Chenoweth from the Lieber Institute for Brain Development, MD, USA. The *EHMT1* heterozygous knockout line was generated by Mouhamed Alsaqati from a modified IBJ4 cell line, containing the pAAVS1-PDi-CRISPRn plasmid (Addgene) inserted into the AAVS1 safe harbour locus. A Tet-inducible Cas9-nuclease was activated with 2 µg/ml Doxycycline, 24 hours prior to transfection with 10pmol each of two ehmt1-specific gRNAs. Successful editing was confirmed by PCR amplification using the flanking primers 5'-AGCAGCATCTCTCACCGTTT-3' and 5'-CTTTTTCAGGTGGACGACTGG-3'. Successful reprogramming was confirmed by way of staining and qRT-PCR. The Kleefstra syndrome patient lines were reprogrammed by Olena Petter from two female patients with microdeletions of the 9q34 region. The first patient was 22 years old, nonverbal (IQ NA), with a history of epilepsy, hypotonia, anxiety and depression. The second patient was 20 years old, FSIQ 53, with a history of ASD, psychotic symptoms, hypotonia, seizures and cardiac mitral valve insufficiency. Both patients were recruited as part of the research study on neurodevelopmental copy number variants at Cardiff University (the Defining Endophenotypes from Integrated Neuroscience [DEFINE] Study). Generation of iPSC lines from patient blood samples were reviewed and approved by the South-East Wales Research Ethics Committee. In cases of diminished responsibility, written informed consent was provided by the patients next of kin on their behalf. PBMCs from each donor were reprogrammed using a CytoTune-iPS 2.0 Sendai reprogramming kit (A16517, ThermoFisher scientific). Karyotype analysis showed 46, XX normal diploid female karyotype (ISCN classification) and possessed a 9q34 deletion.

All iPSC lines were maintained in feeder-free conditions, fed with E8 medium (Thermo Fisher, #A1517001) on a matrix of Cultrex (BioTechne, 3434-010-02). Cell culture plates were prepared by thawing aliquots of frozen Cultrex and diluting 1:100 in cold DMEM/F12 (Thermo Fisher, #11320033), before plating at 1 ml / 9.6 cm2. Coated plates were incubated for at least 1 hour at 37°C and placed at 37°C until needed. Frozen vials of iPSCs were thawed at 37^{o}C for

5 minutes and centrifuged in E8 media at 200g for 5 minutes at room temperature (RT). The supernatant was aspirated, and the cell pellet resuspended in 2ml of E8 with 10 mM Rock inhibitor Y27632 (Stem Cell Technologies, #72302). Cell suspension was plated on a Cultrex coated plate and incubated overnight at 37^{o}C, 5% CO_2. The following day, the media was removed, and the cells washed with 1ml of DPBS (Thermo Fisher, #14190250), before being removed and fed with 2ml of E8 media. Cells were maintained with E8 media changes every other day, until cells reached 70-80% confluency when they were passaged.

2.1.2 iPSC passaging and freezing

Once iPSCs reached confluency spent media was aspirated, and the cells washed with 1ml of DPBS, before 1ml of Gentle cell dissociation agent was added per well (Stem cell technology, #100-0485) and incubated at 37^{o}C for 3 minutes. The gentle cell reagent was then aspirated and 1ml of warm E8 media was added to the well, then cells were manually dissociated by scratching with a serological pipette. The cell suspension was triturated and diluted in a proportional volume of E8 before being re-plated on fresh Cultrex plates and incubated at 37oC, 5% CO^2.

For freezing, confluent iPSCs were first treated with 10 mM Rock inhibitor for 1 hour to overnight. Cells were then dissociated with Gentle cell reagent as previously described, however were resuspended in E8 with 10% dimethyl sulfoxide ([DMSO] Sigma, #D2650). The resulting cell suspension was transferred to a cryovial at a volume of 1ml/vial, before being transferred to a Mr. Frosty™ Freezing Container (Thermo Fisher, #5100-0001) and incubated in a -80oC freezer overnight, and subsequently transferred to vapour phase liquid nitrogen for long term storage.

2.1.3 Differentiation of iPSCs to glutamatergic neurons

All iPSC differentiations were performed using a modified version of the dual SMAD inhibition method described in (Chambers et al., 2009). Basal media components and volumes are summarised in the table below, along with a summary of the modified method.

Table 2.1 Neuronal differentiation media compositions

(DMEM = Dulbecco's Modified Eagle Medium, RA = Retinoic Acid, PSG = Penicillin-Streptomycin-Glutamine, β-ME = Beta Mecaptoethanol)

Components	Media	
	NB27 RA-	**NB27 RA+**
DMEM (Thermo Fisher, #12634028)	100ml	100ml
Neurobasal (Thermo Fisher, #21103049)	50ml	50ml
B27 (50X) (Thermo Fisher, #12587010)	1ml	-
B27 +RA (50X) (Thermo Fisher, #17504044)	-	1ml
N2 (100X) (Thermo Fisher, #17502001)	1ml	1ml
PSG (100X) (Thermo Fisher, #10378016)	1.5ml	1.5ml
β-ME (Sigma, #M3148)	150µl	150µl

Prior to neural induction, iPSCs were passaged as previously mentioned, onto a 12 well plate coated with Cultrex. The cells were maintained with 1ml of E8 every other day until they reach 90-100% confluency, when media was switched (D0) to NB27 RA- media, supplemented with 100 nM LDN193189 ([LDN], Sigma-Aldrich, #SML0559) and 10 nM SB431542 ([SB], Sigma-Aldrich, #S4317) was added.

Cells were maintained with half volume media changes every other day until day 8-10, once cells begin to form multi-layered colonies. Prior to the first passage, cells were treated with 10 mM Rock inhibitor for 1 hour to overnight. This media was removed and saved for later use, before the cells were washed with DPBS and incubated with 0.5ml of Versene (Thermo Fisher, #15040066) at 37^{o}C for 3 minutes. Versene was then aspirated and 1ml of the previously harvested NB27 RA- media +Rock, was added and the cells detached by scratching with a serological pipette. The cells were pooled, diluted to a 2:3 ratio with fresh NB27 RA-, with LDN, SB and rock inhibitor, and passaged onto a 12 well plate coated with fibronectin (Millipore, #FC010) for at least 1 hour prior. From day 12 onwards cells were fed with NB27 RA- only and maintained with half volume feeds every other day until day 20 when multi-layer colonies were formed, and the cells passaged.

At least 2 hours prior to passaging, cells were incubated with 10 mM Rock inhibitor and 12 well plates with 0.1mg/mL poly-D-lysine (Sigma-Aldrich, #P7886) and 20 µg/mL laminin

(Roche, #11243217001) were prepared. This media was removed and saved for later use, before the cells were washed with DPBS and incubated with 0.5ml of Versene (Thermo Fisher, #15040066) at 37^{o}C for 3 minutes. Versene was then aspirated and 1ml of the previously harvested NB27 RA- media + Rock, was added and the cells detached by scratching with a serological pipette. The cells were pooled, diluted to a 1:2 ratio with fresh NB27 RA-, and passaged onto the coated plates. On day 26, medium was changed to NB27 RA+ and maintained with half volume feeds every other day until day 50.

2.1.4 Chemical inhibition of EHMT1/2

For temporal inhibition of *EHMT1/2*, the selective euchromatic histone methyltransferase inhibitor, UNC0638, was used. UNC0638 (Selleckchem, #S8071) was reconstituted in DMSO, before diluting in cell culture media to a final concentration of 400nM. Vehicle controls consisted of the corresponding volume of DMSO being added to cell culture media, with a maximal concentration of 0.5%. Where UNC0638 treatment was to be withdrawn, media was aspirated, and cells washed 3 times with DPBS before adding the required amount of vehicle control media.

2.2 Cell transfection

2.2.1 miRNA sponge

For miRNA/multimiR-sponge optimisation stem cells were grown in 24 well plates until 70% confluent and transfected with both miRNA-sponge (400ng) and luciferase reporter (100ng) using lipofectamine 3000 (Invitrogen, L3000015). An mCherry plasmid was used as a transfection control and a scramble sponge and empty vectors (EV) were used as negative controls. DNA was diluted in 25µl of OptiMEM™ medium, with 1µl of P3000® reagent, whilst 2µl of Lipofectamine®3000 reagent was diluted in 23µl of OptiMEM™ medium. The solutions were mixed at 1:1 and incubated at RT for 15 minutes before gentle resuspension and addition to the cells. Forty-eight hours after transfection, samples were lysed using the Dual-Luciferase® reporter system (Promega, # E1910), luciferase signal was measured using the CLARIOstar microplate reader (BMG Labtech). Treated samples were analysed relative to signal in the EV or scramble controls.

For transient inhibition of *EHMT1*, stem cells were grown in 6 well plates until 70% confluent and treated with either UNC0638 (200nM) or vehicle control (DMSO). Following 24 hours of

treatment cells were transfected with 1-2µg of miRNA/multimiR-sponge plasmid or scramble control as described above. After an additional 48 hours, cells were harvested and analysed by way of qPCR (2.3.3) or western blot (2.5.2).

2.2.2 EHMT1 mutants

For mutated EHMT1 plasmids, stem cells were grown in 6 well plates until 70% confluent, before being transfected with a Flag-EHMT1 (1 µg) and the HA-EZH2 (1 µg), using lipofectamine 3000. The empty pcDNA3-Flag plasmid was used as a negative control. DNA was diluted in 125µl of OptiMEM™ medium, with 4µl of P3000® reagent, whilst 7.5µl of Lipofectamine®3000 reagent was diluted in 125µl of OptiMEM™ medium. The solutions were mixed at 1:1 and incubated at RT for 15 minutes before gentle resuspension and addition to the cells. After 48 hours the cells were harvested and analysed for co-binding, using antibodies against both Flag and HA.

2.3 RNA methods

2.3.1 miRNA/RNA purification

RNA was extracted using the RNeasy kit (Qiagen, #74104), whilst miRNA was extracted using the miRNeasy kit (Qiagen, #217004). In both cases, cells were washed with DPBS, before being manually dissociated by gentle scratching with a serological pipette. Cells were then pelleted by centrifugation at 200g for 5 minutes and the supernatant aspirated.

RNA extraction:

The pellet was resuspended in 600µl of RLT buffer before the suspension was titrated by passing through a 16-gauge needle 10 times. To this, 600µl of 70% ethanol was added before the sample was then passed through a collection column by centrifugation at 5000g for 2 minutes and the flow through discarded. RW1 buffer, followed by RPE buffer and 80% ethanol were each passed through the collection column by centrifugation for 2 minutes at 8000g and discarded. Finally, 20µl of nuclease free water was added to the centre of the column to elute the RNA and incubated for 5 minutes at RT. The column was then centrifuged at 8000g for 5 minutes and the RNA concentration determined by spectrophotometer.

miRNA extraction:

The pellet was resuspended in 700µl of QIAzol lysis buffer before the suspension was titrated by passing through a 16-gauge needle 10 times and incubated for 5 minutes at RT. 140µl of

chloroform was then added to the cell suspension, shaken, and incubated for 3 minutes at RT. The sample was centrifuged at 12,000g at 4°C for 5 minutes, before the upper aqueous phase was transferred to a new tube and 1.5 volumes of 100% ethanol was added. The sample was then passed through a collection column by centrifugation at 5000g for 2 minutes and the flow through discarded. Subsequently, RWT buffer, followed by two additions of RPE buffer were each passed through the collection column by centrifugation for 2 minutes at 8000g and discarded. Finally, 20µl of nuclease free water was added to the centre of the column to elute the RNA and incubated for 5 minutes at RT. The column was then centrifuged at 8000g for 5 minutes and the RNA concentration determined by spectrophotometer.

2.3.2 cDNA synthesis

For cDNA synthesis from RNA the High-Capacity cDNA Reverse Transcription Kit (Thermo Fisher, #4368814) was used. A x2 master mix containing 10X RT Buffer, 25X dNTP Mix (100 mM), 10X RT Random Primers, Reverse Transcriptase, RNase inhibitor and nuclease free water, was added to 1000ng of purified RNA for a total volume of 20µl. Samples were then incubated in a thermocycler at 25°C for 10 minutes, 37°C for 2 hours and 86°C for 5 minutes. Total cDNA concentration was then measured using a ND1000 spectrophotometer (Thermo Scientific) and samples were diluted to 100 ng/mL.

For cDNA synthesis from miRNA the miRCURY LNA RT kit was used (Qiagen, #339340). A master mix containing 5X miRCURY RT Reaction Buffer, 10X Reverse Transcriptase, and nuclease free water, was added to 200ng of purified miRNA for a total volume of 10µl. Samples were then incubated in a thermocycler at 42°C for 60 minutes and 95°C for 5 minutes. Total cDNA concentration was then measured using a ND1000 spectrophotometer (Thermo Scientific) and samples were diluted to 100 ng/mL.

2.3.3 qPCR

Quantitative PCR analysis was performed using the qPCRBIO SyGreen Blue Mix (PCR Biosystems, #PB20.16). 10µl of the x2 master mix was added to 1.6µl of forward and reverse primers, 2.5µl of cDNA (250ng) and nuclease free water to a total volume of 20µl. In the case of miRNAs, a universal primer (underlined) complementary to the unique tag (5'-TCTAGGAAGTCGACCTCGGCATGCGTAACTGGTGCTCGATTC-3') introduced to the cDNA by the miRCURY LNA kit was used. Each sample was run in triplicate on a 96 well plate and the house

keeping genes GAPDH and SNORD48 were used for mRNA and miRNA analysis respectively. All reactions were run on StepOnePlus real time PCR machines (Applied Biosystems), with an initial activation of 95°C for 2 minutes, followed by 34 two stage cycles of: 95°C for 5 seconds and 60°C for 20 seconds. Melt curves were generated to ensure primer specificity. Data was exported to 'R' for analysis using wither the ΔΔCt method or mRNA abundance for relative quantification. A list of primers used is summarised below.

Table 2.2 Primers used for qPCR

Target	Sequence (5'-3')	Target	Sequence (5'-3')
Universal	GAATCGAGCACCAGTTACGC	**miR-101-3p**	GCTACAGTACTGTGATAACTG
miR-142-3p	TGTAGTGTTTCCTACTTTATGGA	**miR-101-5p**	CAGTTATCACAGTGCTGATGCT
miR-142-5p	GCAGCATAAAGTAGAAAGCACT	**miR-10b-3p**	ACAGATTCGATTCTAGGGGAAT
miR-153-3p	TTGCATAGTCACAAAAGTGATC	**miR-124-3p**	TAAGGCACGCGGTGAATGCC
miR-153-3p	GCAGTTGCATAGTCACAAAAGT	**miR-124-5p**	CGTGTTCACAGCGGACCTTGAT
miR-26a-3p	TTATAATACAACCTGATAAGTG	**miR-135b-3p**	ATGTAGGGCTAAAAGCCATGGG
miR-26a-5p	TTCAAGTAATCCAGGATAGGCT	**miR-135b-5p**	TATGGCTTTTCATTCCTATGTGA
miR-26b-3p	CCTGTTCTCCATTACTTGGCT	**miR-140-3p**	TACCACAGGGTAGAACCACGG
miR-26b-5p	GGCTTCAAGTAATTCAGGATAGG	**miR-140-5p**	CAGTGGTTTTACCCTATGGTAG
miR-27b-3p	TTCACAGTGGCTAAGTTCTGC	**miR-144-3p**	GCTACAGTATAGATGATGTACT
miR-27b-5p	AGAGCTTAGCTGATTGGTGAAC	**miR-144-5p**	GCGGATATCATCATATACTGTA
miR-320a-3p	AAAAGCTGGGTTGAGAGGGCGA	**miR-218-3p**	ATGGTTCCGTCAAGCACCATGG
miR-320a-5p	GCCTTCTCTTCCCGGTTCTTCC	**miR-218-5p**	TTGTGCTTGATCTAACCATGT
miR-340-3p	TCCGTCTCAGTTACTTTATAGC	**miR-27a-3p**	TTCACAGTGGCTAAGTTCCGC
miR-340-5p	TTATAAAGCAATGAGACTGATT	**miR-340-5p**	GCAGTTATAAAGCAATGAGACTGA
miR-548f-3p	AAAAACTGTAATTACTTTT	**miR-6835-3p**	AAAAGCACTTTTCTGTCTCCCAG
miR-548f-5p	GCAGTGCAAAAGTAATCACAGT	**miR-6835-5p**	AGGGGGTAGAAAGTGGCTGAAG
miR-653-3p	TTCACTGGAGTTTGTTTCAATA	**miR-9-3p**	ATAAAGCTAGATAACCGAAAGT
miR-653-5p	GTGTTGAAACAATCTCTACTG	**miR-9-5p**	TCTTTGGTTATCTAGCTGTATGA

Gene	Forward Sequence (5'-3')	Reverse Sequence (5'-3')
ACTA1	GGCATTCACGAGACCACCTAC	CGACATGACGTTGTTGGCATAC
ACTL6B	GCGCTGGTCTTTGACATTGG	CCATTCTTGAGGGGCGACAT
AP3B1	GAAGCGGATTGTTGGGATGAT	TCAGCATATCGAACCAGGTAAAC
ASCL1	CGCGGCCAACAAGAAGATG	CGACGAGTAGGATGAGACCG
CALB1	TGGCATCGGAAGAGCAGCAG	TGACGGAAGTGGTTACCTGGAAG
CCND2	ACCTTCCGCAGTGCTCCTA	CCCAGCCAAGAAACGGTCC
CDC42n	GGGACCCAAATTGATCTCAG	GGCAGCTAGGATAGCCTCAT
CDC42u	GGGACCCAAATTGATCTCAG	GATGCGTTCATAGCAGCACA
CDK6	CCAGATGGCTCTAACCTCAGT	AACTTCCACGAAAAAGAGGCTT
CITED2	CCTAATGGGCGAGCACATACA	GGGGTAGGGGTGATGGTTGA
CTDSPL	CCACCAGCTAAGTACCTTCTTCC	GGCCGCTTCAGCACATACA
ETS1	GATAGTTGTGATCGCCTCACC	GTCCTCTGAGTCGAAGCTGTC
EZH2	AATCAGAGTACATGCGACTGAGA	GCTGTATCCTTCGCTGTTTCC
FREM2	CCTGCATGACCTGGTGTTG	GCCAGTGCGTCGTTGTCTA
GAPDH	ACCACAGTCATGCCATCAC	TCCACCACCCTGTTGCTGTA
JAG1	GTCCATGCAGAACGTGAACG	GCGGGACTGATACTCCTTGA
ITGB1	ACTTGAGACGCACATAGGTGA	CCCATAGTACAGCCCTTGATGTT
KIF20A	TGCTGTCCGATGACGATGTC	AGGTTCTTGCGTACCACAGAC
LAMC1	GGACTCCGCCCGAGGAATA	ACTTGAGACGCACATAGGTGA
MAP2	CTGCTTTACAGGGTAGCACAA	TTGAGTATGGCAAACGGTCTG
MAP4n	TCATGGAATGGAGGGGAATA	CTCAGGCATCAGCAGAAAGA
MAP4u	TCATGGAATGGAGGGGAATA	GGGTCCACTGGAGACAAAGA
NCAM1	GGCATTTACAAGTGTGTGGTTAC	TTGGCGCATTCTTGAACATGA
NRXN3	AGTGGTGGGCTTATCCTCTAC	CCCTGTTCTATGTGAAGCTGGA
ONECUT2	GGAATCCAAAACCGTGGAGTAA	CTCTTTGCGTTTGCACGCTG
OTX2	CAAAGTGAGACCTGCCAAAAAGA	TGGACAAGGGATCTGACAGTG
PAX6	GTGTCCAACGGATGTGTGAG	CTAGCCAGGTTGCGAAGAAC
PHF6	AGAGGCACGAAGCTGATGTG	AGTGGTAGTGGTATGTCCTGTG
PRRX1	TGATGCTTTTGTGCGAGAAGA	AGGGAAGCGTTTTTATTGGCT
REST	GCCGCACCTCAGCTTATTATG	CCGGCATCAGTTCTGCCAT
RUFY3n	ATCTCCGGGCTCTTAAGCAT	TGGTGCTTTGGGATCAGTTT
RUFY3u	ATCTCCGGGCTCTTAAGCAT	TCCAGCTGCAGACTGTTGAT

ROCK1	AACATGCTGCTGGATAAATCTGG	TGTATCACATCGTACCATGCCT
SIX3	CTGCCCACCCTCAACTTCTC	GCAGGATCGACTCGTGTTTGT
SIX4	AGCAGCTCTGGTACAAGGC	CTTGAAACAATACACCGTCTCCT
SNORD48	AGTGATGATGACCCCAGGTAACTC	GGTCAGAGCGCTGCGGTG
UNC5C	TGGGACTGGGATACTTGCTG	ACAGTACAGGTTCACAGGCTTAT
VSTM2L	CAGTGGTGGTATGTACGGAGC	CCTGCTTGTCGGTCCAGTC

2.4 DNA methods

2.4.1 Chromatin Immunoprecipitation (ChIP)-qPCR

Samples were collected in triplicate from at least 3 wells of a 12 well plate or one well of a 6 well plate for a total of $1x10^7$ cells. Cells were first washed with DPBS before fixing in situ with 0.75% aqueous formaldehyde (Sigma, #47608) at RT for 5 minutes. To inactivate the reaction, glycine (Sigma, #G7126) was added at a final concentration of 0.125M and incubated at RT for 5 minutes. The solution was aspirated, before cells were washed in ice cold DPBS and manually dissociated by gentle scratching with a serological pipette. They were then centrifuged at 1000g for 5 minutes at 4°C and the supernatant removed.

Table 2.3 Chromatin Immunoprecipitation buffer compositions
(HCL = Hydrogen Chloride, NaCL = Sodium Chloride, LiCL = Lithium Chloride, IGEPAL = Octylphenoxypolyethoxyethanol, SDS = Sodium Dodecyl Sulfate, EDTA = Ethylenediaminetetraacetic Acid, NaHCO3 = Sodium Bicarbonate, PMSF = Phenylmethylsulphonyl Fluoride)

Reagent	**Buffer**						
	Cell lysis	**Nuclear lysis**	**Dilution**	**Wash #1**	**Wash #2**	**Wash #3**	**Elution**
Tris-HCL **(Sigma, #108315)**	10mM	50mM	20mM	20mM	10mM	10mM	
NaCL **(Sigma, #S3014)**	50mM		150mM	50mM			
LiCl **(Sigma, #310468)**					250mM		
IGEPAL CA-630 **(Sigma, #56741)**	0.5%				1%		

Sodium Butyrate **(Sigma, #B5887)**	10mM	10mM	10mM				
SDS **(Sigma, #7910)**		1%	0.01%	0.01%			1%
EDTA **(Sigma, #E4884)**		10mM	2mM	2mM	1mM	1mM	
Triton-X-100 **(Sigma, #X100)**			1%	1%			
Deoxycholic acid **(Sigma, #30960)**					1%		
NaHCO3 **(Sigma, #S5761)**							100mM
PMSF **(Sigma, #PMSF-RO)**	0.3mM	0.3mM	0.3mM				
Leupeptin **(Sigma, #LEU-RO)**	2nM	2nM	2nM				

The cell pellet was resuspended in 150µl of ice-cold cell lysis buffer (CLB) at 4^{o}C for 20 minutes with vigorous vortexing every 5 minutes. Following this the samples were centrifuged at 8000g for 5 minutes at 4^{o}C to collect nuclei, before being resuspended in 1.2ml of nuclear lysis buffer (NLB). The lysis was then passed through a 25-gauge needle 10 times and incubated on ice for 30 minutes. Samples were then transferred to a clean Eppendorf tube, diluted with 720µl of dilution buffer and aliquoted into maximum volumes of 300µl. Chromatin was then sheared to a fragment size of ~200-600bp by sonication in a Bioruptor® PLUS combined with the Minichiller® Water cooler (Diagenode, #B02010003), with 15 cycles of 30 sec ON/30 sec OFF. The resulting chromatin was used to set up the ChIP assay while 270µl was used as the input control.

Primary antibody (10µg) was diluted in 200µl of PBS + 0.1% Tween-20 (PBST) and added to 50ul of magnetic Dynabeads (Thermo Fisher, #10003D) per sample, before incubating for 10 minutes at RT. The bead-Ab complex was then separated by magnet and resuspended in 200ul of PBST. The bead-Ab complex was then separated once more and incubated with chromatin

at 4°C overnight. The following day each sample was washed twice with 750µl of IP wash buffer #1, once with 750µl of IP wash buffer #2 and twice with 750µl of IP wash buffer #3. Then 550µl of elution buffer was added to each sample, which was then heated to 55oC for 15 minutes. Magnetic separation was used to remove the beads from solution and the DNA in was purified using QIAquick PCR Purification Kit (Qiagen, #28104). Samples were analysed by qRT-PCR as previously mentioned, with material detected using PCRBIO SyGreen Blue Mix (PCR Biosystems, #PB20.16) on a StepOnePlus™ Real-Time qPCR System (Applied Biosystems). Primer sets are summarised in the table below. ChIP enrichment was assessed relative to the input DNA in specific genomic regions.

Table 2.4 Primers used for Chromatin Immunoprecipitation
Position denotes location in kilobases from the gene transcription start site (TSS)

Gene	Position	Forward Sequence (5'-3')	Reverse Sequence (5'-3')
OTX2	+1Kb	GAGACGGCATAGTGGTGTTT	AGGGAGTGACTGGGTTATCA
	+0Kb	CACAGCCTCCACTGTGATTA	GAAGGCGGCTAGAGTTCTAAA
	-1Kb	GTGTCCGTCTGTCTTGTCTATATC	AATACATCCGCCTACAGAACTC
	-2Kb	TGGATCGGCCCAGTAAGA	GAGTCACTTGAACGCAACAAC
REST	+1Kb	CCGCTGCGGCTACAATACTA	TCCTCCAGTGATACTCGCTCA
	+0Kb	GCGATGTGGTTTTAAGCCAGT	ACTGCTGGTAAACAGCCCTC
	-1Kb	GGCCAAGTCAAGCACAATGC	GCAGGCTGAAGTTCCACAAC
	-2Kb	GCGGTAACTTTCCGTCCTCT	CCTGCGCTCTCCAACACTAA
	-3Kb	CAGGATCGGGTTACACAGCA	GCCTCAAAGGACCTGACTCG
ROBO3	+1Kb	GTCTCCTACAGGAACTCCTAGAT	GTTTCCATTCCCTCCCAAGT
	+0Kb	AAGAGGCACCGACCGTA	AGTTCATCTGCAGCAGCGT
	-1Kb	CAAGACTCAAGGAAGAGGAAGG	CCCTTCACCTCACATAGGAAAG
	-2Kb	CTCCAAGAGGCCAACTTAACA	GCTTCCAGGTCAGGGTAATG
	-3Kb	CAAAGAGCTCAGCCACTACA	GTCTGAGCTAGATACAGGGAGA
SALL2	+1Kb	GTGGGAATGGAAGTGAGAAAGA	TCTGAGGGCCAGAAGAAGA
	+0Kb	GCTTTCTCACTCCAGCTTCT	ATTGAGGGAGGCGATGG
	-1Kb	GGCCTGAGGGTCACAATAATC	ACTCCTCTCCTCTCCTCTCT
	-2Kb	CCTGTCCAAACCAGCAAGA	GGGTGGTAAAGGTGGAAGAAG
VSTM2L	+1Kb	CTCTCTGCCCATCTGCCTTT	GTGGTATAGGGCTGGGTGTG
	+0Kb	AAATCAAGCGGCAGATCCCT	CCTCCGACTGCGGGACT

	-1Kb	AGGGAAGGAGCCTACAGTCC	TTAGTTGTTGCGGCTCCTGG
	-2Kb	TGCATAGAGTCCAAGACGCC	GCCGTGTTTGCCTGATTCTC
	-3Kb	GTGATGAGCCAACAGAGGCT	GTGCTTGTATGCCTTCCCCT
miR-142	+1Kb	GGTGGACTGGAGACCAAGAC	CAGGACCTTGGGCTGCTATG
	+0Kb	CAAAGCGCCTTGAAACCCTC	CCTTACTCTCCAGCCCTCCT
	-1Kb	GTGTTGGGAAGGGAAGGGAG	TTGAGGGTGACCCCAGAAGA
	-2Kb	GTCACTGAGATCACCAAGAACA	CCACTGCTCGAACCAGAAA
	-3Kb	GACAGCGTGTCTGTGTCTGA	CCTGTGACTGGAACAAGGCT
miR-153	+1Kb	GAGGCATGCGAGATGAGGAA	CCTTCTCCCGAACCTGCAAT
	+0Kb	TAGCGAGGCGCCTACTATTTG	GTCTACATGCCCCTCTCGC
	-1Kb	GGAGCTCGGAAAGATGCGG	CCTGACCGTGGGCACTAAC
	-2Kb	AGTGGTCGTGGTGAAAGAGC	CTTTCTCTCCGTCTGTGCCA
	-3Kb	AGGAAATACAGGTGATATACAGGTT	CATAGACACCATATCCTCTCTCCC
miR-124	+1Kb	CTCTAAGGAGCACCTCACGC	TCCATTCCCTGACAGCCTCT
	+0Kb	AAAGCCTGGATGCGAAAGGA	GAAGGGACCACAGCATCCTC
	-1Kb	TGACAAAGCTGATGAGGGGC	GACCTGGGGATTCAGCCTTC
	-2Kb	TCCAGCCGCATTATACACGA	ACTGTCAGCGGGCTTTACC
	-3Kb	GCAGTGAGAATGACGTGTGC	TCTGCTGACGGTTCCGAAAA
miR-9	+1Kb	TTGCGACTCCCAGGGAAAAG	GACCAGTGCGGAATGGAGG
	+0Kb	GCTTGCAAGGGGTTAACAGT	GTCAGCGGGTCTCACCATTC
	-1Kb	GCTCCCTCTTTGAGCCCTTT	GGGTGGAGAGAGAGAACCCA
	-2Kb	GAACCTCGACTTTCCCCAGG	CTGAAGCCTCCTCCTCTCCT
	-3Kb	CAGAGGCCCGAGTGATTTCG	CACGGGGCTTCTCGAAATCA

2.5 Protein methods

2.5.1 Protein sample collection and measurement

Samples were collected in triplicate from at least one well of a 12 well plate at confluency. Cells were washed with DPBS and either Gentle cell dissociation reagent or Versene was added to the well for iPSCs and differentiated cells respectively. Cells were incubated at 37^{o}C for 1-2 minutes, the DPBS aspirated and fresh DPBS added. Cells were detached by manual scratching using a serological pipette and collected in 1.5ml microtubes. They were then centrifuged at 900g at 4oC for 5 minutes and the supernatant aspirated. The pellet was

resuspended in 150µl of RIPA buffer (SLS, #R0278-50ML) supplemented with MS-SAFE Protease and Phosphatase Inhibitor (Sigma, MS-SAFE-1VL), before being incubated on ice for 30 minutes, vortexing rigorously every 5 minutes. Cells were subsequently centrifuged at 14,000g at 40C for 5 minutes. Of the supernatant, 120µl was transferred to a new tube with 46 µl of LDS sample buffer (4x) and 18 µl of DTT (500mM, 10x), (Thermo Fisher, #NP0007 and #NP0004 respectively), and incubated at 95^{o}C for 5 minutes for protein denaturation. If not used immediately for downstream processes, samples were stored at -80^{o}C.

To measure samples a standard curve was generated using BSA protein standards (Thermo Fisher, #23208). 5µl of each standard, 125-2000 µg/mL, was transferred to a clear 96 well plate in triplicate. Then, 25 µL of working solution A [20 µL reagent S plus 1 mL reagent A], (BioRad, #5000113 and #5000115) was added to each well, followed by 200 µL of reagent B (BioRad, #5000114) before gentle mixing and incubation for 15 minutes at RT. Absorbance values were then read on the CLARIOstar microplate reader (BMG Labtech), and a standard curve plotted for the known values. Using this curve, concentrations of the protein samples were then calculated.

2.5.2 Western Blot

Quantified protein samples from chapter (2.5.1) in DTT and LDS were thawed and 20-30µg of protein was loaded onto a Bolt Bis-Tris 4-12% gel (Thermo Fisher, #NP0323BOX) with Pre-stained Protein Ladder (AbCam, # AB116028). The gel was run at 100V for 1-3 hours in Bolt MES running buffer (Thermo Fisher, #B000202), until the protein of interest was evenly dispersed. The protein was then transferred to a nitrocellulose membrane (BioRad, # 1704158), for 10-15 minutes using the semi-dry Trans Blot Turbo system (BioRad).

The membrane was blocked by soaking in a solution of Tris buffered saline ([TBS], Formedium, #TBSL1000) supplemented with 5% milk powder for 1 hour at RT. The membrane was subsequently incubated with the primary antibody, diluted in a TBS + 5%-milk solution at 4^{o}C overnight. The membrane was then washed 3 times with TBS with 0.1% Tween-20 (Sigma, #P9416) for 5 minutes at RT each time, before being incubated with secondary antibody diluted in a TBS + 0.1% Tween solution for 1 hour at RT. The membrane was again washed 3 times before being visualised in an Odyssey CLx imaging system. Relevant primary and secondary anti-bodies are summarised in the table below.

Table 2.5 Primary and secondary antibodies used for western blotting

Primary Antibodies				
Antibody	**Supplier**	**Cat #**	**Species**	**Dilution**
EHMT1	R&D Systems	(PP-B0422-00)	Rabbit	1:1000
EHMT2	AbCam	(AB185050)	Rabbit	1:1000
EZH2	Cell Signalling Technology	(5246)	Rabbit	1:1000
GAPDH	Abcam	(AB9485)	Rabbit	1:1000
H3K9me2	Merck	(17-648)	Rabbit	1:1000
H3K27me3	Merck	(07-449)	Rabbit	1:500
NEFM	Merck	(AB1987)	Rabbit	1:500
REST	Merck	(07-579)	Rabbit	1:500
SNAP25	AbCam	(AB41455)	Rabbit	1:2000
SYN	AbCam	(AB32127)	Rabbit	1:1000
TUBB3	Cell Signalling Technology	(5568T)	Rabbit	1:1000
Secondary Antibodies				
IRDye® 800CW anti-Rabbit IgG	LiCor	(926-32211)	Goat	1:10000

2.5.3 Co-Immunoprecipitation

Primary antibody (1-10µg) was diluted in 200µl of PBS + 0.1% Tween-20 (PBST) and added to 50ul of magnetic Dynabeads (Thermo Fisher, #10003D) per sample, before incubating for 10 minutes at RT. The bead-Ab complex was then separated by magnet and resuspended in 200ul of PBST. The bead-Ab complex was then separated once more and 500-800µg of quantified protein sample from chapter (2.5.1) was added, before incubating for 20 minutes at RT with rotation. The bead complex was subsequently washed 3 times with RIPA buffer, separating on the magnet between each wash, removing supernatant and resuspending by gentle pipetting. The bead complex was transferred to a new tube to prevent coelution, separated by magnet and resuspended in 20µl of elution buffer (24ul of RIPA buffer + 8ul of NuPAGE LDS). The bead complex was then incubated at 95^{o}C for 5 minutes, before being separated by magnet. The supernatant was then loaded onto a Bolt Bis-Tris 4-12% gel (Thermo Fisher,

#NP0323BOX) with Pre-stained Protein Ladder (AbCam, # AB116028) and processed as previously described in Western Blot Chapter.

Table 2.6 Antibodies used for co-immunoprecipitation

Antibody	Supplier	Cat #	Species
EHMT1	R&D Systems	(PP-B0422-00)	Rabbit
EZH2	Cell Signalling Technology	(5246)	Rabbit
FLAG	AbCam	(AB1257)	Goat
HA	Merck	(05-904)	Mouse
REST	Merck	(07-579)	Rabbit

2.5.4 Immunocytochemistry

Media was aspirated from cells on a 12 well plate, washed with 0.5ml of DPBS and fixed using a 3.7% paraformaldehyde solution ([PFA], Sigma, #P1648) at RT for 20 minutes. Cells were washed 3 times with DPBS, then permeabilized with 0.3% Triton-X-100 (Sigma, #X100PC) for 10 minutes at room temperature and blocked with 5% donkey serum for 1 hour. Cells were then incubated with primary antibodies in PBS-T with 5% donkey serum at 4 °C overnight. Following this, cells were washed 3 times with DPBS. Secondary antibodies were applied in PBS-T for 1.5 h at RT, counterstained with DAPI (Molecular Probes) and mounted in DAKO fluorescent mountant (Life Technologies, #S3023).

Table 2.7 Primary and secondary antibodies used for immunocytochemistry

Primary Antibodies				
Antibody	**Supplier**	**Cat #**	**Species**	**Dilution**
MAP2	AbCam	(AB92434)	Chicken	1:500
PAX6	DSHB	(AB_528427)	Mouse	1:1000
Secondary Antibodies				
Alexa Fluor 488 anti-mouse	Thermo Fisher	(A21202)	Donkey	1:1000
Alexa Fluor 647 anti-chicken	Thermo Fisher	(A78952)	Donkey	1:1000

Samples were imaged on a Leica DMI6000b fluorescent microscope. A minimum of 20 fields were acquired per well at x20 magnification. Image analysis was performed using the FIJI analysis software. Each channel was threshold dependent on protein of interest and maintained between samples. Mean fluorescence intensity measurements were taken from at least 4 biological samples.

2.6 Bioinformatics analysis

2.6.1 RNA Sequencing

Microarray and RNA sequencing datasets of gene expression studies focussed on *EHMT1* depletion or mutation were accessed and downloaded from Gene Expression Omnibus (GEO) Datasets available on the National Centre for Biotechnology Information (NCBI) Database website (http://www.ncbi.nlm.nih.gov/gds/). The search words used were "EHMT1" and "Kleefstra Syndrome" and through filtering the search was restricted to *Homo Sapiens*. From this search the raw data for a single dataset was downloaded (GSE178646) (Fear et al., 2022).

Counts were read into R 4.2.3 (https://www.R-project.org/) and filtered to retain genes with counts greater than 5. Principle Component Analysis Plots indicated no outlying samples. Differential gene expression (DGE) analysis was performed using DESeq2 (R package, v1.30.0), where the difference in gene counts was assessed between the wild type control and SNP samples. P values were adjusted for multiple comparisons using Benjamini-Hochberg correction address false discovery rate (FDR). A gene was considered differentially expressed if it has an adjusted P-value of less than 0.05 and a Log2 fold change of 1.5 or greater.

2.6.2 Functional enrichment analysis

For enrichment analysis, significant genes from RNA seq analysis were grouped into either "upregulated" and "downregulated" datasets. Enrichment analysis was performed for each gene set to determine Gene Ontology – Biological Processes (GOBP), using the fgsea multilevel enrichment test and genes were ranked by minimum significant difference signed msd (fgsea). Enriched terms with a padj value less than 0.01 were considered significant. Enriched GOBP terms were clustered based on semantic similarity using GOSemSim (R package, v2.24.0), and clusters were manually summarized. Disease-gene network analysis was performed using the DisGeNET database (V7.0) (Piñero et al., 2021), calculating overlap significance for DEGs and disease genesets by hypergeometric probability, with adjusted

P<0.001 considered statistically significant. Tissue enrichment analysis was conducted using the TissueEnrich (R package, v1.20.0), with enrichment of tissue specific gene sets assessed within KS DEGs.

2.6.3 Knowledge guided miRNA prediction

For prediction of upregulated miRNAs a knowledge guided bioinformatics model was developed as previously described (Shen et al., 2016). A miRNA-mRNA regulatory network was built based on validated miRNA-mRNA pairs, mined from the TargetScan (McGeary et al., 2019), TarBase (Karagkouni et al., 2017) and miRTarBase (Huang et al., 2022a) databases. The Kleefstra Syndrome specific miRNA-mRNA network was generated by mapping significantly downregulated genes onto the reference network and functional miRNA prediction was achieved by using a 2-step approach (Figure 2.1A).

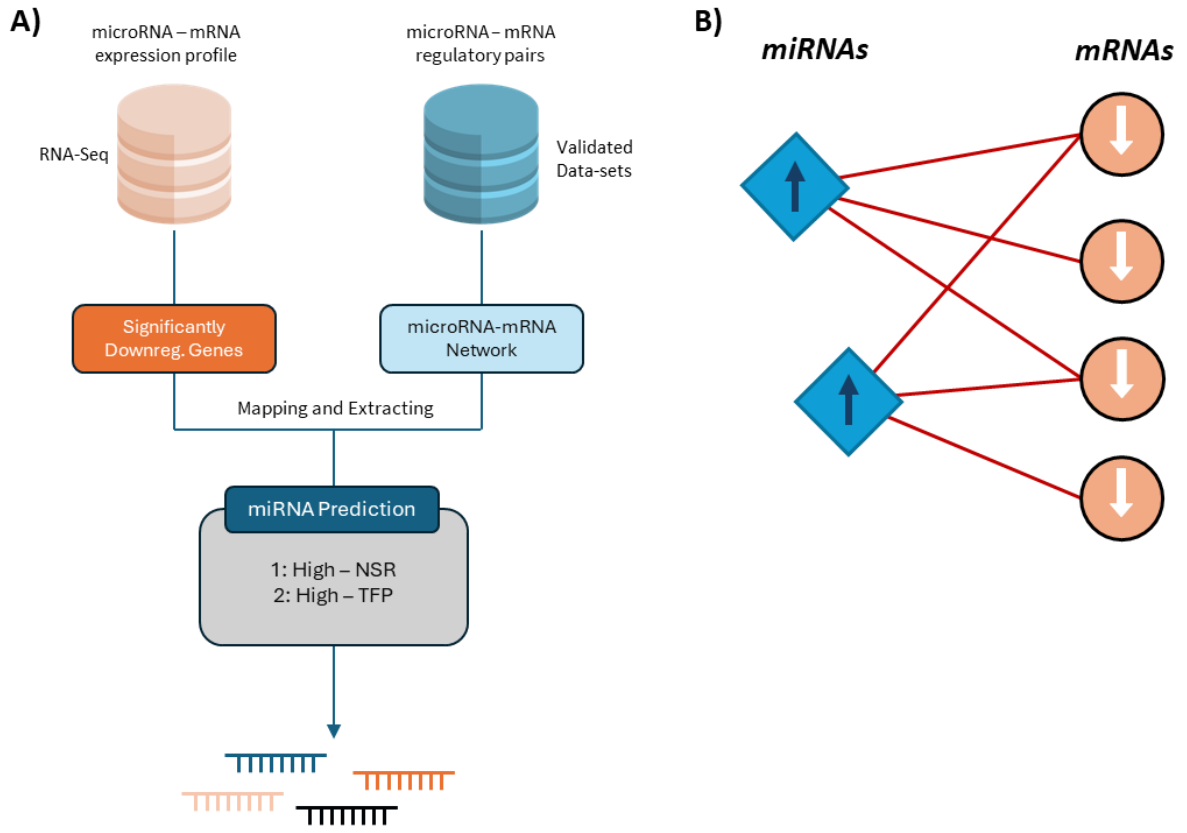

Figure 2.1 Summary of the knowledge guided predictive model
A) *Schematic illustrating the model structure, significantly downregulated genes from KS-RNA sequencing data sets are mapped onto a microRNA-mRNA regulatory network* ***B)*** *Illustration of the many-many network generated to predict upregulated miRNAs based on downregulated target mRNAs from RNA sequencing data*

The Number of Single-line Regulation (NSR) value was calculated to measure the number of genes regulated by a single miRNA and all miRNAs with a significantly high NSR value were

extracted from the KS specific miRNA-mRNA network (p-value <0.01, Wilcoxn signed-rank test). Transcription Factor Percentage (TFP) values were generated to measure the percentage of transcription factors within a target list, before miRNAs with a significant TFP value (p-value <0.01, Wilcoxn signed-rank test) were filtered from those miRNAs in the previous step. Predicted miRNAs were then ranked and presented in order of their NSR values. Using this approach, significantly downregulated genes from an KS specific RNA sequencing dataset was used to predict the functionally significant upregulation of miRNAs in response to the loss of *EHMT1* (Figure 2.1B).

2.7 DNA cloning

2.7.1 Multi-miR sponge construction

The multimiR sponges were constructed from a modified method previously reported (Kluiver et al., 2012b). Three empty sponge cassettes (pmiR-A, pmiR-B, and pmiR-C) were generated by introducing a multiple cloning site (MCS) containing the AgeI, NheI, SbfI and ApaI, restriction sequences, with a nonpalindromic KlfI site positioned between either the 1st and 2nd, 2nd and third, or 3rd and 4th restriction site (Figure 2.2). The donor plasmid, pcDNA3-EGFP a gift from Doug Golenbock (Addgene, plasmid # 13031) was first digested with XbaI and ApaI. Purified plasmid DNA (1µg) was incubated with the restriction enzymes and Cutsmart™ buffer at 37^{o}C for 2 hours. The digested DNA was subsequently run on a 2% agarose gel, before the correct band was identified by size and gel extracted using the Monarch® DNA Gel Extraction Kit (NEB, #T1020L). The MCS oligos were subsequently ligated into the 3' UTR of the digested pcDNA3-EGFP. The oligos were each combined with the purified DNA at a 1:4 ratio, T4 buffer and T4 ligase, before incubation at RT for 30 minutes and then heat inactivation at 65^{o}C for 10 minutes. The ligation mixture was then mixed with a vial of NEB® 5α bacteria (NEB, #C2987H) and incubated on ice for 30 minutes, before transforming into the bacteria by heat-shocking at 42^{o}C for 5 minutes. 950µl of RT Super Optimal broth ([SOC], NEB, B9020S) was added to the solution and incubated at 37^{o}C for 1 hour with shaking at 200rpm. The mixture was then diluted 1:10 and spread on agar plates containing ampicillin (100µg/ml). Colonies were picked and cloning efficacy assessed by diagnostic digest with BamHI and SbfI, and with sanger sequencing.

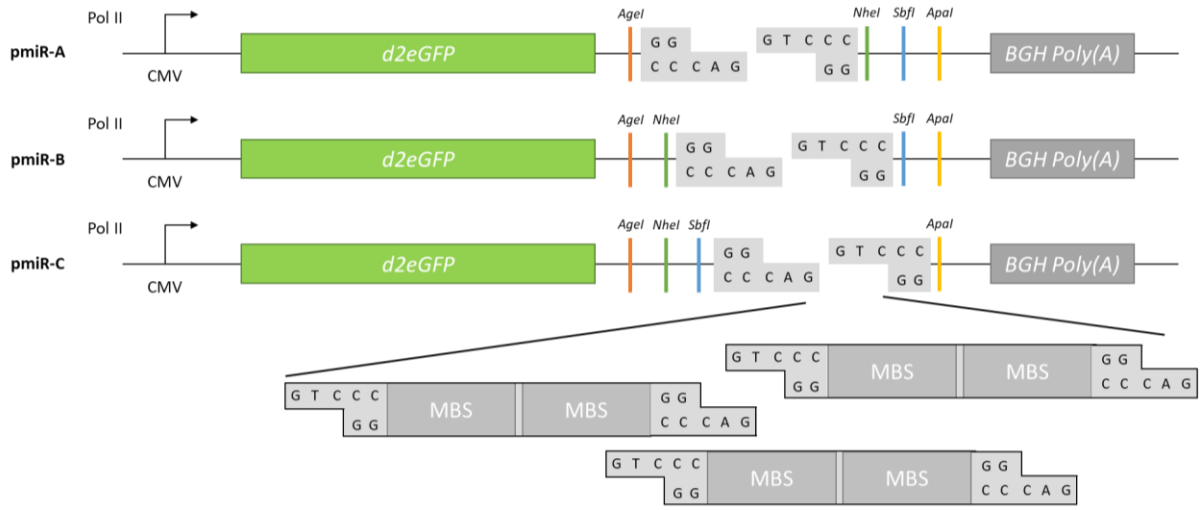

Figure 2.2 Summary of the microRNA-sponge cassette system
Three cassettes allow for quick multimiR-sponge assembly through subcloning

Individual miRNA sponges were designed and tested in-silico using the miRNAsong algorithm to assess on-target and off-target binding efficiency (Barta et al., 2016). A scramble sequence (TCATACTATATGACATCATA), denoted as Empty Vector (EV), was also designed as based on previous studies (Gebeshuber et al., 2013). The scramble sponge was analysed using the miRNAsong algorithm and was not predicted to bind to any miRNA with a free-energy cut off value of -20 kcal/mol. Individual sponges were generated as previously described (Kluiver et al., 2012a), into one of the three MCS cassettes (A, B, C). The relevant pmiR-cassette was digested with KlfI, as described above, before the microRNA binding site (MBS) oligos were ligated with digested cassettes at ratios ranging from 1:3 -1:500. The ligation mixture was transformed into NEB® Stable Competent E. coli (NEB, #C3040H) and spread on agar plates containing ampicillin (100µg/ml). Colonies were picked and cloning efficacy assessed by diagnostic digest with AgeI and ApaI, and with sanger sequencing.

MultimiR-sponges were generated by digesting the individual miR-sponges with the restriction enzymes flanking the MBS insert (AgeI, NheI, SbfI or ApaI), as described above. Digested DNA was separated by gel electrophoresis and purified by gel extraction. Purified DNA was then subcloned into a corresponding individual miRNA sponge and transformed into NEB® Stable bacteria, before spreading on agar plates containing ampicillin (100µg/ml). Colonies were picked and cloning efficacy assessed by sanger sequencing.

Luciferase reporters were again designed and constructed as previously described (Kluiver et al., 2012a). The donor plasmid, pLuc-9, was a gift from Bob Weinberg (Addgene, plasmid

#25037) was digested with HindIII and SpeI, as described above. Digested DNA was purified using the Monarch® PCR & DNA Cleanup Kit (NEB, #T1030S), before being ligated with oligo's specific to each of the miRNA sequences, as described above. Ligation mixture was subsequently transformed into NEB® 5α bacteria and spread on agar plates containing ampicillin (100µg/ml). Colonies were picked and cloning efficacy assessed by sanger sequencing.

For generation of lentiviral multimiR-sponges, the sponge sequence was subcloned into the pBABE-puro retroviral vector, a gift from Hartmut Land & Jay Morgenstern & Bob Weinberg (Addgene plasmid # 1764). Both the donor plasmid and multimiR-sponge were digested with BamHI and ApaI as described above. DNA was separated by gel electrophoresis and purified by gel extraction, before ligation, transformation into NEB® Stable bacteria and spreading onto agar plates containing ampicillin (100µg/ml). Colonies were picked and cloning efficacy assessed by sanger sequencing. The production of amphotropic viruses and infection of target cells were described previously (Stewart et al., 2003).

2.7.2 EHMT1 mutant plasmids

Full length (FL) EHMT1 (ENST00000460843.6 - 5095bp, 1298aa) was amplified from an IBJ4 cDNA library, using primers containing BglII and SalI (NEB, #R0144L, #R0138T) restriction sites. The amplified DNA was digested with BglII and SalI, before being separated by gel electrophoresis and purified by gel extraction. The FL EHMT1 sequence was then subcloned into the donor plasmid pcDNA3-Flag, a gift from Stephen Smale (Addgene, plasmid #20011), digested with BamHI and XhoI (NEB, #R3136T, #R0146L). Amplified EHMT1 FL was ligated with the digested donor using T4 DNA ligase, incubated at RT for 30 minutes and then heat inactivation at 65^{o}C for 10 minutes, before transformation into NEB5α. Colonies were picked, and cloning efficacy assessed by diagnostic digest with NotI-HF (NEB, #R3189L).

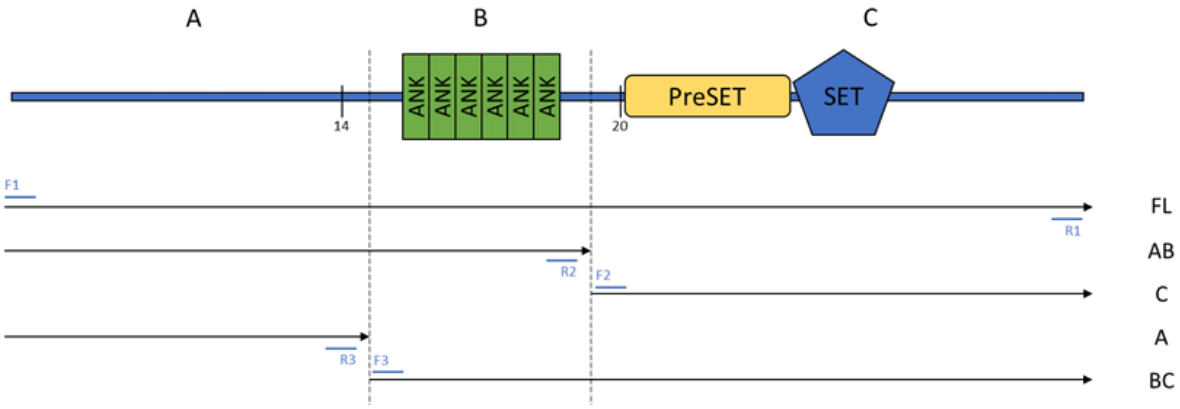

Figure 2.3 Schematic showing the structure of EHMT1 and the deletion constructs

EHMT1 mutant plasmids were then generated, with various truncations of the protein, removing either the N-terminus regions (A), the Ankyrin repeat (B) or the SET domain/C-terminus region (C) (Figure 2.3). A site directed mutagenesis kit (NEB, # E0554S) was used to induce premature termination/STOP codons, with primer pairs for each mutant. Mutant sequences were amplified with respective primers, before each was mixed with a X10 Kinase, Ligase, and DpnI (KLD) enzyme mix and incubated at RT for 10 minutes. The mixture was subsequently transformed into NEB® 5α bacteria and spread on agar plates containing kanamycin (50µg/ml). Colonies were picked and cloning efficacy assessed by sanger sequencing. To investigate binding association of *EHMT1* to *EZH2*, the plasmid pCMVHA hEZH2, a gift from Kristian Helin (Addgene, plasmid #24230), was used.

Table 2.8 Primers used for site directed mutagenesis and sequencing
Underlined sequences denote restriction enzyme sites

Primer	Forward Sequence (5'-3')	Reverse Sequence (5'-3')
***EHMT1* (FL)**	GCTAAGATCT*GT*GAAAACCGAGCTGCTGGG	CGTCGTCGACGGTCGGTCTCCTGACCTCTC
***EHMT1* (A)**	CAGGCAAGGGTAGCTTCAGAAG	GCGGAGAAGTACAGCTGC
***EHMT1* (AB)**	TGCCGCCCGGTAGAACCGCTA	ATGTGCAGTGGCGAGTCTCC
***EHMT1* (BC)**	GTGGACGGAATTGACCCC	CTTATCGTCGTCATCCTTGTAATC
***EHMT1* (C)**	AGGGACATCGCTCGAGGC	AGATCCGCCCGGGCTCTT
Seq (A)	CAGGGACCAGGGAAGGAAAC	CTTCCATCAACGGGGTCCTC
Seq (AB)	AGTACAAGCACGTGGACCTC	TGCAGAGCCTTGCTCATCTG
Seq (Vector)	GGCACCAAAATCAACGGGAC	GGAAGGGCGATCGAGTGAAT

2.7.3 MicroRNA mimics

For gain of function studies, synthetic double stranded miRNA mimics were used (ThermoFisher Scientific). Mimics were transfected into NPCs at 50nM on day 10 of differentiation with Lipofectamine 3000 (ThermoFisher Scientific). Cells were harvested 4 days later, and RNA was isolated for analysis of miRNA expression by qRT-PCR. The mirVana negative control (ThermoFisher Scientific), was used to assess the unspecific effects of mimic treatment.

2.8 Statistical analysis

Statistical analysis was performed in GraphPad Prism (8.4.2), with the exception of miRNA prediction analysis which was performed in R (4.2.3). All data was assessed for normality using the Shapiro-Wilkes test and where normally distributed, parametric testing was conducted. Additionally, outlier analysis was also performed by way of the ROUT method for all experiments. Significant outliers were removed from further analysis. Where two groups were being compared at individual timepoints, students T-tests were implemented to assess statistical significance. When comparing 3 conditions one-way ANOVA was used, whilst multiple conditions across multiple timepoints were assessed by two-way ANOVA. Graphs all display mean values and standard error of the mean (S.E.M). A minimum n value of 3 was always implemented, with higher values denoted on individual figures.

3 Computational analysis of gene expression in cells lacking *EHMT1*

3.1 Introduction

Despite their complexity, psychiatric and neurodevelopmental disorders (NDDs) are increasingly understood to be influenced by both genetic and environmental factors. New genetic evidence shines a light on the critical role of epigenetic modifiers in NDD development. Genome-wide association studies (GWAS) reveal a strong association between mutations in genes encoding these modifiers and a wide range of NDDs (Lasalle, 2013, Yao et al., 2021). This finding is particularly intriguing given the significant overlap in symptoms (phenotypic overlap) across NDDs. For example, autism spectrum disorder (ASD) and intellectual disability (ID) often co-occur at a rate of up to 70% (Coe et al., 2019, Satterstrom et al., 2020). Advanced next-generation sequencing techniques (NGS) have generated complex datasets, when combined with the advent of large-scale computational analysis has shed light on biological mechanisms driven by these epigenes. These analyses reveal that chromatin regulators cluster together in networks with distinct functions and developmental timing (Ciptasari and van Bokhoven, 2020, Moyses-Oliveira et al., 2020). This suggests that disruptions in these networks may contribute to the shared and distinct features observed in various NDDs.

One such epigenetic modifier, *EHMT1*, is consistently associated with autistic features, psychosis and intellectual disability, however the functional pathways involved so far remain unknown (Kirov et al., 2012). Mutations in *EHMT1* are highly penetrant, with heterozygous loss of the gene being causative for the NDD Kleefstra syndrome (KS). The monogenic nature of KS makes it a promising disease model for unveiling commonalities with other NDDs. Computational driven analysis of multiomics data has already proven effective in identifying system-level mechanisms in neurodegenerative conditions such as Alzheimer's disease (AD) (Caldwell et al., 2020). This approach demonstrated that key changes in chromatin modifiers induces a state of de-differentiation within AD cells. Likewise, bioinformatic analysis of publicly available RNA sequencing data from the cortex of ASD patients has been successful in identifying key genetic nodes and essential molecular pathways underlying the disorder (Rahman et al., 2020, Trivedi et al., 2023).

3.2 Chapter Aims

This chapter presents the results of computational analysis of publicly available sequencing data of *EHMT1* depleted cell lines. This work aims to pinpoint the key biological pathways and genetic control points regulated by *EHMT1* that underlie Kleefstra Syndrome and potentially contribute to other widespread neurodevelopmental disorders. In-silico results were subsequently validated in cellular models.

3.3 Results

3.3.1 Bioinformatic analysis of EHMT1$^{+/-}$ cells

Human RNA sequencing data was accessed and downloaded from the Gene Expression Omnibus (GEO) Datasets using the search terms "EHMT1", "Kleefstra Syndrome" and "Neurons". The raw data for a single dataset was downloaded (GSE178646), from KOLF2 iPSCs containing a CRISPR editing induced single nucleotide polymorphism (SNP) in the *EHMT1* gene, which were then differentiated to NPCs at day 24 (Fear et al., 2022). The SNP variant was an EHMT1_c.3430C > T (p.Gln1144*) and identical to a KS patient specific genetic variant. Once the data was processed, I performed differential gene expression (DGE) analysis *EHMT1*$^{+/-}$ NPCs using DESeq2 (Love et al., 2014) with a threshold of |fold change (FC)| > 0.5 and adjusted P value < 0.05. A total of 383 genes were differentially expressed when compared to wild type, with 231 upregulated and 151 downregulated (Figure 3.1). *EHMT1* expression in the SNP line showed reduction in line with pathogenic mutations, though not significant (log2FC = -0.46, p = 0.26).

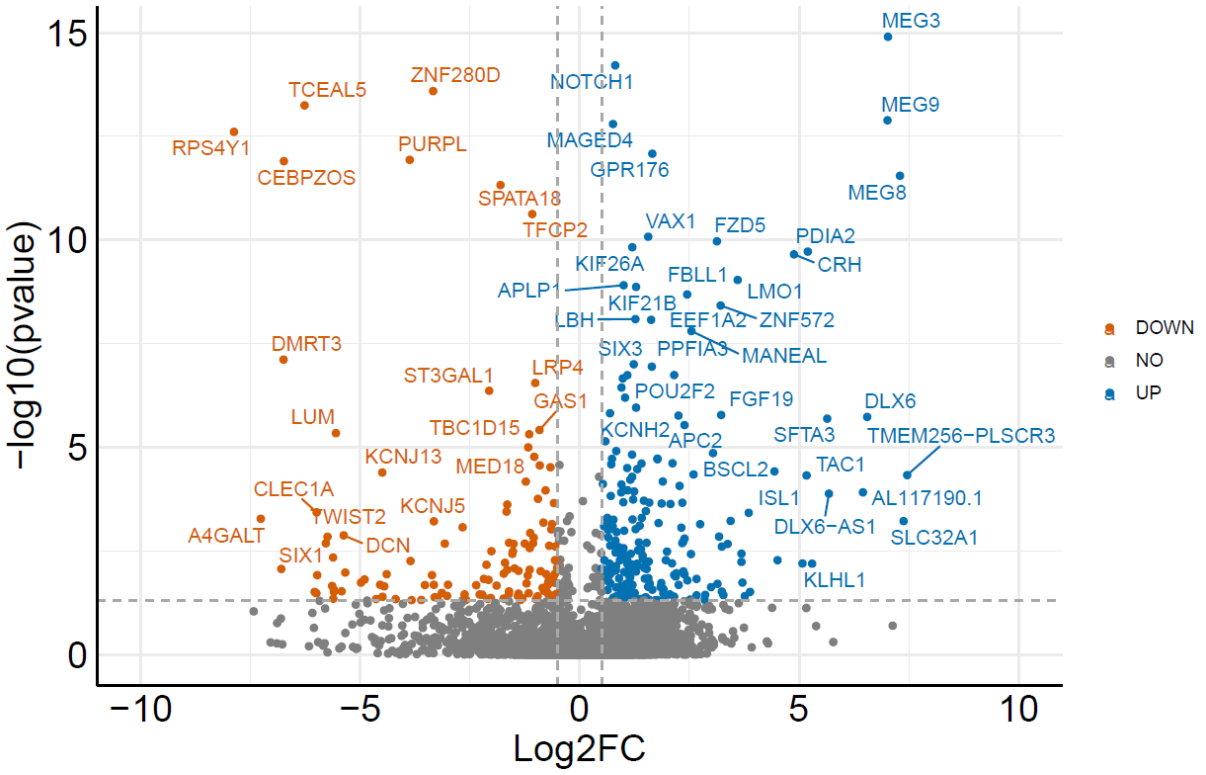

Figure 3.1 RNA sequencing volcano of DEGs in EHMT1$^{+/-}$ mutation relative to WT
As determined by the DESeq2 method with a fold change (FC) threshold of >0.05 and a false discovery rate (FDR)–adjusted P < 0.05

To gain a greater understanding of how the loss of *EHMT1* impacted the gene regulatory network, differentially expressed genes (DEGs) were separated into upregulated and downregulated gene sets, before Gene Set Enrichment Analysis (GSEA) was performed using *fgsea* (Gennady et al., 2021) with the Gene Ontology (GO) database (Figure 3.2). For upregulated genes there was enrichment for GO Biological Processes associated with neuronal development, including Neuron Projection Development, Synaptic Signalling, Brain Development and Synapse Organization. This included a variety of genes including early developmental markers such as *VSTM2L* (LogP = -1.49, Log2FC = 1.06) and *OTX2* (LogP = -1.90, Log2FC = 0.99), adhesion markers, *NCAM1* (LogP = -1.50, Log2FC = 0.98) and neural differentiation markers, *STMN2* (LogP = -1.94, Log2FC = 1.96) In contrast, analysis of downregulated genes showed enrichment for processes including Cell Cycle Regulation, Cell Morphogenesis and Cell Division. Biological processes appeared to show stronger enrichment for upregulated genes compared to downregulated genes, with maximum logP values of -32.15 and -12.68 respectively.

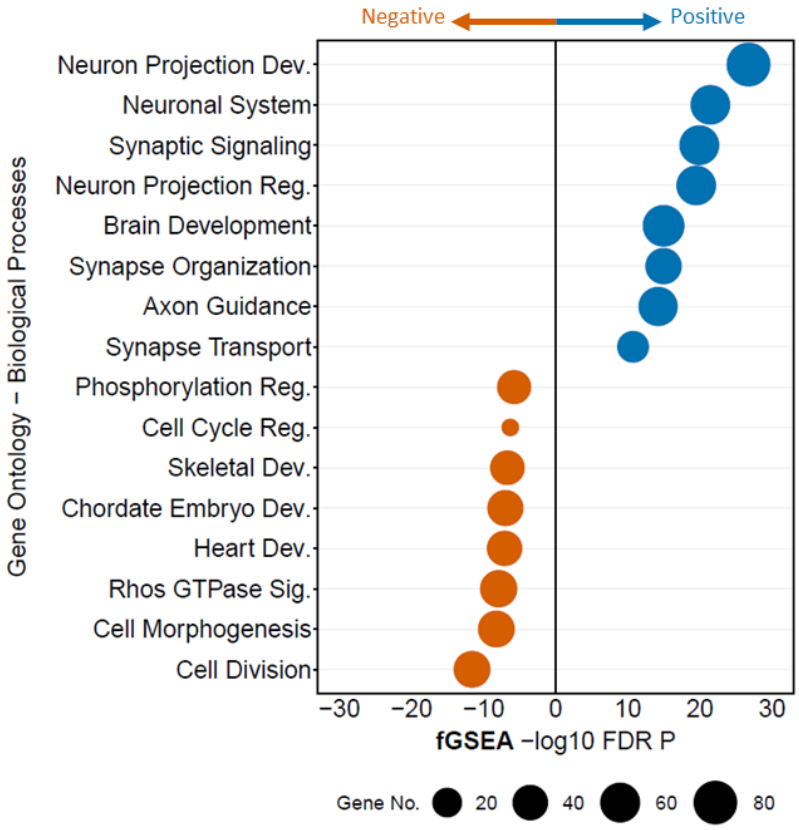

Figure 3.2 Ranked enrichment analysis of EHMT1$^{+/-}$ gene expression
Biological processes ranked using the GOBP database by the fgsea multilevel enrichment test, upregulated genes (blue) and downregulated genes (orange) ranked by minimum significant difference signed msd (fgsea).

Next, to further probe key pathways and identify functionally related genesets, I performed cluster analysis on enriched GOBP terms for upregulated and downregulated genes based on their membership similarities, which were then visualized (Figure 3.3).

For the upregulated geneset (Figure 3.3A), the highest ranked cluster showed enrichment for neuron projection development (GO:0031175, LogP = -32.15), neuron projection morphogenesis (GO:0048812, LogP = -25.96), axon development (GO:0061564, LogP = -22.88), and cell morphogenesis involved in neuron differentiation (GO:0048667, LogP = -18.94). Synaptic signaling pathways were also strongly clustered, with enrichment for trans-synaptic signaling (GO:0099537, LogP = -20.84), chemical synaptic transmission (GO:0007268, LogP = -20.13) and regulation of synaptic plasticity (GO:0048167, LogP = -9.270953337). Likewise, clustering of brain development pathways was also observed, with enrichment for forebrain development (GO:0030900, LogP = -9.61), cerebral cortex development (GO:0021987, LogP = -8.214206926) and neuron migration (GO:0001764, LogP = -6.696903233).

In contrast, analysis of downregulated genes (Figure 3.3B) showed lower levels of clustering. The highest ranked cluster showed enrichment for cell cycling and division, with enrichment for mitotic cell cycle (GO:0000278, LogP = -13.15), chromosome segregation (GO:0007059, LogP = -7.19) and nuclear division (GO:0000280, LogP = -5.12). Other cluster showed enrichment for developmental pathways around skeletal development and cardiac development.

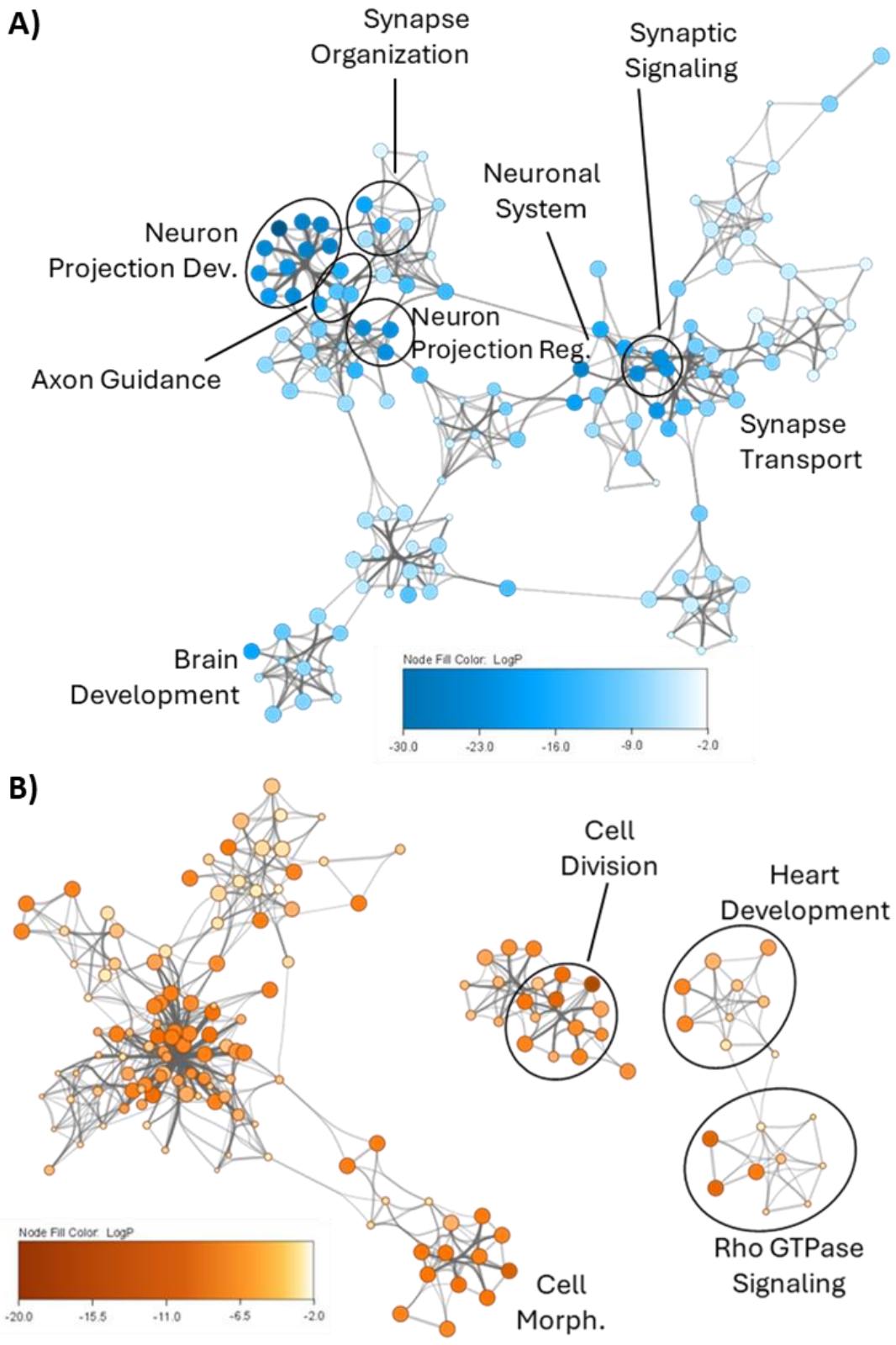

Figure 3.3 Network of enriched GOBP terms in EHMT1$^{+/-}$ neuronal cells
*Clustered by shared ID and coloured by p-value, for both **A)** upregulated DEGs and **B)** downregulated DEGs. Enriched GOBP terms were clustered based on semantic similarity using GOSemSim (R package, v2.24.0), and clusters were manually summarized. Node size indicates the number of genes. Clusters are identified by the most statistically significant term.*

3.3.2 Functional enrichment analysis

This hypothesis of neuronal enrichment was further supported by Tissue analysis (Figure 3.4A-B), which indicated huge enrichment for brain specific gene expression (LogP = -28.30), as well as nerve tissue (LogP = -26.25). Modest enrichment was also seen for the ovaries (LogP = -7.49), heart (LogP =-7.08) and pancreas (LogP = -5.07). Given the significant enrichment in brain specific expression, brain cell type enrichment analysis was subsequently performed using single cell sequencing reference datasets from human brain tissue (Lake et al., 2018). *EHMT1*$^{+/-}$ cells showed a clear genetic shift toward neuronal commitment with significant enrichment for all subtypes of neuron found within the brain including, granule (LogP = -3.7), inhibitory (LogP = -2.61), excitatory (LogP = -2.41) and Purkinje (LogP = -2.26) cells (Figure 3.4C). In contrast there was no enrichment for other non-neuronal cell types.

Next, given the considerable genetic and phenotypic overlap observed between Neurodevelopmental disorders, I assessed the gene-disease association using the *DisGeNET* database (Piñero et al., 2017). Of the 13 associated diseases, Neurodevelopmental Disorders showed the highest enrichment, as well as the greatest overlap in Differentially Expressed Genes (DEGs) (Figure 3.4D). Gene ontology analysis of overlapping genes again showed significant enrichment for biological process involved in neuronal development, with the top three processes as Nervous System Development (GO:0007399, LogP = -4.65), Synapse Organization (GO:0050808, LogP = -3.80) and Neuron Projection Morphogenesis (GO:0048812, LogP = -3.77). Interestingly, the remaining diseases/disorders showed significant overlap with documented KS phenotypes (facial features, speech delay, dystonia). Genes common between enriched genes included *MAPT*, *NLGN3*, *KIF1A*, *EEF1A2 and MAST1*, and with exception of *MAPT*, de-novo mutations for each gene being linked to a range of neurodevelopmental symptoms (Quartier et al., 2019, Tomaselli et al., 2017, Kaneko et al., 2021, Tripathy et al., 2018, Cooper et al., 2011).

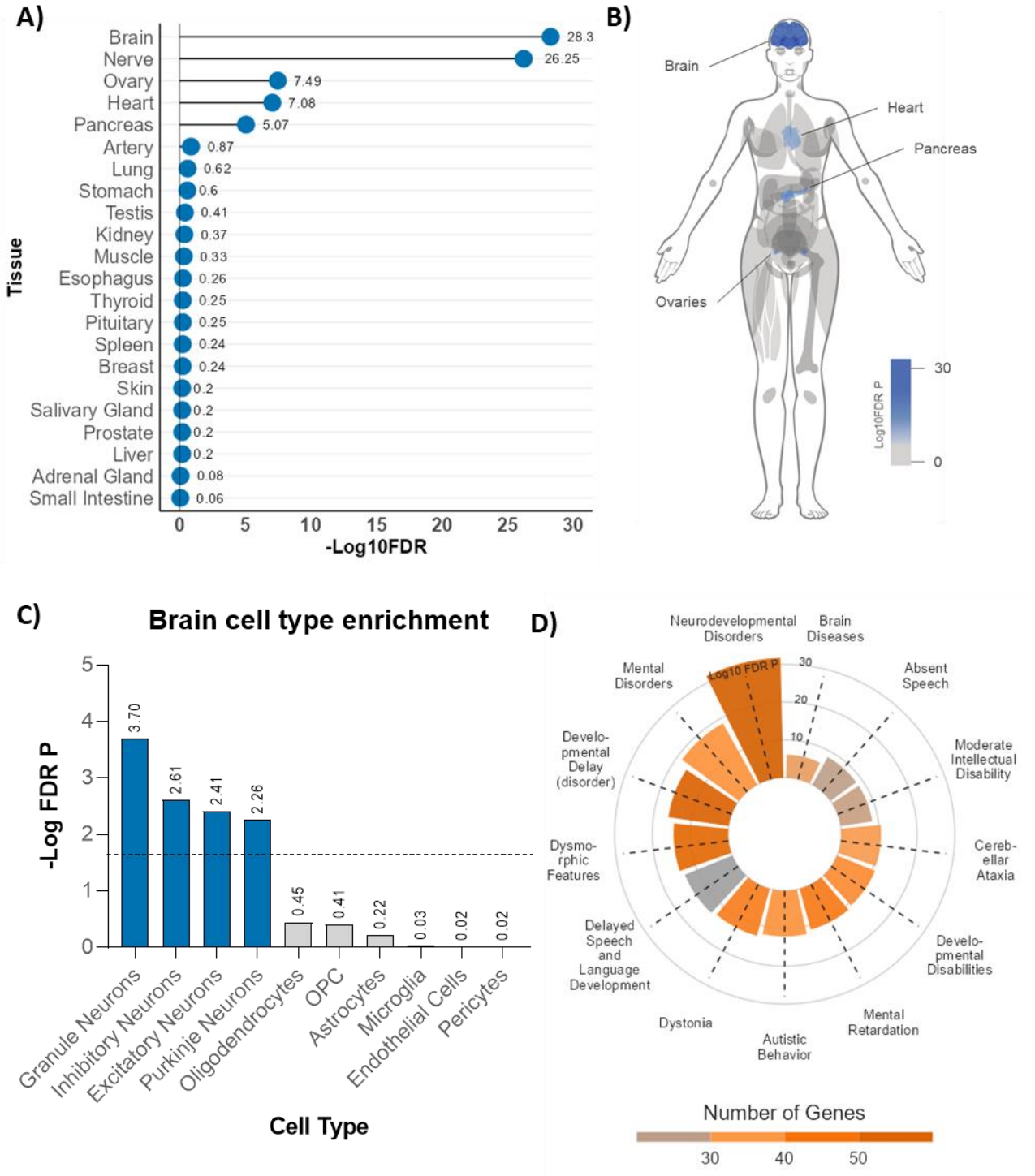

Figure 3.4 Enrichment analysis of EHMT1$^{+/-}$ neuronal cells

A) *Tissue enrichment analysis using gene expression per tissue based on GTEx RNA-seq data for general tissues* ***B)*** *Schematic body map of significantly enriched tissues.* ***C)*** *Brain cell type enrichment analysis using gene expression per tissue based on brain tissue single cell data. Significant tissues P>0.05, are in blue.* ***D)*** *Disease-gene enrichment analysis performed for all DEGs and disease associations from DisGeNET, with significance determined as P < 0.001. Bar plot colour indicates the number of enriched genes within a given disease gene-set.*

3.3.3 *Transcription motif analysis*

Collectively, enrichment results indicate cells depleted in *EHMT1* suggested a gene enrichment indicative of increased neuronal differentiation and maturation. To characterise the transcriptional changes of this altered gene architecture I performed transcription factor (TF) analysis using Integrated System for Motif Activity Response (ISMARA) (Balwierz et al., 2014), for the upregulated and downregulated genesets (Figure 3.5A-B).

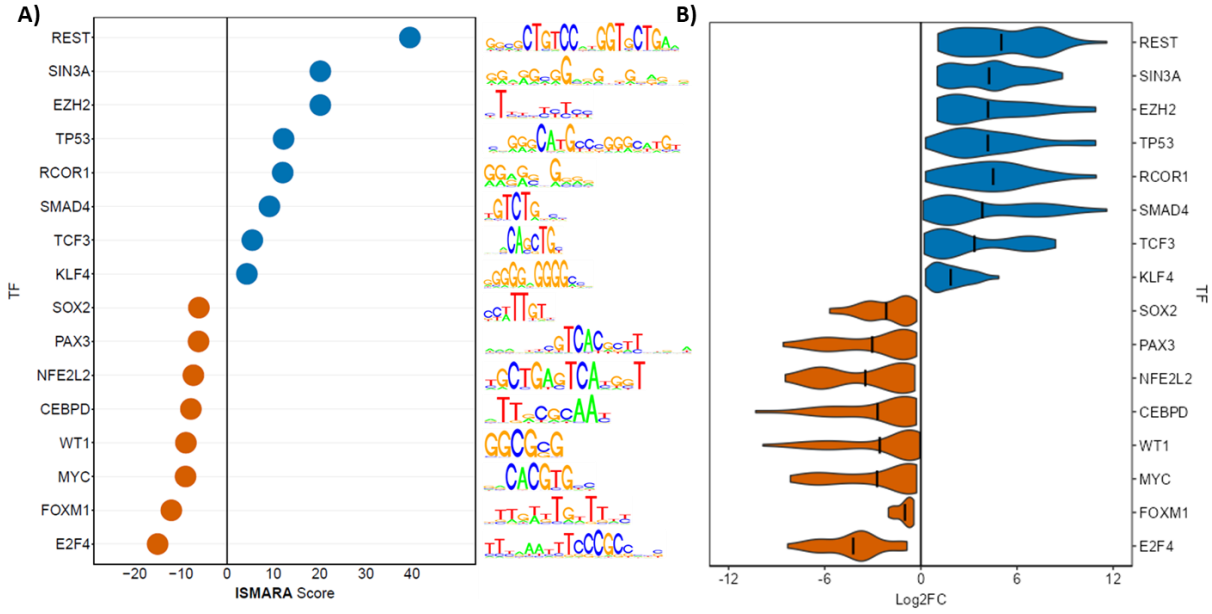

Figure 3.5 ISMARA motif analysis of EHMT1$^{+/-}$ neurons
A) *ISMARA motif analysis (based on z score) for upregulated (blue) and downregulated (orange) genesets, with identified motif sequence.* ***B)*** *Violin plot of TF target expression for upregulated (blue) and downregulated (orange) genes.*

The top transcriptional regulator for the upregulated gene set was REST (RE1 Silencing Transcription Factor) (Z-score = 39.49), a neuron specific gene repressor, often referred to as the master regulator of neurogenesis (Mozzi et al., 2017). Indeed, of the 231 upregulated genes, 52 contained REST RE1 motifs. Interestingly, amongst the remaining enriched TFs is EZH2 (Z-score = 20.13), another epigenetic repressor, known to directly bind to the REST protein (Dietrich et al., 2012). Additionally, SIN3A (Z-score = 20.14) and RCOR1 (Z-score = 12.01) are both TFs within the REST complex and known to regulate the balance of proliferation and differentiation of developing neurons (Monaghan et al., 2017). These findings suggest a dysregulation of the REST complex, principally around the REST protein itself, leading to strong activation of the neurogenesis pathway. This supports previous GOBP analysis that suggested the enrichment of neuronal differentiation pathways. Conversely,

within the downregulated gene set, enriched TFs included E2F4, FOXM1, MYC and SOX2. A negative association with FOXM1 and SOX2 suggests a loss of stemness as they are directed to neuronal cell differentiation (Besharat et al., 2018, Favaro et al., 2009).

3.3.4 Analysis of REST expression

Bioinformatic analysis indicated that REST function was disrupted in response to a loss of *EHMT1*. REST is a critical regulator of development and is highly expressed in both stem cells and neural stem cells (Johnson et al., 2008). To assess the impact of depletion on REST function, hiPSCs were treated with the selective euchromatic histone methyltransferase inhibitor, UNC0638, for 48 hours.

Stem cells were treated with concentrations of UNC0638, from 0-800nM and the levels of REST protein were analysed (Figure 3.6A). Analysis by One-way ANOVA with Bonferroni post-hoc testing revealed levels of REST protein were inversely proportional to UNC0638 concentrations, with significant decreases at 400, 600 and 800nM as compared to control (0nM 1.404±0.196, 200nM 0.989±0.243, 400nM 0.539+0.100, 600nM 0.399±0.048, 600nM 0.204±0.090). Half maximal change was seen around 400nM of UNC0638. This data indicates that a loss of *EHMT1* does indeed lead to a reduction in REST protein as early as the stem cell stage.

To assess if this reduction in protein translated to functional changes, expression of *NRXN3*, *ACTA1*, *CALB1* and *ACTL6B* were measured as targets of REST, in hiPSCs treated with UNC0638 (400nM) (Figure 3.6C). The expression of these three targets begins early in neuronal development in response to decreased REST, however, they are not present in stem cells (Bruce et al., 2004, Ballas et al., 2005, Wu and Xie, 2006). Treatment of hiPSCs with UNC06368 lead to a reduction in *REST* transcript levels (0.703±0.125), although this reduction was not significant. However significant increases were observed in the REST targets, *NRXN3* (3.663±0.455), *ACTA1* (3.400±1.223), *CALB1* (6.517±0.613) and *ACTL6B* (7.183±1.262). This data indicates that the loss of REST protein leads to de-repression of its targets and a premature increase in their expression.

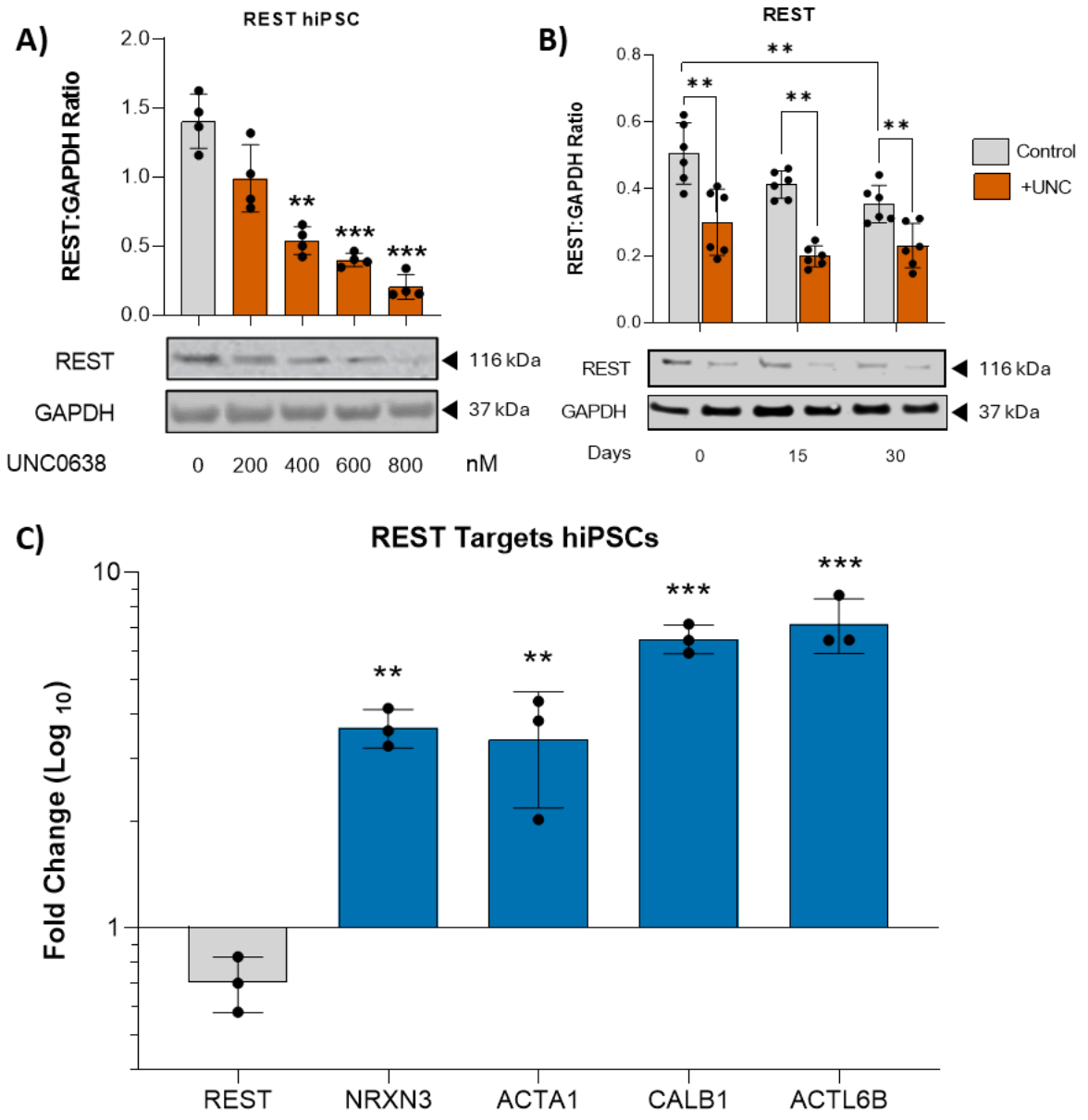

Figure 3.6 Expression of REST following EHMT1 inhibition
A) *Analysis of REST protein levels in hiPSCs treated with varying concentrations of UNC0638, from 0-800nM. Analysis by One way ANOVA with Bonferroni post hoc analysis relative to control* ***B)*** *Analysis of REST protein levels during neuronal differentiation, of cells treated with UNC0638 (400nM).* ***C)*** *Expression analysis of REST and its targets in hiPSCs treated with UNC0638 (400nM) (* p>0.05; ** p>0.01; *** p>0.001). Figure A shows summary data from 3 samples, figure B shows summary data from 6 samples and figure C shows summary data from 3 samples.*

Given that REST expression is known to decrease as neural differentiation progresses, I wanted to assess how protein expression changes in *EHMT1* depleted cells during differentiation. Cells were treated with UNC0638 (400nM) starting two days prior and differentiated, with samples taken at day 0, 15 and 30.

REST protein levels were significantly lower in UNC0638 treated cells compared to control at day 0 (0.301±0.099 vs 0.506±0.091), day 15 (0.198±0.031 vs 0.413±0.041) and day 30 (0.230±0.066 vs 0.355±0.056) (Figure 3.6B). Importantly REST levels were significantly decreased in controls cells compared between day 0 and day 30 (0.506±0.091 vs 0.355±0.056), however this was not the case UNC0638 treated cells which remained low from day 0 and no significant change was observed between timepoints.

To visualize the effects of UNC0638 on protein expression, hiPSCs were continuously exposed to the drug (400nM) throughout their differentiation process into neurons for 30 days. Following differentiation, the cells were stained for REST protein (Figure 3.7A). Analysis of the images showed a significant drop REST protein intensity relative to DAPI (1621±126 vs. 529±233) (Figure 3.7B). This data suggests initial loss of REST protein is sustained throughout differentiation and globally affecting all cells in culture.

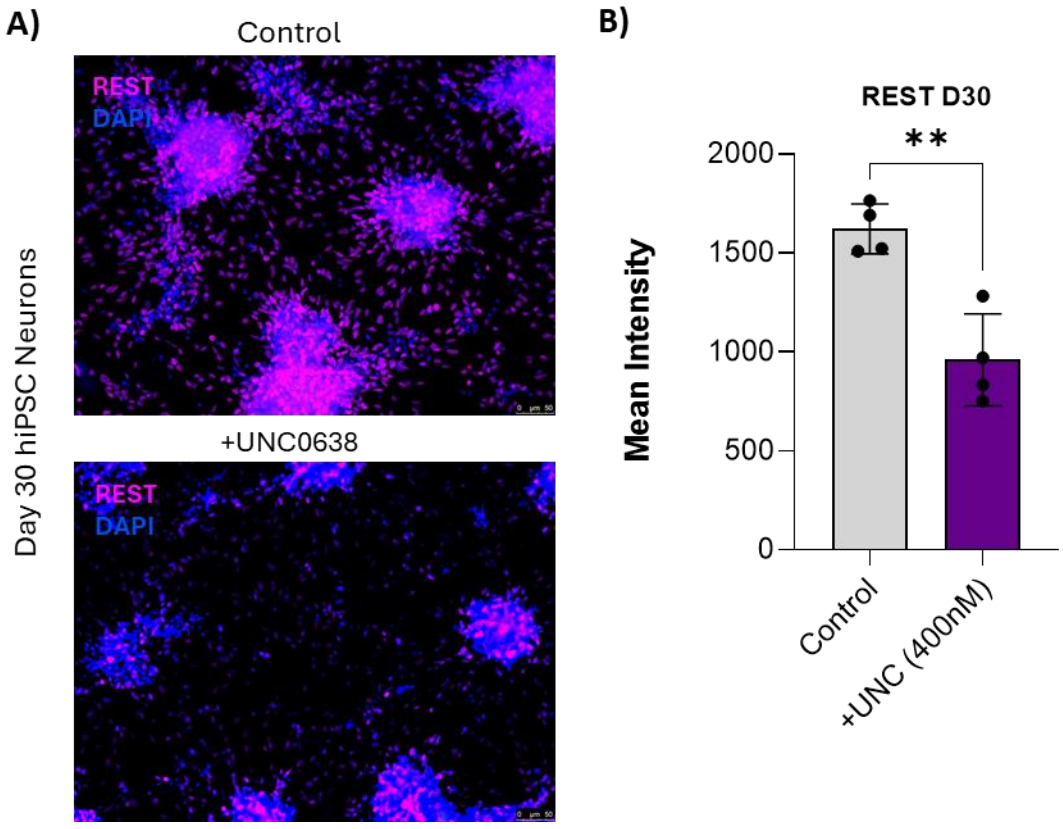

Figure 3.7 Immunostaining of REST (purple) and DAPI (blue) in control and UNC0638 treated neurons, day 30*. A) Example-stained images, scale Bar, 50µm. B) Quantification of protein expression as REST mean fluorescence intensity, with DAPI nuclear counterstain. (** p>0.01). Figure B shows summary data from 4 samples across 4 differentiations.*

3.4 Discussion

This chapter describes how reduced *EHMT1* function, a mutation linked to Kleefstra Syndrome, affects gene expression in human induced pluripotent stem cells (hiPSCs) as they progress to neurons. Publicly available RNA sequencing data from *EHMT1*$^{+/-}$ cells was processed and revealed global changes. A limitation in the availability of *EHMT1*$^{+/-}$ RNA sequencing data meant only a single dataset was analysed. Subsequently published results by the authors of the KS-RNA sequencing dataset (GSE178646), performed differential gene expression analysis on combined iPSC and NPC data between SNP and WT cells (Fear et al., 2022). In contrast, given that EHMT1 is not required to maintain a pluripotent state, my analysis focused solely on data from the NPC stage, identifying 231 significantly upregulated genes and 151 downregulated genes, as opposed to 89 and 19 respectively. 54 DEG were common to the results of both analyses. Results from both mine and the authors analysis identified a significant dysregulation of REST targets as previously identified in our work (Alsaqati et al., 2022). Work by the authors also identified associated changes with targets of the transcription factor SP1, not identified in my analysis. This may indicate a function of SP1 as cells transition out of the pluripotent stage. Within my own work, by utilising approaches such as fGSEA, ISMARA and tissue enrichment analysis, I identified novel changes in neuronal maturation, key transcription factors, histone methylation marks and cell type specification.

Genes involved in neuronal development and maturation, such as those related to neuron projection and synaptic signalling, were upregulated. Conversely, genes associated with cell cycle and division were downregulated. Analysis of brain-specific tissues showed an enrichment of the differentially expressed genes, suggesting their relevance to brain development. Interestingly, several genes commonly altered in this work have been previously linked to neurodevelopmental disorders. Further investigation pointed towards a potential role for the protein REST, a critical regulator of neuronal differentiation, in the observed effects. Loss of *EHMT1* function appeared to disrupt REST, leading to decreased protein levels in hiPSCs. This inactivation of REST resulted in the premature expression of genes typically activated during later stages of development. These findings suggest *EHMT1* plays a key role in neuronal development and the regulation of key neuronal genes.

My findings of enhanced neuronal differentiation are corroborated by omics studies examining the early stages of neural differentiation in human stem cells (Samara et al., 2022,

Su et al., 2017). These studies identified a significant overlap in enriched biological processes, including nervous system development, synaptic signalling, neuron projection development, and neuron development itself. Notably, all these processes were enriched in *EHMT1*+/- neurons, and clustering analysis revealed a strong association, suggesting a highly organized network. Furthermore, these studies reported increased expression of specific genes that were also upregulated in *EHMT1*+/- neurons. These genes included early neurodevelopmental markers like *OTX2* and *VSTM2L*, alongside neuronal differentiation markers such as *STMN2* and *NCAM1*. Conversely, the enrichment of cell cycle-related genes among downregulated genes suggests a disruption of the cell cycle, potentially indicative of premature neuronal differentiation (Pauklin et al., 2016).

However, these results contradict previous results of KS derived neurons, which show increased expression of proliferation related genes, alongside a decrease in maturation and migration genes (Nagy et al., 2017). This may in part be explained by the study design, in which the researchers shortlisted 197 targets from the SFARI autism dataset (Abrahams et al., 2013), as representative of the differentiation state. Upregulated genes which the authors associated with increased proliferation, *SIX3*, were also upregulated in the *EHMT1*$^{+/-}$ neurons. Meanwhile maturation markers *CUX2* and *HCN2* which were shown to be downregulated in the study, were instead upregulated in my analysis. At the timepoint investigated, day 10, increases in the homeobox gene SIX3 are more indicative of increased neuronal differentiation (Shrestha et al., 2023), whilst accompanying morphological maturation analysis is performed significantly later at the 8-week mark.

In this study tissue enrichment analysis also indicated a genetic shift toward neuronal development in response to a loss of *EHMT1*. By far the strongest genetic signatures in upregulated genes were for brain and nerve tissues., whilst cell type analysis showed enrichment for all neuronal cell types within the brain. Interestingly, disease analysis also showed significant enrichment for various conditions, including the top result, neurodevelopmental disorders. These findings are in line with other studies which have shown significant genetic overlap between neurodevelopmental disorders, including *EHMT1* (Gigek et al., 2015, Chen et al., 2014). Importantly, as seen in my work, these expression changes are characteristic to differentiating neural cells, with decreases in proliferation associated genes. This suggests the loss of *EHMT1* is driving precocious neuronal

differentiation and leading to a premature exit from the cell cycle. This hypothesis aligns with the disease phenotype, in which microencephaly and reduced brain size are a common observation of Kleefstra Syndrome (Stewart and Kleefstra, 2007). This precocious maturation has been demonstrated in other neurodevelopmental disorders such as Kabuki syndrome, Wiedemann-Steiner syndrome, Rett syndrome and Tuberous Sclerosis Complex disorder (Carosso et al., 2019, Huang et al., 2015, Patrizi et al., 2019, Magri et al., 2011). Indeed, deficits in neuronal differentiation and proliferation have been posited as major convergence points for NDDs and may go some way to explaining the observed phenotypic overlap (Ernst, 2016). The effect of *EHMT1* on neuronal maturation rate has also been highlighted in a very recent study, demonstrating that a temporary loss of the epigenetic regulator leads to premature maturation of iPSC derived neurons (Ciceri et al., 2024). Many of the upregulated markers observed in this work were also identified as being upregulated in my own analysis, such as *NEFM* and *STX1A*.

Transcription factor analysis indicated the driving force behind this accelerated maturation was a loss of the REST complex, with almost a quarter of upregulated genes targeted by REST. This finding strongly corroborates previous findings that indicate REST is a key mediator of the Kleefstra Syndrome phenotype (Alsaqati et al., 2022). Multiple known components of the REST complex were identified in motif analysis, including SIN3A and RCOR1, which in themselves are important regulators of neurodevelopment. RCOR1 is a core protein of the BRAF-HDAC (BHF) complex and is vital for the recruitment of HDAC for the repression of neuronal genes (Lee et al., 2005). Despite being closely associated with the REST complex, the protein is also capable of REST independent regulation and is required for proper timing and migration of cortical neurons (Fuentes et al., 2012). Mutations in the gene have also been closely associated with the developmental disorder Joubert Syndrome 1 (Braun et al., 2016).

Likewise, SIN3A is a core member of the REST complex, required for the recruitment of HDACs to repress gene expression (Huang et al., 1999). Intriguingly, a study by Halder et al. demonstrated that reducing SIN3A levels promotes neuronal differentiation while inhibiting the formation of astrocytes (Halder et al., 2017). This finding aligns with results of my cell type enrichment analysis, which revealed a preferential shift towards neuronal subtypes compared to astrocytes and oligodendrocytes. Similar to *RCOR1*, mutations of *SIN3A* are causative for the neurodevelopmental disorder Witteveen-Kolk syndrome, characterised by intellectual

disability, seizures, hypotonia and epilepsy (Balasubramanian et al., 2021), all classical symptoms of the *EHMT1* disorder, Kleefstra Syndrome.

Another highly enriched transcription factor was the epigenetic regulator EZH2, a methyltransferase responsible for depositing H3K27me3. EZH2 is crucial for the proper development of neurons, particularly in balancing between self-renewal and differentiation (Pereira et al., 2010). Though not a core member of the REST complex, EZH2 has been found to associate with the complex, whilst REST is required for the recruitment of EZH2 at specific targets (Dietrich et al., 2012). Furthermore, alongside *EHMT1* and *DOT1L*; *EZH2* was identified as a key regulator of neural differentiation timing (Ciceri et al., 2024).

Collectively these results demonstrate the close relationship between these epigenetic regulators and the significant overlap seen in their functions. Despite this, results of the motif analysis indicated enrichment appeared primarily around the REST protein itself. Moreover, of all transcription factors identified, REST showed the largest change in *EHMT1*$^{+/-}$ cells. Beyond the control of REST gene expression, the protein's activity is further fine-tuned through various chemical modifications (ubiquitination, phosphorylation, methylation), as well as alternative splicing mechanisms (Nishihara et al., 2003, Ohnishi et al., 2017). To assess if the dysregulation of REST was at the transcriptional or translational level, cells were treated with an EHMT inhibitor, UNC0638. I demonstrated that although a modest decrease is seen in REST transcript, the most significant reductions were seen in protein levels. This indicates the regulation of REST by EHMT1 is most likely post-translational in nature. To note, UNC0638 inhibits not only EHMT1 but also its dimer, EHMT2, meaning I cannot conclusively exclude an action of EHMT2 on REST levels at this stage.

Widely recognized as the master regulator of neurogenesis, REST functions by suppressing genes that maintain neural stem cells in an undifferentiated state. Conversely, activation of these REST target genes is sufficient to drive neuronal differentiation (Su et al., 2004). To test if the loss of REST protein was sufficient to cause de-repression of its targets, I analysed expression levels following *EHMT1* inhibition. Expression of early NPC markers were significantly upregulated as early as the stem cell stage, indicating the loss of REST protein has a functional implication on its targets. These results underline that REST decreases are driving precocious neuronal differentiation in *EHMT1* depleted cells. This mirrors our previous findings that indicate REST protein shows a marked decrease in *EHMT1* deficient cells

(Alsaqati et al., 2022). This aligns with studies implicating the role of REST in maintaining an undifferentiated state in stem cells (Mukherjee et al., 2016). In this work, depletion of REST not only induced premature differentiation of neurons, but also a decrease in cell cycling genes, as previously highlighted in my findings. This is not the first association of a methylase and REST impairment with neurodevelopmental disorders. Mutations in the histone demethylase, *KDM5C* (also referred to as *JARID1C*) was found to impair the REST mediated repression of various neuronal genes, ultimately culminating in X-linked intellectual disability (Tahiliani et al., 2007).

Although REST expression decreases as stem cells progress through neural differentiation, several studies have demonstrated elevated levels of REST are expressed later in adult post-mitotic neurons (Gao et al., 2011, Calderone et al., 2003). To understand if REST levels changed as differentiation progresses, I differentiated *EHMT1* depleted cells until day 30 and compared to control cells. As before REST levels were decreased in stem cells in response to a loss of *EHMT1*, however as differentiation progressed these levels remained repressed. Conversely, levels in control cells decreased sequentially as differentiation progressed, however by day 30 were still significantly higher than *EHMT1* depleted cells. Taking this information together suggests beyond simply an acceleration of REST reduction, the loss of *EHMT1* causes a sustained repression of REST. This was supported by imaging analysis of day 30 neurons which showed a significant reduction in REST levels across the culture. There is a possibility that prolonged culture of these *EHMT1* depleted cells may lead to subsequent increases in REST levels, particularly for specific neuronal phenotypes. Most likely expression would take the form of the alternatively spliced isoform, REST4, a truncated protein that unlike its full-length counterpart functions as an activator (Raj et al., 2011).

3.5 Conclusion

This chapter delves into the computational analysis of gene expression patterns within neurons possessing a heterozygous mutation in the *EHMT1* gene (*EHMT1*+/-). The work demonstrates the ramifications of reduced *EHMT1* levels on the overall architecture of gene expression. The findings reveal a compelling shift in this architecture, favouring the gene expression profile characteristic of differentiating cells. This shift manifests as an upregulation of genes intimately involved in the development of neuronal structures, particularly those facilitating communication and connection between neurons. These findings collectively

suggest that *EHMT1* plays a critical role in orchestrating the timely progression of neurogenesis, ensuring the proper development of neurons within a defined timeframe. Notably, the genes exhibiting dysregulation displayed a significant overlap with genes implicated in various developmental disorders. This observation highlights a potential convergence pathway with other disorders that share similar symptomatic presentations. The research provides compelling evidence for a degree of functional convergence between *EHMT1* and a subset of rare neurodevelopmental disorders. The central driver behind this shift in gene expression appears to be the dysregulation of the master regulator REST. The study successfully confirmed that the ablation of *EHMT1* leads to a subsequent downregulation of REST protein levels. This downregulation, in turn, prematurely derepresses the vast network of genes associated with neuronal function. Interestingly, these alterations in REST function are not solely confined to the stem cell stage, but rather persist as the process of neural differentiation unfolds.

4 Analysis of miRNAs in *EHMT1* deficient cell models

4.1 Introduction

As a master regulator of neurogenesis, the regulation of REST is complex and regulated at various levels. Mechanisms of REST regulation are dependent on cell type and differentiation stage, with a multistep system regulating how cells progress to mature neurons. During the transition to the neuronal progenitor state, REST protein levels undergo a tightly regulated reduction. This precisely controlled degradation ensures that neuronal gene chromatin remains in a transcriptionally repressed yet inducible state (Ballas et al., 2005). Subsequently, as these progenitors differentiate into mature neurons, REST along with its co-repressors dissociate from the RE1 element on neuronal gene promoters. This dissociation event triggers the transcriptional activation of the neuronal gene network.

In the early stages of neuronal differentiation, post-translational regulation mechanisms appear to be the dominant regulator of REST levels. For example, retinoic acid (RA) induced differentiation has been shown to stimulate proteasomal degradation of REST through the elevation of β-TRCP E3 ubiquitin ligase (Westbrook et al., 2008, Singh et al., 2011). However more recently studies have implicated sncRNAs are instrumental in the regulation of REST, with a particular inference on microRNAs. MicroRNAs are small, non-coding RNAs that function as post-transcriptional regulators by binding to target mRNAs and promoting their degradation or inhibiting translation (Gebert and MacRae, 2019).

Studies on the role of RA demonstrated that in addition to the effect on β-TRCP E3, there was also a significant increase in miR-29a-3p, which acted to directly degrade REST (Wang et al., 2018b). Interestingly, treatment with inhibitors for miR-29a-3p lead to a reduction in neuronal differentiation and increases in proliferation. Other studies have demonstrated that initial loss of REST is driven by increases in the miR-26 family (Sauer et al., 2021). Administration of miR-26 mimics were shown to directly inhibit REST and lead to both accelerated differentiation and reduced proliferation.

The regulatory relationship between REST and miRNAs is intricate. While some miRNAs may target REST for downregulation, REST itself acts as a transcriptional repressor for a subset of miRNAs. For example, REST directly inhibits miR-124-3p, miR-9-5p, miR-132-3p, miR-153-3p and let-7-5p, whilst simultaneously being targeted by these miRNAs (Wu and Xie, 2006, Otto

et al., 2007) This reciprocal interaction creates a feedback loop, making it challenging to definitively identify which miRNAs act upstream of the REST complex in a given context.

In the absence of high-throughput biological assays, computational methods have emerged as a valuable tool for the rapid identification of miRNAs and their putative targets. The cornerstone of most algorithms for predicting miRNA targets lies in the analysis of complementarity between the miRNA's seed region, typically nucleotides 2-7, and a potential target site within the 3' untranslated region (UTR) of an mRNA transcript (Min and Yoon, 2010). Despite this, various techniques are used, each considering differences in pairing matches, evolutionary conservation, and target accessibility. As such these databases can produce significantly differing results, with one analysis of 5 databases showing an overlap of only 16 miRNA-target interactions from a total of 2,869 (0.56%) (Kariuki et al., 2023). Moreover, a study aiming to validate these databases by studying the global impact of knocking out a single miRNA found the best algorithm, TargetScan (V4.1), still displayed a false discovery rate of approximately 66% (Baek et al., 2008).

This discrepancy can in part be explained by the failure of these algorithms to acknowledge the highly complex reality of miRNA binding *in-vivo*. It has been demonstrated that a single miRNA can bind to many target genes, but perhaps even more importantly that multiple miRNAs can bind to a single target simultaneously and in concert with one another (Wu et al., 2010, Hashimoto et al., 2013). Combined with other factors such as competitive binding between miRNAs (Gardiner et al., 2015) and dosage response (Cui et al., 2024), it is little surprise that algorithms display such high rates of false positives.

In attempts to embrace this complexity some studies have incorporated target prediction results with omics data, including mRNA expression profiles. Such approaches have involved generating disease specific miRNA-mRNA networks, using a biological systems approach to overcome issues of many-many relationships (Zhu et al., 2017, Zhang et al., 2014b, Lin et al., 2018). This approach has been successful in identifying novel biomarkers in various cancers, but also in highly polygenic disorders such as autism spectrum disorder (ASD) (Shen et al., 2016).

4.2 Chapter Aims

The aim of this chapter will be to develop a novel Kleefstra syndrome specific miRNA-mRNA network, utilising previously analysed RNA-sequencing data from chapter 3.3.1. The goal is to identify dysregulated miRNAs that may be driving the disease phenotype and confirm these results in-vitro using disease models. Critically, the work also aims to discern the temporal differences in this network throughout neuronal differentiation.

4.3 Results

4.3.1 Knowledge guided miRNA prediction analysis

The results in Chapter 3 demonstrated that REST protein is significantly repressed in response to a loss of *EHMT1*. To further probe the potential role of miRNAs in this system I developed a model based on integrative analysis of a miRNA-mRNA regulatory network and the disease specific expression profile of RNA-seq data analysed at day 30, modified from previously described pipelines (Shen et al., 2016, Zhang et al., 2014b). This model predicts and ranks enriched miRNAs, utilising three network measurements, namely single-line regulation, the percentage of transcription factor genes and the closeness proximity score.

Based on the expression data from *EHMT1*$^{+/-}$ cells at day 30, a total of 18 miRNAs were predicted to be enriched (P≤0.01) (Figure 4.1A). Interestingly, of these 18 miRNAs, 8 are known to contain RE1 binding sites and have been shown to be directly regulated by the REST complex (Wu and Xie, 2006). Next to confirm the results of the model, qRT-PCR was performed on samples taken from day 30 of differentiation and treated with UNC0638 (400nM). Of the 18 predicted miRNAs, an astonishing 14 (78%) were shown to be upregulated (Figure 4.1B), including 7 of those known to be regulated by the REST complex (Wu and Xie, 2006). This included brain specific miRNAs such as miR-124-3p and miR-9-5p, which are known to induce neuronal differentiation and drive maturation (Richner et al., 2015).

Given that previous studies have suggested specific miRNAs may act upstream of the REST complex, I next analysed the expression of the predicted miRNAs in pluripotent cells treated with UNC0638 (400nM) for 48 hours. Of the total 18 miRNAs, 10 (56%) were shown to be significantly upregulated following the UNC treatment (Figure 4.1C). Interestingly, with the exception of miR-153-3p, the remaining REST targeted miRNAs were not upregulated, suggesting although REST was decreased at the pluripotent stage, a residual level of activity was sufficient for repression. Furthermore, although upregulated at the pluripotent stage, the expression of several miRNAs (miR-653-3p, miR-10b-3p and miR-140-5p) appear to reduce by day 30, whilst the remaining miRNAs remain elevated. To determine if the pluripotent upregulated miRNAs may be acting upstream of the REST complex, target analysis was performed. Four of these miRNAs (miR-142-3p, miR-153-3p, miR-140-5p and miR-26a-5p), were predicted to target REST mRNA based on the TargetScan database (V8.0).

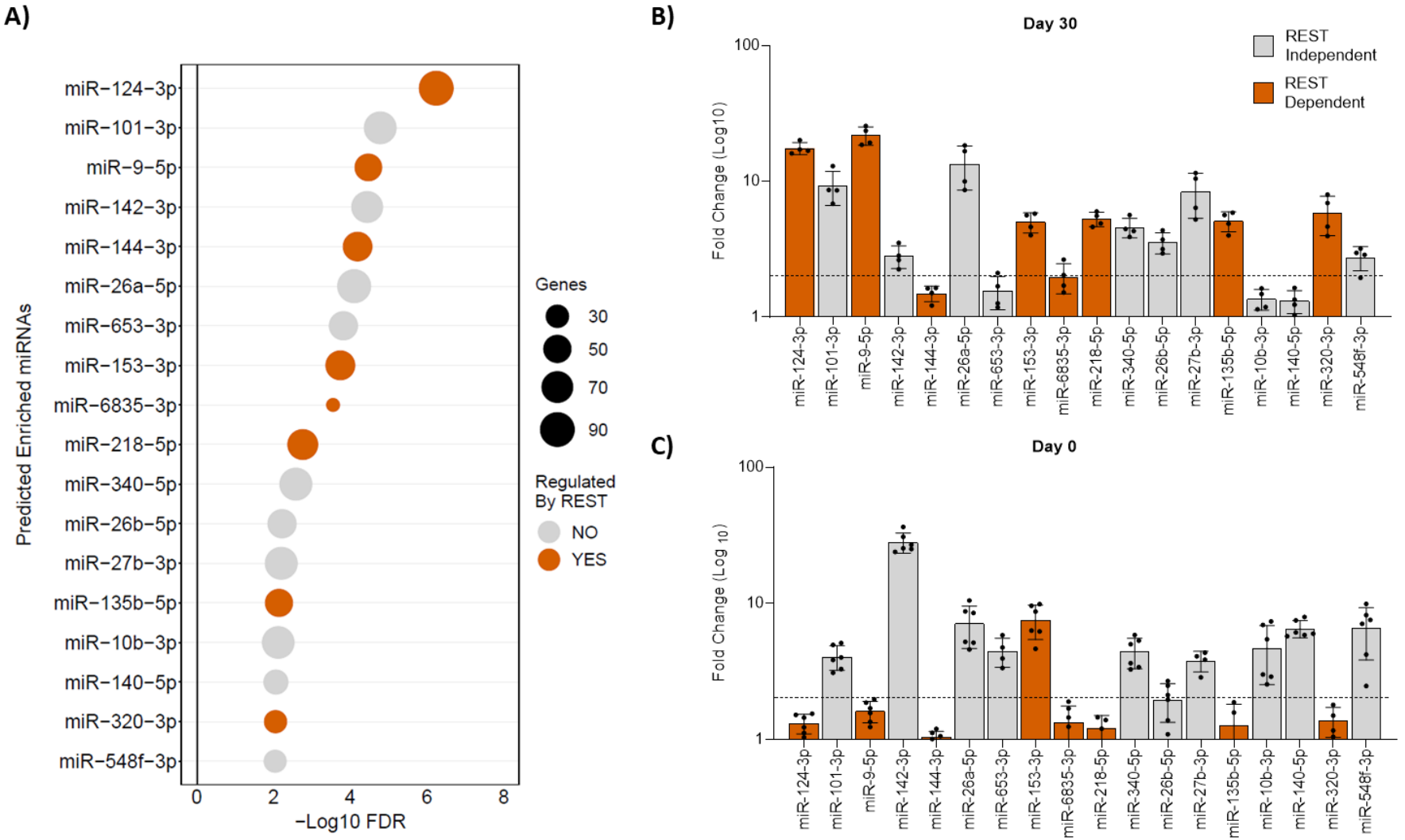

Figure 4.1 Dysregulation of miRNAs in EHMT1 depleted cells.

A) *Prediction enrichment analysis of upregulated miRNAs based on EHMT1$^{+/-}$ day 30 transcriptomic data, where orange miRNAs are those known to be regulated by the REST complex. Prediction was considered significant when P < 0.01, plot size indicates the number of DEGs predicted to be targeted by the relevant miRNA.* ***B,C*** *Analysis of predicted miRNA expression by qRT-PCR. Mean fold change over vehicle control, n ≥ 4 independent experiments, log10 scale axis. Increased miRNA expression = FC > 2.* ***B)*** *Day 30 hiPSC derived neurons following constitutive treatment with 400nM UNC0638.* ***C)*** *hiPSC following treatment with 400nM UNC0638 for 4 days. Data were presented as Mean±SEM and analysed by student's t-test or One-way ANOVA with post hoc comparisons using Tukey's multiple comparisons test comparing to control samples.*

4.3.2 EHMT1 mediated regulation of miRNAs

To determine if these miRNAs were indeed directly targeted by *EHMT1*, ChIP-qPCR was performed for all four miRNAs to determine the levels of H3K9me2 methylation. For the gene encoding each miRNA, primer pairs were designed for the transcription start site (TSS), 1Kb downstream of the TSS, or up to 3Kb upstream of the TSS at 1Kb intervals (Figure 4.2A). A control region, 8Kb upstream of the TSS was also assessed. H3K9me2 levels were then analysed for each of the four miRNA genes (miR-142, miR-153, miR-140 and miR-26a) in hiPSCs treated with UNC0638 (400nM) for 48 hours (Figure 4.2B-E).

Genes for all four miRNAs showed greater than two-fold enrichment for repressive H3K9me2 marks in control samples. The largest mean fold enrichment was 18.73±2.09 for MIR142, 12.11±1.67 for MIR153, 10.46±1.44 for MIR140 and 6.53±0.44 for MIR26a. Control regions, at -8Kb showed no enrichment for H3K9me2. With the exception of MIR26a, all genes show clear peaks of H3K9me2 enrichment. Following treatment with UNC0638, all genes showed a significant reduction in repressive H3K9me2 levels across all regions as compared to controls, with the exception of MIR26a -2Kb ($P>0.05$). Mean fold enrichment for previous peaks dropped to 4.37±0.75 for MIR142, 4.91±1.29 for MIR153, 2.43±0.39 for MIR140 and 1.13±0.43 for MIR26a.

Collectively data indicates enrichment for H3K9me2 marks around each of the miRNA genes that is significantly reduced following treatment with the methyltransferase inhibitor, UNC0638.

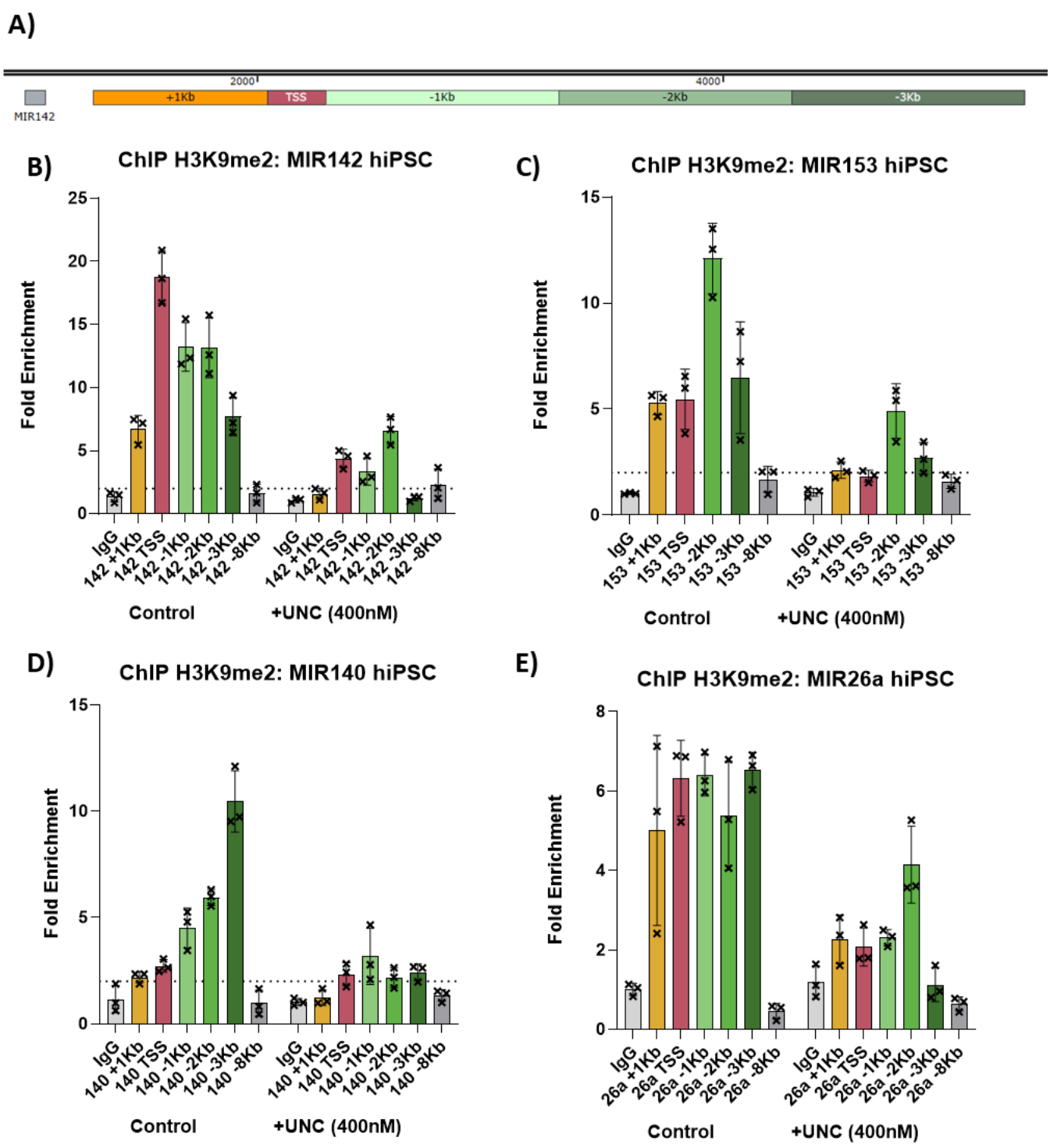

Figure 4.2 ChIP-qPCR analysis of H3K9me2 marks on miRNA targets
A) *Schematic of regions in the MIR142 gene analysed by qPCR. Primer pairs were designed at the transcription start site (TSS), 1Kb downstream of the TSS, or up to -3Kb upstream of the TSS at 1Kb intervals.* ***B-E*** *Analysis of miRNAs in hiPSCs treated with 400nM UNC0638 as compared to vehicle control. Mean fold change over vehicle control, n = 3 independent experiments* ***B)*** *MIR142* ***C)*** *MIR-153, successful primers were not possible for -1Kb downstream of the TSS* ***D)*** *MIR140* ***E)*** *MIR26a. Data were presented as Mean±SEM*

To further probe the link between *EHMT1* and the four miRNAs, I assessed their expression in iPSCs derived from Kleefstra Syndrome patients (KS). Unlike the UNC0638 inhibitor, the KS cell lines are only deficient in *EHMT1*, whilst EHMT2 remains unchanged. With the exception of miR-142-3p in cell line KS1, analysis by two way ANOVA revealed all miRNAs were significantly increased compared to control (Figure 4.3A), indicating *EHMT1* is directly responsible for the regulation of the H3K9me2 marks noted previously. No significant difference was observed between the two patient lines, however miR-153-3p was significantly higher than all other miRNAs ($P<0.05$).

To further support this finding, I assessed expression of the miRNAs in a previously generated *EHMT1* heterozygous mutant cell line (*EHMT1*$^{+/-}$). Expression of all four miRNAs was increased relative to controls (Figure 4.3B). To understand if abnormal increase in miRNA expression was reversible, I generated a full length *EHMT1* plasmid and subsequently transfected the plasmid into the *EHMT1*$^{+/-}$ cells. Exogenous overexpression of *EHMT1* in the *EHMT1*+/- cell line was sufficient to significantly reduce expression levels of all four mature miRNAs, (miR-142-3p p=0.0013; miR-153-3p p=0.00015, miR-140-5p p=0.0082, miR-26a-5p p=0.0050) reversing the effects of the *EHMT1* loss (Figure 4.3B). Together this data suggests *EHMT1* is directly responsible for the repression of miRNAs targeting *REST* in hiPSCs, whilst the loss of *EHMT1* and its effects of miRNA expression are reversible.

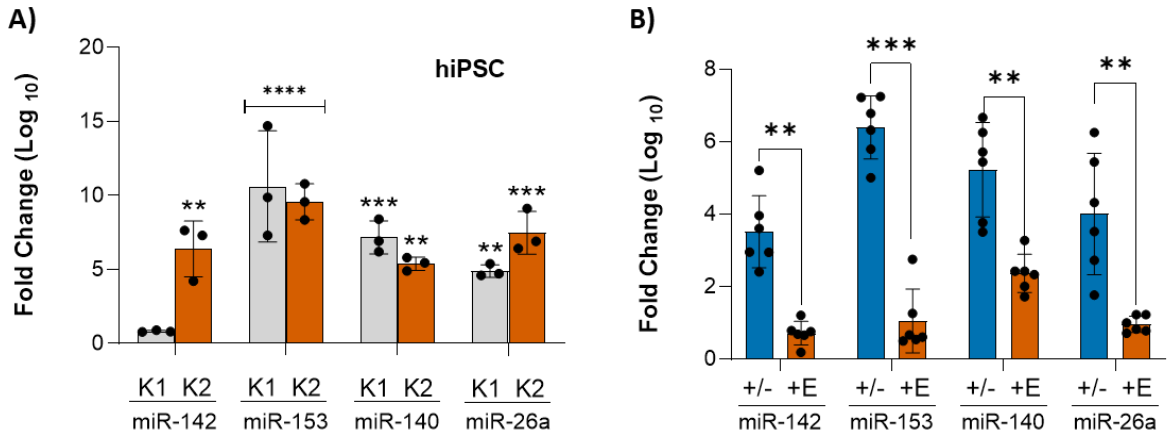

Figure 4.3 EHMT1 directly regulates miRNAs

A) *Mature miRNA expression analysis of miRs predicted to target REST by qRT-PCR in patient hiPSCs (KS1, KS2). Mean fold change over control, n = 3 independent experiments.* ***B)*** *Mature miRNA expression analysis by qRT-PCR in CRISPR edited EHMT1*$^{+/-}$ *cells only, or with exogenous EHMT1 plasmid (+E). The qRT-PCR data were shown as Mean±SEM and analysed by two-way ANOVA comparing between samples and miRNAs. *P < 0.05, **P < 0.01, ***P < 0.001, ****P < 0.0001, n ≥ 3.*

4.3.3 Development of a multimiR-sponge

It has been previously demonstrated that several miRNAs are capable of targeting the same mRNA simultaneously (Wu et al., 2010) and I hypothesised this may also be the case with my shortlisted miRNAs and REST. To test this hypothesis, I generated a novel multimiR-sponge based on previous sponge approaches (Ebert et al., 2007), capable of repressing multiple miRNAs simultaneously.

To generate the multimiR-sponges, individual sponges were first generated by ligating multiple miRNA binding sites (MBS) into the 3'UTR of one of three empty GFP vectors (Figure 4.4A). The efficacy of a miRNA sponge is determined both by the binding sequence and the number of those sequences in the sponge. The number of MBS inserts was regulated by varying the ratio of insert to vector, ranging from 1:3 up to 1:500 (Figure 4.4B). Increased ratios showed a greater number of average repeated MBS per sponge, 1:3 (4.27±0.42), 1:50 (6.07±0.56), 1:100 (7.80±0.68), 1:300 (9.33±0.80) and 1:500 (12.67±1.22).

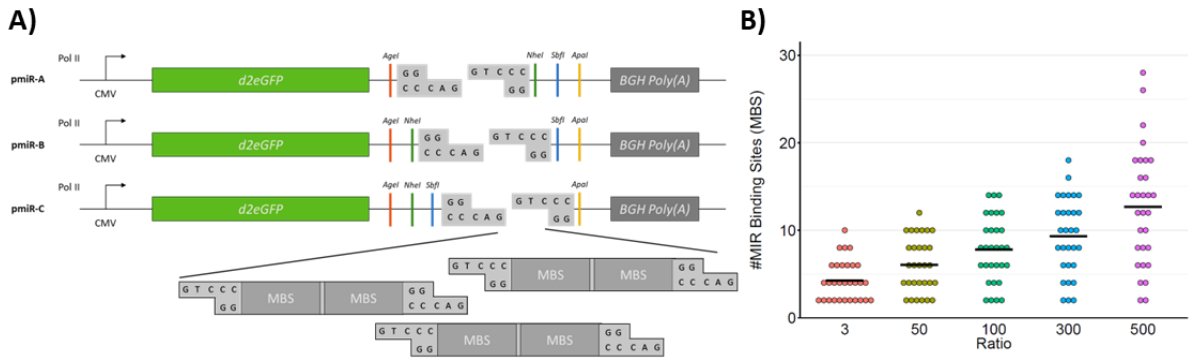

Figure 4.4 MultimiR-sponge cloning
***A**) Overview of the multimiR sponge cloning approach. Three vector libraries allow for subcloning of individual miR sponges to generate the combined multimiR-sponges. **B)** Analysis of microRNA binding site inserts proportional to insert ratio (3-500), n = 30 bacterial colonies. Black bar denotes average number of microRNA binding sites (MBS)*

Next to test the efficacy, I generated sponges specific to miR-142-3p (pmiR-142) with either a perfect binding sequence or bulged sequence with a slight 4bp mismatch (Figure 4.5A), as this has been reported to prevent cleavage of the sponge and thus increase efficacy. Sponges were generated with either 2, 6 or 12 repeated MBS inserts and co-transfected with either an empty luciferase vector or one containing the binding sequence for miR-142-3p (Figure 4.5C). Analysis by two-way ANOVA revealed bulged sponges showed significantly increased luciferase levels compared to perfect sponges (0.64±0.16 vs. 0.15±0.090, $p<0.0001$). This was

most likely due to the cleavage of perfect sponges by mRISC complexes, a hypothesis that was supported by the lack of GFP signal in cells transfected with perfect sponges (Figure 4.5B).

Furthermore, significant increases in luciferase signal were seen between x2 and x12 MBS inserts for both perfect (0.074±0.026 vs. 0.26±0.063, p=0.045) and bulged (0.45±0.086 vs. 0.76±0.047, p=0.0006) sponges. However, no significant increase was observed in bulged sponges beyond x6 MBS inserts (p=0.93), suggesting an upper level of inhibition was reached. Importantly, even the largest increase in luciferase signal seen in pmiR-142-bulged-x12 MBS was significantly lower when compared to empty vector (p=0.0064).

To determine if the miR-sponge was capable of inhibiting its target miRNA in a KS model, a sponge was designed against the most robustly elevated miRNA, miR-153. Stem cells were treated with UNC0638 for 48 hours and transfected with either an empty vector or pmiR-153(x12). Three validated targets of miR-153, *KIF20A*, *CITED2* and *UNC5C* (Rahman et al., 2023, Gao et al., 2020, Zhao et al., 2022), were selected and their expression measured using qRT-PCR. Following treatment with UNC0638 and the empty vector, significant decreases in expression were seen for both *KIF20A* (0.35±0.12, p=0.0085) and *UNC5C* (0.61±0.015, P<0.00012) (Figure 4.5D). *CITED2* also showed a decrease, however this was not significant (0.69±0.098, p=0.0576). Conversely, in samples transfected with UNC0638 and the pmiR-153 sponge, expression of *KIF20A*, *CITED2* and *UNC5C* were greater than the empty vector samples, with a 3.4-fold (1.20±0.15, p=0.0045), 1.3-fold (0.94±0.12, p=0.11) and 1.9-fold (1.15±0.028, =0.0001) increase respectively.

Next, I generated a multimiR-sponge for miR-142-3p and miR-153-3p by subcloning together individual pmiR-142 and pmiR-153 bulged sponges with x12 MBS each. To assess the efficacy of the multimiR sponge it was co-transfected into stem cells with either an empty luciferase vector or one containing the binding sequence for miR-142/153. Analysis by one-way ANOVA revealed there was no significant difference in luciferase signal between the multimiR-sponge and the individual pmiR-142 or pmiR-153 sponges (Figure 4.5E). Despite this luciferase signal in samples treated with the multimiR-sponge remained significantly lower than the empty vector (0.80±0.066 vs. 1.03±0.11, p=0.0014).

Collectively these results demonstrate that miR-sponges are capable of inhibiting the effects of miRNAs, while multimiR-sponges are equally as capable as their individual counterparts.

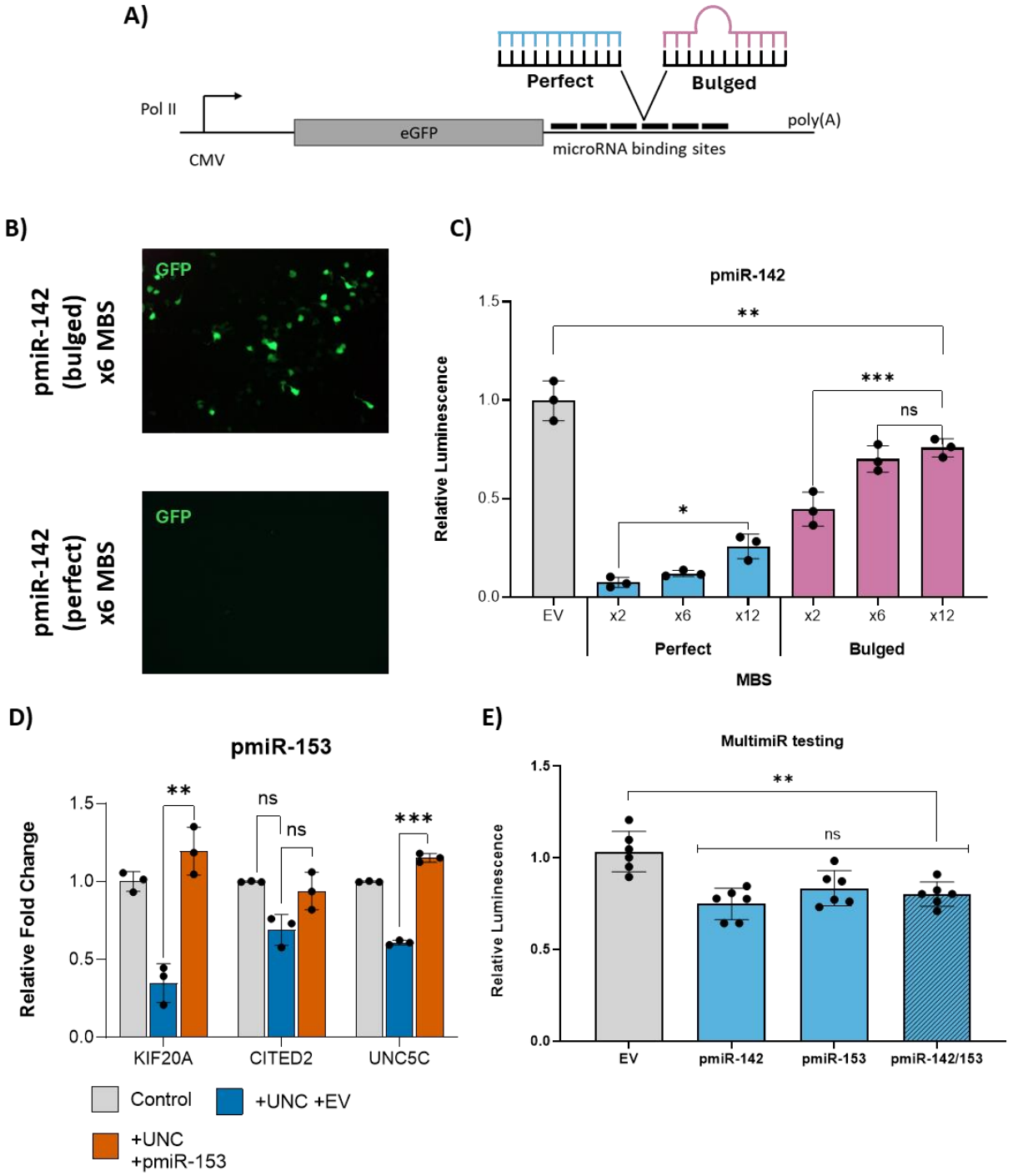

Figure 4.5 MultimiR-sponge efficacy

A) *Illustration of the perfect vs. bulged sponge designs, in which an individual sponge will contain either one or the other* ***B, C*** *Efficacy analysis of individual sponge inserts using luciferase reporters.* ***B)*** *Immunofluorescence imaging of stem cells transfected with either the bulged or perfect pmiR-142 sponges.* ***C)*** *Luciferase reporter analysis of perfect and bulged miR-142 sponges relative to empty vector (EV).* ***D)*** *Gene analysis using qRT-PCR of hiPSCs treated with 400nM UNC0638 + Empty vector (EV) miR-sponge, or pmiR-153 sponge, as compared to vehicle treated control. Mean fold change over vehicle control, n = 3 independent experiments, log10 scale axis* ***E)*** *Luciferase reporter analysis of individual and multimiR-sponges relative to empty vector (EV). Luciferase data shown as Mean±SEM and analysed by One-way ANOVA with post hoc comparisons using Tukey's multiple comparisons test comparing to control samples. *P < 0.05, **P < 0.01, **P < 0.001 n ≥ 3.*

4.3.4 MicroRNA regulation of REST

Given that miRNAs have been shown to target genes simultaneously and that a number of miRNAs upregulated in my cell model are predicted to target REST, I aimed to probe this relationship further. To achieve this, I first treated stem cells with UNC0638 (400nM) inhibitor, before transfecting these cells with either miRNA-specific sponges targeting miR-142-3p, miR-140-5p, miR-26a-5p, and miR-153-3p individually or a multimiR-sponge targeting up to three miRNAs simultaneously. To assess the impact on REST function I assessed the expression of REST targets known to be dysregulated following UNC0638 treatment, *NRXN3*, *ACTA1*, *CALB1*.

As previously demonstrated the expression of all three targets, *NRXN3*, *ACTA1* and *CALB1*, were significantly elevated following treatment with UNC0638 and scramble control, with fold changes of (4.82±1.07, 4.24±1.48, and 8.36±1.39 respectively) (Figure 4.6A-C). With the exception of pmiR-153 and *CALB1*, which showed a 1.7-fold reduction vs scramble control (FC 4.85±2.34 vs. FC 8.36±1.39, p=0.02), none of the individual sponges were capable of significantly reducing the elevated expression of REST targets following UNC0638 treatment (Figure 4.6A-C). Analysis by two-way ANOVA revealed multimiR-sponges collectively elicited a stronger effect on REST target expression, with a significant reduction compared to individual sponges for *NRXN3* (p=0.034), *ACTA1* (p=0.049) and *CALB1* (p=0.012).

Of the multimiR-sponges, the sponge lacking miR-153-3p (pmiR-142/140/26a) showed the weakest response of all the multimiR sponges, only capable of significantly reducing *CALB1* vs scramble control 1.8-fold following treatment with UNC0638 (FC 4.67±0.82 vs. 8.36±1.39, p=0.013). Conversely, pmiR-142/26a/153 and pmiR-142/140/153 both showed stronger repression for *NRXN3* (FC 2.12±0.69, p=0.0021 and 2.34±0.77, p=0.0047 respectively), *ACTA1* (FC 1.65±0.36, p=0.015 and 1.83±0.54, p=0.026 respectively) and *CALB1* (FC 3.45±0.58, p=0.0009 and 2.91±0.31, p=0.0003 respectively). In contrast the combined repression of miR-140-5p, miR-26a-5p and miR-153-3p (pmiR-140/26a/153) consistently showed the greatest reduction in REST target expression, with relative FC of (1.56±0.56, p=0.0003; 1.10±0.30, p=0.0027 and 2.37±0.42, P<0.0001) for *NRXN3*, *ACTA1* and *CALB1* respectively. These results indicate that miR-153-3p appears to be the central driver behind the REST degradation, however the combined action of multiple miRNAs, enact a more significant reduction in REST function.

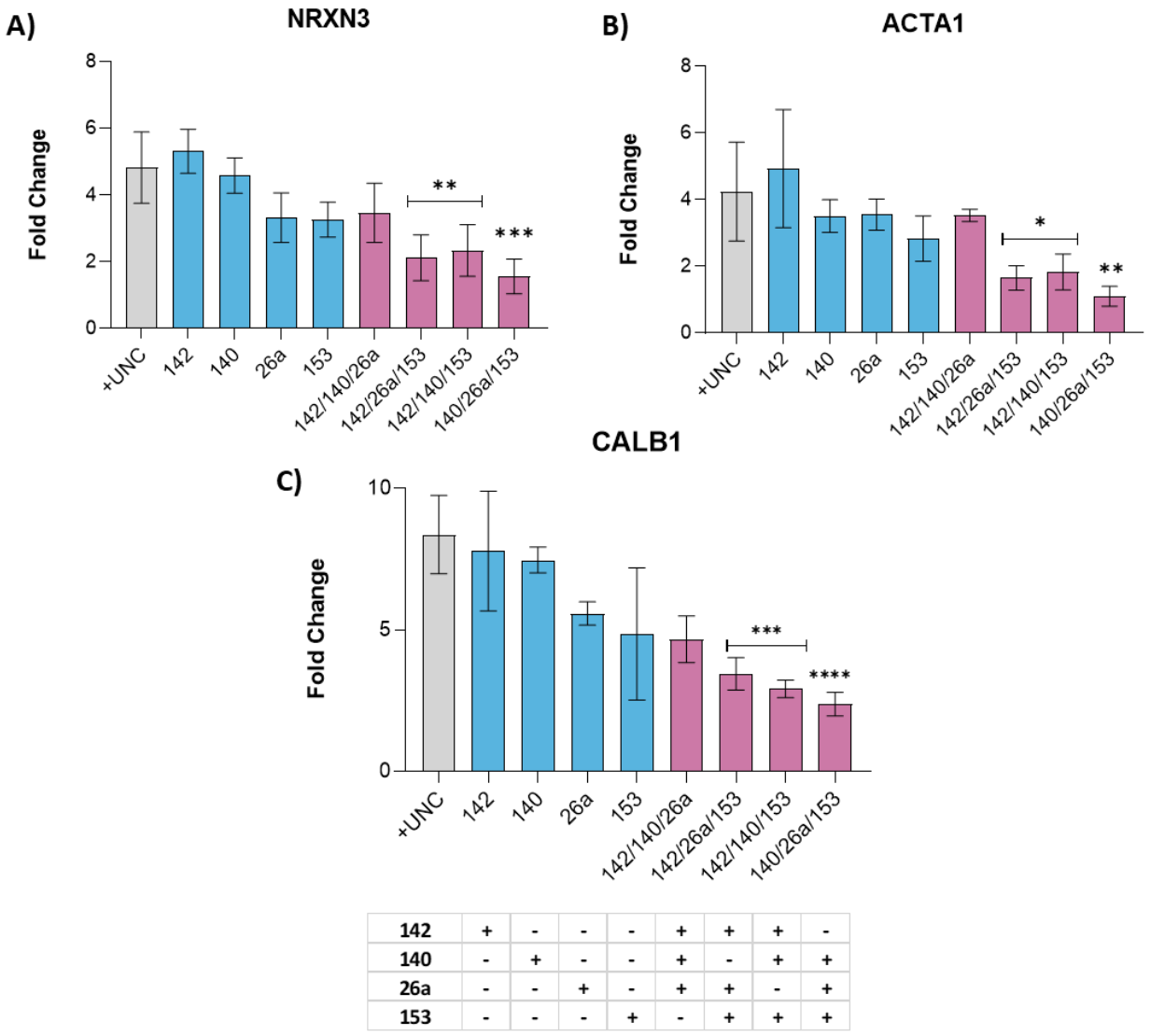

Figure 4.6 Analysis of miRNA regulation of REST using multimiR-sponges
A-C *Analysis of REST targets by qRT-PCR in hiPSCs treated with 400nM UNC0638 and varying individual (blue) or multi (pink) pmiR-sponges, as compared to EV control. Mean fold change over vehicle control±SEM and analysed by two-way ANOVA with post hoc comparisons using Tukey's multiple comparisons test. n ≥ 3 independent experiments, log10 scale axis.* ***A)*** *NRXN3 expression, only multimiR-sponges containing pmiR-153 suppressed increased expression.* ***B)*** *ACTA1 expression, only multimiR-sponges containing pmiR-153 suppressed increased expression.* ***C)*** *CALB1 expression, all multimiR-sponges were capable of reducing increased target expression, in addition to pmiR-153 alone. n ≥ 3 independent experiments, log10 scale axis*

To assess if the *EHMT1* regulated miRNAs were leading to a reduction in REST protein, western blot analysis was performed on hiPSCs treated with UNC0638 and transfected with multimiR-140/26a/153. As demonstrated previously treatment with UNC0638 and empty vector resulted in a significant reduction in REST protein levels by almost 2-fold compared to

control (1.24±0.27 vs. 0.66±0.09, p=0.0003) (Figure 4.7A). In contrast simultaneous treatment with the multimiR sponge led to no significant change in REST protein levels.

To ensure this de-repression of REST was specifically linked to the loss of *EHMT1*, *EHMT1*$^{+/-}$ cells were transfected with the multimiR-140/26a/153 sponge. Again, REST protein levels were significantly decreased in empty vector samples (p<0.0001), whilst those treated with the multimiR sponge showed a modest but non-significant change in expression (Figure 4.7B). Collectively, this data demonstrates that a defined group of *EHMT1* regulated miRNAs act simultaneously to repress REST levels at the pluripotent stage. Moreover, this repression can be effectively reversed using novel multimiR-sponge technology, allowing for tuneable repression of each target miRNA simultaneously.

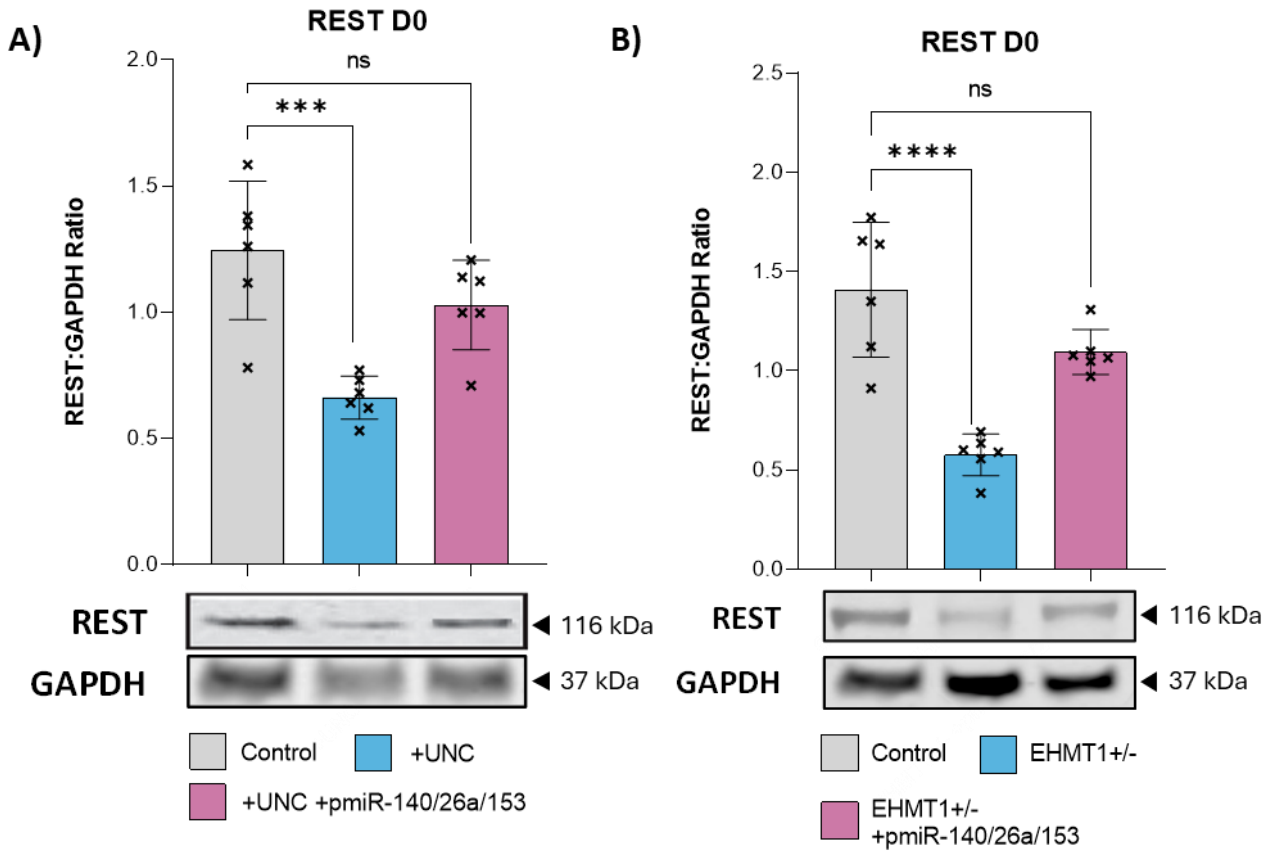

Figure 4.7 Analysis of REST protein levels following multimiR sponge treatment
Western blot analysis of REST protein expression following treatment with Empty vector (EV) miR-sponge, or multimiR-140/26a/153 sponge, as compared to control samples. Plotted as Western band intensity normalized to GAPDH, n = 6. ***A)*** *Control hiPSCs treated with UNC0638 for 4 days.* ***B)*** *EHMT1+/– hiPSCs compared to isogenic control hiPSCs. Data were presented as Mean±SEM and analysed by One-way ANOVA with post hoc comparisons using Tukey's multiple comparisons test comparing to control samples. ***P < 0.001, ****P<0.0001.*

4.4 Discussion

The work in this chapter demonstrates that *EHMT1* deficiency induces substantial miRNA dysregulation throughout the differentiation process, from pluripotency to early neuronal stages. The relationship between epigenetic modifiers and miRNAs is highly complex, as each are known to regulate both genetic targets and one-another in a temporal fashion. Existing miRNA prediction algorithms relying solely on seed sequence pairing have exhibited limited success in translating simple miRNA-gene interactions into the complex human transcriptome environment, with peak accuracy results of up to approximately 66% (Maragkakis et al., 2009). Consequently, to address these limitations studies have demonstrated that by using a systems biology approach and deriving prediction models from known validated omics data, the efficacy of these predictions is significantly improved (Zhang et al., 2014b).

I therefore developed a novel predictive model informed by prior transcriptomic data obtained from *EHMT1*-haplodeficient NPCs. This model identified a number of upregulated miRNAs and confirmation by qRT-PCR revealed successfully predicted with an efficacy rate of 78%. A recent study compared 5 of the most common miRNA prediction tools, miRanda, PicTar, PITA, RNA22 and TargetScan, with positive rates ranging from 3.6-6% (Plotnikova and Skoblov, 2018). One suggested approach has been to combine multiple prediction tools, however as the previous study demonstrated this only increases efficiency rates to 14%. Conversely, significant progress has been achieved with machine learning models that capitalize on curated databases of miRNA-mRNA interactions with confirmed biological relevance. This approach offers an alternative to solely relying on novel predictions and Predication rates have been reported from 54-88% (Grigaitis et al., 2020). Despite this, machine learning models are often prone to overfitting and training datasets are often representative of heterogenous disorders (Kuang et al., 2023).

Considering that fluctuations in miRNAs are reflected in the expression of their target genes, paring miRNA regulatory data with experimental specific transcriptomic data gives a systematic approach to miRNA prediction. Results of similar approaches in Autism spectrum disorder show highly similar data, with positive identification rates of 72.7% (Shen et al., 2016). This model has been shown to be particularly for identifying dysregulated miRNAs regulating genes with known roles in biological processes. My data shows comparative results, with a high accuracy in identifying miRNAs functionally relevant to the disorder.

Positive targets included a number of brain-related miRNAs including miR-9-5p, miR-124-3p, miR-135b-5p, miR-153-3p and miR-26-5p, shown to be upregulated in healthy mouse and human brains (Sempere et al., 2004). MiR-153-3p has been shown to promote neuronal differentiation, whilst reducing self-proliferation and the self-renewal capacity of NPCs (Mandemakers et al., 2013, Liang et al., 2012, Stappert et al., 2013). Similarly, miR-135b-5p is upregulated during brain development, inducing neuronal differentiation through inhibition of the BMP/TGFβ pathway (Bhinge et al., 2014). Additionally, the miR-26 family has also been found to be required for neuronal differentiation, inhibiting neuronal repressors including its own host gene CTDSP (Sauer et al., 2021, Dill et al., 2012). Two of the most powerful miRNAs are the brain specific miR-124-3p and miR-9-5p, which have been shown to be key drivers of neuronal maturation (Suzuki et al., 2020). MiR-124-3p targets a number of non-neuronal genes, ensuring there repression during differentiation (Lim et al., 2005). Likewise, miR-9-5p promotes neural differentiation and reduces proliferation, whilst it's inhibition significantly impairs neuronal differentiation capacity (Nowak et al., 2014, Yuan et al., 2021b). Upregulation of these miRNAs coincides with previous findings in this work that a loss of *EHMT1* leads to accelerated maturation of neurons. These results suggest, the loss of *EHMT1* and subsequent increased expression of brain related miRNAs contributes to the accelerated differentiation and maturation of neuronal cells.

Perhaps unsurprisingly considering the previous results identifying a loss of REST protein, a number of these dysregulated miRNAs contain RE1 sites and are known to be regulated by the REST complex (Wu and Xie, 2006). This finding aligns with the loss of REST protein observed in Chapter 3, further suggesting it promotes the significant upregulation of a specific subset of miRNAs. Furthermore, studies have shown a number of these miRNAs, miR-9-5p, miR-124-3p, miR-135b-5p, act to repress REST, establishing a negative feedback loop (Lee et al., 2017, Giusti et al., 2014, Reed et al., 2018). The control of this feedback loop during neurogenesis is complex; however, it has been demonstrated that the miR-26 family act as one potential upstream regulator, working to repress the REST complex (Sauer et al., 2021).

Hypothesising that one or more of the REST independent miRNAs identified may be acting upstream of REST I assessed the expression of all predicted miRNAs at the pluripotent stage. The observation that numerous miRNAs were upregulated at this early developmental stage strongly suggests that *EHMT1* plays a crucial role in regulating miRNA expression from the

earliest stages onwards. Despite having previously observed a loss of REST protein at the pluripotent stage, analysis revealed REST regulated miRNAs were not upregulated. Repression by REST/NRSF is dynamic and there may be several reasons for this lack of expression. Previous work analysing targets of the REST complex, have identified two gene classes. The first class exhibits automatic increases in expression upon REST loss, while the second class retains associated co-repressors even in the absence of REST (Ballas et al., 2005). Despite a potential loss of REST protein binding to the miRNA targets identified in this study, these targets may still be repressed during the pluripotent stage due to the action of other co-repressors, such as co-REST and MECP2. Further work investigating the repressive elements bound to these miRNAs at the embryonic stage may further elucidate their regulation by epigenetic factors.

In contrast, several REST-independent miRNAs, including miR-142-3p, miR-153-3p, miR-140-5p, and miR-26a-5p, were upregulated at the pluripotent stage. Computational analysis indicated these miRNAs targeted REST, suggesting a potential link between *EHMT1* and REST regulation. To validate this hypothesis, chromatin immunoprecipitation (ChIP) assays were performed to assess the enrichment of the *EHMT1*-mediated methylation mark H3K9me2 at the promoter regions of all four miRNA genes. Notably, these regions showed significant enrichment of H3K9me2, which was ablated upon treatment with the EHMT1 inhibitor, UNC0638. However, a limitation of UNC0638 is its potential to inhibit both EHMT1 and its paralog, EHMT2. Therefore, to achieve greater target specificity, miRNA expression was evaluated in induced pluripotent stem cells (iPSCs) derived from Kleefstra Syndrome (KS) patients, a condition associated with *EHMT1* deficiency, as well as EHMT1-haplodeficient cell lines (*EHMT1*$^{+/-}$). In both models, all four miRNAs exhibited elevated expression, strongly suggesting their primary regulation by EHMT1-deposited H3K9me2 marks. Further supporting this conclusion, ectopic overexpression of *EHMT1* in *EHMT1*$^{+/-}$ iPSCs effectively repressed the expression of all four target miRNAs. This also demonstrates the repression of these miRNAs by *EHMT1* is dynamic and reversible.

EHMT1/2 has previously been shown to regulate miRNAs in various contexts. Studies have demonstrated that EHMT2 alongside EZH2 and CDYL2 acts to repress miR-124-3p/5p in cancer cells (Siouda et al., 2020). Likewise, EHMT2 directly represses miR-200c-3p/5p in response to leptin signalling (Chang et al., 2015). STAT3 upregulation of *EHMT2* has also been shown to

repress miR-145-3p/5p in lung cancer lines (Chang et al., 2019). Beyond cancers, EHMT2 is required for the suppression of maternal specific miRNA clusters (Zeng et al., 2021). Furthermore, miRNAs have shown to regulate EHMT2 expression, with both miR-122-5p and miR-217 targeting the epigene (Yuan et al., 2021a, Thienpont et al., 2017). Despite significant evidence of miRNA regulation by EHMT2, there is comparatively significantly less evidence of regulation by EHMT1. Given the homology between the two methyltransferases it is reasonable to expect EHMT1 is also capable of miRNA regulation. This has been shown to be true for other histone methyltransferases such as SETD1A, which modulate cell cycle progression through the repression of various miRNAs (Tajima et al., 2015). My work demonstrates that alongside EHMT2, EHMT1 acts as a powerful regulator of various miRNAs and is capable of independently repressing key miRNAs in pluripotent cells.

Based on these previous experiments it appeared the repression of REST by one or more of these EHMT1 regulated miRNAs was the most plausible explanation. Although miRNAs are typically thought to act on a single mRNA target in a one-to-one fashion, they have also been shown to act simultaneously on a single target (Wu et al., 2010, Hashimoto et al., 2013). Working in a collaborative fashion, individual miRNAs often act at the centre of a hub with other miRNAs to synergistically fine-tune protein levels (Chen et al., 2017). To this end I wanted to answer the question of whether these miRNAs were targeting REST independently or in a cooperative fashion.

While various approaches exist for miRNA inhibition, achieving multiplexed repression necessitates the delivery of equal inhibitor concentrations to individual cells. To address this challenge, I developed a novel multiplexed miRNA inhibition system that facilitates the simultaneous repression of multiple miRNAs. Initially developed individual sponges revealed that those with perfect binding miRNA sequences were significantly less effective at repressing target miRNAs than sponges with a 4bp mismatched bulge. Perfect binding between miRNA and mRNA is rare in mammals, however such binding leads to cleavage of the target (Yekta et al., 2004). This increased efficacy of bulged miRNA sponges has been previously noted (Jung et al., 2015). Therefore, the reduced efficacy of perfect sponges is most likely explained by a premature degradation of the miRNA sponge. Within bulged sponges an increased number of miRNA binding sites showed an increase in miRNA repression but plateaued beyond 6 repeated binding sites. This is most likely representative of an upper limit

of miR-sponge repression and maximal efficacy. A similar effect was not seen in the perfect sponges, as supported by the absence of visible GFP in transfected cells. This sub saturation presence of GFP is replicated in similar GFP sponge approaches (Malmevik et al., 2015). Such thresholds have been demonstrated previously with miR-sponges, but maximal inhibition numbers likely vary depending on the abundance of target miRNA present (Ebert et al., 2007).

Results of gene expression analysis indicated individual miR-sponges were capable of rescuing target genes inhibited by elevated levels of miR-153-3p in response to UNC0638 treatment. Although two targets showed significant reduction, *CITED2* a validated target of miR-153-3p was not significantly reduced following UNC0638 treatment. One explanation for this result may be the competitive binding action of the remaining two targets, *KIF20A* and *UNC5C*. RNAs themselves have been shown to act as miR-sponges, influencing each-others expression levels by sequestering away miRNAs (Bosia et al., 2017). Alternatively, the modest decrease seen at the transcript level may be representative of a more significant reduction in translation levels, however analysis by western blot would be required to confirm this. These results indicate the constructed sponges were effective at repressing the target miRNA, as has been shown previously with sponges targeting miR-124-3p and the miR-132/212 family (Malmevik et al., 2015, Lavenniah et al., 2020).

To evaluate the efficacy of a multimiR-sponge compared to individual counterparts, luciferase assays were performed. These assays utilized individual sponges targeting either miR-142-3p or miR-153-3p, alongside a multimiR-sponge targeting both miRNAs. The results demonstrated that the multimiR-sponge effectively inhibited both miRNAs, achieving comparable efficacy to the individual sponges. However, none of the sponges fully restored luciferase activity to control levels observed with the empty reporter vector. As mentioned previously, this is likely due to a ceiling effect in miRNA inhibition.

The multimiR-sponge platform emerges as a powerful tool for comprehensively investigating the influence of multiple miRNAs simultaneously. This approach offers several key advantages. Firstly, the presence of antibiotic resistance and fluorescent markers enables positive selection of transfected cells, minimizing signal contamination from non-transfected cells. Secondly, the single-cassette design incorporating multiple miRNA inhibitors ensures consistent delivery ratios within individual cells. This eliminates potential variability associated with separate transfection events or between individual cells. Lastly, the flexibility

to tailor the number of miRNA binding sites per target allows for adaptable inhibition levels, enabling fine-tuning of the degree of miRNA suppression for each target.

Encouraged by the effectiveness of the multimiR-sponges, I sought to investigate the connection between the miRNAs regulated by *EHMT1* and the observed dysfunction of the REST complex. To achieve this, I generated both individual miRNA sponges targeting specific miRNAs and multimiR-sponges targeting combinations of three miRNAs. The efficacy of these sponges on REST was measured in UNC0638 treated cells by measuring the expression of REST targets. As anticipated, UNC0638 treatment resulted in a notable increase in REST target gene expression. While individual miRNA sponges partially counteracted this rise, the reductions observed were statistically insignificant. In contrast the combined effect of multiple miRNA inhibitions was much stronger, significantly reducing all three REST target genes compared to individual sponges. The results strongly indicate that the loss of REST is caused by the collective repression of multiple miRNAs, simultaneously, rather than the action of a single miRNA.

Further analysis revealed that a multi-sponge lacking miR-153-3p had the weakest effect, while sponges containing miR-153-3p alongside miR-140-5p and/or miR-26a-5p showed the strongest reduction in REST target levels. These findings suggest that miR-153-3p may be a key node in reducing REST function. This finding is supported by data that has shown similar miRNA hubs centred around a primary miRNA (Chen et al., 2017). However, the combined action of multiple miRNAs appears to be even more effective. This directly contradicts previous work that suggests separate miRNA binding sites within the same target UTR act antagonistically (Gam et al., 2018). Importantly this study had a number of limitations, the principle of which was utilising exogenous plasmids with perfect miRNA binding sites to measure the binding kinetics of several miRNAs. Both results from my work, along with that of others have demonstrated perfect binding sequences lead to poor binding of miRNAs and are not representative of the typical miRNA-mRNA interactions seen within animals (Jung et al., 2015). In contrast, others have cloned the binding sites of validated miRNA targets into exogenous plasmids, with imperfect binding and have demonstrated a clear additive and collaborative effect of multiple miRNAs on a single transcript (Diener et al., 2023). One key finding of this study was that miRNA binding sites within 40 base pairs of one another lead to significantly increases in repression comparted to further distances. Given that none of the

binding sites I studied in *REST* fell within a 40bp window, it is unlikely the repressive action can be attributed to a combinatorial effect. However future studies may consider cloning of the binding sites in an exogenous plasmid at varying distances to assess this possibility.

Since the most significant changes in REST activity were observed at the protein level, I investigated the multimiR-sponges' effect on REST protein itself. Notably, the multimiR-sponges effectively restored REST protein levels close to normal in both UNC0638-treated and *EHMT1*-haplodeficient cells. This finding suggests that *EHMT1*-regulated miRNAs, miR-140-5p, miR-26a-5p and miR-153-3p, function upstream of REST, directly and collectively reducing protein levels. My observations are consistent with previous studies, where miR-26-5p was shown to function independently of the REST complex to suppress REST expression during neurogenesis (Sauer et al., 2021). Interestingly, the miR-26 family also target their host genes, CTDSP, a central element of the REST complex (Han et al., 2012).

Neuronal development is characterized by a gradual decline in REST protein levels, even though it remains bound to target genes in neural stem cells (Sun et al., 2005). My findings suggest that a specific subset of miRNAs regulated by *EHMT1* contributes to this initial reduction. However, when *EHMT1* is absent, REST loss accelerates dramatically, starting as early as the embryonic stage. Since REST plays a crucial role in fine-tuning neuronal and synaptic genes (Rodenas-Ruano et al., 2012), it's likely that these *EHMT1*-regulated miRNAs help to precisely regulate REST expression and function throughout development. Further research is needed to confirm this hypothesis.

Interestingly, my work also revealed a reciprocal regulatory role for REST. It appears to inhibit a set of brain-specific miRNAs that target a wide range of non-neuronal genes. By repressing these miRNAs, REST effectively prevents a large-scale genetic shift towards a neuronal phenotype, further amplifying the regulatory reach of the REST complex. The upregulation of these miRNAs upon *EHMT1* loss suggests a second phase of neurodevelopment, where several of these miRNAs actively suppress REST, creating a feedback loop that reinforces neuronal differentiation. MicroRNAs within this feedback loop such as miR-9-5p and miR-124-3p, are crucial for the balance of neural stem cell proliferation and differentiation (Qu et al., 2010).

4.5 Conclusion

This chapter describes the role of *EHMT1*, an epigenetic regulator, in microRNA (miRNA) dysregulation during neuronal differentiation. The findings reveal a complex interplay between *EHMT1*, miRNAs, and the REST complex, a key player in neuronal development. Novel transcriptomic guided prediction pipelines accurately predicted a number of dysregulated miRNAs in a response to a lack of EHTM1. In neurons a significant number of these miRNAs were known to be targeted by the REST complex and key to neuronal development and maturation. Likewise, miRNAs were upregulated that are known to directly target the REST complex. At early pluripotent stages, miRNAs upstream of REST were significantly elevated. Novel multimiR sponges revealed these miRNAs targeted REST in synergistically, with miR-153-3p a key regulator of this process. Importantly, the inhibitory influence of these miRNAs on REST could be both prevented and reversed.

Collectively these findings have elucidated the complex regulatory network between epigenetic modifiers and miRNAs, and the implications on neuronal development and maturation. The novel predictive models and multimiR sponges represent significant advancements in the study of the interactive role of miRNAs in a systems approach.

5 The effect of *EHMT1* loss on neuronal development and maturation

5.1 Introduction

Neurodevelopment is a meticulously timed process, and research has revealed that microRNAs (miRNAs) play a key role in this orchestration. This was first demonstrated during loss-of-function studies, probing key components of the miRNA biogenesis pathways such as Dicer and DGCR8 (Davis et al., 2008, Stark et al., 2008). In these studies, the subsequent global loss of miRNAs resulted in microcephaly, reduced synaptic connectivity, and reduced neuronal branching, incidentally all phenotypes of *EHMT1* deficient Kleefstra Syndrome cells. Interestingly, stage specific ablation of Dicer in neural stem cells indicates miRNAs are required for the generation of novel neurons, but dispensable for astrocytes (Pons-Espinal et al., 2017). This work highlights the importance of miRNAs throughout the various stages of neurogenesis. The advent of human stem cell derived models over the last two decades has enabled researchers to reveal the specific roles of various miRNAs. Analysis of miRNAs expression as cells transitioned from pluripotent stem cells to mature neurons identified over 100 miRNAs that differed in expression (Giorgi Silveira et al., 2020).

As our understanding of neural development has advanced, miRNAs have been found to impact on almost biological processes during brain development, with varying effects. Quite often the impacts of an individual miRNA are dependent on the developmental timing and transcriptomic environment. Mammalian neurogenesis has been shown to be strongly regulated by the highly conserved miR-153-3p, through its direct repression of the Notch signalling pathway (Qiao et al., 2020, Xu et al., 2019). Likewise, the miR-128 also acts to positively affect neurogenesis through the inhibition of *UPF1*, ensuring nonsense mediated decay does not impinge on differentiation (Bruno et al., 2011). Conversely, as neuronal differentiation progresses miR-128 also plays a negative role, preventing migration through the inhibition of the zinc finger PHF6 (Franzoni et al., 2015). This dual role is also demonstrated in other miRNAs such as miR-137. Early in neural development the miRNA acts to induce differentiation of NSCs by repressing the nuclear receptors *TLX1* and *LSD1*, the latter of which is found in the REST complex (Sun et al., 2011). At later stages, miR-137 has a negative effect on neurogenesis, targeting the epigenetic regulator, *EZH2* (Szulwach et al.,

2010). These studies demonstrate that the roles of miRNAs in neurodevelopment are dynamic and often dependent on the developmental stage.

Profiling of miRNAs across all cell types in the human brain has shown enrichment in at least one cell type, including intermediate progenitors, radial glial cells and interneurons (Nowakowski et al., 2018). During differentiation, distinct sequential transcriptional waves are required guiding development through cell phases, something mirrored with miRNAs (Telley et al., 2016, Kumar et al., 2020). As such a number of these miRNAs are vital for the correct regulation of timing for both neuronal differentiation and development. This is exemplified by Dicer knockout cells which remain arrested at progenitor stages until transient reintroduction of Dicer leads to irreversible terminal differentiation (Andersson et al., 2010). This control is seen also in individual miRNAs such as the miR-200 family which establishes a feedback loop with both *SOX2* and *KLF4*. Inhibition of miR-200 miRs leads to reduced neuronal differentiation and significantly increased proliferation, whilst overexpression leads to premature exit from the cell cycle (Peng et al., 2012, Pandey et al., 2015).

In the case of mature post-mitotic neurons, miR-124-3p shows the most consistent enrichment (Nowakowski et al., 2018), whilst from differentiation of stem cell to mature neuron both miR-124-3p and miR-9-5p are the most markedly altered (Liu et al., 2012). Collectively miR-124-3p and miR-9-5p are typically regarded as master regulators of neuronal differentiation and are only significantly upregulated in terminally differentiating neural stem cells (Fedorova et al., 2023). Both miR-124-3p and miR-9-5p are downstream targets of the REST complex and simultaneously both target the complex in a feedback loop (Visvanathan et al., 2007, Packer et al., 2008). Simultaneous overexpression of the two miRNAs is sufficient to reprogram fibroblasts to a neuronal state, in part through the downregulation of REST protein levels (Lee et al., 2018). Temporal single cell sequencing of this process reveal this is a sequential stepwise process, with an initial erasure of the fibroblast genetic network, before activation of the neuronal program (Cates et al., 2021). Analysis has revealed synergism with *ELAVL3* is required for a significant portion of the neuronal activation profile (Lu et al., 2021). However, inhibition of *ELAVL3* and the miRNAs in adult neurons is not sufficient to de-differentiate the cells, indicating the pathway is irreversible. The synergistic effects of the two miRNAs are also important for neuronal differentiation, with studies demonstrating that

expression of both miRNAs is required for the suppression of common targets such as *RAP2A*, to support dendritic branching (Xue et al., 2016).

5.2 Chapter Aims

This chapter aims to assess the dysregulation of epigenetically regulated miRNAs throughout neuronal development and assess the impact on timing and maturation. Stem cell models will be utilised to determine changes in miRNA targets, whilst miRNA mimics and sponges will be used to aid in implicating the role of individual miRNAs. Markers of neuronal development will be analysed to assess changes on cell maturation with regards to developmental timing.

5.3 Results

5.3.1 Analysis of miR-124 and miR-9 in EHMT1 depleted cells

Having already demonstrated that a lack of REST leads to increased levels of brain specific miRNAs, miR-124-3p and miR-9-5p by day 30 but not at day 0, I sought to better understand the timeframe of this dysregulation. To do this two of the most important miRNAs in neuron differentiation, miR-9-5p and miR-124-3p were selected and their expression tracked over 70 days of neuronal differentiation in *EHMT1*$^{+/-}$ cells. These miRNAs are known to be repressed directly by REST and their overexpression is sufficient to induce a fate change of fibroblasts to late-stage neurons (Wu and Xie, 2006, Lee et al., 2018).

Despite a rise, neither miR-124-3p or miR-9 showed a significant increase in *EHMT1* depleted cells in the first 20 days. However, from day 30 onwards significant increases were seen in the expression of both miRNAs in *EHMT1*$^{+/-}$ cells as compared to control (Figure 5.1A-B). At day 30 average abundance levels of miR-124-3p were 3.76-fold higher compared to control ($p<0.0001$), and miR-9-5p levels were 2.88-fold higher ($p<0.0001$). At day 40, average levels of miR-124-3p in control rose but remained 1.92-fold higher in *EHMT1*$^{+/-}$ cells ($p<0.0001$), whilst miR-9-5p was 2.35-fold higher than control ($p<0.0001$). By day 50 both miRNAs remained elevated, with miR-124 an average of 1.76-fold higher than control ($p<0.0001$) and miR-9-5p slightly lower at 1.36-fold ($p=0.002$). Average abundance was more comparable by day 60, with no significant difference in miR-9-5p levels and miR-124-3p levels 1.23-fold higher than control ($p=0.029$). Finally at day 70, neither miR-124-3p or miR-9-5p showed any significant change, with levels of miR-9-5p slightly lower than control. These results demonstrate both miRNAs displayed a significant and premature upregulation in *EHMT1*-deficient cells, with control levels gradually approaching those of the *EHMT1*-deficient group by day 60. Taken together, these results indicate a shift in the normal expression of these proneural, REST regulated miRNAs.

To better understand the effect of this dysregulation on transcription, expression of validated miR-124-5p and miR-9-3p targets were assessed at peak differential expression, day 30. Across 14 targets analysed, all showed a significant reduction in expression (Figure 5.1C). For miR-124-3p, 7 targets showed an average fold change of 0.48±0.18 and for miR-9-5p, four targets showed an average fold change of 0.50±0.20. Targets common to both miRNAs were

also assessed and showed an average fold change of 0.24±0.10, significantly lower than the individual targets (p=0.024). Two of these targets, *REST* and *CTDSPL*, are components of the REST complex and know to negatively regulate miR-9-5p and miR-124-3p, hence their depletion further increases miRNA expression. The remaining targets are typically downregulated in mature neurons, including developmental markers such as *ONECUT2* and *SIX4* that prevent premature differentiation (Chen et al., 2021b) and genes such as *JAG1* required for the balance between NSCs and mature neurons (Blackwood, 2019). These results further suggest that a lack of REST is leading to accelerated neuronal differentiation as a result of increased miR-9-5p and miR-124-3p.

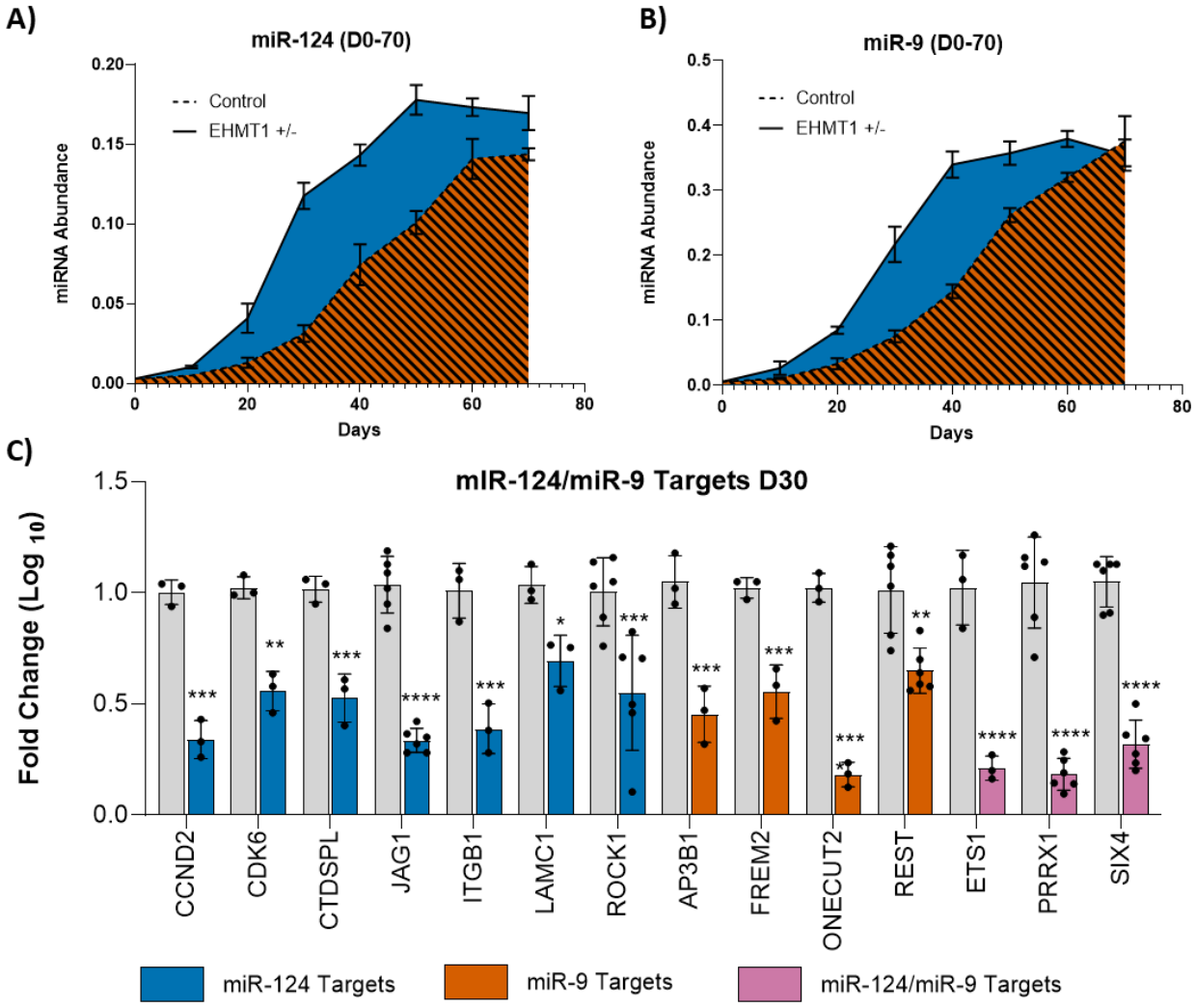

Figure 5.1 REST dysregulation of brain specific miRNAs
A,B *Relative miRNA abundance measured by qRT-PCR in EHMT1$^{+/-}$ hiPSC derived neurons, from day 0-70, as compared to wild type control.* ***A)*** *Expression of miR-124, EHMT1$^{+/-}$ cells show a premature increase in expression that remains elevated.* ***B)*** *Expression of miR-9, EHMT1$^{+/-}$ cells show a premature increase that is elevated until day 70. n ≥ 3 independent experiments* ***C*** *Analysis of miR-124 and miR-9 validated targets by qRT-PCR in EHMT1$^{+/-}$ hiPSC derived neurons at day 30 Targets were all decreased in EHMT1$^{+/-}$ cells. n ≥ 3 independent experiments*

5.3.2 Alternative neuronal splicing

One of the accompanying changes in miR-124-3p positive neuronal cells is the induction of alternative brain specific pre-mRNA splicing. It has been shown the increased expression of miR-124-3p represses *PTBP1*, resulting in an isoform switch to *PTBP2* (Makeyev et al., 2007).

The culmination of this isoform switch is a change in the splicing patterns of a number of genes. To determine if brain specific splicing is altered in *EHMT1* depleted cells, three genes, *CDC42, RUFY3 and MAP4*, known to be alternatively spliced in response to increased levels of *PTBP2* were selected. Primers were then designed, specific to either the neuronal isoform or the universally spliced isoform. Expression was then analysed in UNC0638 (400nM) treated progenitor cells transfected with either a scramble sponge or miR-124-3p specific sponge.

For all three genes, analysis by two-way ANOVA revealed a significant increase in the expression of the neuronally spliced isoform. *CDC42n* showed a 7.43-fold increase relative to control (7.43±1.75, $p<0.0001$), *RUFY3n* a 5.02-fold increase (5.02±1.56, $p=0.0004$), and *MAP4n* a 7.19-fold increase (7.19±2.25, $p=0.0003$) (Figure 5.2A-C). In contrast no significant change was observed in the expression levels of the universally spliced isoform for any of the three genes.

Importantly, samples treated with sponges targeting miR-124-3p showed drastic reductions in the expression of neuronally spliced variants. *CDC42n* showed only a 2.71-fold increase relative to control (2.71±0.85, $p<0.014$), *RUFY3n* displayed a 2.03-fold increase (2.03±1.03, ns), and *MAP4n* a 2.86-fold increase (2.86±0.94, $p=0.032$) (Figure 5.2A-C). Once more as with scramble sponge samples, no change was observed in the universally spliced isoforms.

Together these results suggest increased expression of miR-124-3p in *EHMT1* depleted cells causes a significant shift toward a brain specific pattern of alternative splicing. Importantly miR-sponges are capable of ablating these affects by repressing the action of miR-124-3p, most likely restoring expression levels of the PTBP1 protein.

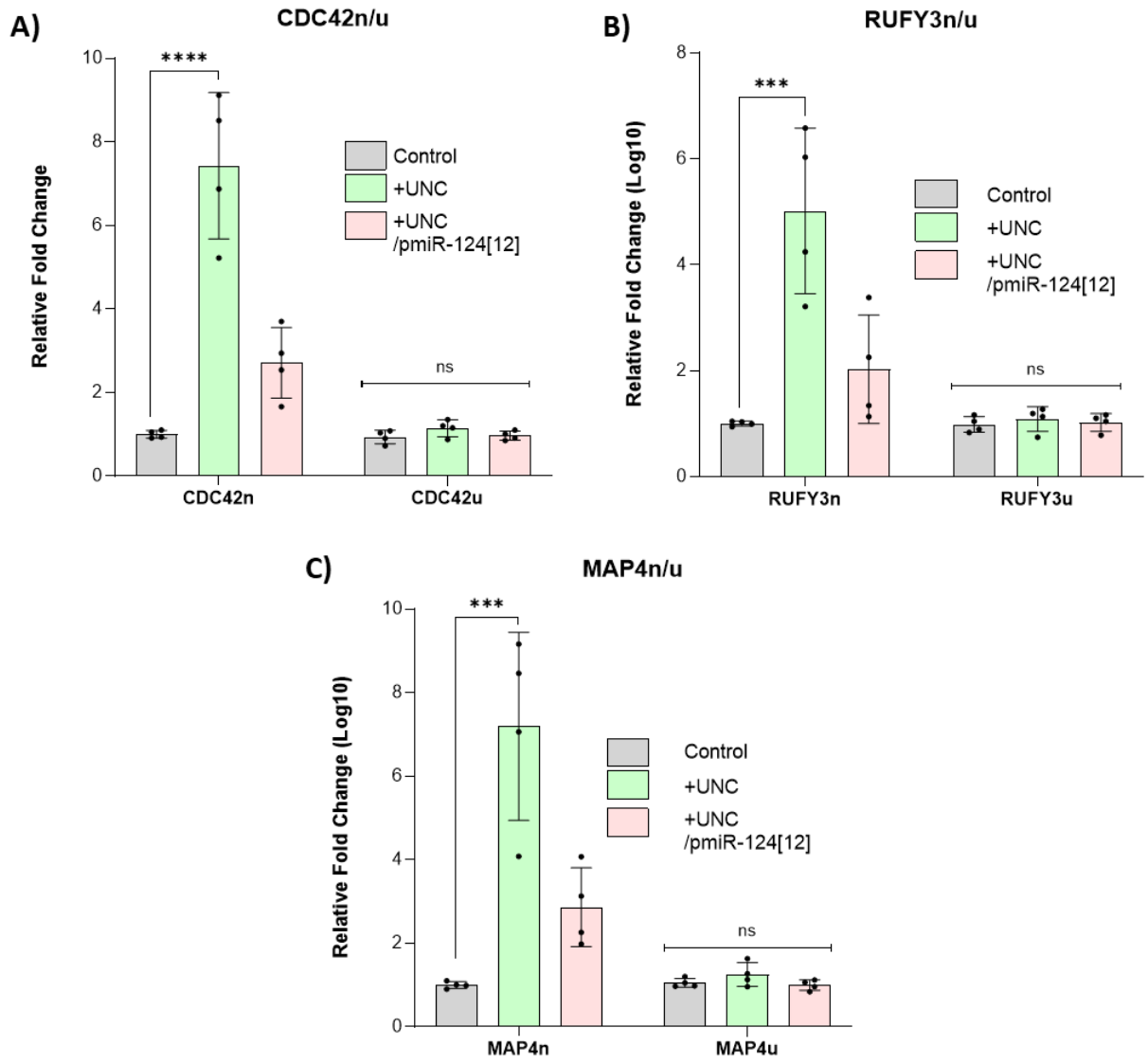

Figure 5.2 miRNA induced alternatively spliced isoforms

A-C *Analysis of neuronally spliced (n) or ubiquitously spliced (u) isoforms in cells treated with UNC and wither a scramble sponge or a miR-sponge against mIR-124, with x12 binding repeats. The qRT-PCR analysis for* ***A)*** *CDC42,* ***B)*** *RUFY3 and* ***C)*** *MAP4. Data were presented as Mean±SEM and analysed by Two-way ANOVA with post hoc comparisons using Dunnett's multiple comparisons test comparing to control samples. *P < 0.05, **P < 0.01, ***P < 0.001, ****P < 0.0001.*

5.3.3 miRNA – REST neuronal network

Unlike miR-124-3p and miR-9-5p, previous work suggested miR-26a-5p and miR-140-5p do not contain RE1 sites and are not regulated by the REST complex, hence they are most likely upstream of brain specific miRNAs in neurogenesis. To determine if this was the case, I transfected WT cells with miRNA-mimics of miR-26a-5p, miR-26b-5p and miR-140-5p into NPC cultures at day 10 and measured the expression of REST regulated miR-9-3p and miR-124-3p 3 days later. Following transfection of the mimics, increases were seen in the expression of both miR-9-5p (2.79±0.19, p=0.003) and miR-124-3p (1.89±0.18, p=0.015) (Figure 5.3A). These results are consistent with previous findings that miR-26a-5p and miR-140-5p act independently and upstream of the REST controlled miRNAs.

Based on previous studies which demonstrated that inhibition of miR-124-3p in adult neurons was not sufficient to induce dedifferentiation (Lu et al., 2021), I wanted to assess if the precocious elevation of miR-124-3p and miR-9-5p was reversible. To this end cells were either treated with UNC0638 (400nM) continually or transiently treated from d0 to d20, before withdrawing the inhibitor until d30. Cells treated with UNC0638 continually, showed increased expression of both miR-124-3p (8.17±1.14) and miR-9-5p (9.42±2.74) as expected (Figure 5.3B). However, despite withdrawal of the inhibitor, levels of both miR-124-3p (7.16±1.36) and miR-9-5p (8.43±1.38) remained elevated.

Both these miRNAs are directly regulated by the REST, which has already shown in my work to be downregulated following a loss *EHMT1*. To determine if the loss of REST protein is also fixed following restoration of *EHMT1* western blot analysis was also performed on cells transiently treated with UNC0638 (400nM). As expected, treatment with UNC0638 resulted in a significant drop in REST protein levels at day 30 as compared to control (0.32±0.052) (Figure 5.3C). As seen with the miRNAs, the removal of UNC0638 did not result in a de-repression of REST protein levels (0.37±0.039). Together these results suggest the shift in brain specific REST-miRNAs in response to a loss of *EHMT1* is already fixed at the NPC stage.

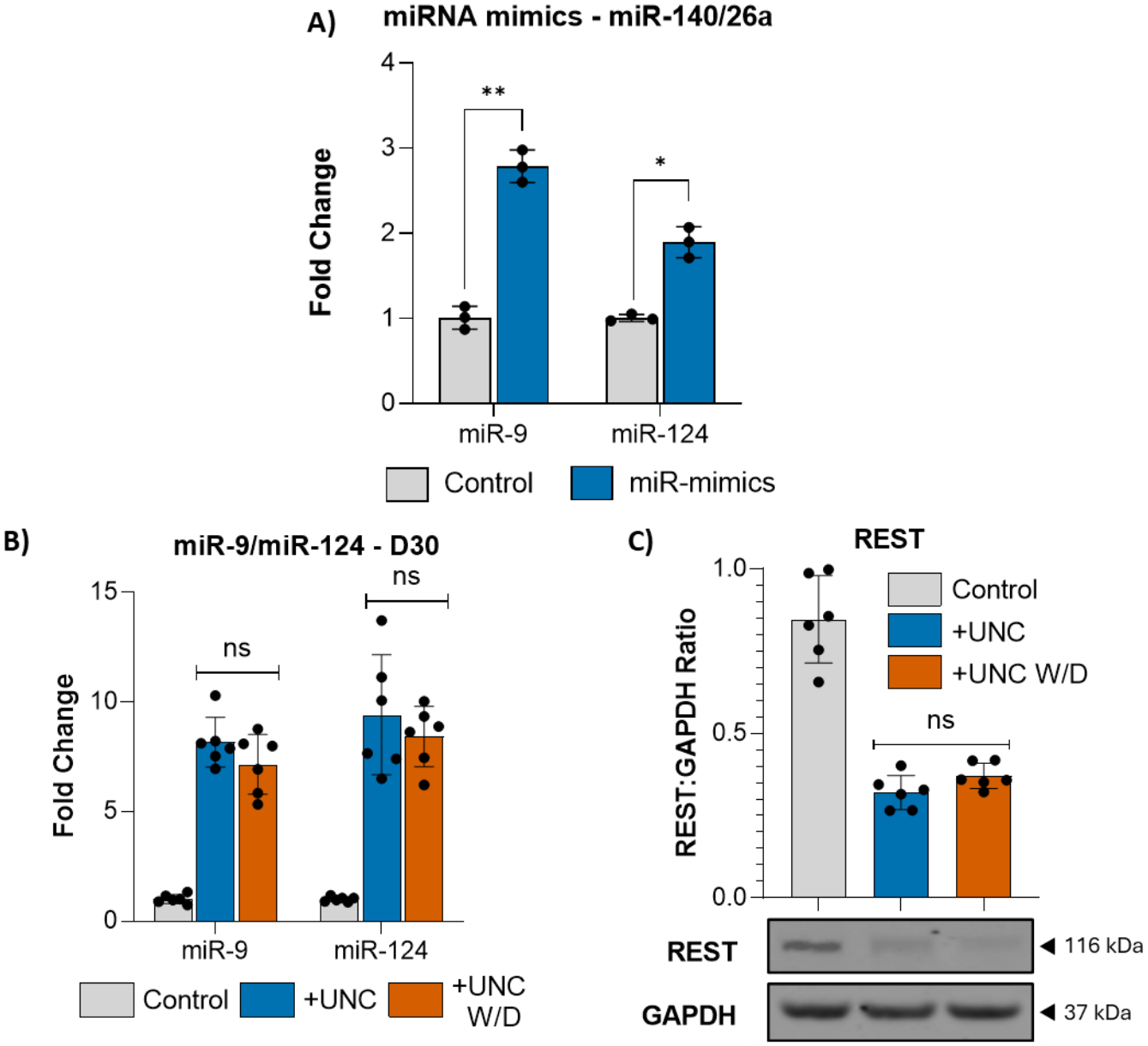

Figure 5.3 miRNA-REST network

A) *Mature miRNA expression analysis of miR-9-5p and miR-124-3p by qRT-PCR in hiPSC derived neurons treated with miRNA mimics. At day 10 of differentiation cells were treated with mimics for miR-140-5p and miR-26a-5p, 3 days later samples were collected and both miR-9-5p and miR-124-3p expression was elevated. n = 3 independent experiments* ***B)*** *Mature miRNA expression analysis of miR-9-5p and miR-124-3p by qRT-PCR in hiPSC derived neurons at day 30 following treatment with UNC0638 from days 0-20, as compared to vehicle control. n = 6 independent experiments. The withdrawal of UNC0638 did not reduce miR-9-5p or miR-124-3p expression.* ***C)*** *Western blot analysis of REST protein expression in hiPSC derived neurons at day 30 following treatment with UNC0638 from days 0-20, as compared to vehicle control. Withdrawal of UNC0638 did not restore REST expression. Data were presented as Mean±SEM and analysed by student's t-test or One-way ANOVA with post hoc comparisons using Tukey's multiple comparisons test comparing to control samples. *P < 0.05, **P < 0.01, ***P < 0.001.*

5.3.4 Impact on early neuronal markers

In an attempt to understand how a loss of REST and the accompanying increase in REST-miRNAs affected neuronal differentiation, control cells and UNC0638 (400nM) treated cells were differentiated into neurons using a standard dual-SMAD inhibition protocol (Chambers et al., 2009). Expression of two non-REST regulated genes, *PAX6* and *MAP2*, were analysed as markers of development. *PAX6* is a transcription factor and a marker of early neuroectoderm cells, typically associated with neural progenitor cells (Zhang et al., 2010). Meanwhile, MAP2 is a cytoskeletal protein and a marker of neurons, its dysregulation has been associated with disorders including schizophrenia and autism (Przyborski and Cambray-Deakin, 1995, DeGiosio et al., 2019, Westphal et al., 2018).

Expression levels of *PAX6* showed significant elevation in UNC0638 treated cells both at day 10 with a fold difference of 2.78 (14.41±4.39 Vs. 40.13±7.59, p=0.0071) and at day 20 with a fold difference of 1.86 (57.23±8.14 vs. 106.55±23.43, p=0.026) (Figure 5.4A). Likewise, expression levels of *MAP2* were significantly elevated at day 20 with a fold difference of 8.39 (42.30±3.08 Vs. 103.0±21.05, p=0.0077) and at day 30 with a fold difference of 2.50 (84.30±7.96 Vs. 211.70± 32.77, p=0.0028) (Figure 5.4B). These results suggest a precocious, sustained increase in REST independent maturation markers.

Next to understand if these transcriptional changes were reflected at the translational level, control cells, along with UNC0638 (400nM) treated cells and *EHMT1*$^{+/-}$ cells were again differentiated into neurons. *EHMT1*$^{+/-}$ were included to ensure the observed effects were directly caused by the loss of *EHMT1* and not a dual effect of *EHMT1/2* induced by UNC0638. Cells were either stained for the PAX6 NPC marker at day 20 or the neuronal MAP2 marker at day 30 (Figure 5.4C). Analysis revealed at day 20 mean fluorescence levels for PAX6 were significantly higher in *EHMT1* deficient cells as compared to control, by a factor of 2.06 (410.73±113.04, p=0.0021) for UNC0638 treated cells and a factor of 2.35 (410.73±113.04 Vs. 963.41±161.08, p=0.0004) (Figure 5.4D). Analysis of MAP2 at day 30 also showed significant increases in mean fluorescence in UNC0638 treated cells, by a factor of 2.67 (515.60±89.14 Vs. 1375.58±158.62, p<0.0001) and also for *EHMT1*$^{+/-}$ cells by a factor of 1.91 (515.60±89.14 Vs. 983.24±97.70, p=0.0009) (Figure 5.4E). Of note, no significant difference was observed between UNC0638 treated cells or *EHMT1*$^{+/-}$ cells for either PAX6 or MAP2.

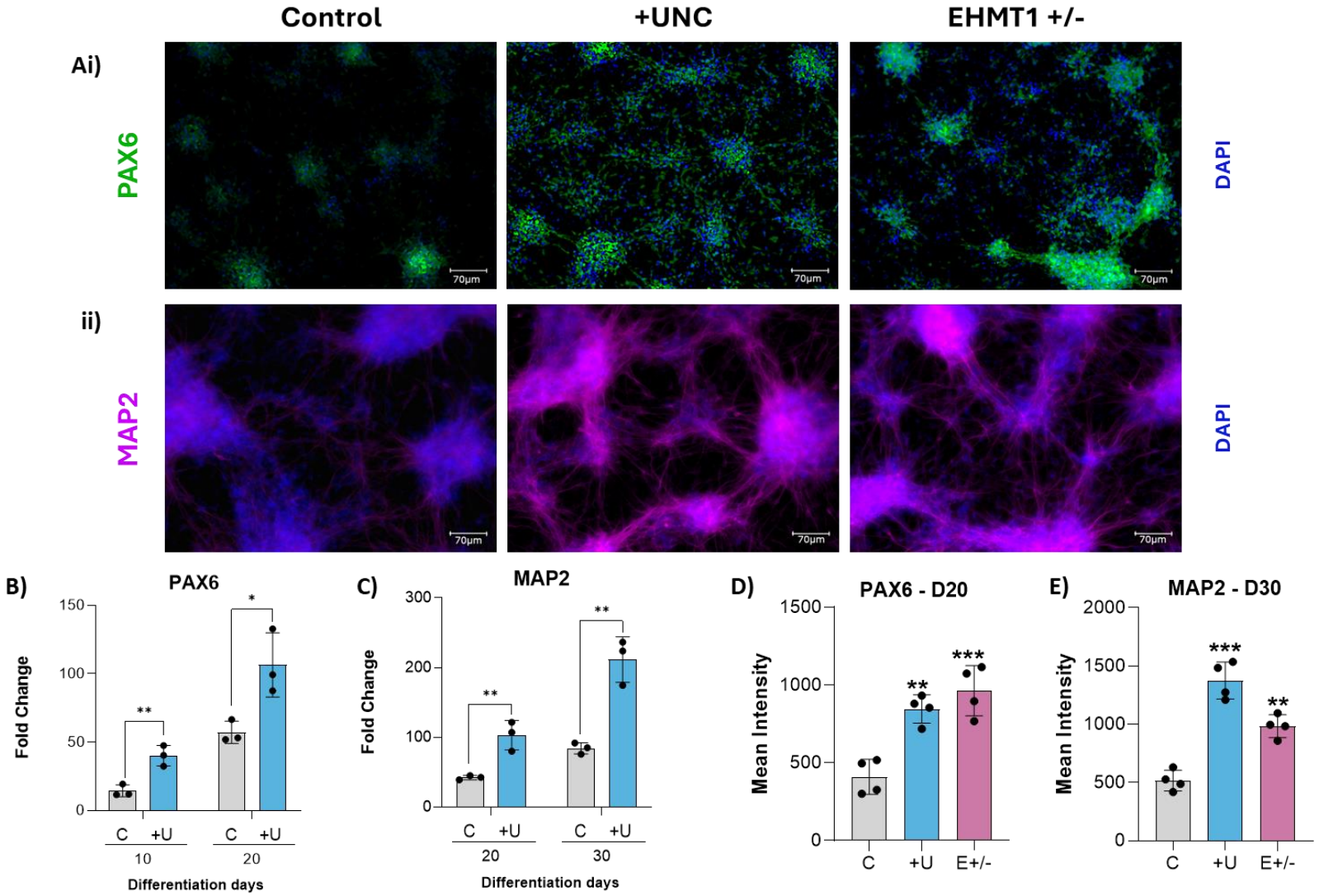

Figure 5.4 EHMT1 depletion leads to precocious neuron differentiation

A) *Cell staining of hiPSCs treated with UNC0638 and EHMT1+/- hiPSCs, subsequently differentiated to either day 20 or day 30. Day 20 cells were stained for PAX6 protein, whilst day 30 cells were stained for MAP2 expression. Scale Bar, 70 µm.* ***B-C*** *Gene expression analysis by qRT-PCR in hiPSC derived NPCs following treatment with 400nM UNC0638, as compared to vehicle control.* ***B)*** *PAX6 expression at day 10 and day 20 of differentiation.* ***C)*** *MAP2 expression at day 20 and day 30 of differentiation. n = 3 independent experiments.* ***D-E*** *Graphs show quantitation of protein expression as* ***D)*** *MAP2 or* ***E)*** *PAX6 mean fluorescence intensity, with DAPI nuclear counterstain.*

5.3.5 Impact on ealy to late neuronal markers

Next, expression of early determinators of neuronal fate, *NCAM1* and *ASCL1*, were assessed in order to understand if the effects on differentiation were limited to only day 20 onwards. *NCAM1* is a neural adhesion molecule which promotes the determination to a neuronal fate (Shin et al., 2002b), whilst *ASCL1* (also known as *MASH1*) is a protein specifically expressed in cells undergoing the critical transition from neural progenitor to mature neuron (Kim et al., 2007). At 15 days there was no discernible difference in the expression of *NCAM1* between samples, however by day 30 there was a 2.57-fold increase in UNC0638 treated cells (23.12±6.76 Vs. 59.44±12.2.27, p=0.011) (Figure 5.5A). Comparatively, *ASCL1* showed a modest 2.26-fold increase compared to control at day 15 (2.56±0.58 Vs. 5.79±1.91, p=0.049) and a larger 4-fold increase at day 30 (19.49±5.21 Vs. 78.50±5.75, 0.00019) (Figure 5.5B). These results indicate the loss of *EHMT1* and subsequent increase in brain specific miRNAs induces a shift in neuronal maturation toward a greater expression of mid stage neuronal markers.

Theorising that the upregulation of brain specific miRNAs had induced a precocious shift in neuronal maturation, two markers of mature neurons were assessed in *EHMT1* depleted cells at day 40/50 of differentiation. TUBB3 (also known as TUJ1) is a beta tubulin protein almost exclusively expressed in neurons (Pang et al., 2011), whilst SNAP25 is a synaptic protein, essential for healthy neuronal communication (Nazir et al., 2018). Protein levels of TUBB3 was analysed at day 40 in both UNC0638 (400nM) treated and *EHMT1*$^{+/-}$ cells. UNC0638 treated cells showed a 2.02-fold increase (0.070±0.009 Vs. 0.14±0.023, p=0.008) compared to control, whilst *EHMT1*$^{+/-}$ cells displayed a comparable 1.86-fold increase (0.070±0.009 Vs. 0.13±0.033, p=0.017) (Figure 5.5C).

Levels of SNAP25 protein were assessed at day 50 in UNC0638 treated, *EHMT1*$^{+/-}$ and Kleefstra syndrome patient cells. For all three sample types SNAP25 showed a sustained and significant increase in protein levels. Treatment with UNC0638 induced a 2.95-fold increase relative to control (0.37±0.11 Vs. 1.09±0.16, p=0.0017), in *EHMT1*$^{+/-}$ cells a 2.11-fold increase (0.74±0.082 Vs. 1.56±0.26, p=0.0006) and in KS1 cells a 1.51-fold increase (0.81±0.16 Vs. 1.25±0.28, p=0.048) (Figure 5.5D). Collectively, results indicate the lack of *EHMT1* leads to significant increases in TUBB3 and SNAP25, indicating a greater shift toward maturing neurons.

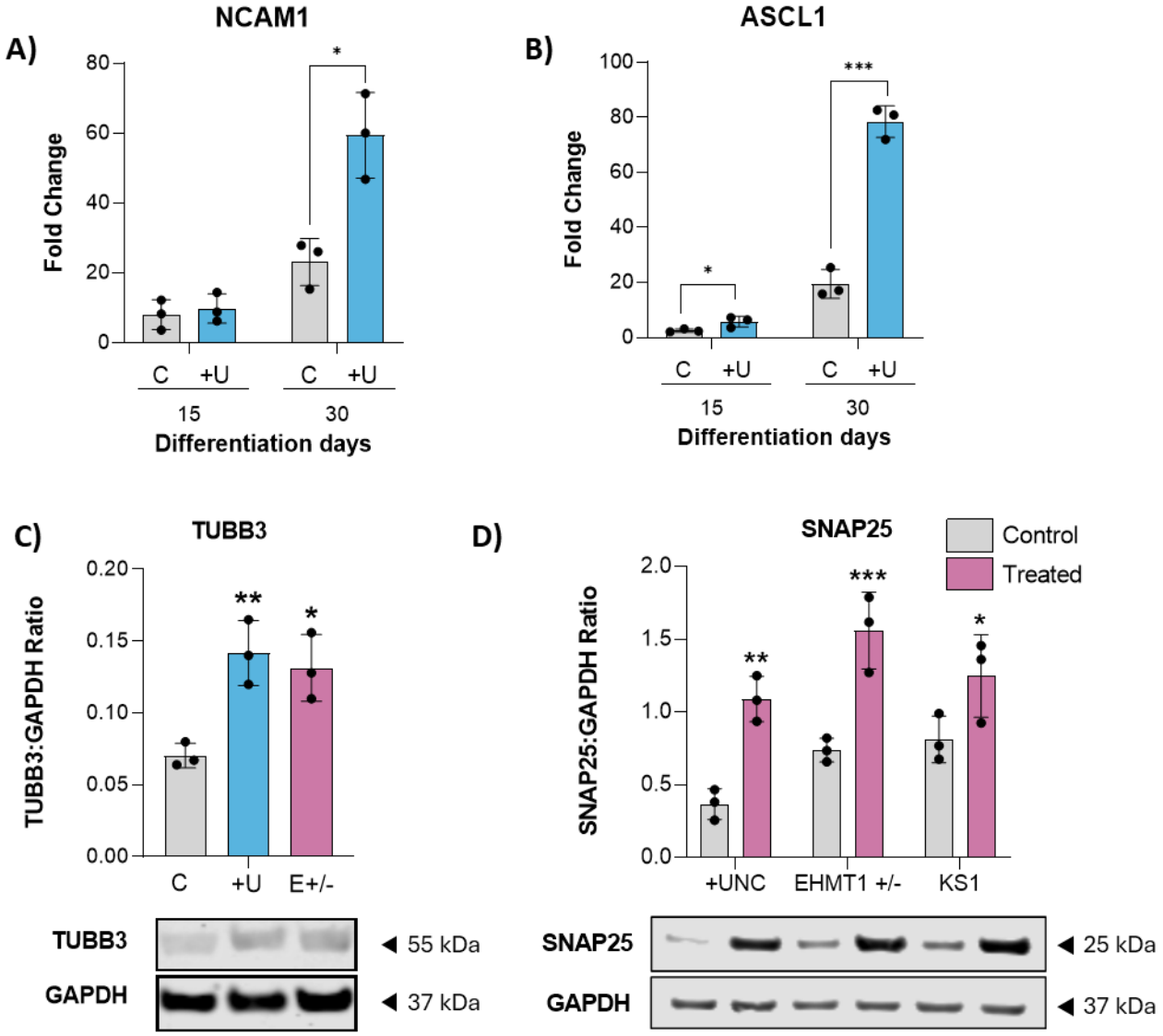

Figure 5.5 Increases in maturation markers

A,B *qRT-PCR analysis of early neuronal markers in hiPSC following treatment with UNC0638 and differentiation.* ***A)*** *NCAM1 expression is elevated at day 30.* ***B)*** *ASCL1 expression is strongly increased at both day 15 and day 30.* ***C*** *Western blot analysis of TUBB3 protein expression in hiPSCs treated with UNC0638 and EHMT1+/- hiPSCs, differentiated to neurons, day 40, as compared to vehicle control or isogeneic control respectively.* ***D*** *Western blot analysis of pre-synaptic SNAP25 protein expression in hiPSC treated with UNC0638, EHMT1+/- hiPSCs and patient KS hiPSCs, all differentiated to day 50 neurons and relative to vehicle control or isogenic controls. Data were presented as Mean±SEM and analysed by One-way ANOVA with post hoc comparisons using Tukey's multiple comparisons test comparing to control samples. *P < 0.05, **P < 0.01, ***P < 0.001.*

5.3.6 Rescue of precocious maturation

Having previously identified that *EHMT1* mediated dysregulation leads to repressed levels of REST, elevated brain specific miRNAs and in turn precocious neuronal differentiation, I wanted to determine if stable repression of these *EHMT1* mediated miRNAs could restore normal developmental timing.

To this end a stable multimiR sponge against miR-140-5p/26a-5p/153-3p was transduced into hiPSCs using retroviral vectors or a scramble sponge. Cells were then either treated with UNC0638 (400nm) or vehicle control and differentiated to day 30 neurons. Given that these miRNAs have already been shown to repress REST, protein expression was analysed in both stable and scramble sponges at day 0. Relative to control, scramble sponges showed a significant drop in protein levels (0.41±0.096 Vs. 0.94±0.045, p=0.0007), however stable sponge samples showed no significant changes compared to control (Figure 5.6A).

Next, to assess whether the restoration of REST translates to changes in brain specific miRNAs, both miR-124-3p and miR-9-5p expression was analysed in day 30 neurons. In line with previous results in this chapter, both miRNAs were significantly elevated in scramble sponge samples following continuous treatment with UNC0638 (Figure 5.6B). Importantly however, multimiR sponge samples showed a marked decrease in expression relative to scramble samples for both miR-9-5p (3.30±1.33 Vs. 6.92±1.52, p=0.0014) and miR-124-3p (3.47±1.09 Vs. 6.11±0.75, p=0.0006). These results indicate stable sponges not only significantly reduce the inhibition of REST protein, but also the premature expression of REST regulated/brain specific miRNAs.

Finally, to identify if this reduction in brain specific miRNAs restores the developmental timing of neurons, two mature markers were assessed in treated samples at day 40 of differentiation. NEFM is a medium neurofilament protein associated with terminal neuronal differentiation and exit from the cell cycle (Mao et al., 2011). SYN (also known as synapsin) is a neuron specific phosphoprotein, which is only expressed in mature late-stage neurons (Kim et al., 2019). Following treatment with UNC0638, the scramble sponges showed increases relative to control in both NEFM protein levels (1.047±0.066 Vs. 0.74±0.14, p=0.0011) and SYN protein levels (0.86±0.083 Vs. 0.56±0.12, p=0.008) (Figure 5.6C,D). In contrast multimiR sponge samples showed significantly lower protein levels compared to scramble samples, for

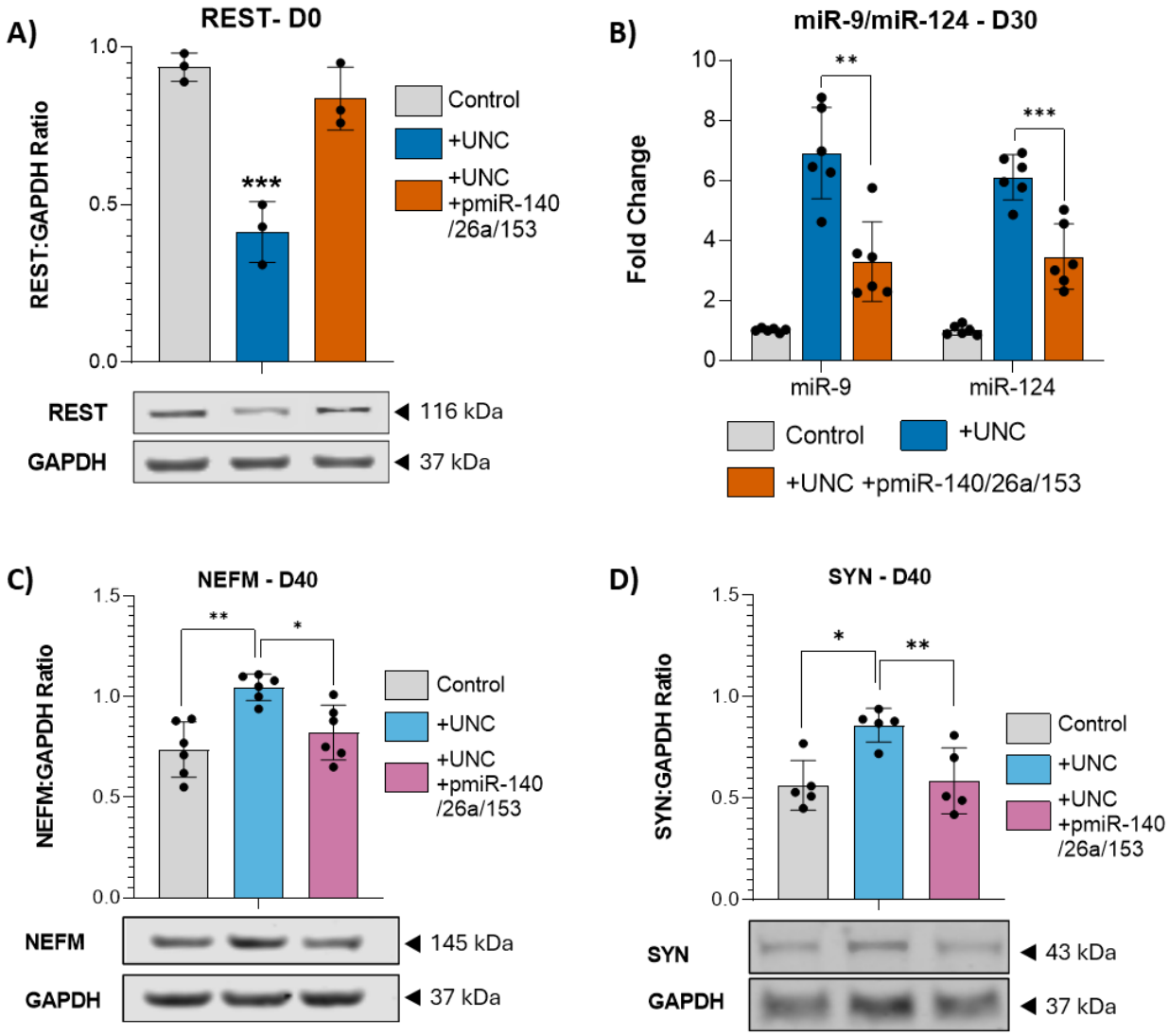

Figure 5.6 EHMT1 controls an epigenetic window that dictates neurodevelopmental timing
A) *Western blot analysis of REST protein expression in hiPSC s treated with 400nM UNC0638, and samples infected with lentiviral multimiR-sponge against miR-140-5p/26a-5p/153-3p or scramble sequence, as relative to vehicle control.* ***B)*** *Mature miRNA expression analysis of miR-9-5p and miR-124-3p by qRT-PCR in hiPSC derived neurons at day 30 following treatment with UNC0638 and samples infected with lentiviral multimiR-sponge against miR-140-5p/26a-5p/153-3p or scramble sequence, as relative to vehicle control. n = 6 independent experiments.* ***C-D*** *Western blot analysis in hiPSC derived neurons (day 40) treated with 400nM UNC0638, and samples infected with lentiviral multimiR-sponge against miR-140-5p/26a-5p/153-3p or scramble sequence, as relative to vehicle control.* ***C)*** *Mature neuronal marker NEFM protein levels and* ***D)*** *mature neuronal marker SYN, at day 40. Data were presented as Mean±SEM and analysed by One-way ANOVA with post hoc comparisons using Tukey's multiple comparisons test comparing to control samples. *P < 0.05, **P < 0.01, ***P < 0.001.*

both NEFM (0.82±0.14 Vs. 1.047±0.066, p=0.013) and SYN (0.59±0.16 Vs. 0.86±0.083, p=0.008). Taken together this data demonstrates that through its action on miRNAs, *EHMT1* controls the timing of neurodevelopment, and disruption results in abnormal neuronal and brain development.

Based on these findings I propose a model for the regulation of neurodevelopmental timing by the epigenetic regulator, *EHMT1* (Figure 5.7A, B). Loss of *EHMT1* leads to a premature downregulation in REST through the de-repression of *EHMT1* regulated miRNAs (miR-140-5p/26a-5p/153-3p). This in turn induces a temporal shift, prematurely increasing levels of brain specific miRNAs and in turn leading to the precocious differentiation and maturation of neurons.

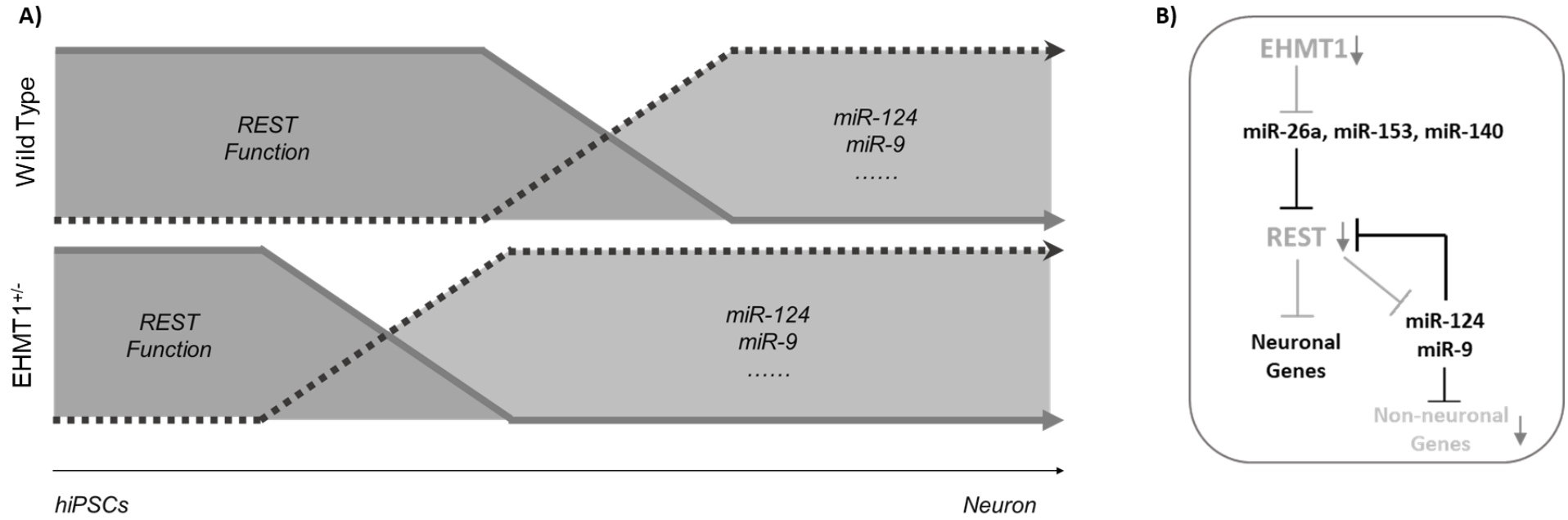

Figure 5.7 EHMT1 mediation of neuronal differentiation timing

A) *Diagram depicting the shift in normal REST protein reduction in response to a loss of EHMT1, accompanied by a premature increase in REST regulated miRNAs (miR-9-5p, miR-124-3p), culminating in premature neuronal maturation.* ***B)*** *Premature reduction in REST protein is caused by elevated levels of a cooperative subset of miRNAs (miR-26a-5p, miR-153-3p, miR-140-5p) directly regulated by EHMT1.*

5.4 Discussion

This chapter describes the role of *EHMT1* on regulating epigenetic windows which determine the timing and progression of neuronal development. Analysis of brain specific miRNAs, miR-124-3p and miR-9-5p, indicated a clear shift in expression, with peak differences seen around day 30 of differentiation. Significant increases in expression were not seen for either miRNA in the first 20 days, which is in-line with previous work from Chapter 4.3.1 that showed no increase in either mIR-124-3p or miR-9-5p at the pluripotent stage. As mentioned previously, despite the loss of REST protein, certain gene targets retain REST complex co-repressors potentially maintaining initial repression (Ballas et al., 2005). My results are strongly supported by other studies, which have demonstrated knockdown of REST leads to its absence from the promotor of MIR9, however this is not sufficient to induce transcriptional activation (Laneve et al., 2010). Furthermore, other factors beyond the REST complex are involved in the regulation of miR-9-5p and miR-124-3p. For example, miR-9-5p has been to shown to form a feedback-loop with the nuclear receptor *TLX* directly repressing the miRNA (Zhao et al., 2009). Similarly, miR-124-3p forms a feedback loop with the membrane protein, ephrin-B1, which acts to repress miR-124-3p via signalling (Arvanitis et al., 2010). Adding complexity to this regulation, miR-124-3p has also been shown to be differentially regulated at the post-translational level, both in the brain and by RNA binding proteins during erythropoiesis (Maiorano and Mallamaci, 2010, Wang et al., 2017). Therefore, my results indicate that although REST most likely acts as the master regulator of mIR-124-3p and miR-9-5p expression, other factors appear to maintain repression until neural induction.

Beyond day 20 of differentiation, both miRNAs remain significantly elevated until day 60, during which time expression of both increases. Beyond this point miR-124-3p levels were comparable to control, and miR-9-5p levels began to drop. This expression pattern mirrors that seen in-vivo, where miR-124-3p and miR-9-5p are the most abundant brain miRNAs, their expression begins at the same time and increases throughout neural development, and expression of miR-9-5p is decreased postnatally (De Pietri Tonelli et al., 2008, Xue et al., 2016). Collectively the data indicates a shift in the expression of these miRNAs in response to the loss of REST. Expression of various miR-124-3p and miR-9-5p targets were found to be significantly downregulated in response to the precocious elevation of the miRNAs. Several of these genes are cell cycle regulators, including *CCND2* and *CDK6*. During neural

development, *CDK6* has been shown to regulate the proliferation of NPCs and control the number of newborn neurons (Beukelaers et al., 2011). Likewise, expression of *CCND2* in asymmetrically dividing NPCs promotes either self-renewal or terminal differentiation (Tsunekawa et al., 2012). The downregulation of these cell cycling regulators is reflected in the role of miR-124-3p, where inhibition of the miRNA results in delayed cell cycle exit of NPCs (Cheng et al., 2009).

Alongside cell-cycle regulators, dysregulated targets also included genes involved in cell adhesion, namely *ITGB1*, *LAMC1* and *FREM2*. Both *LAMC1* and *ITGB1* have been shown to be post-transcriptionally regulated by miR-124-3p during neurogenesis, typically in post-mitotic neurons (Cao et al., 2007). Both *ITGB1* and *LAMC1* are highly expressed in neural progenitors where they are essential for neuronal migration through interactions with the ligand *RELN* (Schmid and Anton, 2003, Dulabon et al., 2000). Indeed overexpression of miR-124-3p lead to structural abnormalities in the cortex of effected animals (Cao et al., 2007). The downregulation of these cell adhesion molecules suggests reduced cell motility in response to elevated miR-124-3p, although further studies ideally in-vivo would be required to discern the extent of this disruption.

Regulators of early neuronal development, *ONECUT2*, *PRRX1* and *SIX4* were also shown to be repressed in response to miRNA elevation. Expression of *ONECUT2* is vital for accessibility of neuronal genes and inducing gene expression (van der Raadt et al., 2019). However, levels of *ONECUT2* decrease as cells progress to neuronal fate in direct response to increasing levels of miR-9-5p (Pöstyéni et al., 2021). Knockdown mutations of *ONECUT* genes show a significant reduction in the number of neurons, however this may have a reduced implication in-vivo due to the redundant nature of the *ONECUT* family (Sapkota et al., 2014, Kabayiza et al., 2017). Despite this, the decreased expression of *ONECUT2* is most likely indicative of a developmental shift toward a mature state. Similarly, PRRX1 plays a significant role in NPC stemness and is required for commitment to neuronal differentiation (Shimozaki et al., 2013). However, overexpression of *PRRX1* induced a greater number of NPC like cells at the expense of neurons. Again, the loss of *PRRX1* suggests a premature maturation beyond the point of NPCs to mature neurons. Finally, *SIX4* is a homeobox gene essential for the maintenance of NPCs and preventing premature differentiation. Knockdown studies have demonstrated that a loss of *SIX4* at the progenitor stage leads to the premature differentiation to terminally

dividing cells (Chen et al., 2021b). Together this suggests the downregulation of these early neuronal regulators leads to an acceleration through the progenitor stages of neuronal differentiation.

One of the well reported actions of miR-124-3p during neuronal differentiation is the induction of alternative brain specific splicing due to the direct reduction of *PTBP1*. Analysis of three reported genes, *CDC42*, *RUFY3* and *MAP4*, demonstrated a clear shift, with significant upregulation of the neuronally spliced isoforms. These findings replicate previous studies, which demonstrated upregulation of miR-124-3p during neuronal differentiation directly repressed *PTBP1* expression, causing the isoform switch (Makeyev et al., 2007). Reduced levels of *PTBP1* were found to prevent exon skipping in the homolog *PTBP2* which would typically lead to nonsense mediated decay. Moreover, this *PTBP1* repression was shown to be essential for the efficient differentiation of neurons (Makeyev et al., 2007). Importantly, these differentially spliced variants appear to have significant impacts on neurogenesis. For example, despite differing by only 9 amino acids, the two variants of the *CDC42* gene show uniquely distinct functions in neurogenesis. Whilst the general or ubiquitously expressed variant (*CDC42u*) drives the formation of progenitor cells, the brain specific variant, typically limited to mature neurons is essential for the transition to a terminally differentiated state (Endo et al., 2020). Furthermore, analysis of human neurogenesis has indicated a gradual transition of *CDC42* isoforms rather than a sharp switch is instrumental for proper structural and functional polarization of neurons (Yap et al., 2016). Therefore, not only do these results indicate the premature upregulation of miR-124-3p has global cellular implications, but also a dysregulation of proper neurogenesis due to an expeditiousness of developmental timing.

In addition to changes in spliced variants, analysis also revealed downregulation of target genes including *REST* and its associated protein *CTDSPL* (CTD Small Phosphatase Like). This further emphasizes the disruption of the REST-miRNA feedback loop previously observed. Since REST targets both miR-124-3p and miR-9, I investigated if the elevated levels of these miRNAs were caused by the downregulation of REST by using mimics against *EHMT1*-regulated miRNAs.

The results supported this hypothesis. Upregulation of miR-26a and miR-140, both under *EHMT1* control, led to the increase in miR-124-3p and miR-9, suggesting these *EHMT1*-regulated miRNAs act upstream of REST. Interestingly, while previous studies have shown

EHMT1/2 directly represses miR-124-3p in cancer (Siouda et al., 2020), my findings suggest that the miR-124-3p increase here is a consequence of decreased REST, rather than direct *EHMT1* action. ChIP studies could be useful in the future to confirm the presence of H3K9me2 marks on the *MIR124* gene during differentiation.

Previous results suggest that as differentiation progresses, the loss of REST derepresses miR-9-5p expression, which in turn actively downregulates REST further (Laneve et al., 2010). Given the overexpression of miR-124-3p and miR-9-5p is sufficient to transdifferentiate cells to a neuronal state by targeting REST (Lee et al., 2018), I questioned whether the elevation of these miRNAs marked a ratchet like state change, preventing de-differentiation. As such, cells were treated with UNC0638 inhibitor until day 20 before the chemical was removed until day 30. Results indicated that despite the removal of the EHMT inhibitor, levels of miR-124-3p and miR-9-5p remained elevated. Likewise, levels of REST protein remained significantly lower at day 30, in-spite of UNC0638 withdrawal. Together this suggests a dynamic shift in REST regulation from upstream *EHMT1* regulated miRNAs, to downstream destabilisation of the REST-miRNA feedback loop. In this manner, elevation of miR-124-3p and miR-9-5p act as a transcriptional ratchet, ensuring neuronal fate commitment and preventing de-differentiation of neuronal cells. This sequential progression toward differentiation is supported by studies which demonstrate despite being sufficient to induce neuronal differentiation, overexpression of miR-124-3p and miR-9-5p is only partially responsible for the inhibition of REST (Drouin-Ouellet et al., 2017). This would suggest for proper and total neuronal differentiation, the correct regulation and timing of multiple transcriptional stages is required.

This work strengthens the evidence for a time-dependent role of miR-124-3p and miR-9-5p in neuronal differentiation, initiated by *EHMT1* regulation. Supporting this concept, previous research has shown that while overexpressing miR-9-5p alone cannot trigger neuronal differentiation, it significantly accelerates this process in neuronal progenitor cells that are already primed for differentiation (Zhao et al., 2009). Conversely, inhibiting miR-124-3p has been linked to delayed neurogenesis or even blocked neuronal differentiation, highlighting its importance in the precise timing of neuronal development (Cheng et al., 2009).

Having demonstrated that a loss of *EHMT1* induces a temporal shift in neurodevelopment and precocious elevation of miR-124-3p and miR-9, I wanted to understand if this had an

implication on neuronal maturation. Indeed, previous studies have demonstrated that synthetically inhibiting REST levels, whilst simultaneously elevating miR-124-3p and miR-9-5p drastically accelerates neuronal maturation (Lee et al., 2018). Both miRNAs act to progress maturation, by repressing a range of genes. By targeting the stemness gene *FOXG1*, miR-9-5p acts to transit cells away from the progenitor state (Garaffo et al., 2015). Likewise, miR-124-3p inhibits the *SOX9* gene, responsible for maintaining a stem like state in neuronal progenitor cells (Cheng et al., 2009). Meanwhile, miR-124-3p also promotes neuronal differentiation and axonal branching by targeting the homeobox gene, *LHX2* (Sanuki et al., 2011).

To gain insight into the speed of maturation, I investigated the expression of the progenitor marker *PAX6* and the neuronal marker *MAP2* in *EHMT1* deficient cells. If a shift in acceleration was present, earlier increases in neuronal progenitors would be expected, accompanied by subsequent premature increases in neuronal cells. Analysis revealed this was the case, with significant elevation of *PAX6* by day 20, accompanied by a greater number of *PAX6* positive cells, indicating an increase in the number of progenitor cells. Despite this, levels of *PAX6* were not significantly elevated at day 10, which was surprising as *PAX6* levels increase very early during neuronal differentiation. One possible explanation is that *PAX6* is not a target of REST and hence not initially impacted by the loss of REST. Expression of *MAP2* was elevated at day 20 and to an even greater extent by day 30. Accompanied by the increased number of *MAP2* positive cells in both UNC0638 treated and *EHMT1* haplodeficient cells, this strongly suggests an increase in the number of neuronally committed cells in direct response to the loss of *EHMT1*. Comparing the results from *PAX6* and *MAP2* analysis, it is possible that cells are transitioning very quickly from the progenitor to neuronal cell types, as indicated by the more pronounced increase in *MAP2*. Future work should further investigate the transition of *EHMT1* depleted cells through the neuronal pathway and single cell sequencing tools will be particularly advantageous in defining the unique subpopulations of cells.

To further probe the temporal effects of *EHMT1* depletion on neuronal maturation, I assessed expression of neuronal markers *NCAM1* and *ASCL1*. Despite being known to be regulated by REST (Kreisler et al., 2010), *NCAM1* showed no discernible increases compared to control at day 15. However significant increases were seen at day 30, in line with peak miRNA differences. Interestingly elevation of *NCAM1* has been shown in cells where miR-124-3p and miR-9-5p are overexpressed, indicating a shift toward a neuronal state (Lu et al., 2021).

Moreover it has long been known exogenous addition of soluble NCAM1 has been shown to actively promote differentiation of progenitor cells (Shin et al., 2002a), again supporting an acceleration of neural differentiation in *EHMT1* deficient cells.

In contrast, *ASCL1* was elevated as early as day 15 and showed even greater increases at day 30. *ASCL1* is a highly influential proneural gene, capable of converting astrocytes to induced neurons (Rao et al., 2021). The transcription factor has been found to be vital for neuronal specification and activating a plethora of neuronal subtype markers, including neurodevelopmental factors such as *OLIG1*, *OLIG2* and *SOX2* (Aydin et al., 2019, Vue et al., 2020). Overexpression of *ASCL1* is sufficient to generate transdifferentiated neurons, however these cells initially display slower maturation kinetics (Chanda et al., 2014). However, the efficacy of *ASCL1* reprogramming is significantly enhanced with ectopic overexpression of miR-124-3p and miR-9-5p (Yoo et al., 2011). My results indicate the increased expression of *ASCL1* is indicative of a transcriptional shift towards neuronal subtypes as seen in previous chapters. To assess if neuronal fate was increased in *EHMT1* deficient cells, protein levels of the neuronal marker β-tubulin III (TUBB3) were analysed in *EHMT1* depleted cells. TUBB3 expression is restricted to neurons and levels peak during early postnatal periods (Radwitz et al., 2022). Even at day 40, levels of TUBB3 remained elevated, suggesting a significant enrichment of neuronal cells as compared to control samples. Importantly this effect was observed in both UNC0638 treated cells, but also in *EHMT1*$^{+/-}$ cells, suggesting the increase is directly due to mis-regulation by *EHMT1* loss. This finding is in-line with similar studies, which demonstrate a lack of REST, or upstream miRNAs result in elevated expression levels of TUBB3 (Sauer et al., 2021). However, decreased levels of TUBB3 during neurodevelopment have been found to boost regulate synaptogenesis and long-term potentiation (Radwitz et al., 2022). As such, elevated levels of TUBB3 in response to a loss of *EHMT1* may lead to issues regarding synaptogenesis in Kleefstra syndrome patients. Further work would be required to prolong differentiation of these cells and analyse the effects at later stages.

To understand if this increased maturation was sustained at later stages of differentiation, expression levels of the mature neuronal marker SNAP25 were analysed in various *EHMT1* depleted models at day 50 of differentiation. Results showed SNAP25 levels were elevated in UNC0638 treated, *EHMT1*$^{+/-}$ and Kleefstra syndrome cells, demonstrating a clear *EHMT1*

specific effect. *SNAP25* is highly regulated by REST, containing two RE1 sites within its sequence (Cheong et al., 2005). Furthermore, as with other targets, overexpression of miR-124-3p and miR-9-5p leads to significant elevation of SNAP25 expression (Lu et al., 2021). Results indicate SNAP25 is consistently elevated in the absence of *EHMT1*, most likely as a direct result of REST loss. Moreover, it indicates the increase in neuronal maturation is sustained, rather than a transient effect at the progenitor stages.

Based on previous experiments in Chapter 5.3.3-5.3.5, loss of *EHMT1* appeared to induce a shift in neuronal maturation that was fixed beyond day 20. Moreover, the ectopic expression of *EHMT1* regulated miRNAs was sufficient to induce upregulation of brain specific miRNAs underpinning this precocious maturation. Therefore, in an attempt to uncouple these elevated miRNAs and restore the normal timing of neurodevelopment, I generated stable multimiR sponges against either *EHMT1*-miRNAs (miR-140-5p/miR-153-3p/miR-26a-5p) or a scramble sequence, using a retroviral system. Results of *EHMT1* depleted hiPSCs replicated previous findings that inhibition of these miRNAs is sufficient to rescue REST expression. Rescue of REST protein levels was almost indistinguishable from control, most likely due to the stable and continuous expression of the multimiR-sponge. These hiPSCs were differentiated to day 30 and the expression of miR-9-5p and miR-124-3p was analysed. As expected, given the rescue of REST protein, miR-124-3p and miR-9-5p levels were significantly decreased in multimiR-sponge samples compared to scramble control. This finding supports previous results of mimic experiments that demonstrated *EHMT1*-miRNAs were responsible for the elevation of brain specific miRNAs.

Inhibition of brain-specific miRNAs in adult neurons has shown not to be sufficient to reverse differentiation (Lu et al., 2021). However, miR-124-3p inhibition during early neural development can prevent neuronal differentiation altogether (Cheng et al., 2009). With this in mind, I aimed to determine if the rescue of brain specific miRNAs at day 30 translated to a restoration of the neurodevelopmental timeline. To do this I analysed the protein expression of two markers of mature neurons, NEFM and SYN at differentiation day 40, in control, scramble and multimiR sponge samples following continual treatment with UNC0638. Results of both NEFM and SYN protein analysis in scramble sponge samples showed significant elevation relative to control. NEFM is highly expressed in mature neurons and is directly involved in dendrite outgrowth and axon organisation (Yuan et al., 2017). Likewise, SYN is

highly expressed in mature neurons, where it plays a distinct role in the regulation of adult neurogenesis (Barbieri et al., 2018). Transformation studies, utilising overexpression of miR-124-3p and miR-9-5p also display strong increases in SYN expression, as seen in my results (Yoo et al., 2011). As such the increase in scramble cells indicates precocious maturation seen in early neuronal cells is sustained, as indicated by earlier SNAP25 results in *EHMT1*+/- and patient cells.

Importantly, multimiR-sponge samples demonstrated significant reduction in both NEFM and SYN protein, back to levels comparable with control. Inhibition of the *EHMT1* miRNAs from the hiPSC stage was able to restore the timing of maturation comparable to healthy cells. Collectively this work demonstrates that intervention at the hiPSC stage, either by stable miRNA repression or by *EHMT1* overexpression as shown in Chapter 4.3.2, could prevent premature maturation. This suggests *EHMT1* controls an epigenetic window in which its effects can be reversed, acting like a ratchet to progress neural development and timing.

These findings are strongly supported by a very recent study that has demonstrated a similar link, in which *EHMT1* was transiently inhibited from day 12 to 20 of neuronal differentiation (Ciceri et al., 2024). In contrast to my findings no change was seen in *PAX6* expression at day 20, most likely due the transient inhibition of *EHMT1*. However significant increases were seen in the neurofilament heavy (NEFH) protein, a heteropolymer of the NEFM, at day 35. Moreover, early postnatal supply of *EHMT1* in Ehmt1$^{+/-}$ mice has been shown to drastically improve but not fully reverse KS phenotypes (Yamada et al., 2021). Together with my results, these findings strongly suggest an epigenetic window prior to day 20 dictates the temporal regulation of neuronal differentiation, whereby disruptions during this time lead to accelerated maturation toward a neuronal phenotype.

The association between precocious differentiation and neurodevelopmental disorders are not unique to Kleefstra syndrome. Kabuki syndrome is a rare congenital disorder characterised by intellectual disability, caused by mutations in the methyltransferases *KMT2D* (Ng et al., 2010). Studies analysing the effects of *KMT2D* loss of neuronal differentiation similarly demonstrated an accelerated rate of neuronal maturation (Carosso et al., 2019). Results of this work revealed premature increases in *MAP2*, *TUBB3* and *ASCL1* as seen in my results, along with various other proneural genes. Similarly, Wiedemann-Steiner syndrome is disorder caused by mutations of the methyltransferase *KMT2A*, characterised by intellectual

disabilities and brain malformations (Nardello et al., 2021). The loss of *KMT2A* has been shown to lead to premature decrease in neuronal progenitors, accompanied by increases in differentiated neurons (Cederquist et al., 2020). Furthermore, analysis of *KMT2A* deficient zebrafish embryos revealed although proliferation remained unaffected, neurons showed precocious differentiation as early as 16 hours post-fertilisation (Huang et al., 2015). Mutations in the histone methyltransferase, *EZH2*, have also been shown to directly cause premature neuronal differentiation. Following an initial increase, *PAX6* levels are significantly decreased and developmental timing is drastically advanced, with increased numbers of initial neurons, but reduced brain size overall (Pereira et al., 2010). These findings demonstrate premature neuronal differentiation and reduced proliferation are distinct convergence points for a number of neurodevelopmental disorders.

5.5 Conclusion

This chapter demonstrated the significant disruption of brain specific miRNAs following the *EHMT1* induced loss of REST. The precocious elevation of both miR-124-3p and miR-9-5p induced accelerated neuronal maturation to a terminally differentiated neuronal state. This precocious maturation was shown to be as a direct cause of *EHMT1* loss and seen in inhibitor treatment, as well as CRISPR edited and patient cell lines. Importantly, these effects by *EHMT1* loss were reversible in the early stages of neuronal development but fixed beyond day 20 of differentiation. Thus, *EHMT1* controls an important epigenetic window in neurodevelopment, ensuring the timely progression of neuronal differentiation in the healthy brain.

6 Epigenetic crosstalk during neuronal differentiation

6.1 Introduction

Epigenetic modifiers create complex networks, independent of DNA sequence which act to regulate the transcriptome throughout development. Within these networks, histone modifiers do not act independently from one another, and as our understanding of epigenetics grows, there is significant evidence for epigenetic co-occupancy and crosstalk. Importantly this epigenetic crosstalk appears to play significant roles in the regulation of neurodevelopment.

One of the most long standing examples is that of bivalent genes, which display opposing repressive and activating marks, H3K27me3 and H3K4me3 respectively (Bernstein et al., 2006). Such bivalent genes are often developmental and frequently found in stem cells leading many to hypothesise such marks enable fine-tuning of development and timing (Nagarajan and Johnsen, 2016). This is supported by the fact that the loss of H3K27me3 marks on these genes do not automatically translate to increased expression (Banaszynski et al., 2013). Bivalent genes have also been found in neural progenitor cells, where paused genes were most often those activated in neurons (Liu et al., 2017a). Once more, loss of H3K27me3 marks did not immediately lead to an increase in gene expression. Moreover, bivalent domains have also been shown to be instrumental to cerebellum development, primarily around H3K27me3, with disruption leading to accelerated neuronal maturation (Matlik et al., 2023). These results suggest bivalent genes play a significant role in the regulation and timing of proper brain development.

Co-occupancy of histone marks is not limited to opposing mechanisms and cooperative epigenetic modifications are often seen on the same transcripts or histone tails. For example, the repressive marks H3K9me2 (encoded by EHMT2) and H3K27me3 (encoded by EZH2) share a number of common targets. Simultaneous inhibition of both EZH2 and EHMT2 was found to be significantly more effective at inducing gene expression than individual inhibition (Curry et al., 2015). Importantly, a number of genes were not expressed following individual inhibition, inferencing dual targeting develops a level of expression patterning for fine-tuned expression. Similar results have also been seen in multiple myeloma samples, where EHMT2

and EZH2 collectively target genes involved in the regulation of proliferation (Ishiguro et al., 2021).

Beyond their close proximity, recent research suggests a more intertwined role for H3K9me2 and H3K27me3 writers. Studies have shown that the EZH2 containing complex PRC2 and its mark H3K27me3, cooperate with the H3K9me2 mark to ensure the stability and function of heterochromatin protein 1 alpha (HP1α) (Boros et al., 2014). Whilst H3K9me2 marks are required for the recruitment of HP1α to the chromatin, which in turn recruits the PRC2 complex to deposit H3K27me3 repressive marks. This relationship was further demonstrated in neural progenitor cells, where it was demonstrated H3K9me2/3 recruits HP1 to neuronal specific genes to recruit H3K27me3 and protect against demethylases (Naruse et al., 2020). Interestingly, loss of HP1 led to the loss of H3K27me3 at various neuronal specific genes and resulted in significant increased expression. Such work demonstrates the unique crosstalk between the H3K9me2/3 and H3K27me3 marks in neurodevelopment.

In addition to histone mark interaction, crosstalk has also been demonstrated between *EHMT1/2* and the PRC2 complex. Interplay between the two modifiers found that they not only physically interact, but that this binding had functional implications on target genes (Mozzetta et al., 2014). Interestingly, not only does EHMT2 recruit the PRC2 complex via EZH2, but this recruitment is specifically required for H3K27me3 activity at specific genomic loci. Moreover, the catalytic activity of EHMT2 was also shown to be vital for this functional recruitment. This unique binding activity was not global, but instead restricted to a subset of primarily neuronal determinant genes.

In contrast global changes have been identified across the zygote genome. Despite primarily methylating H3K9me2 residues, EHMT1 was found to be instrumental for the establishment of H3K27me2 within the male pronucleus (Meng et al., 2020). Interestingly, this function appears to be specific to the EHMT1 protein rather than the more prolific EHMT2 methyltransferase. Furthermore, the establishment of H3K27me2 was a prerequisite for the EZH2 mediated establishment of de-novo H3K27me3 marks. Despite these clear interactions between EHMT1 and EZH2 at various levels epigenetic control, their specific role in mediating neuronal differentiation and its time course remains unclear.

6.2 Chapter Aims

This chapter will investigate the epigenetic crosstalk between EHMT1 and EZH2, in relation to its role in neurodevelopment. Co-binding of epigenetic factors will be assessed, alongside specific genomic targets. To further assess the exact binding mechanics, various *EHMT1* mutant models will be generated and their impact on joint function analysed.

6.3 Results

6.3.1 Analysis of epigenetic co-binding

Transcription factor motif analysis in Chapter 3, identified significant enrichment for members of the REST complex in upregulated genes. Additionally, enrichment for the methyltransferase, EZH2 responsible for the methylation mark H3K27me3, was also identified. To better understand the global changes to global histone states induced by the loss of *EHMT1*, epigenomic enrichment analysis was performed on the upregulated genes of the *EHMT1*$^{+/-}$ day 30 RNA sequencing data set. Analysis revealed 14 methylation states were enriched, all of which were for the EZH2 methylation mark, H3K27me3 (Figure 6.1A). These results suggest significant enrichment of H3K27me3 targeted genes in *EHMT1* depleted neurons. The top three enriched sets were H3K27me3 H1 BMP4 derived trophoblast cultured cells (-Log=4.92), H3K27me3 Brain Hippocampus Middle (-Log=4.9) and H3K27me3 Neurosphere Cultured Cells Cortex Derived (-Log=4.57). Two of these top three targets are brain/neural specific, further implicating a disruption of H3K27me3 methylation in brain development. Indeed, of the remaining 11 enriched states, 2 are related to brain environment, H3K27me3 Brain Germinal Matrix (-Log=1.99) and H3K27me3 Brain Substantia Nigra (-Log=1.53). Interestingly the remaining methylation states, although all H3K27me3, appear to be from differing cell backgrounds, primarily pluripotent and haematopoietic. No enrichment was seen for H3K9me2 as it was not assessed across the 111 reference epigenomes (Kundaje et al., 2015).

Next, given that it has been reported that REST recruits both EHMT1/2 and EZH2 for genetic repression, Coimmunoprecipitation (Co-IP) was performed in hiPSCs to determine if the proteins colocalise and bind. Results of the pulldown analysis indicated a direct interaction between the EZH2 and EHMT1 proteins (Figure 6.1B). Likewise, analysis demonstrated a similar physical interaction for the REST protein (Figure 6.1C). These results demonstrate EZH2 is capable of forming a complex with both EHMT1 and REST, as has previously been reported. Furthermore, this suggests a number of neuronal targets potentially contain both H3K9me2 and H3K27me3 marks, deposited by EHMT1 and EZH2 respectively.

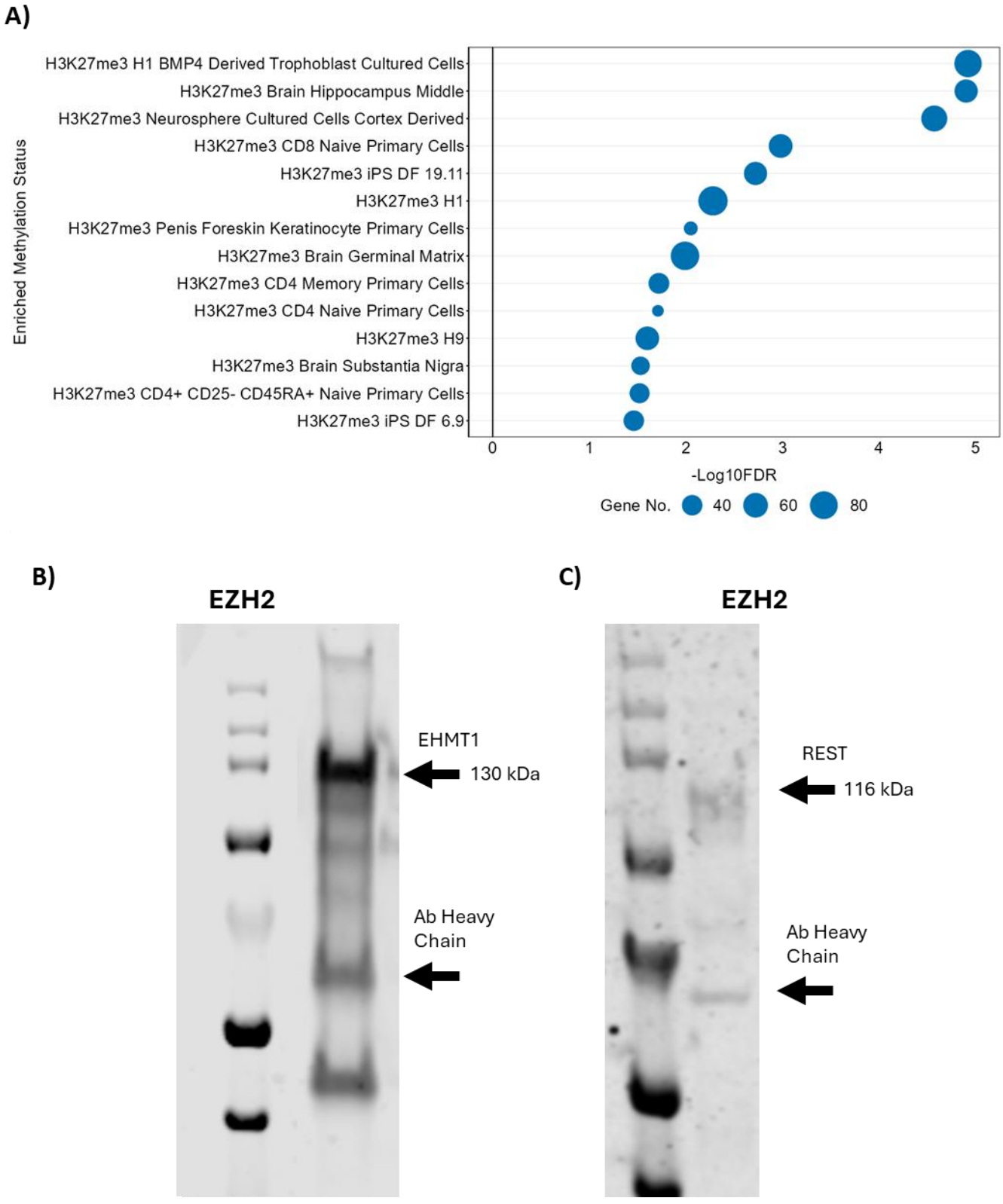

Figure 6.1 Co-binding analysis of epigenetic factors
A) *Methylation state enrichment analysis based on human ChIP-seq datasets.* ***B-C*** *Co-immunoprecipitation of EZH2 in hiPSCs by monoclonal antibody* ***B)*** *probed with EHMT1 antibody and* ***C)*** *probed with REST antibody. Ab heavy chain is present on the western blot and indicated by lower arrow.*

6.3.2 *Analysis of EZH2 in EHMT1 deficient cells*

From methylation enrichment results I reasoned H3K27me3 appears to be significantly dysregulated in *EHMT1* deficient neurons and therefore wanted to assess whether this was caused by a disruption in EZH2. To do this I analysed EHMT1 protein levels by western blot at the previously identified timepoints of differentiation day 0 (hiPSCs) and day 30 following treatment with UNC0638 (400nM).

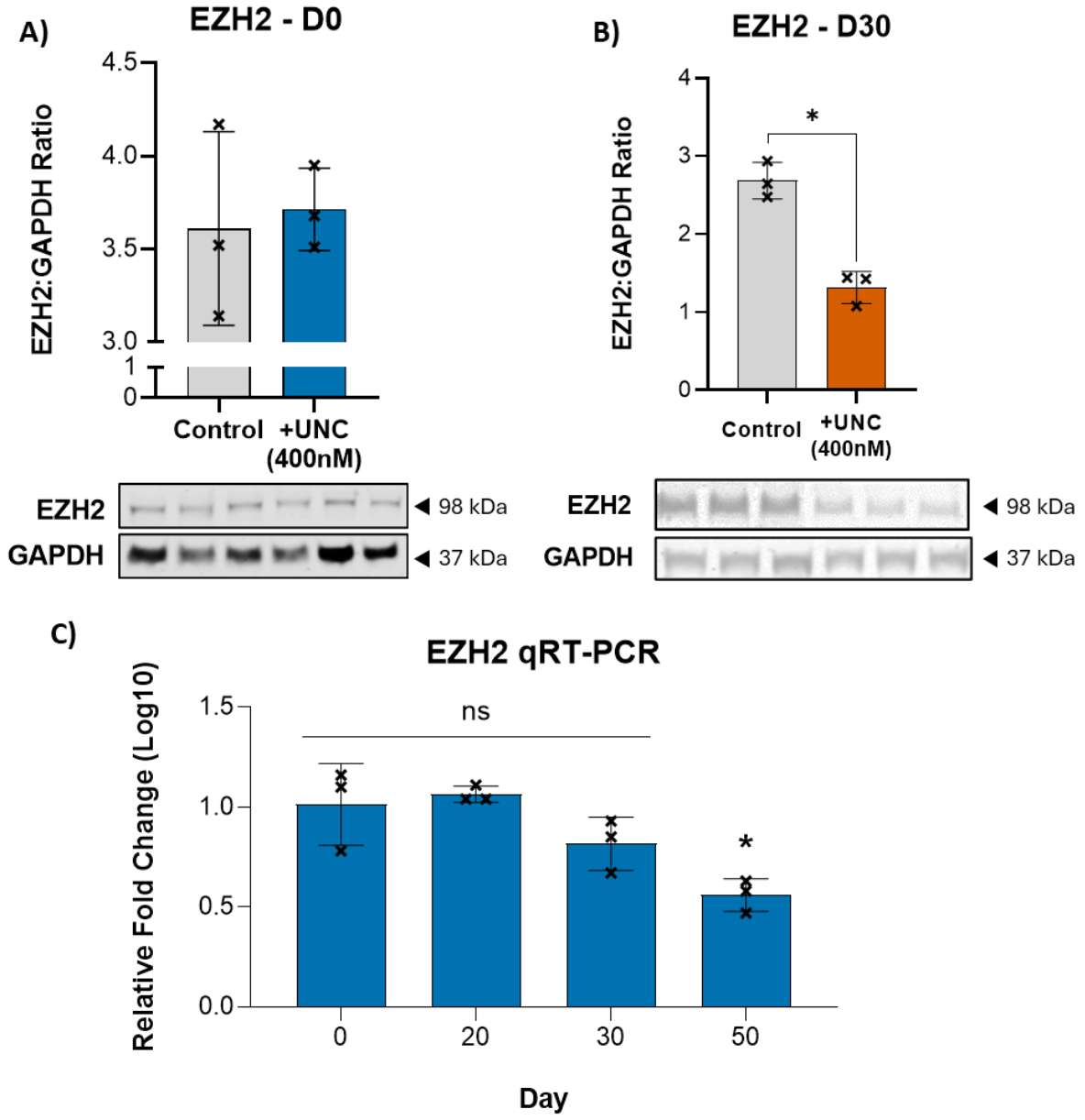

Figure 6.2 Analysis of EZH2 expression in EHMT1 depleted cells during neuronal differentiation
A) *Western blot analysis of EZH2 protein expression in hiPSCs (Day 0) treated with 400nM UNC0638.* ***B)*** *Western blot analysis of EZH2 protein expression in neurons (Day 30) treated with 400nM UNC0638.* ***C)*** *Expression analysis of EZH2 by qRT-PCR during various days of neuronal differentiation (Day 0-50), with each timepoint relative to vehicle only control. Data were presented as Mean±SEM and analysed by student's t-test. *P < 0.05. n=3 independent experiments.*

Analysis indicated no change in EZH2 protein levels at day 0 despite inhibition of EHMT1 (Figure 6.2A). In contrast, levels at day 30 were significantly lower than control, with a 50% reduction (1.32±0.21 Vs. 2.69±0.23, p=0.032) (Figure 6.2B).

In an attempt to understand if this change in EZH2 protein was reflected in the transcriptional expression, qRT-PCR analysis was performed on cells treated with UNC0638 (400nM) and differentiated until day 50 (Figure 6.2C). As seen with protein levels, expression of *EZH2* remained unchanged at day 0, with levels highly comparable to control. Likewise at day 20 there was no significant change in expression. Although modestly decreased at day 30, the change in expression was not significant (0.82±0.13, p=0.057). This is contrast to the results of the western blot, which indicated a significant reduction at day 30, however a similar response was seen with REST in chapter 3 which demonstrated significant reductions in protein but not transcription. These results suggest a global loss of *EZH2* in *EHMT1* depleted cells beyond day 30 of neuronal differentiation.

6.3.3 Epigenetic crosstalk of EHMT1 and EZH2

Although a global loss of EZH2 was not identified in hiPSCs, given the colocalization of EHMT1, EZH2 and REST, paired with the discovery that REST is lost following EHMT1 inhibition, I wanted to probe this connection further. Previous studies have identified the paralog EHMT2 forms a ternary complex with the EZH2 containing PRC2 complex and REST, at the promoter of neuronal genes (Mozzetta et al., 2014). I therefore performed ChIP-qPCR on the neuronal genes *VSTM2L* and *ROBO3* in *EHMT1* heterozygous mutant cells (*EHMT1*$^{+/-}$). Both *VSTM2L* and *ROBO3* showed significant enrichment for H3K9me2 in control samples, with mean peak fold changes of 20.85±3.02 and 14.81±1.35 as compared to IgG respectively (Figure 6.3Ai, Bi). Similarly, both *VSTM2L* and *ROBO3* also showed significant enrichment for H3K27me3 in control samples, with mean peak fold changes of 19.28±1.66 and 18.30±2.72 compared to IgG respectively (Figure 6.3Aii, Bii). Importantly, in *EHMT1*$^{+/-}$ samples, mean peak H3K9me2 fold change for *VSTM2L* and *ROBO3* drops to 4.03±0.43 and 2.11±0.79 respectively. Even more interestingly however, large drops are also seen in H3K27me3 marks, with mean peak fold change for *VSTM2L* and *ROBO3* decreasing to 4.72±0.62 and 2.48±1.45 respectively. These results strongly indicate that both EHMT1 and EZH2 target common neuronal genes. Moreover, the loss of EHMT1 is sufficient to also induce significant loss of the EZH2 mark, H3K27me3 on these coregulated genes.

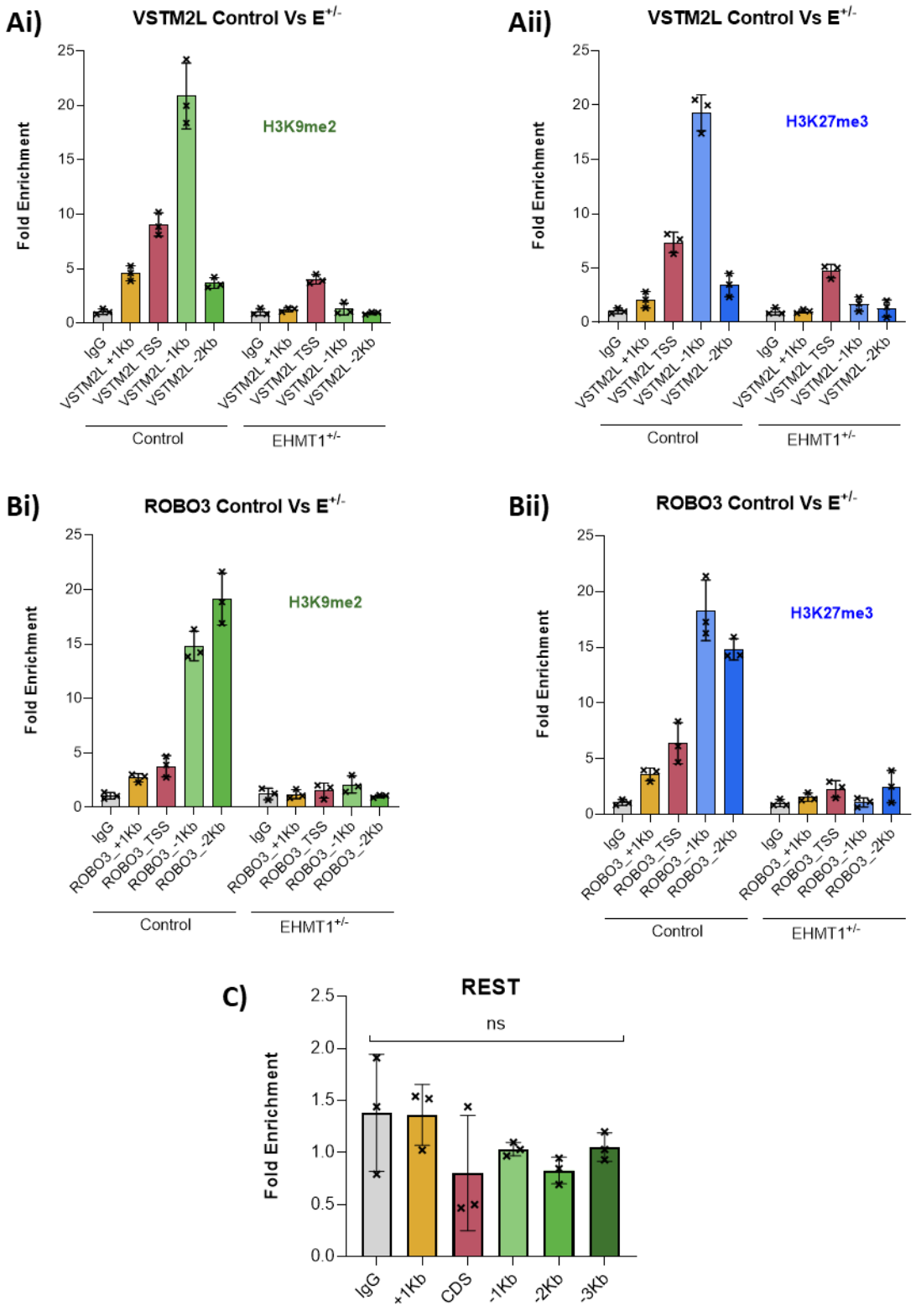

Figure 6.3 ChIP-qPCR analysis of neuronal genes in EHMT1 depleted cells
*ChIP-qPCR analysis of **A)** VSTM2L in EHMT1 heterozygous mutant hiPSCs for **i)** H3K9me2 marks and **ii)** H3K27me3 marks. **B)** ROBO3 in EHMT1 heterozygous mutant hiPSCs for **i)** H3K9me2 marks and **ii)** H3K27me3 marks. **C)** ChIP-qPCR to analyse H3K9me2 marks on the REST promoter in control hiPSCs. Data were presented as Mean±SEM. n=3 independent experiments.*

As REST was also shown to be in a ternary complex with both EHMT1 and EZH2, the *REST* gene itself was analysed for potential methylation by H3K9me2. No enrichment was seen for H3K9me2 marks on *REST*, indicating the gene was not directly regulated by EHMT1 (Figure 6.3C).

Given that both these genes are targeted by REST, it would be natural to assume the loss of H3K27me3 could be explained by the failure of REST to recruit EZH2. However, EHMT2 and EZH2 are also reported to target REST independent genes involved in early differentiation (Zylicz et al., 2015). In order to analyse the interaction of EHMT1 and EZH2 independently of REST, ChIP-qPCR was again performed on the developmental genes *OTX2* and *SALL2* in *EHMT1* heterozygous mutant cells (*EHMT1*$^{+/-}$). Neither *OTX2* or *SALL2* contain RE1 sites and are not regulated by the REST complex. As such interactions between EHMT1 and EZH2 on these genes are not mediated by the REST complex.

Both *OTX2* and *SALL2* were strongly enriched for H3K9me2 methylation in control samples, with mean peak fold enrichment of 152.27±15.26 and 19.36±6.79 as compared to IgG respectively (Figure 6.3Ai, Bi). Again, as seen previously with neuronal genes, both *OTX2* and *SALL2* displayed enrichment for H3K27me3 methylation also, with mean peak increases of 27.23±9.54 and 8.61±3.01 respectively (Figure 6.3Aii, Bii). These results demonstrate EHMT1 and EZH2 are able to colocalise on developmental genes independently of the REST complex.

As seen previously, *EHMT1*$^{+/-}$ samples displayed significant reductions in H3K9me2 enrichment for both *OTX2* and *SALL2*, with mean peak fold enrichment of 24.85±13.69 and 2.18±0.37 respectively. Likewise, enrichment of H3K27me3 was simultaneously also reduced, with mean peak fold enrichment of 6.94±0.77 and 2.45±2.71 respectively. This further implicates a cooperative function for EHMT1 and EZH2, indicating either the presence or catalytic function of EHMT1 is required for H3K27me3 methylation at specific genes. Importantly conducting these experiments in the *EHMT1* heterozygous lines demonstrate it is the function of EHMT1 and not only its paralog EHMT2 that is capable of epigenetic crosstalk with factors such as EZH2 and REST.

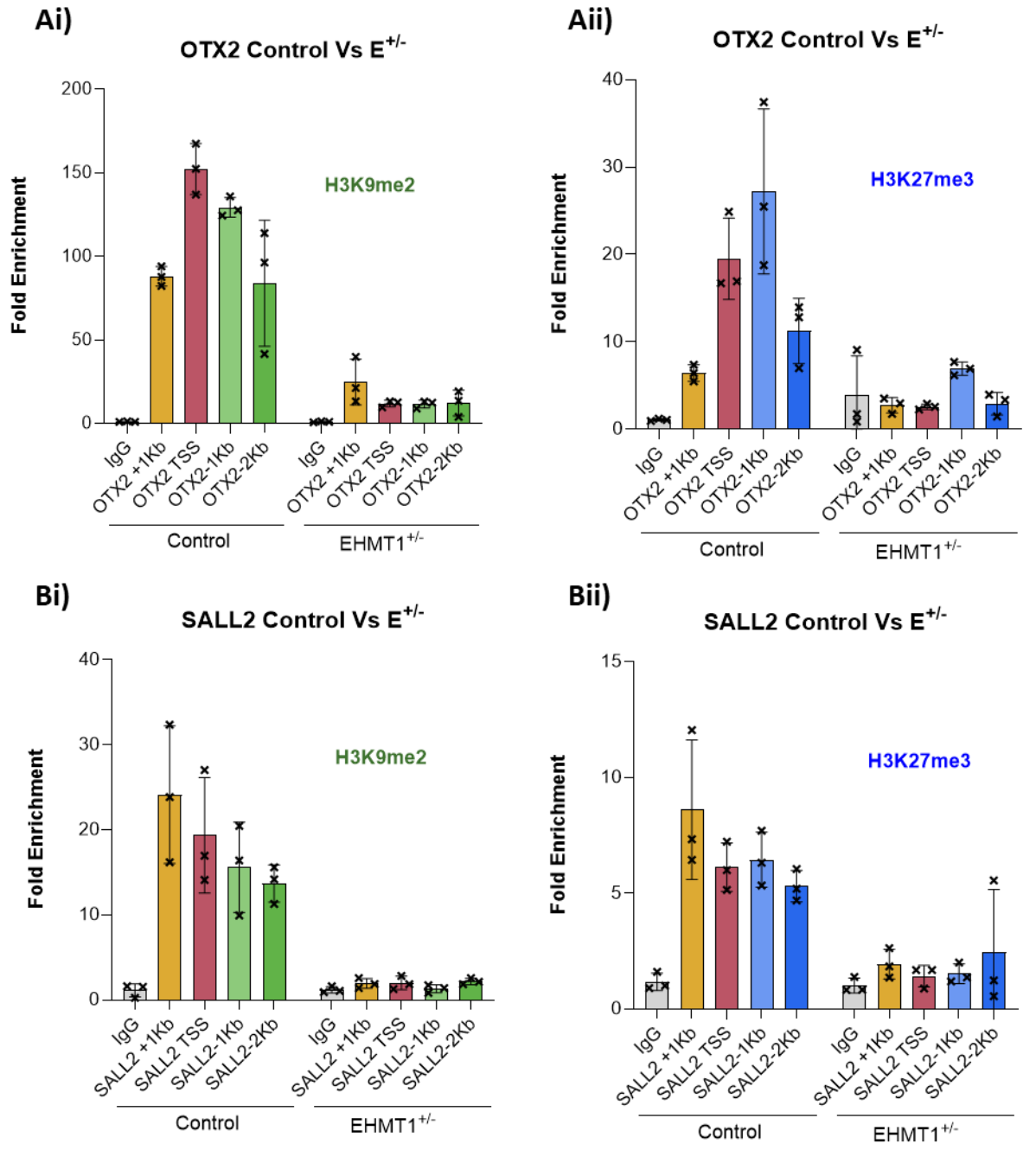

Figure 6.4 ChIP-qPCR analysis of developmental genes in EHMT1 depleted cells
*ChIP-qPCR analysis of **A)** OTX2 in EHMT1 heterozygous mutant hiPSCs for **i)** H3K9me2 marks and **ii)** H3K27me3 marks. **B)** SALL2 in EHMT1 heterozygous mutant hiPSCs for **i)** H3K9me2 marks and **ii)** H3K27me3 marks. Data were presented as Mean±SEM. n=3 independent experiments.*

6.3.4 EHMT1 mutants and EZH2 function

Previous studies probing epigenetic crosstalk between EHMT2 and EZH2 have suggested that not only are the two proteins capable of physical binding, but also that this interaction is instrumental for their function at specific genomic targets (Mozzetta et al., 2014). To test if EHMT1 and EZH2 could similarly bind directly and at what region of the protein, I generated

various *EHMT1* mutants. The EHMT1 protein is comprised of a N-terminus, Ankyrin repeat region, pre-SET and SET domain, and C-terminus (Figure 6.5A). To probe the binding potential of each of these I generated a HA-tagged EZH2 protein, along with flag tagged full length *EHMT1* (FL) and various mutants with missing regions of the protein. To assess the binding capacity, HA-tagged EZH2 was co-transfected with the various *EHMT1* mutants or eGFP as a negative control before Co-IP was performed (Figure 6.5B). Results of the Co-IP indicated strong binding between the full length EHMT1 (EHMT1-FL) and EZH2 (Figure 6.5C), demonstrating the two proteins do indeed directly bind to one another. In addition to the full-length EHMT1, the SET (AB) and the ankyrin repeat (A) deletion mutants also demonstrated binding with EZH2, however no binding was seen with the N-terminal deletion (BC). These results strongly suggest EHMT1 binds EZH2 via its N-terminal region.

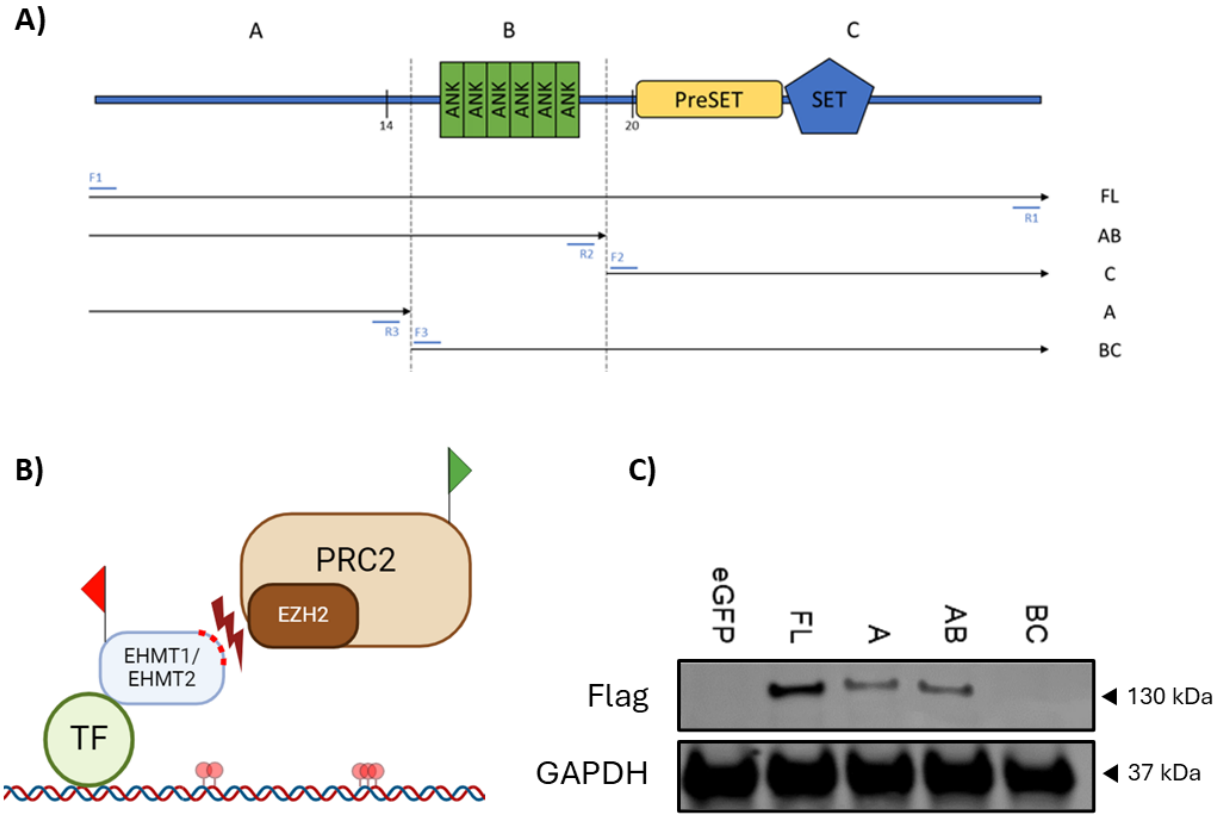

Figure 6.5 Generation and testing of EHMT1 mutants
A) *Schematic showing the structure of the* EHMT1 protein *and the associated mutants. Region A contains the C-terminus, region B the ankyrin repeats and C the pre-Set and Set domains. Exons 14 and 20 are marked on the schematic.* ***B)*** *The hypothesised binding between EHMT1 and EZH2, mutants contain either a flag tag (red) or HA-tag (green).* ***C)*** *Western blot against a flag tag antibody following immunoprecipitation with HA-tag. eGFP was used as a negative control.*

I reasoned that if EHMT1 could directly bind to EZH2, it may also recruit the protein to specific genomic regions and regulate its methylating function, H3K27me3. To test this theory a GAL4 reporter system was used to localise the various EHMT1 mutant proteins to the promoter of a reporter gene. The recruitment of EHMT1 and EZH2, and their methylation marks H3K9me2 and H3K27me3 at the reporter were then assessed by ChIP-qPCR to assess the impact of the various mutants (Figure 6.6A). To further understand the EHMT1 recruitment dynamics a catalytically inactive mutant (EHMT1ΔCat), with a point mutation in the SET domain was also included. This is a structurally intact protein but lacks the ability to deposit H3K9me2 methylation. Additionally, KMT5A, a methyltransferase responsible for the methylation of H4K20 and with no co-reactivity with EHMT1, was utilised as a negative control.

Analysis by ChIP-qPCR indicated all GAL4 fusion proteins were successfully recruited to the promoter of the reporter gene (Figure 6.6B). Subsequently H3K9me2 analysis revealed only EHMT1-FL showed significant enrichment, with a 7.52-fold increase (% Input 0.67±0.13, $p<0.0001$) compared to KMT5A control (% Input 0.089±0.015) (Figure 6.6C). EHMT1-AB (% Input 0.11±0.024), EHMT1-BC (% Input 0.14±0.033) and EHMT1ΔCat (% Input 0.19±0.036) all appeared incapable of depositing H3K9me2 despite binding to the reporter promoter.

The binding of EZH2 was then assessed by ChIP-qPCR for all samples. In this instance EHMT1-FL (% Input 0.23±0.071, $P<0.0001$), EHMT1-AB (% Input 0.19±0.058, $p<0.0001$) and EHMT1ΔCat (% Input 0.21±0.061, $p<0.0001$), all showed significant enrichment for EZH2 binding as compared to KMT5A control (% Input 0.0078±0.0015) (Figure 6.6D). However, EHMT1-BC (% Input 0.016±0.0047), the only fusion protein lacking the N-terminus region showed no enrichment for EZH2. This supports the previous results which indicate *EHMT1* binds via its N-terminal region to EZH2.

Finally, enrichment for the EZH2 methylation mark, H3K27me3 was assessed. As expected, EHMT1-FL showed significant enrichment (% Input 0.69±0.17, $p<0.0001$) as compared to KMT5A control (% Input 0.089±0.011) (Figure 6.6E). Likewise, EHMT1ΔCat also showed significant enrichment (% Input 0.58±0.10, $p<0.0001$) for H3K27me3 as compared to KMT5A, indicating the catalytic activity of EHMT1 was not required for H3K27me3 methylation. Conversely, neither EHMT1-AB or EHMT1-BC were able to induce H3K27me3 methylation at the reporter gene. In the case of the AB mutant this is most likely due to a lack of EZH2 binding

and recruitment. However, for the BC mutant it appears the SET domain, but not its catalytic activity is required for H3K27me3 methylation.

Collectively these results indicate EHMT1 binds via its N-terminus to EZH2 and is required for its recruitment to specific genomic regions. The SET domain of EHMT1, but not its catalytic activity is also required for H3K27me3 methylation at these genes. This suggests the structural presence of the EHMT1 SET domain is integral to this process.

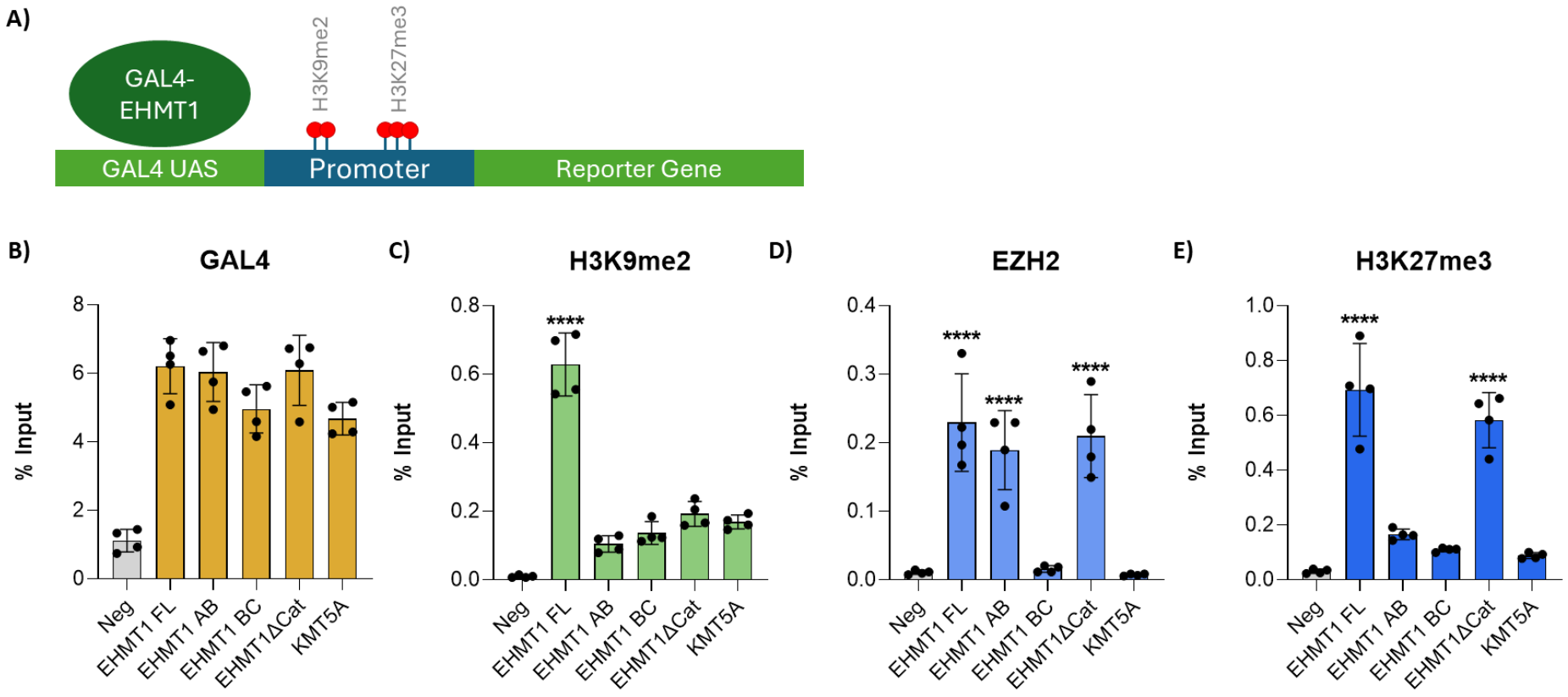

Figure 6.6 EHMT1 mediated recruitment of EZH2

Samples were transfected with a GAL4 UAS reporter and varying GAL4 fused mutants. ***A)*** *Overview of the GAL4 reporter system. Samples were subsequently immunoprecipitated and ChIP-qPCR analysis was performed at the reporter promoter for* ***B)*** *Gal4* ***C)*** *H3K9me2* ***D)*** *EZH2* ***E)*** *H3K27me3. Data were presented as Mean±SEM. and analysed by One-way ANOVA with post hoc comparisons using Tukey's multiple comparisons test comparing to KMT5A control samples. *P < 0.05, **P < 0.01, ***P < 0.001. n=4 independent experiments.*

6.4 Discussion

Here I focused on deciphering the interplay between EHMT1 and other epigenetic factors, particularly how this interaction is disrupted when *EHMT1* levels are depleted. Results of my bioinformatic analysis on *EHMT1*$^{+/-}$ neurons revealed significant enrichment for the REST motif around upregulated genes (Figure 3.5A). Within this analysis, the histone methyltransferase EZH2 also showed significant enrichment.

To better understand the implications of EHMT1 loss on various other histone modifications across the genome, enrichment analysis was performed using the epigenomes roadmap model. Histone modifications in the *EHMT1*$^{+/-}$ RNA seq dataset revealed huge enrichment for the H3K27me3 methylation mark on upregulated genes, indicating a dysregulation of its catalytic protein, EZH2. Importantly, a majority of these enriched epigene datasets were from neuronal cells or tissues, again reinforcing a genetic shift toward a neuronal subtype.

Previous work has shown that EHMT1*/2*, EZH2 and REST form a ternary complex (Mozzetta et al., 2014). Results of co-immunoprecipitation analysis in iPSCs revealed EZH2 was indeed capable of binding to both the EHMT1 and REST protein, indicating a closely associated role for the three proteins. Interestingly REST is well known to recruit the EZH2 containing PRC2 complex to co-regulate a number of neuronal genes. Despite this, most REST targets appear to be regulated independently of the PRC2 complex (McGann et al., 2014). Indeed, REST knockdown studies in mESCs show that although global levels of EZH2 and H3K27me3 remain unchanged, REST-PRC2 appears to regulate a subset of genes including, *BRUNOL6*, *BEST2* and *PRRXL1* (Dietrich et al., 2012). This study also highlighted this recruitment is potentially context dependent, with PRC2-EZH2 preferentially recruited to RE1 sites in CPG islands. These results were supported by other studies which also demonstrated REST-PRC2 co-bound preferentially on CGP rich sequences (Arnold et al., 2013). Previous work has also shown that the REST protein binds to EHMT2 via its C-terminal domain (Roopra et al., 2004). Moreover, results indicated EHMT2 function was essential for efficient repression of neuronal REST target genes. Studies inhibiting both REST and EHMT2 indicate that the two proteins work to induce a reversible plastic state in neuronal development (Crews et al., 2023).

Following the histone modification analysis, I wanted to further probe the role of EZH2 in neuronal development. The deregulation of so many H3K27me3 marked and EZH2 targeted

genes in *EHMT1*$^{+/-}$ early neurons strongly suggested a global loss of EZH2 regulation. Hypothesising that this may be due to a significant loss of EZH2 protein, western blot analysis was performed on *EHMT1* depleted neurons and stem cells. As proposed, *EHMT1* depleted cells showed a significant reduction in EZH2 protein at the early neuronal stage, but no change was seen in stem cells. This drop in protein was accompanied by a significant decrease in transcription at later stages, indicating a systemic loss of EZH2 expression during differentiation. This differs from earlier results that demonstrated a loss of REST from the stem cell stage and throughout neuronal differentiation. This finding strongly aligns with REST knock out studies which demonstrated a loss of REST leads to no significant change in global H3K27me3 levels at the stem cell stage but saw significant reductions at the NPC stage (Arnold et al., 2013). This work also demonstrated that REST is also associated with a transient H3K27me3 peak in neuronal progenitors. This finding is in line with a recent study that demonstrated EZH2 and EHMT1 induce a temporal epigenetic roadblock, holding progenitor cells in a poised state that is gradually released as differentiation progresses (Ciceri et al., 2024).

A likely explanation for this premature loss of EZH2 is the significant increases in brain specific miRNAs. Recent studies have presented substantial evidence that EZH2 expression is directly regulated by miRNAs during neuronal differentiation. Overexpression of miR-124-3p was shown to activate a fraction of neuronal specific EZH2 targets, whilst expression of a mutant EZH2 lacking miR-124-3p binding sites resulted in a shift from neuronal to astrocyte specific cells (Neo et al., 2014). Similarly, overexpression of miR-124-3p and miR-9-5p in fibroblasts leads to neuronal trans-differentiation, accompanied by a significant reduction in EZH2 protein (Lee et al., 2018). Not only did miR-124-3p directly inhibit EZH2, but the combined effects of the miRNAs also inhibited the deubiquitinating enzyme *USP14* which normally stabilises EZH2. Finally, analysis of mature hippocampal neurons revealed increased miR-124-3p expression during neuronal maturation directly targets EZH2 and downregulates the protein (Guajardo et al., 2020). Importantly this work also demonstrated that EZH2 remains elevated in early progenitor cells, indicating this loss aligns with a maturation of neuronal cells. Beyond neuronal cells, reduced miR-124-3p expression has also been shown to lead to elevated EZH2 and in turn increased proliferation in prostate, bile and gastric cancer (Song et al., 2023, Ma et al., 2018, Xie et al., 2014). Based on my previous findings that *EHMT1*

mediated loss of REST culminates in the premature and sustained increase of miR-124-3p and miR-9-5p, it is highly likely this leads to the observed loss of EZH2. This indicates a second irreversible epigenetic ratchet in normal brain development that is disrupted following the loss of *EHMT1*. However, further work is required to confirm this hypothesis, with experiments focusing on miR-sponges against miR-124-3p or the generation of 3'UTR deficient EZH2 mutants required.

Although no change was seen in total EZH2 protein levels at the stem cell stage, I wanted to probe the possible disruption of EHMT1-EZH2 co-bound target genes. Previous work has demonstrated that the EHMT1 paralog, EHMT2, co-binds with the PRC2 complex to regulate a number of early neuronal targets in stem cells (Mozzetta et al., 2014). Therefore, I aimed to assess if such targets were impacted following the loss of *EHMT1* at the pluripotent stage. A ChIP-qPCR analysis targeting *VSTM2L* and *ROBO3*, markers of early neuronal development, showed these genes co-localized with repressive histone marks H3K9me2 and H3K27me3 deposited by EHMT1 and EZH2, respectively. Crucially, analysis of *EHMT1*$^{+/-}$ cells indicated a loss of not only H3K9me2 methylation, but also H3K27me3 at these genes, despite no change in global H3K27me3. This data implies the loss of *EHMT1* in turn leads to the loss of H3K27me3 in a gene specific manner.

One plausible explanation for this loss of H3K27me3 is the concurrent loss of REST already established at the pluripotent stage. As neither EHMT1/2 or EZH2 are capable of independently binding to DNA, they are reliant on other factors to recruit them to specific regions. As discussed previously, REST is capable of recruiting both EHMT1/2 (Roopra et al., 2004) and EZH2 (Dietrich et al., 2012) to DNA regions, potentially mediating silencing in a cell specific manner. Therefore, the loss of REST may result in the inability of EZH2 to bind and hence the almost total loss of H3K27me3 at *VSTM2L* and *ROBO3* promoters. Indeed the REST complex has been shown to actively recruit both EHMT2 and EZH2 to silence active HIV virus in microglia (Ye et al., 2022). It has also been suggested that the dual activity of both EHMT2 and EZH2 are required to establish HIV-1 latency (Nguyen et al., 2017), thus highlighting the functional importance of this dual binding.

Additionally, EHMT1/2 is known to undergo auto methylation, which was found to be fundamental for its binding to factors such as CDYL and HP1 (Sampath et al., 2007, Chin et al., 2007). It is therefore plausible that *EHMT1* regulates its binding to other factors, including

REST and EZH2, via its auto methylation of itself and EHMT2. Furthermore, EZH2 has been found to directly methylate EHMT2, increasing its ability to recruit repressive complexes (Pham et al., 2020). Surprisingly, one recent publication suggested EHMT1/2 directly repressed the REST protein in direct contrast to my findings. Importantly analysis of the REST promoter indicated that it was devoid of H3K9me2 marks, indicating a lack of EHMT1/2 regulation.

Although the loss of REST seems a logical explanation for the gene specific reduction in H3K27me3 levels, both EHMT1 and EZH2 have also been reported to co-bind to other non-REST target genes (Zylicz et al., 2015). Two REST independent genes, *OTX2* and *SALL2*, were selected to assess if they were similarly dual targeted. The correct expression of *SALL2* is vital for proper neurodevelopment (Böhm et al., 2008), while the loss of SALL proteins leads to the premature differentiation of pluripotent cells (Pantier et al., 2021). Conversely, *OTX2* is an essential developmental regulator, acting to repress neuronal differentiation (Bai et al., 2012). As with the REST dependent targets, both *OTX2* and *SALL2* were enriched for H3K9me2 and H3K27me3 methylation at their promoter. Interestingly, as before *EHMT1*$^{+/-}$ cells showed both a loss of H3K9me2 and H3K27me3 methylation specific to the two genes. This finding strongly suggests the site-specific loss of H3K27me3 is not simply due to a loss of REST as a binding factor. Moreover, it implies the co-binding of EHMT1 and EZH2 is not specific to REST and other transcription factors are likely able to recruit the HMTs.

One factor that is routinely found to co-bind to EZH2 and often referred as a recruitment factor is JARID2 (Sreeshma and Devi, 2023, Pasini et al., 2010, Kaneko et al., 2014). Importantly, knockout of JARID2 significantly impacts the ability of pluripotent cells to undergo multilineage differentiation (Li et al., 2010, Landeira et al., 2010). Likewise JARID2 has also been shown to bind and recruit EHMT1/2 to genes such as *CCND1*, which it subsequently methylates (Shirato et al., 2009). Additionally JARID2 also displays significant target overlap with EHMT1/2 binding sites (Mozzetta et al., 2014), further implicating it as a potential HMT co-binding partner.

Recently, studies have also demonstrated the nuclear receptor PALI1 (also known as LCOR) may also be a strong candidate as a common partner between the two HMTs. Research suggests that PALI1 has evolved as a conserved mimic to the JARID2 protein, allosterically activating the PRC2 complex through EED binding (Zhang et al., 2021a). Importantly this work

demonstrated PALI1 acts as a bridge between both EHMT1/2 and EZH2, suggesting this dual binding is required to maintain PALI1 stability. Another more recent study has demonstrated that PALI1-EZH2 is actively recruited by EHMT2 to methylate H3K27 at a subset of specific genes (Fong et al., 2022). Astonishingly it was demonstrated that knockdown of EHMT2 lead to a global loss of H3K9me2, accompanied by the specific loss of H3K27me3 at specific genes. This aligns directly with my own results which indicate a similar response following the loss of *EHMT1*. Moreover, the PALI1 co-binding of the two HMTs was shown to induce dedifferentiation of cells, again further demonstrating the role of epigenetic crosstalk in developmental regulation.

In addition to JARID2 and PALI1, the chromatin binding protein CDYL has also been implicated in joint EHMT/EZH2 binding. Research into the role of CDYL has demonstrated the chromodomain protein is required for the proper deposition of histone marks during cell replication (Liu et al., 2017b). The CDYL protein jointly recruits both EHMT1/2 and EZH2 simultaneously to induce H3K9me2 and H3K27me3 marks. Interestingly, work has also shown that CDYL relies on H3K9me2 marks for its association with chromatin and implicates the combined effects of EHMT2 and EZH2 as prerequisites for CDYL binding (Escamilla-Del-Arenal et al., 2013). Adding complexity to this regulation, CDYL has also been found to bind to the REST complex, where it recruits EZH2 and G9a to regulate BDNF expression during neuronal development (Qi et al., 2014). More recently, CDYL was also shown to simultaneously recruit both EHMT2 and EZH2 to MIR124 genes in breast cancer cells, depositing both H3K9me2 and H3K27me3 marks (Siouda et al., 2020). This work suggested that although CDYL is capable of binding to EZH2 weakly, primary binding between the two proteins was via EHMT2. Again, this would align with my results, where a loss of *EHMT1* would concurrently lead to a reduction in both H3K9me2 and H3K27me3 at target genes. Collectively these findings suggest *EHMT1* and EZH2 co-regulate a subset of developmentally enriched target genes via various nuclear binding factors. Several studies implicate binding of these factors and EZH2 is facilitated by EHMT1/2 as an intermediate. Further work is required to determine both the specific factors involved and categorising the specific genes targeted.

While extensive research has documented a physical interaction between EHMT2 and EZH2, similar studies investigating its paralog, EHMT1, are currently lacking. Given that the sequence for EHMT1 and EHMT2 are over 75% identical, I wanted to understand if EHMT1 and EZH2

physically bind in the same fashion. To this end I generated various *EHMT1* truncated mutants fused to a Flag tag, in addition to an HA fused EZH2 protein. The EHMT1 protein consists of roughly three main domains, the N-terminus containing a cysteine rich region, an ankyrin repeat responsible for reading H3K9 marks and a catalytic SET domain that generates de-novo H3K9me1/2 marks (Collins and Cheng, 2010). Both EHMT1 and EHMT2 form a heterodimer, in which they both bind via their respective SET domains (Tachibana et al., 2005). Mutant plasmids absent for each of these three regions was generated to understand both if and how EHMT1 may bind to EZH2. Results of a pulldown assay showed for the first time that EHMT1 does in fact bind to the EZH2 protein. Comparatively, the mutant lines showed slightly lower pulldown signal as compared to the full-length protein, most likely owing to the altered structure of the protein. Only the mutant lacking the cysteine rich N-terminus was unable to recover HA tagged EZH2 protein, indicating the two proteins bind via the N-terminus of EHMT1. These results replicate the previous finding of EHMT2 and EZH2, which was also found to bind at the N-terminus of EHMT2 (Mozzetta et al., 2014). In contrast binding to factors such as PALI1 was shown to occur at the ankyrin repeat region of EHMT2 (Fong et al., 2022) whilst factors such as SNAI1 bind at the C-terminal region of EHMT2 (Dong et al., 2012). These results indicate various mechanisms of protein binding by EHMT1 and EHMT2, though this appears consistent between paralogs. Additionally, shortened splice variants of human EHMT2 exist with a reduced N-terminal region (Brown et al., 2001). Levels of this splice variant have been shown to increase during neuronal differentiation (Fiszbein et al., 2016). Future work may benefit from exploring the EZH2 binding capacity of this splice variant and whether splicing is altered in *EHMT1*$^{+/-}$ cells.

Results have already demonstrated that a loss of *EHMT1* impairs both H3K9me2 and H3K27me3 methylation at specific genes. Moreover, *EHMT1* is able to directly bind via its N-terminus region to the EZH2 protein. Therefore, I wanted to further understand if *EHMT1* activity is required for H3K27me3 methylation by EZH2. To this end I generated GAL4 fused EHMT1 mutants for the SET deficient and N-terminal deficient mutants. Additionally, a catalytically inactive mutant was generated with a point mutation, which retained the SET domain of EHMT1 but lacked its methylating capability. As expected only the full length EHMT1 protein was capable of depositing H3K9me2 methylation marks on the luciferase reporter. In contrast all proteins with the exception of N-terminal deficient mutant were

capable of recruiting EZH2 protein to the promoter. This further supports binding of EHMT1 and EZH2 via the N-terminus region. Finally, both the full length EHMT1 and catalytic mutants were able to induce H3K27me3 methylation of the promoter. As expected, the N-terminal deficient mutant showed a loss of H3K27me3, explained by the absence of EZH2 recruitment. Studies have demonstrated that the paralog EZH1 can compensate for the loss of EZH2, particularly at bivalent promoters (Mochizuki-Kashio et al., 2015). However, my results indicate, at least in a reporter system, that the *EHMT1* mediated activity of EZH2 acts independently of EZH1 function. Interestingly, the SET deficient mutant also failed to induce H3K27me3 methylation, despite the successful recruitment of EZH2 protein. This suggests the structural function of the SET domain but not its catalytic activity is required for EHMT1 mediated H3K27me3 methylation. One possible explanation is that EHMT1 forms a heterodimer with EHMT2 via its SET domain. EHMT2 is capable of monomethylating H3K27 and disruption of this process has been shown to impede further H3K27 methylation (Wu et al., 2011).

This finding is supported by other studies which indicate the structural presence of EHMT1/2, but not their methylating activity is required for the recruitment of DNA methyltransferases (Collins and Cheng, 2010). However, another study indicated that a catalytically inactive EHMT2 protein was unable to recruit either EZH2 or induce H3K27me3 methylation (Mozzetta et al., 2014). This work suggests the catalytic activity of EHMT2 is somehow essential for the establishment of H3K27me3 marks at specific gene targets.

In contrast to this a recent study investigating the role of EHMT1 in the human zygote, demonstrated EHMT1, but not EHMT2 was indispensable for the establishment of de-novo H3K27me2 and in turn H3K27me3 methylation (Meng et al., 2020). It has been suggested the establishment of H3K27me2 marks are a prerequisite for H3K27me3 methylation, acting as both a substrate and protecting the lysine residue from antagonistic acetylation (Margueron and Reinberg, 2011). It is therefore possible EHMT1, independent of EHMT2, contributes to H3K27me2 methylation and in turn EZH2 mediated establishment of H3K27me3 at specific developmental genes. Importantly as seen in my work, this research demonstrated the SET domain was not required for EZH2 binding, whilst the structural presence of the SET domain but not its catalytic activity was required for H3K27me2/3 methylation. Hence as indicated in my findings the structural presence of the SET domain appears crucial for the establishment

of H3K27me3 methylation at specific targets. Future work would benefit from investigating the levels of H3K27me2 in addition to H3K27me3 at these genes regulated by both EHMT1 and EZH2.

Results of this chapter have demonstrated a number of developmental genes key to neurodevelopment are dually targeted by EHMT1 and EZH2, depositing H3K9me2 and H3K27me3 marks respectively. The abundance of chromatin marks in pluripotent cells has more recently been shown as a key mechanism in fine-tuning the transcriptional expression of genes during development and neuronal commitment. Traditionally this has most commonly been demonstrated within bivalent genes, marked simultaneously by both repressive H3K27me3 and activating H3K4me3 methylation marks (Voigt et al., 2012). The most recent data suggests bivalent genes are protected from irreversible silencing by DNA methylation, but maintained in a reversible silenced state (Kumar et al., 2021).

It has also been shown that trivalent states exist, in which bivalent genes are additionally marked with H3K9me3 methylation (Alder et al., 2010). Interestingly, trivalent marked genes have been shown to predict the neuronal trans-differentiation capacity of cells, with an absence of these trimethylated genes resulting in the inability to generate induced neurons (Wapinski et al., 2013). It was suggested this trivalent signature allows for a quick transition from a repressed to an active state. Both *OTX2* and *SALL2* highlighted in this work have been shown to be bivalent genes, displaying both H3K27me3 and H3K4me3 marks (Bunt et al., 2013, Huang et al., 2022b). Results of my work indicate these genes may also represent a trivalent state, marked by H3K4me3, H3K27me3 and H3K9me2 methylation. In this manner, EHMT1 appears to act alongside EZH2 at key developmental genes, recruiting the PRC2 complex in a cell state specific manner and stabilising the repressed state of these target genes.

6.5 Conclusion

Work in this chapter demonstrated that EHMT1 and EZH2 are capable of physically binding. *EHMT1* deficient cells show a significant premature reduction in in global levels of EZH2 in early neurons compared to controls. Interestingly although no change is seen in global EZH2 levels at the pluripotent stage several specific developmental genes demonstrated both a

simultaneous loss of H3K9me2 and H3K27me3. This effect was seen in both REST regulated and non-REST regulated genes. Subsequent reporter experiments demonstrated EHMT1 binds via its N-terminus to the EZH2 protein. Moreover, the SET domain of *EHMT1* but not its catalytic activity was required for the deposition of H3K27me3 in a reporter system. These results indicate EHMT1 and EZH2 are responsible for the dual regulation of various developmental genes during differentiation and lineage commitment. Whilst the loss of *EHMT1* leads to the premature de-repression of EZH2 globally, further committing to premature neuronal differentiation.

7 General Discussion

7.1 Summary of Findings

7.1.1 Chapter 3 Computational analysis of gene expression in cells lacking EHMT1

The main aim of this work was to identify key transcriptional changes in *EHMT1* deficient neuronal cells and the implications on cell type and development. To do this various bioinformatic analysis was conducted on publicly available RNA sequencing data from neurons with a heterozygous mutation. The chapter summarises the analysis of this data.

Key Findings:

- Depletion of *EHMT1* lead to a significant genetic shift toward a neuronal cell type, with a particular enrichment for brain specific neuronal cells
- Dysregulated genes showed significant overlap with various neurodevelopmental disorders
- Transcriptional changes are primarily driven by a loss of the REST protein
- The loss of REST protein was confirmed in pluripotent cells and persisted throughout neuronal differentiation

7.1.2 Chapter 4 Analysis of miRNAs in EHMT1 deficient cell models

Previous studies have suggested miRNAs play a key role in regulating REST protein levels. This chapter aimed to identify dysregulated miRNAs in response to the loss of *EHMT1*, performed using novel bioinformatic predictive pipelines. A novel multimiR sponge was then generated to probe the simultaneous activity of miRNAs on REST expression.

Key Findings:

- The novel predictive algorithm correctly predicted 14 upregulated miRNAs in *EHMT1* deficient neurons with an accuracy of 78%
- A significant number of miRNAs were known to be regulated by the REST complex
- Four *EHMT1* regulated miRNAs (miR-142-3p, miR-153-3p, miR-26a-5p, miR-140-5p) predicted to target REST upstream of the protein were identified as upregulated in pluripotent cells

- A novel multimiR-sponge was generated, capable of repressing up to three miRNAs simultaneously to probe the effect of multiple miRNAs in concert
- Multiple miRNAs, centred around miR-153-3p acted collaboratively to repress REST in *EHMT1* deficient cells, with multimiR-sponge treatment reversing this premature loss

7.1.3 Chapter 5The effect of EHMT1 loss on neuronal development and maturation

Previous studies have demonstrated miR-124-3p and miR-9-5p as the primary drivers of neuronal differentiation. This chapter describes the effect of *EHMT1* loss on these brain specific miRNAs and the subsequent implications on neuronal maturation and timing.

Key Findings:

- *EHMT1* depleted cells showed a significant premature increase in the expression of both miR-124 and miR-9-5p, demonstrating a temporal shift
- This shift was fixed by day 20 and could not be reversed with the reintroduction of H3K9me2 methylation
- Increased expression of these brain specific miRNAs at earlier timepoints culminated in increased neuronal maturation
- Treatment with multimiR-sponges at day 0 reversed the premature increases in brain specific miRNAs, as well as the accelerated rate of neuronal maturation

7.1.4 Chapter 6 Epigenetic crosstalk during neuronal differentiation

Alongside REST depletion, a loss of the epigenetic regulator EZH2 was also predicted in *EHMT1* deficient neurons following bioinformatic analysis. Previous studies demonstrated an epigenetic crosstalk existed between both EHMT1 and EZH2. This chapter describes the dysregulation of EZH2 at the neuronal and pluripotent stages.

Key findings:

- The EZH2 protein was shown to associate with both EHMT1 and EZH2 in control pluripotent cells

- The predicted loss of EZH2 was confirmed in neurons, with a significant global loss of protein seen in neuronal cells but not pluripotent cells
- Despite the lack of EZH2 loss in pluripotent cells, its methylation mark H3K27me3 was absent in a subset of developmentally significant genes, along with H3K9me2
- The combined loss of H3K9me2 and H3K27me3 occurred in both REST regulated and non-REST regulated genes
- Mutant plasmid experiments revealed the direct binding between EHMT1 and EZH2 is possible and occurs via the N-terminus of EHMT1
- GAL4 reporter work indicated the EHMT1 N-terminus is required for EZH2 recruitment, and the SET domain but not its catalytic activity is required for H3K27me3 methylation at specific gene targets

7.2 Context and points of discussion

7.2.1 Computational modelling of epigenetic disorders

Increasing numbers of genome wide association studies (GWAS) have revealed a clear association between epigenetic regulators and neurodevelopmental disorders that share similar clinical symptoms. While a strong link has been established, the precise functions and underlying mechanisms by which epigenetic regulators influence neurodevelopment remain largely unknown. In part this been convoluted by the complex networks consisting of epigenetic modifiers, protein coding genes and non-coding RNAs such as microRNAs. The development of induced pluripotent stem cells and CRISPR editing, combined with complex computational modelling, have provided the opportunity to contextualise these multilayered interactions throughout neurodevelopment. The computational modelling demonstrated in Chapter 3 and 4, presented a rapid and robust approach to identify the key genetic and phenotypic changes in a rare disease from high content omics data.

This is by no means the first study to combine these multiple modalities to probe neural conditions with similar backgrounds. Similar studies have used computational analysis of high content RNA sequencing and ChIP-sequencing data to demonstrate specific factors driving system level changes, such as de-differentiation in Alzheimer's disease (Caldwell et al., 2020). However, to date no such approach has been taken for the study of *EHMT1* and Kleefstra syndrome (KS). Following the discovery that mutations in the *EHMT1* gene are the causative factor behind KS (Kleefstra et al., 2006a), research surrounding KS has primarily focussed on the functional implications of the disorder. Work in heterozygous *EHMT1* mouse models, attempted to understand the effect on learning, memory, and cranial abnormalities (Benevento et al., 2017, Balemans et al., 2013). On the other hand, studies using cell models have explored how imbalances in the proportions of different neuronal cell types can underlie the disease pathobiology (Frega et al., 2019). Attention has also been placed on the molecular convergence between KS and similar disorders (Frega et al., 2020, Koemans et al., 2017), though the driving molecular mechanisms behind the disorder remained unclear. The work in Chapter 3 leveraged computational approaches to show the loss of *EHMT1* caused a dynamic transcriptional shift toward a neuronal subtype and an acceleration through progenitor stages. Importantly, motif analysis revealed that a lack of REST, as implicated by the collective de-repression of its targets, was the main cause for this precocious maturation.

Similarly, the development of novel miRNA prediction pipelines guided by transcriptomic data in Chapter 4, enabled the rapid and accurate identification of dysregulated miRNAs in EHTM1$^{+/-}$ cells. This transcriptomic approach importantly enables the consideration of many-many relationships of miRNAs that exist in disease states (Hashimoto et al., 2013). The approach reported here has been successfully reported in similar studies identifying novel biomarkers for Autism Spectrum Disorder (Shen et al., 2016). Indeed, the novel prediction pipelines developed in this work would be well suited to predicting and contextualising differentially expressed miRNAs in other rare diseases, alongside identifying potential novel biomarkers common to these disorders. Importantly, the proximity score provides for the first time the ability to consider the co-operation of neighbouring bound miRNAs as recently reported (Diener et al., 2023). Though previous studies have highlighted differences in *EHMT1*$^{+/-}$ miRNA expression previously using whole genome miRNA sequencing (Chen et al., 2014), the work failed to highlight the functional significance of these enriched miRNAs. The work presented here not only identified the key transcriptional driver in Kleefstra Syndrome but was also able to link the collective action of various miRNAs in a temporal manner.

Collectively, the computational methods developed and utilised in this work should provide a reliable technique for the investigation of various rare disease and neurodevelopmental disorders. Motif, enrichment, and miRNA prediction analysis can be performed concurrently on bulk RNA sequencing data from hiPSC derived neurons. One limitation of such analysis is the heterogeneity seen in disorders such as Autism or 22q deletion syndrome, leading to variable results between datasets. However, the increasing availability of public sequencing datasets paired with the rapid analysis enabled by the pipelines, will allow for the relatively high throughput screening of various datasets. Such repeat analysis should help to reveal key driving nodes in the network. While the computational modelling described in this work does not provide the same level of accuracy as compared to miRNA-sequencing or functional electrophysiological analysis, the contextual multisystem approach enables rapid contextualisation of the results. Such methods could be exploited to provide large scale screening studies, importantly helping to identify novel common pharmaceutical targets for further screening and analysis. The work presented here lay the groundwork for a unique and valuable approach to investigating the functionality of hPSC disease models, paving the way for the discovery of novel therapies.

7.2.2 Combinatorial microRNA analysis

Recent developments in the understanding of miRNA binding kinetics have demonstrated that rather than acting independently from one another, multiple miRNAs can simultaneously work to target a single gene transcript. This was first demonstrated when two miRNAs were able to repress the same synthetic mRNA transcript (Doench and Sharp, 2004). Subsequent work in 2010 through multiple mutation experiments, demonstrated 28 miRNAs were capable of targeting *CDKN1A*, with 5 miRNAs driving this action (Wu et al., 2010). Interestingly, research in 2017 revealed that even non-functional miRNAs could still amplify the silencing effects of other locally bound miRNAs (Flamand et al., 2017). Results presented in Chapter 4 highlighted this mechanism, for the first time indicating that multiple miRNAs acted collaboratively and simultaneously to repress the activity of the REST protein. This work builds on previous studies that demonstrate the link between several of these individual miRNAs and REST (Sauer et al., 2021, Gebhardt et al., 2014). Though studies have demonstrated the ability of miRNAs to repress *EHMT1*, particularly in cancer (Xiao et al., 2022), this work clearly indicates *EHMT1* is directly capable of regulating multiple miRNAs in stem cells. This suggests a broader role for *EHMT1*, potentially influencing a much wider range of genes by affecting these various miRNAs.

A primary aim of Chapter 4 was to develop a novel system for the simultaneous regulation of multiple miRNAs. MiRNA sponges are not a novel technology, and various other molecular tools exist for manipulation of miRNAs, including tough decoys, antimiRs and locked nucleic acids (Bernardo et al., 2018, Krutzfeldt et al., 2005). A significant challenge associated with these high-throughput miRNA target exploration tools lies in their inability to guarantee uniform introduction of each miRNA construct at the same copy number into every cell. The multimiR-sponge described in this Chapter overcomes this issue by delivering up to three miRNA constructs in a single plasmid. Moreover, the ability to visualise and select for treated cells enables a pure population of inhibited cells, refining background noise when studying these complex interactions. Following the completion and testing of the multimiR-sponge, an almost identical method for generating ‘multi-targeted sponges’ was published (Jie et al., 2022). The study yielded equally positive results in reporter assays, however the system targets only two miRNAs and relies on lengthy subcloning to developed multiple repeats of the miRNA insert. Conversely the multimiR-sponge system offers a quicker ratio ligation

approach for introducing anywhere from 2 to 46 microRNA binding sites. Importantly by varying these ratios prior to subcloning the multimiR-sponge, the inhibition can be fine-tuned on a single miRNA basis.

The multimiR-sponge system emerges as a powerful tool for swiftly investigating the combined effects of multiple miRNAs within a cell type. This versatile platform utilizes plasmids driven by the CMV promoter for transient inhibition or lentiviral vectors for stable miRNA knockdown. The system's ease of use makes it ideal for exploring the collective influence of multiple miRNAs in various neurodevelopmental disorders or across different stages of human brain development. Notably, this approach captures the combinatorial effects of miRNAs on their targets, a challenge for traditional computational methods and molecular assays. While historically used in biological research, miRNA sponges may also hold significant therapeutic potential, particularly in scenarios where manipulating multiple miRNAs is crucial.

7.2.3 Accelerated neuronal maturation

The overarching finding of Chapters 3, 4 and 5 were the precocious and accelerated maturation of neuronal differentiation. The work demonstrates that *EHMT1* is crucial for regulating the proper timing and sequential development of neurons within the human brain. The loss of *EHMT1* led to immediate reduction in the master neuronal regulator REST, which in turn lead to the upregulation of the neuronal drivers miR-124-3p and miR-9-5p, which most likely drive the subsequent repression of EZH2. Each stage appears to act as an epigenetic ratchet, initially reversibly at the pluripotent stage, but quickly enacting an irreversible progression toward neuronal determination. In this manner, *EHMT1* repression acts to prolong the initial plastic neural progenitor state of the cells, which appears as an essential step in the highly protracted process of human neurodevelopment (Petanjek et al., 2019). Indeed, very recent studies have indicated *EHMT1* specifically acts as an epigenetic barrier that must be overcome for neuronal differentiation to occur, whilst premature ablation drastically accelerates maturation (Ciceri et al., 2024). Strikingly, the increased expression of brain specific miR-124-3p and miR-9-5p appear to mark an intrinsic system transition to irreversible neurogenesis. This idea of an epigenetic ratchet has also been posited in other

developmental settings, including the polarization and specification of macrophages within the innate immune system (Daniel et al., 2018). Here the mechanism is suggested to ensure long-term directionality to a process that would otherwise be transient.

Within human brain development physiological maturation occurs in a fine-tuned sequential manner, and perturbation of these stages leads to significant implications on neural structure and networks (Wallois et al., 2020). Accelerated maturation is thought to be a key contributor to a number of neurodevelopmental disorders, potentially explaining the strong phenotypic convergence. For example, *BRAF* patient derived iPSC neurons display rapid onset of neuronal maturation and a depleted progenitor pool (Yeh et al., 2018). Similarly, *PCDH12* mutations associated with severe neurodevelopmental disorders, result in premature maturation as well as disruption of neuronal migration in organoid models (Rakotomamonjy et al., 2023). This precocious maturation is not only specific to rare genetic diseases, accelerated neuronal maturation has also been reported in iPSC generated cerebral organoids from patients with Schizophrenia (Sawada et al., 2020). The fact that this study was conducted in monozygotic twins discordant for psychosis, strongly indicates a significant epigenetic role in the regulation of neurodevelopmental timing and its connection to disease occurrence. So too in Kleefstra syndrome the symptoms of reduced brain size and microencephaly (Stewart and Kleefstra, 2007) point toward the possibility of a depleted neuronal progenitor pool, indicative of premature maturation. The premature exit from the cell cycle and transcriptional shift toward a mature state as indicated in Chapter 3, along with the premature increases in maturation markers in Chapter 5 certainly support this hypothesis. This study reveals that the absence of *EHMT1* triggers premature differentiation of neural cells and unique features specific to certain neuronal types. These findings suggest a common disease mechanism underlying Kleefstra syndrome and potentially other neurological conditions.

7.2.4 Epigenetic priming

One of the most interesting findings from this project was epigenetic crosstalk that occurred between EHMT1 and EZH2. The discovery that EHMT1 and EZH2 co-regulated what appear to be primarily neurodevelopmental regulators in stem cells, suggests the two epigenetic modifiers are specifically gatekeeping the key regulators of neural induction. This idea was

further supported when considering that several of these targets are bivalent genes, implying they are held in a poised state (Kumar et al., 2021). Indeed, the default fate of embryonic stem cells appears to be neural tissue (Levine and Brivanlou, 2007), implying ESCs are genetically primed for neuronal differentiation. Certainly, in the absence of extrinsic morphogens, ESCs readily form primitive neuronal stem cells (Tropepe et al., 2001).

Formative studies by Mozzetta et al for the first time demonstrated that EHMT2 and EZH2 could jointly target a specific subset of key developmental regulators (Mozzetta et al., 2014). Findings in Chapter 6 demonstrate that rather than being an addendum to the activity of EHMT2, EHMT1 plays its own independent role both in the regulation of EZH2 and its recruitment to specific genetic targets. In this manner, many of these gene targets appear epigenetically primed, that is containing both activation and repressive mark, but without changes in transcription. This feature appears to be uniquely enriched within brain development when compared to other lineages (Xu et al., 2009). Epigenetic priming has been suggested as one possible model for neurodevelopmental disorders, whereby disruption in this epigenetic priming predisposes pluripotent cells to perturbation of neuronal differentiation and timing (Ernst and Jefri, 2021). Hence, the *EHMT1* mediated crosstalk with, EZH2 and REST observed in pluripotent cells appear to directly prime the neuronal genome for response to external stimuli during development.

7.2.5 Patient impact

Beyond the scientific findings, the results of this work have potential implications for patients with Kleefstra Syndrome. Although approximately 50% of patients are diagnosed before the age of 3 years old, almost 10% receive their diagnosis at 18 years or older (Kleefstra-Syndrome-UK, 2018). The identification of common circulating microRNAs, acting as biomarkers, may allow for accurate and rapid diagnosis for patients in the future. With a more distant view, the combined results of other studies that KS symptoms can be rescued postnatally and my identification of key dysregulated miRNAs, offer the potential for unique anti-miR therapies. Such approaches would offer the first disorder specific treatments for people with KS.

7.3 Study Limitations

7.3.1 hPSC derived neuronal maturation

A significant portion of the results in this project focus on the accelerated neuronal maturation of *EHMT1* depleted iPSCs. However, it is important to understand that pragmatically speaking, these iPSC derived neurons remain immature and may be prone to more significant changes than those seen in-vivo. Very recent publications have utilised small molecules targeting epigenetic regulators to produce more mature PSC derived neurons (Hergenreder et al., 2024), however these still fall short of the levels of maturation seen in human brains. Given the primary focus of this work has been surrounding the early stages of neurodevelopment, the immature nature of the PSC derived neurons is less of a concern. Despite this, for the study of *EHMT1* loss at later stages of neural development this is should be an important consideration.

7.3.2 Use of patient and isogenic cell lines

For the *EHMT1* mutant cell lines within this study a combination of patient derived human iPSCs and CRISPR edited iPSCs were employed. The iPSCs derived from Kleefstra syndrome have the advantage of more directly recapitulating both the genetic and phenotypic landscape of the disease, due to the lack of both the causative gene, *EHMT1*, and other genes within the microdeletion. This also presents the disadvantage of increased genetic variability, making it more difficult to isolate the effects of specific genetic variations. This was perhaps best demonstrated by the increased levels of miR-142-3p observed in the KS2 patient line, but not in the KS1 line. It has been argued that for the detailed understanding of disease etiology, they is a requirement for large cohorts of patient-derived iPSCs (Doss and Sachinidis, 2019). Given the very low incidence rate of Kleefstra Syndrome the large-scale generation of patient iPSC libraries is impractical. However, the *EHMT1* mutation is highly penetrant (Alsaqati et al., 2022), meaning this is also likely unnecessary. The use of the CRISPR edited cell line, which contains a SNP in the *EHMT1* gene, also helped to isolate the effects of the gene specific effects. It is though important to remember the use of this CRISPR edited cell line may lead to the loss of specific phenotypes and a lack of clinical relevance should always

be considered. Obviously both iPSC lines have the distinct advantage of scalability, enabling the production of millions of neuronal cells that would otherwise not be possible.

Furthermore, both patient derived cells lines were sourced from female only patients, despite females and males displaying equal incidence rates (Kleefstra et al., 2006b). This is certainly a limitation when considering the genetic differences between males and females and the known implications for neurodevelopmental disorders. One classic example is that of fragile X syndrome, where despite comparable incidence rates, males primarily display more severe symptoms. This is due to compensation of a healthy X chromosome in female patients (Hunter et al., 2014). Although male and female KS patients appear equally affected, unique genetic, mechanistic and phenotypic differences may exist. Most importantly the EHMT1 methylation mark, H3K9me2, is well known to be involved in X-linked inactivation (Keniry et al., 2016), potentially positing a significant role for EHMT1 in sex linked differences. This is partially answered by the *EHMT1*$^{+/-}$ CRISPR line, which is a male cell line. However future work should aim to include patient derived cell lines from both males and females.

7.3.3 Use of UNC0638 inhibitor

For many of the results presented here, the UNC0638 chemical inhibitor was used to induce a loss of *EHMT1* function and in turn H3K9me2 methylation levels. However, the UNC inhibitor is well known to target both the EHMT1 and EHMT2 proteins equally (Vedadi et al., 2011), making it hard to distinguish whether results are directly or primarily caused by the loss of *EHMT1* alone. Where possible results were confirmed in CRISPR edited cell lines or patient derived iPSCs, both of which contain only a mutation for the *EHMT1* gene. One examples of discrepancies include the robust upregulation of miR-142-3p observed following UNC treatment, which was not observed in one of the patient derived lines. However, the UNC inhibitor remains a powerful tool for transiently and temporarily inhibiting the EHMT proteins. One potential solution for future work may be to utilise methodologies such as CRISPR Cas13 or dCas9, to transiently and effectively repress *EHMT1* specifically.

7.3.4 Implications of multiple miRNAs

Given the significant number of miRNAs shown to be dysregulated at the neuronal stage, it is hard to determine whether there could be indirect effects on other signalling pathways that also contribute to the observed phenotypes. In particular the effects of miR-124-3p and miR-9-5p as key drivers of premature neuronal maturation could be jointly impacted by numerous other miRNAs. One solution to this problem would be to use multimiR-sponges against the two miRNAs to ascertain the specific role of these miRNAs in the disorder phenotype. Likewise, predictive miRNA models were based on RNA sequencing data from *EHMT1*$^{+/-}$ neurons and subsequent targets validated in both neurons and pluripotent cells. Generating models based on RNA sequencing data from *EHMT1*$^{+/-}$ pluripotent cells may help to identify further dysregulated miRNAs specific to the embryonic timepoint.

7.3.5 MultimiR-sponges

The multimiR-sponges developed in Chapter 4 overall appeared to be highly effective, with the consistent repression of individual and multiple miRNAs. However, the system presents some innate limitations. Where expression levels of miRNAs are very high, repression may require significant and possibly unachievable concentrations of the sponge. Moreover, the greater number of repeated binding sites required to repress a given miRNA, the more likely there are to be copy errors when the sponge is transcribed. Additionally, identifying the efficacy of these multimiR-sponges can be difficult. Reporter results may not always reflect the true nature of the sponge in a cell model, where the messy inclusion of circular RNA and non-coding RNA can competitively bind to the sponge. The varying discrepancies between repression of transcript levels and protein levels also make target validation complex and potentially costly. Delivery of the sponges is also challenging during neuronal differentiations, where cells remain tightly bound and transfection rates remain very low. Finally, the inclusion of multiple miRNA inhibitors in a single cassette, drastically increases the potential for off-target inhibition that may indirectly affect cellular function and results. Similar results may be seen with miRNA families such as miR-26-5p highlighted in this work, which can differ by as little as a single base pair. Despite these considerations the multimiR-sponge remains an effective tool for simultaneous miRNA manipulation.

7.3.6 Bioinformatic data set

For the bioinformatic results discussed in Chapter 3 only a single RNA sequencing dataset was used due to availability. This presents a number of limitations such as reduced statistical power, potentially leading to an inability to identify subtle changes in gene expression. Interestingly, the results of bulk RNA sequencing data, such as the one used in this study, appear highly reproducible with minimal systemic changes (Jeon et al., 2023). Performing differential meta-analyses of RNA-seq from multiple independent studies would also allow for more robust results, potentially reducing genetic variability and identifying core mechanistic and genetic nodes within the KS disorder (Rau et al., 2014). Such approaches have also been shown to identify uniquely differentially expressed genes, not identified in the original datasets (Alimadadi et al., 2020). As more datasets undoubtably become available further comparative analysis will help to further consolidate key nodes within the KS disorder.

7.4 Future Directions

7.4.1 Comparison of different KS mutations

Kleefstra syndrome was originally categorised by a microdeletion in the 9q34 region impacting a loss of *EHMT1*. As the understanding of neurodevelopmental disorders has increased, mutations in four other epigenetic regulators, *MBD5*, *MLL3*, *SMARCB1* and *NR1I3* have been shown to cause a comparable NDD termed Kleefstra 2. Based on the highly similar phenotypes and the functional interaction seen between these various epigenetic modifiers, there is a strong basis for further work on identifying the common mechanisms between these mutations. The same iPSC derived modelling and computational approach could be used to identify system level pathways and genetic nodes common to the various mutations. Such work would also provide the opportunity to identify novel biomarkers, common to the subset of Kleefstra disorders. Furthermore, in addition to *EHMT1* microdeletions, specific microduplications have also been associated with subtle forms of NDDs (Bonati et al., 2019). It would therefore be interesting to investigate the effect of increased *EHMT1* dosage on neurodevelopment and the potential causative role in NDD occurrence.

7.4.2 Identification of EHMT1-EZH2 regulated genes

This work has successfully identified several key genes jointly regulated by EHMT1 and EZH2, that are dependent on the action of EHTM1. However, there is significant overlap between EHMT1 and EZH2 gene targets, implying a greater number of these co-regulated targets exist. Therefore, further work using techniques such as ChIP-sequencing and CRISPR, is required to identify all co-regulated targets and understand their role in neurodevelopment. Additionally, further work is required to understand the exact mechanisms behind the EHMT1 dependent methylation of H3K27me3. Various possibilities exist including the direct methylation of accessory proteins required for proper H3K27me3 deposition, or the prerequisite H3K27me2 methylation by EHMT1. Beyond H3K27 methylation, the study of other methylation marks such as H3K4me3 will be vital in understanding the activation state of these genes, particularly in a temporal manner. Again ChIP-sequencing data would allow for a better understanding of the global changes in methylation marks, as well as the specific EHMT1-EZH2 coregulated subsets.

7.4.3 Neuronal maturation and subtype specification

Results in this project strongly suggest an accelerated neuronal maturation in response to the loss of *EHMT1*. Results in Chapter 5 suggest a precocious elevation of first progenitor and subsequently maturation markers. Other studies researching NDDs, and accelerated neurons have demonstrated a shift from direct to indirect neurogenesis and a depletion of neural progenitors (Rakotomamonjy et al., 2023). A time course single cell sequencing analysis of *EHMT1* depleted cells would demonstrate the developmental trajectory taken by these cells, determining which transcriptional route they take to mature neurons. There is also the potential for a dynamic shift in the percentage of progenitor to neuronal cells. Immunofluorescent experiments would help to determine the populations of progenitor to mature neurons and help identify displacements at given timepoints. Proliferation assays, such as BrdU pulse-chase experiments would also help determine if these cells are displaying an early exit from the cell cycle.

The primary focus of this work was on the earlier stages of neuronal development, however it has been suggested that the loss of *EHMT1* seen in KS neurons leads to an imbalance in the number of excitatory and inhibitory neurons (Frega et al., 2019). The current differentiation protocol in this study favours the generation of excitatory glutamatergic cortical neurons, with only a small portion becoming GABAergic neurons. This composition doesn't accurately reflect the developing human cortex, where GABAergic neurons constitute nearly 20% (Ouellet and de Villers-Sidani, 2014). Future studies should address this limitation to fully understand *EHMT1*'s role in neuronal subtype specification. One approach would be to differentiate cells with one copy of *EHMT1* (*EHMT1*+/-) into mature glutamatergic and GABAergic neurons. Additionally, co-culturing these differentiated neurons would enable investigation of how *EHMT1* loss affects their interactions. Furthermore, the use of Multi Electrode Array (MEA) analysis could provide valuable insights into the electrophysiological consequences of *EHMT1* loss on neuronal function.

7.5 Conclusions

The work in this project has demonstrated a significant impact of *EHMT1* on the timing and progression of neuronal development. Loss of *EHMT1* leads to a premature downregulation of the master neuronal regulator REST, through the de-repression of several miRNAs. These *EHMT1* regulated miRNAs act simultaneously and in a cooperative fashion to target and inhibit the REST protein. Premature loss of REST was sufficient to induce precocious differentiation toward a neuronal phenotype, primarily driven by the brain specific miRNAs, miR-124-3p and miR-9-5p. Novel computational models developed were key to identifying the dysregulated miRNAs within *EHMT1* deficient cells, whilst newly developed multimiR-sponges enabled for the concurrent manipulation of these miRNAs. Significant epigenetic crosstalk was also identified between EHMT1 and EZH2 for the first time, demonstrating EHMT1 was crucial for the recruitment of EZH2 function at a subset of neurodevelopmental genes.

References

ABRAHAMS, B. S., ARKING, D. E., CAMPBELL, D. B., MEFFORD, H. C., MORROW, E. M., WEISS, L. A., MENASHE, I., WADKINS, T., BANERJEE-BASU, S. & PACKER, A. 2013. SFARI Gene 2.0: a community-driven knowledgebase for the autism spectrum disorders (ASDs). *Molecular Autism,* 4**,** 36.

ADAM, M. A. & ISLES, A. R. 2017. EHMT1/GLP; Biochemical Function and Association with Brain Disorders. *Epigenomes,* 1**,** 15.

ADHIKARI, A., MAINALI, P. & DAVIE, J. K. 2019. JARID2 and the PRC2 complex regulate the cell cycle in skeletal muscle. *Journal of Biological Chemistry,* 294**,** 19451-19464.

AISINA, D., NIYAZOVA, R., ATAMBAYEVA, S. & IVASHCHENKO, A. 2019. Prediction of clusters of miRNA binding sites in mRNA candidate genes of breast cancer subtypes. *PeerJ,* 7**,** e8049.

ÅKERBLOM, M., SACHDEVA, R., BARDE, I., VERP, S., GENTNER, B., TRONO, D. & JAKOBSSON, J. 2012. MicroRNA-124 Is a Subventricular Zone Neuronal Fate Determinant. *The Journal of Neuroscience,* 32**,** 8879-8889.

ALDER, O., LAVIAL, F., HELNESS, A., BROOKES, E., PINHO, S., CHANDRASHEKRAN, A., ARNAUD, P., POMBO, A., O'NEILL, L. & AZUARA, V. 2010. Ring1B and Suv39h1 delineate distinct chromatin states at bivalent genes during early mouse lineage commitment. *Development,* 137**,** 2483-2492.

ALIMADADI, A., MUNROE, P. B., JOE, B. & CHENG, X. 2020. Meta-Analysis of Dilated Cardiomyopathy Using Cardiac RNA-Seq Transcriptomic Datasets. *Genes,* 11**,** 60.

ALSAQATI, M., DAVIS, B. A., WOOD, J., JONES, M. M., JONES, L., WESTWOOD, A., PETTER, O., ISLES, A. R., LINDEN, D., VAN DEN BREE, M., OWEN, M., HALL, J. & HARWOOD, A. J. 2022. NRSF/REST lies at the intersection between epigenetic regulation, miRNA-mediated gene control and neurodevelopmental pathways associated with Intellectual disability (ID) and Schizophrenia. *Translational Psychiatry,* 12**,** 438.

ANDERSSON, T., RAHMAN, S., SANSOM, S. N., ALSIÖ, J. M., KANEDA, M., SMITH, J., O'CARROLL, D., TARAKHOVSKY, A. & LIVESEY, F. J. 2010. Reversible Block of Mouse Neural Stem Cell Differentiation in the Absence of Dicer and MicroRNAs. *PLOS ONE,* 5**,** e13453.

ANDRÉS, M. E., BURGER, C., PERAL-RUBIO, M. J., BATTAGLIOLI, E., ANDERSON, M. E., GRIMES, J., DALLMAN, J., BALLAS, N. & MANDEL, G. 1999. CoREST: A functional corepressor required for regulation of neural-specific gene expression. *Proceedings of the National Academy of Sciences,* 96**,** 9873-9878.

AOKI, H., HARA, A., ERA, T., KUNISADA, T. & YAMADA, Y. 2012. Genetic ablation of Rest leads to in vitro-specific derepression of neuronal genes during neurogenesis. *Development,* 139**,** 667-677.

ARENTS, G., BURLINGAME, R. W., WANG, B.-C., LOVE, W. E. & MOUDRIANAKIS, E. N. 1991. The nucleosomal core histone octamer at 3.1 A resolution: a tripartite protein assembly and a left-handed superhelix. *Proceedings of the National Academy of Sciences,* 88**,** 10148-10152.

ARNOLD, P., SCHÖLER, A., PACHKOV, M., BALWIERZ, P. J., JØRGENSEN, H., STADLER, M. B., VAN NIMWEGEN, E. & SCHÜBELER, D. 2013. Modeling of epigenome dynamics identifies transcription factors that mediate Polycomb targeting. *Genome Res,* 23**,** 60-73.

ARVANITIS, D. N., JUNGAS, T., BEHAR, A. & DAVY, A. 2010. Ephrin-B1 Reverse Signaling Controls a Posttranscriptional Feedback Mechanism via miR-124. *Molecular and Cellular Biology,* 30**,** 2508-2517.

AUYEUNG, VINCENT C., ULITSKY, I., MCGEARY, SEAN E. & BARTEL, DAVID P. 2013. Beyond Secondary Structure: Primary-Sequence Determinants License Pri-miRNA Hairpins for Processing. *Cell,* 152**,** 844-858.

AYDIN, B., KAKUMANU, A., ROSSILLO, M., MORENO-ESTELLÉS, M., GARIPLER, G., RINGSTAD, N., FLAMES, N., MAHONY, S. & MAZZONI, E. O. 2019. Proneural factors Ascl1 and Neurog2 contribute to neuronal subtype identities by establishing distinct chromatin landscapes. *Nature Neuroscience,* 22**,** 897-908.

AZUARA, V., PERRY, P., SAUER, S., SPIVAKOV, M., JØRGENSEN, H. F., JOHN, R. M., GOUTI, M., CASANOVA, M., WARNES, G. & MERKENSCHLAGER, M. 2006. Chromatin signatures of pluripotent cell lines. *Nature cell biology,* 8**,** 532-538.

BAEK, D., VILLÉN, J., SHIN, C., CAMARGO, F. D., GYGI, S. P. & BARTEL, D. P. 2008. The impact of microRNAs on protein output. *Nature,* 455**,** 64-71.

BAER, S., AFENJAR, A., SMOL, T., PITON, A., GÉRARD, B., ALEMBIK, Y., BIENVENU, T., BOURSIER, G., BOUTE, O., COLSON, C., CORDIER, M.-P., CORMIER-DAIRE, V., DELOBEL, B., DOCO-FENZY, M., DUBAN-BEDU, B., FRADIN, M., GENEVIÈVE, D., GOLDENBERG, A., GRELET, M., HAYE, D., HERON, D., ISIDOR, B., KEREN, B., LACOMBE, D., LÈBRE, A.-S., LESCA, G., MASUREL, A., MATHIEU-DRAMARD, M., NAVA, C., PASQUIER, L., PETIT, A., PHILIP, N., PIARD, J., RONDEAU, S., SAUGIER-VEBER, P., SUKNO, S., THEVENON, J., VAN-GILS, J., VINCENT-DELORME, C., WILLEMS, M., SCHAEFER, E. & MORIN, G. 2018. Wiedemann-Steiner syndrome as a major cause of syndromic intellectual disability: A study of 33 French cases. *Clinical Genetics,* 94**,** 141-152.

BAI, R. Y., STAEDTKE, V., LIDOV, H. G., EBERHART, C. G. & RIGGINS, G. J. 2012. OTX2 represses myogenic and neuronal differentiation in medulloblastoma cells. *Cancer Res,* 72**,** 5988-6001.

BALASUBRAMANIAN, M., DINGEMANS, A. J. M., ALBABA, S., RICHARDSON, R., YATES, T. M., COX, H., DOUZGOU, S., ARMSTRONG, R., SANSBURY, F. H., BURKE, K. B., FRY, A. E., RAGGE, N., SHARIF, S., FOSTER, A., DE SANDRE-GIOVANNOLI, A., ELOUEJ, S., VASUDEVAN, P., MANSOUR, S., WILSON, K., STEWART, H., HEIDE, S., NAVA, C., KEREN, B., DEMIRDAS, S., BROOKS, A. S., VINCENT, M., ISIDOR, B., KÜRY, S., SCHOUTEN, M., LEENDERS, E., CHUNG, W. K., HAERINGEN, A. V., SCHEFFNER, T., DEBRAY, F. G., WHITE, S. M., PALAFOLL, M. I. V., PFUNDT, R., NEWBURY-ECOB, R. & KLEEFSTRA, T. 2021. Comprehensive study of 28 individuals with SIN3A-related disorder underscoring the associated mild cognitive and distinctive facial phenotype. *Eur J Hum Genet,* 29**,** 625-636.

BALEMANS, M. C., HUIBERS, M. M., EIKELENBOOM, N. W., KUIPERS, A. J., VAN SUMMEREN, R. C., PIJPERS, M. M., TACHIBANA, M., SHINKAI, Y., VAN BOKHOVEN, H. & VAN DER ZEE, C. E. 2010. Reduced exploration, increased anxiety, and altered social behavior: Autistic-like features of euchromatin histone methyltransferase 1 heterozygous knockout mice. *Behav Brain Res,* 208**,** 47-55.

BALEMANS, M. C., NADIF KASRI, N., KOPANITSA, M. V., AFINOWI, N. O., RAMAKERS, G., PETERS, T. A., BEYNON, A. J., JANSSEN, S. M., VAN SUMMEREN, R. C. & EEFTENS, J. M. 2013. Hippocampal dysfunction in the Euchromatin histone methyltransferase 1 heterozygous knockout mouse model for Kleefstra syndrome. *Human molecular genetics,* 22**,** 852-866.

BALEMANS, M. C. M., ANSAR, M., OUDAKKER, A. R., VAN CAAM, A. P. M., BAKKER, B., VITTERS, E. L., VAN DER KRAAN, P. M., DE BRUIJN, D. R. H., JANSSEN, S. M., KUIPERS, A. J., HUIBERS, M. M. H., MALIEPAARD, E. M., WALBOOMERS, X. F., BENEVENTO, M., NADIF KASRI, N., KLEEFSTRA, T., ZHOU, H., VAN DER ZEE, C. E. E. M. & VAN BOKHOVEN, H. 2014. Reduced Euchromatin histone methyltransferase 1 causes developmental delay, hypotonia, and

cranial abnormalities associated with increased bone gene expression in Kleefstra syndrome mice. *Developmental Biology,* 386**,** 395-407.

BALLAS, N., BATTAGLIOLI, E., ATOUF, F., ANDRES, M. E., CHENOWETH, J., ANDERSON, M. E., BURGER, C., MONIWA, M., DAVIE, J. R. & BOWERS, W. J. 2001. Regulation of neuronal traits by a novel transcriptional complex. *Neuron,* 31**,** 353-365.

BALLAS, N., GRUNSEICH, C., LU, D. D., SPEH, J. C. & MANDEL, G. 2005. REST and its corepressors mediate plasticity of neuronal gene chromatin throughout neurogenesis. *Cell,* 121**,** 645-657.

BALWIERZ, P. J., PACHKOV, M., ARNOLD, P., GRUBER, A. J., ZAVOLAN, M. & VAN NIMWEGEN, E. 2014. ISMARA: automated modeling of genomic signals as a democracy of regulatory motifs. *Genome Res,* 24**,** 869-84.

BANASZYNSKI, L. A., WEN, D., DEWELL, S., WHITCOMB, S. J., LIN, M., DIAZ, N., ELSÄSSER, S. J., CHAPGIER, A., GOLDBERG, A. D., CANAANI, E., RAFII, S., ZHENG, D. & ALLIS, C. D. 2013. Hira-dependent histone H3.3 deposition facilitates PRC2 recruitment at developmental loci in ES cells. *Cell,* 155**,** 107-20.

BARBIERI, R., CONTESTABILE, A., CIARDO, M. G., FORTE, N., MARTE, A., BALDELLI, P., BENFENATI, F. & ONOFRI, F. 2018. Synapsin I and Synapsin II regulate neurogenesis in the dentate gyrus of adult mice. *Oncotarget,* 9**,** 18760-18774.

BARTA, T., PESKOVA, L. & HAMPL, A. 2016. miRNAsong: a web-based tool for generation and testing of miRNA sponge constructs in silico. *Scientific reports,* 6**,** 1-8.

BARTEL, D. P. 2018. Metazoan micrornas. *Cell,* 173**,** 20-51.

BAZZINI, A. A., LEE, M. T. & GIRALDEZ, A. J. 2012. Ribosome profiling shows that miR-430 reduces translation before causing mRNA decay in zebrafish. *Science,* 336**,** 233-237.

BEHM-ANSMANT, I., REHWINKEL, J., DOERKS, T., STARK, A., BORK, P. & IZAURRALDE, E. 2006. mRNA degradation by miRNAs and GW182 requires both CCR4: NOT deadenylase and DCP1: DCP2 decapping complexes. *Genes & development,* 20**,** 1885-1898.

BENEVENTO, M., IACONO, G., SELTEN, M., BA, W., OUDAKKER, A., FREGA, M., KELLER, J., MANCINI, R., LEWERISSA, E., KLEEFSTRA, T., STUNNENBERG, H. G., ZHOU, H., VAN BOKHOVEN, H. & NADIF KASRI, N. 2016. Histone Methylation by the Kleefstra Syndrome Protein EHMT1 Mediates Homeostatic Synaptic Scaling. *Neuron,* 91**,** 341-355.

BENEVENTO, M., OOMEN, C. A., HORNER, A. E., AMIRI, H., JACOBS, T., PAUWELS, C., FREGA, M., KLEEFSTRA, T., KOPANITSA, M. V., GRANT, S. G. N., BUSSEY, T. J., SAKSIDA, L. M., VAN DER ZEE, C. E. E. M., VAN BOKHOVEN, H., GLENNON, J. C. & KASRI, N. N. 2017. Haploinsufficiency of EHMT1 improves pattern separation and increases hippocampal cell proliferation. *Scientific Reports,* 7**,** 40284.

BERNARDO, B. C., GREGOREVIC, P., RITCHIE, R. H. & MCMULLEN, J. R. 2018. Generation of MicroRNA-34 Sponges and Tough Decoys for the Heart: Developments and Challenges. *Frontiers in Pharmacology,* 9.

BERNSTEIN, B. E., MIKKELSEN, T. S., XIE, X., KAMAL, M., HUEBERT, D. J., CUFF, J., FRY, B., MEISSNER, A., WERNIG, M. & PLATH, K. 2006. A bivalent chromatin structure marks key developmental genes in embryonic stem cells. *Cell,* 125**,** 315-326.

BERNSTEIN, E., KIM, S. Y., CARMELL, M. A., MURCHISON, E. P., ALCORN, H., LI, M. Z., MILLS, A. A., ELLEDGE, S. J., ANDERSON, K. V. & HANNON, G. J. 2003. Dicer is essential for mouse development. *Nature genetics,* 35**,** 215-217.

BESHARAT, Z. M., ABBALLE, L., CICCONARDI, F., BHUTKAR, A., GRASSI, L., LE PERA, L., MORETTI, M., CHINAPPI, M., D'ANDREA, D., MASTRONUZZI, A., IANARI, A., VACCA, A., DE SMAELE, E., LOCATELLI, F., PO, A., MIELE, E. & FERRETTI, E. 2018. Foxm1 controls a pro-stemness microRNA network in neural stem cells. *Scientific Reports,* 8**,** 3523.

BEUKELAERS, P., VANDENBOSCH, R., CARON, N., NGUYEN, L., BELACHEW, S., MOONEN, G., KIYOKAWA, H., BARBACID, M., SANTAMARIA, D. & MALGRANGE, B. 2011. Cdk6-dependent regulation of G(1) length controls adult neurogenesis. *Stem Cells,* 29**,** 713-24.

BHATTACHARYYA, S. N., HABERMACHER, R., MARTINE, U., CLOSS, E. I. & FILIPOWICZ, W. 2006. Relief of microRNA-mediated translational repression in human cells subjected to stress. *Cell,* 125**,** 1111-1124.

BHINGE, A., POSCHMANN, J., NAMBOORI, S. C., TIAN, X., JIA HUI LOH, S., TRACZYK, A., PRABHAKAR, S. & STANTON, L. W. 2014. Mi R-135b is a direct PAX 6 target and specifies human neuroectoderm by inhibiting TGF-β/BMP signaling. *The EMBO journal,* 33**,** 1271-1283.

BILLINGSLEY, K. J., MANCA, M., GIANFRANCESCO, O., COLLIER, D. A., SHARP, H., BUBB, V. J. & QUINN, J. P. 2018. Regulatory characterisation of the schizophrenia-associated CACNA1C proximal promoter and the potential role for the transcription factor EZH2 in schizophrenia aetiology. *Schizophr Res,* 199**,** 168-175.

BILODEAU, S., KAGEY, M. H., FRAMPTON, G. M., RAHL, P. B. & YOUNG, R. A. 2009. SetDB1 contributes to repression of genes encoding developmental regulators and maintenance of ES cell state. *Genes Dev,* 23**,** 2484-9.

BIRNBAUM, R. & WEINBERGER, D. R. 2017. Genetic insights into the neurodevelopmental origins of schizophrenia. *Nature Reviews Neuroscience,* 18**,** 727-740.

BLACKBURN, P. R., TISCHER, A., ZIMMERMANN, M. T., KEMPPAINEN, J. L., SASTRY, S., KNIGHT JOHNSON, A. E., COUSIN, M. A., BOCZEK, N. J., OLIVER, G., MISRA, V. K., GAVRILOVA, R. H., LOMBERK, G., AUTON, M., URRUTIA, R. & KLEE, E. W. 2017. A Novel Kleefstra Syndrome-associated Variant That Affects the Conserved TPLX Motif within the Ankyrin Repeat of EHMT1 Leads to Abnormal Protein Folding. *J Biol Chem,* 292**,** 3866-3876.

BLACKWOOD, C. A. 2019. Jagged1 is Essential for Radial Glial Maintenance in the Cortical Proliferative Zone. *Neuroscience,* 413**,** 230-238.

BÖHM, J., BUCK, A., BOROZDIN, W., MANNAN, A. U., MATYSIAK-SCHOLZE, U., ADHAM, I., SCHULZ-SCHAEFFER, W., FLOSS, T., WURST, W. & KOHLHASE, J. 2008. Sall1, sall2, and sall4 are required for neural tube closure in mice. *The American journal of pathology,* 173**,** 1455-1463.

BOLLATI, V. & BACCARELLI, A. 2010. Environmental epigenetics. *Heredity,* 105**,** 105-112.

BONATI, M. T., CASTRONOVO, C., SIRONI, A., ZIMBALATTI, D., BESTETTI, I., CRIPPA, M., NOVELLI, A., LODDO, S., DENTICI, M. L., TAYLOR, J., DEVILLARD, F., LARIZZA, L. & FINELLI, P. 2019. 9q34.3 microduplications lead to neurodevelopmental disorders through EHMT1 overexpression. *neurogenetics,* 20**,** 145-154.

BONEV, B., STANLEY, P. & PAPALOPULU, N. 2012. MicroRNA-9 modulates Hes1 ultradian oscillations by forming a double-negative feedback loop. *Cell reports,* 2**,** 10-18.

BOROS, J., ARNOULT, N., STROOBANT, V., COLLET, J.-F. & DECOTTIGNIES, A. 2014. Polycomb Repressive Complex 2 and H3K27me3 Cooperate with H3K9 Methylation To Maintain Heterochromatin Protein 1α at Chromatin. *Molecular and Cellular Biology,* 34**,** 3662-3674.

BOSIA, C., SGRÒ, F., CONTI, L., BALDASSI, C., BRUSA, D., CAVALLO, F., CUNTO, F. D., TURCO, E., PAGNANI, A. & ZECCHINA, R. 2017. RNAs competing for microRNAs mutually influence their fluctuations in a highly non-linear microRNA-dependent manner in single cells. *Genome Biol,* 18**,** 37.

BOUTIN, C., HARDT, O., DE CHEVIGNY, A., CORÉ, N., GOEBBELS, S., SEIDENFADEN, R., BOSIO, A. & CREMER, H. 2010. NeuroD1 induces terminal neuronal differentiation in olfactory neurogenesis. *Proceedings of the National Academy of Sciences,* 107**,** 1201-1206.

BOYER, L. A., PLATH, K., ZEITLINGER, J., BRAMBRINK, T., MEDEIROS, L. A., LEE, T. I., LEVINE, S. S., WERNIG, M., TAJONAR, A., RAY, M. K., BELL, G. W., OTTE, A. P., VIDAL, M., GIFFORD, D. K., YOUNG, R. A. & JAENISCH, R. 2006. Polycomb complexes repress developmental regulators in murine embryonic stem cells. *Nature,* 441**,** 349-353.

BRACKEN, A. P., DIETRICH, N., PASINI, D., HANSEN, K. H. & HELIN, K. 2006. Genome-wide mapping of Polycomb target genes unravels their roles in cell fate transitions. *Genes & development,* 20**,** 1123-1136.

BRAUN, D. A., SCHUELER, M., HALBRITTER, J., GEE, H. Y., PORATH, J. D., LAWSON, J. A., AIRIK, R., SHRIL, S., ALLEN, S. J., STEIN, D., AL KINDY, A., BECK, B. B., CENGIZ, N., MOORANI, K. N., OZALTIN, F., HASHMI, S., SAYER, J. A., BOCKENHAUER, D., SOLIMAN, N. A., OTTO, E. A., LIFTON, R. P. & HILDEBRANDT, F. 2016. Whole exome sequencing identifies causative mutations in the majority of consanguineous or familial cases with childhood-onset increased renal echogenicity. *Kidney International,* 89**,** 468-475.

BRISKIN, D., WANG, P. Y. & BARTEL, D. P. 2020. The biochemical basis for the cooperative action of microRNAs. *Proc Natl Acad Sci U S A,* 117**,** 17764-17774.

BRODERICK, J. A., SALOMON, W. E., RYDER, S. P., ARONIN, N. & ZAMORE, P. D. 2011. Argonaute protein identity and pairing geometry determine cooperativity in mammalian RNA silencing. *Rna,* 17**,** 1858-69.

BRODSKI, C., BLAESS, S., PARTANEN, J. & PRAKASH, N. 2019. Crosstalk of Intercellular Signaling Pathways in the Generation of Midbrain Dopaminergic Neurons In Vivo and from Stem Cells. *J Dev Biol,* 7.

BROUGHTON, J. P., LOVCI, M. T., HUANG, J. L., YEO, G. W. & PASQUINELLI, A. E. 2016. Pairing beyond the seed supports microRNA targeting specificity. *Molecular cell,* 64**,** 320-333.

BROWN, J., BARRY, C., SCHMITZ, M. T., ARGUS, C., BOLIN, J. M., SCHWARTZ, M. P., VAN AARTSEN, A., STEILL, J., SWANSON, S., STEWART, R., THOMSON, J. A. & KENDZIORSKI, C. 2021. Interspecies chimeric conditions affect the developmental rate of human pluripotent stem cells. *PLOS Computational Biology,* 17**,** e1008778.

BROWN, S. E., CAMPBELL, R. D. & SANDERSON, C. M. 2001. Novel NG36/G9a gene products encoded within the human and mouse MHC class III regions. *Mammalian genome,* 12**,** 916-924.

BRUCE, A. W., DONALDSON, I. J., WOOD, I. C., YERBURY, S. A., SADOWSKI, M. I., CHAPMAN, M., GÖTTGENS, B. & BUCKLEY, N. J. 2004. Genome-wide analysis of repressor element 1 silencing transcription factor/neuron-restrictive silencing factor (REST/NRSF) target genes. *Proceedings of the National Academy of Sciences,* 101**,** 10458-10463.

BRUCE, A. W., KREJČÍ, A., OOI, L., DEUCHARS, J., WOOD, I. C., DOLEŽAL, V. & BUCKLEY, N. J. 2006. The transcriptional repressor REST is a critical regulator of the neurosecretory phenotype. *Journal of neurochemistry,* 98**,** 1828-1840.

BRUNO, I. G., KARAM, R., HUANG, L., BHARDWAJ, A., LOU, C. H., SHUM, E. Y., SONG, H. W., CORBETT, M. A., GIFFORD, W. D., GECZ, J., PFAFF, S. L. & WILKINSON, M. F. 2011. Identification of a microRNA that activates gene expression by repressing nonsense-mediated RNA decay. *Mol Cell,* 42**,** 500-10.

BUNT, J., HASSELT, N. A., ZWIJNENBURG, D. A., KOSTER, J., VERSTEEG, R. & KOOL, M. 2013. OTX2 sustains a bivalent-like state of OTX2-bound promoters in medulloblastoma by maintaining their H3K27me3 levels. *Acta Neuropathol,* 125**,** 385-94.

CAINELLI, E. & BISIACCHI, P. 2022. Neurodevelopmental Disorders: Past, Present, and Future. *Children (Basel),* 10.

CALDERONE, A., JOVER, T., NOH, K.-M., TANAKA, H., YOKOTA, H., LIN, Y., GROOMS, S. Y., REGIS, R., BENNETT, M. V. L. & ZUKIN, R. S. 2003. Ischemic Insults Derepress the Gene Silencer REST in Neurons Destined to Die. *The Journal of Neuroscience,* 23**,** 2112-2121.

CALDWELL, A. B., LIU, Q., SCHROTH, G. P., GALASKO, D. R., YUAN, S. H., WAGNER, S. L. & SUBRAMANIAM, S. 2020. Dedifferentiation and neuronal repression define familial Alzheimer's disease. *Science Advances,* 6**,** eaba5933.

CAO, X., PFAFF, S. L. & GAGE, F. H. 2007. A functional study of miR-124 in the developing neural tube. *Genes Dev,* 21**,** 531-6.

CAROSSO, G. A., BOUKAS, L., AUGUSTIN, J. J., NGUYEN, H. N., WINER, B. L., CANNON, G. H., ROBERTSON, J. D., ZHANG, L., HANSEN, K. D., GOFF, L. A. & BJORNSSON, H. T. 2019. Precocious neuronal differentiation and disrupted oxygen responses in Kabuki syndrome. *JCI Insight,* 4.

CASTINO, M. R., BAKER-ANDRESEN, D., RATNU, V. S., SHEVCHENKO, G., MORRIS, K. V., BREDY, T. W., YOUNGSON, N. A. & CLEMENS, K. J. 2018. Persistent histone modifications at the BDNF and Cdk-5 promoters following extinction of nicotine-seeking in rats. *Genes, Brain and Behavior,* 17**,** 98-106.

CATES, K., MCCOY, M. J., KWON, J.-S., LIU, Y., ABERNATHY, D. G., ZHANG, B., LIU, S., GONTARZ, P., KIM, W. K., CHEN, S., KONG, W., HO, J. N., BURBACH, K. F., GABEL, H. W., MORRIS, S. A. & YOO, A. S. 2021. Deconstructing Stepwise Fate Conversion of Human Fibroblasts to Neurons by MicroRNAs. *Cell Stem Cell,* 28**,** 127-140.e9.

CEDERQUIST, G. Y., TCHIEU, J., CALLAHAN, S. J., RAMNARINE, K., RYAN, S., ZHANG, C., RITTENHOUSE, C., ZELTNER, N., CHUNG, S. Y., ZHOU, T., CHEN, S., BETEL, D., WHITE, R. M., TOMISHIMA, M. & STUDER, L. 2020. A Multiplex Human Pluripotent Stem Cell Platform Defines Molecular and Functional Subclasses of Autism-Related Genes. *Cell Stem Cell,* 27**,** 35-49.e6.

CHAMBERLAIN, S. J., YEE, D. & MAGNUSON, T. 2008. Polycomb Repressive Complex 2 Is Dispensable for Maintenance of Embryonic Stem Cell Pluripotency. *Stem Cells,* 26**,** 1496-1505.

CHAMBERS, S. M., FASANO, C. A., PAPAPETROU, E. P., TOMISHIMA, M., SADELAIN, M. & STUDER, L. 2009. Highly efficient neural conversion of human ES and iPS cells by dual inhibition of SMAD signaling. *Nature Biotechnology,* 27**,** 275-280.

CHANDA, S., ANG, CHEEN E., DAVILA, J., PAK, C., MALL, M., LEE, QIAN Y., AHLENIUS, H., JUNG, SEUNG W., SÜDHOF, THOMAS C. & WERNIG, M. 2014. Generation of Induced Neuronal Cells by the Single Reprogramming Factor ASCL1. *Stem Cell Reports,* 3**,** 282-296.

CHANDRADOSS, S. D., SCHIRLE, N. T., SZCZEPANIAK, M., MACRAE, I. J. & JOO, C. 2015. A dynamic search process underlies microRNA targeting. *Cell,* 162**,** 96-107.

CHANG, C. C., WU, M. J., YANG, J. Y., CAMARILLO, I. G. & CHANG, C. J. 2015. Leptin-STAT3-G9a Signaling Promotes Obesity-Mediated Breast Cancer Progression. *Cancer Res,* 75**,** 2375-2386.

CHANG, Y., ZHANG, X., HORTON, J. R., UPADHYAY, A. K., SPANNHOFF, A., LIU, J., SNYDER, J. P., BEDFORD, M. T. & CHENG, X. 2009. Structural basis for G9a-like protein lysine methyltransferase inhibition by BIX-01294. *Nature Structural & Molecular Biology,* 16**,** 312-317.

CHANG, Y. F., LIM, K. H., CHIANG, Y. W., SIE, Z. L., CHANG, J., HO, A. S. & CHENG, C. C. 2019. STAT3 induces G9a to exacerbate HER3 expression for the survival of epidermal growth factor receptor-tyrosine kinase inhibitors in lung cancers. *BMC Cancer,* 19**,** 959.

CHASE, K. A., FEINER, B., RAMAKER, M. J., HU, E., ROSEN, C. & SHARMA, R. P. 2019. Examining the effects of the histone methyltransferase inhibitor BIX-01294 on histone modifications

and gene expression in both a clinical population and mouse models. *PLoS One,* 14**,** e0216463.

CHASE, K. A., GAVIN, D. P., GUIDOTTI, A. & SHARMA, R. P. 2013. Histone methylation at H3K9: evidence for a restrictive epigenome in schizophrenia. *Schizophr Res,* 149**,** 15-20.

CHASE, K. A., ROSEN, C., RUBIN, L. H., FEINER, B., BODAPATI, A. S., GIN, H., HU, E. & SHARMA, R. P. 2015. Evidence of a sex-dependent restrictive epigenome in schizophrenia. *Journal of Psychiatric Research,* 65**,** 87-94.

CHASE, K. A. & SHARMA, R. P. 2013. Nicotine induces chromatin remodelling through decreases in the methyltransferases GLP, G9a, Setdb1 and levels of H3K9me2. *International Journal of Neuropsychopharmacology,* 16**,** 1129-1138.

CHATURVEDI, C. P., SOMASUNDARAM, B., SINGH, K., CARPENEDO, R. L., STANFORD, W. L., DILWORTH, F. J. & BRAND, M. 2012. Maintenance of gene silencing by the coordinate action of the H3K9 methyltransferase G9a/KMT1C and the H3K4 demethylase Jarid1a/KDM5A. *Proc Natl Acad Sci U S A,* 109**,** 18845-50.

CHEN, D., LIU, J., WU, Z. & LI, S. H. 2021a. Role of miR-132/methyl-CpG-binding protein 2 in the regulation of neural stem cell differentiation. *Neural Regen Res,* 16**,** 345-349.

CHEN, E. S., GIGEK, C. O., ROSENFELD, J. A., DIALLO, A. B., MAUSSION, G., CHEN, G. G., VAILLANCOURT, K., LOPEZ, J. P., CRAPPER, L., POUJOL, R., SHAFFER, L. G., BOURQUE, G. & ERNST, C. 2014. Molecular convergence of neurodevelopmental disorders. *Am J Hum Genet,* 95**,** 490-508.

CHEN, R., HOU, Y., CONNELL, M. & ZHU, S. 2021b. Homeodomain protein Six4 prevents the generation of supernumerary Drosophila type II neuroblasts and premature differentiation of intermediate neural progenitors. *PLoS Genet,* 17**,** e1009371.

CHEN, S., ZHANG, Y., DING, X. & LI, W. 2022. Identification of lncRNA/circRNA-miRNA-mRNA ceRNA Network as Biomarkers for Hepatocellular Carcinoma. *Front Genet,* 13**,** 838869.

CHEN, X., ZHAO, W., YUAN, Y., BAI, Y., SUN, Y., ZHU, W. & DU, Z. 2017. MicroRNAs tend to synergistically control expression of genes encoding extensively-expressed proteins in humans. *PeerJ,* 5**,** e3682.

CHEN, Z.-F., PAQUETTE, A. J. & ANDERSON, D. J. 1998. NRSF/REST is required in vivo for repression of multiple neuronal target genes during embryogenesis. *Nature Genetics,* 20**,** 136-142.

CHENG, L.-C., PASTRANA, E., TAVAZOIE, M. & DOETSCH, F. 2009. miR-124 regulates adult neurogenesis in the subventricular zone stem cell niche. *Nature Neuroscience,* 12**,** 399-408.

CHEONG, A., BINGHAM, A. J., LI, J., KUMAR, B., SUKUMAR, P., MUNSCH, C., BUCKLEY, N. J., NEYLON, C. B., PORTER, K. E., BEECH, D. J. & WOOD, I. C. 2005. Downregulated REST transcription factor is a switch enabling critical potassium channel expression and cell proliferation. *Mol Cell,* 20**,** 45-52.

CHEREJI, R. V. & CLARK, D. J. 2018. Major Determinants of Nucleosome Positioning. *Biophys J,* 114**,** 2279-2289.

CHIN, H. G., ESTÈVE, P. O., PRADHAN, M., BENNER, J., PATNAIK, D., CAREY, M. F. & PRADHAN, S. 2007. Automethylation of G9a and its implication in wider substrate specificity and HP1 binding. *Nucleic Acids Res,* 35**,** 7313-23.

CHU, C.-Y. & RANA, T. M. 2006. Translation repression in human cells by microRNA-induced gene silencing requires RCK/p54. *PLoS biology,* 4**,** e210.

CICERI, G., BAGGIOLINI, A., CHO, H. S., KSHIRSAGAR, M., BENITO-KWIECINSKI, S., WALSH, R. M., AROMOLARAN, K. A., GONZALEZ-HERNANDEZ, A. J., MUNGUBA, H., KOO, S. Y., XU, N., SEVILLA, K. J., GOLDSTEIN, P. A., LEVITZ, J., LESLIE, C. S., KOCHE, R. P. & STUDER, L. 2024.

An epigenetic barrier sets the timing of human neuronal maturation. *Nature,* 626**,** 881-890.

CIPTASARI, U. & VAN BOKHOVEN, H. 2020. The phenomenal epigenome in neurodevelopmental disorders. *Hum Mol Genet,* 29**,** R42-r50.

COE, B. P., STESSMAN, H. A. F., SULOVARI, A., GEISHEKER, M. R., BAKKEN, T. E., LAKE, A. M., DOUGHERTY, J. D., LEIN, E. S., HORMOZDIARI, F., BERNIER, R. A. & EICHLER, E. E. 2019. Neurodevelopmental disease genes implicated by de novo mutation and copy number variation morbidity. *Nature Genetics,* 51**,** 106-116.

COHEN, J. L., JACKSON, N. L., BALLESTAS, M. E., WEBB, W. M., LUBIN, F. D. & CLINTON, S. M. 2017. Amygdalar expression of the microRNA miR-101a and its target Ezh2 contribute to rodent anxiety-like behaviour. *Eur J Neurosci,* 46**,** 2241-2252.

COLLINS, R. & CHENG, X. 2010. A case study in cross-talk: the histone lysine methyltransferases G9a and GLP. *Nucleic Acids Research,* 38**,** 3503-3511.

COLLINS, R. E., NORTHROP, J. P., HORTON, J. R., LEE, D. Y., ZHANG, X., STALLCUP, M. R. & CHENG, X. 2008. The ankyrin repeats of G9a and GLP histone methyltransferases are mono-and dimethyllysine binding modules. *Nature structural & molecular biology,* 15**,** 245-250.

CONACO, C., OTTO, S., HAN, J.-J. & MANDEL, G. 2006. Reciprocal actions of REST and a microRNA promote neuronal identity. *Proceedings of the National Academy of Sciences,* 103**,** 2422-2427.

CONSTANTINO, J. N. & MARRUS, N. 2017. The early origins of autism. *Child and Adolescent Psychiatric Clinics,* 26**,** 555-570.

COOPER, G. M., COE, B. P., GIRIRAJAN, S., ROSENFELD, J. A., VU, T. H., BAKER, C., WILLIAMS, C., STALKER, H., HAMID, R., HANNIG, V., ABDEL-HAMID, H., BADER, P., MCCRACKEN, E., NIYAZOV, D., LEPPIG, K., THIESE, H., HUMMEL, M., ALEXANDER, N., GORSKI, J., KUSSMANN, J., SHASHI, V., JOHNSON, K., REHDER, C., BALLIF, B. C., SHAFFER, L. G. & EICHLER, E. E. 2011. A copy number variation morbidity map of developmental delay. *Nat Genet,* 43**,** 838-46.

CORRELL, C. U. & SCHOOLER, N. R. 2020. Negative Symptoms in Schizophrenia: A Review and Clinical Guide for Recognition, Assessment, and Treatment. *Neuropsychiatr Dis Treat,* 16**,** 519-534.

CREWS, F. T., FISHER, R. P., QIN, L. & VETRENO, R. P. 2023. HMGB1 neuroimmune signaling and REST-G9a gene repression contribute to ethanol-induced reversible suppression of the cholinergic neuron phenotype. *Molecular Psychiatry,* 28**,** 5159-5172.

CUI, Y., QI, Y., DING, L., DING, S., HAN, Z., WANG, Y. & DU, P. 2024. miRNA dosage control in development and human disease. *Trends in Cell Biology,* 34**,** 31-47.

CURRY, E., GREEN, I., CHAPMAN-ROTHE, N., SHAMSAEI, E., KANDIL, S., CHERBLANC, F. L., PAYNE, L., BELL, E., GANESH, T., SRIMONGKOLPITHAK, N., CARON, J., LI, F., UREN, A. G., SNYDER, J. P., VEDADI, M., FUCHTER, M. J. & BROWN, R. 2015. Dual EZH2 and EHMT2 histone methyltransferase inhibition increases biological efficacy in breast cancer cells. *Clinical Epigenetics,* 7**,** 84.

DANIEL, B., NAGY, G., CZIMMERER, Z., HORVATH, A., HAMMERS, D. W., CUARANTA-MONROY, I., POLISKA, S., TZERPOS, P., KOLOSTYAK, Z., HAYS, T. T., PATSALOS, A., HOUTMAN, R., SAUER, S., FRANCOIS-DELEUZE, J., RASTINEJAD, F., BALINT, B. L., SWEENEY, H. L. & NAGY, L. 2018. The Nuclear Receptor PPARγ Controls Progressive Macrophage Polarization as a Ligand-Insensitive Epigenomic Ratchet of Transcriptional Memory. *Immunity,* 49**,** 615-626.e6.

DAVIS, T. H., CUELLAR, T. L., KOCH, S. M., BARKER, A. J., HARFE, B. D., MCMANUS, M. T. & ULLIAN, E. M. 2008. Conditional Loss of Dicer Disrupts Cellular and Tissue Morphogenesis in the Cortex and Hippocampus. *The Journal of Neuroscience,* 28**,** 4322-4330.

DE BOER, A., VERMEULEN, K., EGGER, J. I. M., JANZING, J. G. E., DE LEEUW, N., VEENSTRA-KNOL, H. E., DEN HOLLANDER, N. S., VAN BOKHOVEN, H., STAAL, W. & KLEEFSTRA, T. 2018. EHMT1 mosaicism in apparently unaffected parents is associated with autism spectrum disorder and neurocognitive dysfunction. *Molecular Autism,* 9**,** 5.

DE PIETRI TONELLI, D., PULVERS, J. N., HAFFNER, C., MURCHISON, E. P., HANNON, G. J. & HUTTNER, W. B. 2008. miRNAs are essential for survival and differentiation of newborn neurons but not for expansion of neural progenitors during early neurogenesis in the mouse embryonic neocortex. *Development,* 135**,** 3911-3921.

DEGIOSIO, R., KELLY, R. M., DEDIONISIO, A. M., NEWMAN, J. T., FISH, K. N., SAMPSON, A. R., LEWIS, D. A. & SWEET, R. A. 2019. MAP2 immunoreactivity deficit is conserved across the cerebral cortex within individuals with schizophrenia. *npj Schizophrenia,* 5**,** 13.

DI FEDE, E., GRAZIOLI, P., LETTIERI, A., PARODI, C., CASTIGLIONI, S., TACI, E., COLOMBO, E. A., ANCONA, S., PRIORI, A., GERVASINI, C. & MASSA, V. 2022. Epigenetic disorders: Lessons from the animals–animal models in chromatinopathies. *Frontiers in Cell and Developmental Biology,* 10.

DI FEDE, E., LETTIERI, A., TACI, E., CASTIGLIONI, S., REBELLATO, S., PARODI, C., COLOMBO, E. A., GRAZIOLI, P., NATACCI, F., MARCHISIO, P., PEZZANI, L., FAZIO, G., MILANI, D., MASSA, V. & GERVASINI, C. 2024. Characterization of a novel HDAC2 pathogenetic variant: a missing puzzle piece for chromatinopathies. *Human Genetics,* 143**,** 747-759.

DIENER, C., HART, M., FECHER-TROST, C., KNITTEL, J., RHEINHEIMER, S., MEYER, M. R., MAYER, J., FLOCKERZI, V., KELLER, A. & MEESE, E. 2023. Outside the limit: questioning the distance restrictions for cooperative miRNA binding sites. *Cell Mol Biol Lett,* 28**,** 8.

DIETRICH, N., LERDRUP, M., LANDT, E., AGRAWAL-SINGH, S., BAK, M., TOMMERUP, N., RAPPSILBER, J., SÖDERSTEN, E. & HANSEN, K. 2012. REST-mediated recruitment of polycomb repressor complexes in mammalian cells. *PLoS Genet,* 8**,** e1002494.

DIETS, I. J., PRESCOTT, T., CHAMPAIGNE, N. L., MANCINI, G. M., KROSSNES, B., FRIČ, R., KOCSIS, K., JONGMANS, M. C. & KLEEFSTRA, T. 2019. A recurrent de novo missense pathogenic variant in SMARCB1 causes severe intellectual disability and choroid plexus hyperplasia with resultant hydrocephalus. *Genetics in Medicine,* 21**,** 572-579.

DILL, H., LINDER, B., FEHR, A. & FISCHER, U. 2012. Intronic miR-26b controls neuronal differentiation by repressing its host transcript, ctdsp2. *Genes Dev,* 26**,** 25-30.

DING, N., ZHOU, H., ESTEVE, P.-O., CHIN, H. G., KIM, S., XU, X., JOSEPH, S. M., FRIEZ, M. J., SCHWARTZ, C. E. & PRADHAN, S. 2008. Mediator links epigenetic silencing of neuronal gene expression with x-linked mental retardation. *Molecular cell,* 31**,** 347-359.

DJURANOVIC, S., NAHVI, A. & GREEN, R. 2012. miRNA-mediated gene silencing by translational repression followed by mRNA deadenylation and decay. *Science,* 336**,** 237-240.

DOENCH, J. G. & SHARP, P. A. 2004. Specificity of microRNA target selection in translational repression. *Genes Dev,* 18**,** 504-11.

DONG, C., WU, Y., YAO, J., WANG, Y., YU, Y., RYCHAHOU, P. G., EVERS, B. M. & ZHOU, B. P. 2012. G9a interacts with Snail and is critical for Snail-mediated E-cadherin repression in human breast cancer. *The Journal of Clinical Investigation,* 122**,** 1469-1486.

DOSS, M. X. & SACHINIDIS, A. 2019. Current Challenges of iPSC-Based Disease Modeling and Therapeutic Implications. *Cells,* 8.

DROUIN-OUELLET, J., LAU, S., BRATTÅS, P. L., RYLANDER OTTOSSON, D., PIRCS, K., GRASSI, D. A., COLLINS, L. M., VUONO, R., ANDERSSON SJÖLAND, A., WESTERGREN-THORSSON, G.,

GRAFF, C., MINTHON, L., TORESSON, H., BARKER, R. A., JAKOBSSON, J. & PARMAR, M. 2017. REST suppression mediates neural conversion of adult human fibroblasts via microRNA-dependent and -independent pathways. *EMBO Molecular Medicine,* 9**,** 1117-1131.

DUAN, P., SUN, S., LI, B., HUANG, C., XU, Y., HAN, X., XING, Y. & YAN, W. 2014. miR-29a modulates neuronal differentiation through targeting REST in mesenchymal stem cells. *PLoS One,* 9**,** e97684.

DULABON, L., OLSON, E. C., TAGLIENTI, M. G., EISENHUTH, S., MCGRATH, B., WALSH, C. A., KREIDBERG, J. A. & ANTON, E. 2000. Reelin binds α3β1 integrin and inhibits neuronal migration. *Neuron,* 27**,** 33-44.

EBERT, M. S., NEILSON, J. R. & SHARP, P. A. 2007. MicroRNA sponges: competitive inhibitors of small RNAs in mammalian cells. *Nature Methods,* 4**,** 721-726.

ENDO, M., DRUSO, J. E. & CERIONE, R. A. 2020. The two splice variant forms of Cdc42 exert distinct and essential functions in neurogenesis. *J Biol Chem,* 295**,** 4498-4512.

ERNST, C. 2016. Proliferation and Differentiation Deficits are a Major Convergence Point for Neurodevelopmental Disorders. *Trends in Neurosciences,* 39**,** 290-299.

ERNST, C. & JEFRI, M. 2021. Epigenetic priming in neurodevelopmental disorders. *Trends Mol Med,* 27**,** 1106-1114.

ESCAMILLA-DEL-ARENAL, M., DA ROCHA, S. T., SPRUIJT, C. G., MASUI, O., RENAUD, O., SMITS, A. H., MARGUERON, R., VERMEULEN, M. & HEARD, E. 2013. Cdyl, a New Partner of the Inactive X Chromosome and Potential Reader of H3K27me3 and H3K9me2. *Molecular and Cellular Biology,* 33**,** 5005-5020.

ESPUNY-CAMACHO, I., MICHELSEN, K. A., GALL, D., LINARO, D., HASCHE, A., BONNEFONT, J., BALI, C., ORDUZ, D., BILHEU, A. & HERPOEL, A. 2013. Pyramidal neurons derived from human pluripotent stem cells integrate efficiently into mouse brain circuits in vivo. *Neuron,* 77**,** 440-456.

ESTÈVE, P. O., CHIN, H. G., SMALLWOOD, A., FEEHERY, G. R., GANGISETTY, O., KARPF, A. R., CAREY, M. F. & PRADHAN, S. 2006. Direct interaction between DNMT1 and G9a coordinates DNA and histone methylation during replication. *Genes Dev,* 20**,** 3089-103.

EYRING, K. W. & GESCHWIND, D. H. 2021. Three decades of ASD genetics: building a foundation for neurobiological understanding and treatment. *Human Molecular Genetics,* 30**,** R236-R244.

EZHKOVA, E., PASOLLI, H. A., PARKER, J. S., STOKES, N., SU, I. H., HANNON, G., TARAKHOVSKY, A. & FUCHS, E. 2009. Ezh2 orchestrates gene expression for the stepwise differentiation of tissue-specific stem cells. *Cell,* 136**,** 1122-35.

FAVARO, R., VALOTTA, M., FERRI, A. L. M., LATORRE, E., MARIANI, J., GIACHINO, C., LANCINI, C., TOSETTI, V., OTTOLENGHI, S., TAYLOR, V. & NICOLIS, S. K. 2009. Hippocampal development and neural stem cell maintenance require Sox2-dependent regulation of Shh. *Nature Neuroscience,* 12**,** 1248-1256.

FEAR, V. S., FORBES, C. A., ANDERSON, D., RAUSCHERT, S., SYN, G., SHAW, N., JAMIESON, S., WARD, M., BAYNAM, G. & LASSMANN, T. 2022. CRISPR single base editing, neuronal disease modelling and functional genomics for genetic variant analysis: pipeline validation using Kleefstra syndrome EHMT1 haploinsufficiency. *Stem Cell Research & Therapy,* 13**,** 69.

FEDOROVA, V., AMRUZ CERNA, K., OPPELT, J., POSPISILOVA, V., BARTA, T., MRAZ, M. & BOHACIAKOVA, D. 2023. MicroRNA Profiling of Self-Renewing Human Neural Stem Cells Reveals Novel Sets of Differentially Expressed microRNAs During Neural Differentiation In Vitro. *Stem Cell Rev Rep,* 19**,** 1524-1539.

FILION, G. J. & VAN STEENSEL, B. 2010. Reassessing the abundance of H3K9me2 chromatin domains in embryonic stem cells. *Nature Genetics,* 42**,** 4-4.

FISZBEIN, A., GIONO, LUCIANA E., QUAGLINO, A., BERARDINO, BRUNO G., SIGAUT, L., VON BILDERLING, C., SCHOR, IGNACIO E., ENRIQUÉ STEINBERG, J. H., ROSSI, M., PIETRASANTA, LÍA I., CARAMELO, JULIO J., SREBROW, A. & KORNBLIHTT, ALBERTO R. 2016. Alternative Splicing of G9a Regulates Neuronal Differentiation. *Cell Reports,* 14**,** 2797-2808.

FLAMAND, M. N., GAN, H. H., MAYYA, V. K., GUNSALUS, K. C. & DUCHAINE, T. F. 2017. A non-canonical site reveals the cooperative mechanisms of microRNA-mediated silencing. *Nucleic Acids Research,* 45**,** 7212-7225.

FONG, K. W., ZHAO, J. C., LU, X., KIM, J., PIUNTI, A., SHILATIFARD, A. & YU, J. 2022. PALI1 promotes tumor growth through competitive recruitment of PRC2 to G9A-target chromatin for dual epigenetic silencing. *Mol Cell,* 82**,** 4611-4626.e7.

FRAGOLA, G., GERMAIN, P. L., LAISE, P., CUOMO, A., BLASIMME, A., GROSS, F., SIGNAROLDI, E., BUCCI, G., SOMMER, C., PRUNERI, G., MAZZAROL, G., BONALDI, T., MOSTOSLAVSKY, G., CASOLA, S. & TESTA, G. 2013. Cell reprogramming requires silencing of a core subset of polycomb targets. *PLoS Genet,* 9**,** e1003292.

FRANZONI, E., BOOKER, S. A., PARTHASARATHY, S., REHFELD, F., GROSSER, S., SRIVATSA, S., FUCHS, H. R., TARABYKIN, V., VIDA, I. & WULCZYN, F. G. 2015. miR-128 regulates neuronal migration, outgrowth and intrinsic excitability via the intellectual disability gene Phf6. *elife,* 4**,** e04263.

FREGA, M., LINDA, K., KELLER, J. M., GÜMÜŞ-AKAY, G., MOSSINK, B., VAN RHIJN, J.-R., NEGWER, M., KLEIN GUNNEWIEK, T., FOREMAN, K., KOMPIER, N., SCHOENMAKER, C., VAN DEN AKKER, W., VAN DER WERF, I., OUDAKKER, A., ZHOU, H., KLEEFSTRA, T., SCHUBERT, D., VAN BOKHOVEN, H. & NADIF KASRI, N. 2019. Neuronal network dysfunction in a model for Kleefstra syndrome mediated by enhanced NMDAR signaling. *Nature communications,* 10**,** 4928-4928.

FREGA, M., SELTEN, M., MOSSINK, B., KELLER, J. M., LINDA, K., MOERSCHEN, R., QU, J., KOERNER, P., JANSEN, S., OUDAKKER, A., KLEEFSTRA, T., VAN BOKHOVEN, H., ZHOU, H., SCHUBERT, D. & NADIF KASRI, N. 2020. Distinct Pathogenic Genes Causing Intellectual Disability and Autism Exhibit a Common Neuronal Network Hyperactivity Phenotype. *Cell Rep,* 30**,** 173-186.e6.

FRIEDMAN, R. C., FARH, K. K., BURGE, C. B. & BARTEL, D. P. 2009. Most mammalian mRNAs are conserved targets of microRNAs. *Genome Res,* 19**,** 92-105.

FUENTES, P., CÁNOVAS, J., BERNDT, F. A., NOCTOR, S. C. & KUKULJAN, M. 2012. CoREST/LSD1 Control the Development of Pyramidal Cortical Neurons. *Cerebral Cortex,* 22**,** 1431-1441.

FUKAO, A., MISHIMA, Y., TAKIZAWA, N., OKA, S., IMATAKA, H., PELLETIER, J., SONENBERG, N., THOMA, C. & FUJIWARA, T. 2014. MicroRNAs trigger dissociation of eIF4AI and eIF4AII from target mRNAs in humans. *Molecular cell,* 56**,** 79-89.

FUKAYA, T., IWAKAWA, H.-O. & TOMARI, Y. 2014. MicroRNAs block assembly of eIF4F translation initiation complex in Drosophila. *Molecular cell,* 56**,** 67-78.

GAM, J. J., BABB, J. & WEISS, R. 2018. A mixed antagonistic/synergistic miRNA repression model enables accurate predictions of multi-input miRNA sensor activity. *Nature Communications,* 9**,** 2430.

GAO, L., ZHAO, Y., MA, X. & ZHANG, L. 2021. Integrated analysis of lncRNA–miRNA–mRNA ceRNA network and the potential prognosis indicators in sarcomas. *BMC Medical Genomics,* 14**,** 67.

GAO, Y., XIE, M., GUO, Y., YANG, Q., HU, S. & LI, Z. 2020. Long Non-coding RNA FGD5-AS1 Regulates Cancer Cell Proliferation and Chemoresistance in Gastric Cancer Through miR-153-3p/CITED2 Axis. *Front Genet,* 11**,** 715.

GAO, Z., DING, P. & HSIEH, J. 2012. Profiling of REST-Dependent microRNAs Reveals Dynamic Modes of Expression. *Front Neurosci,* 6**,** 67.

GAO, Z., URE, K., DING, P., NASHAAT, M., YUAN, L., MA, J., HAMMER, R. E. & HSIEH, J. 2011. The Master Negative Regulator REST/NRSF Controls Adult Neurogenesis by Restraining the Neurogenic Program in Quiescent Stem Cells. *The Journal of Neuroscience,* 31**,** 9772-9786.

GARAFFO, G., CONTE, D., PROVERO, P., TOMAIUOLO, D., LUO, Z., PINCIROLI, P., PEANO, C., D'ATRI, I., GITTON, Y., ETZION, T., GOTHILF, Y., GAYS, D., SANTORO, M. M. & MERLO, G. R. 2015. The Dlx5 and Foxg1 transcription factors, linked via miRNA-9 and -200, are required for the development of the olfactory and GnRH system. *Mol Cell Neurosci,* 68**,** 103-19.

GARDINER, A. S., TWISS, J. L. & PERRONE-BIZZOZERO, N. I. 2015. Competing Interactions of RNA-Binding Proteins, MicroRNAs, and Their Targets Control Neuronal Development and Function. *Biomolecules,* 5**,** 2903-18.

GAUGLER, T., KLEI, L., SANDERS, S. J., BODEA, C. A., GOLDBERG, A. P., LEE, A. B., MAHAJAN, M., MANAA, D., PAWITAN, Y., REICHERT, J., RIPKE, S., SANDIN, S., SKLAR, P., SVANTESSON, O., REICHENBERG, A., HULTMAN, C. M., DEVLIN, B., ROEDER, K. & BUXBAUM, J. D. 2014. Most genetic risk for autism resides with common variation. *Nature Genetics,* 46**,** 881-885.

GAVIN, D. P., ROSEN, C., CHASE, K., GRAYSON, D. R., TUN, N. & SHARMA, R. P. 2009. Dimethylated lysine 9 of histone 3 is elevated in schizophrenia and exhibits a divergent response to histone deacetylase inhibitors in lymphocyte cultures. *Journal of Psychiatry and Neuroscience,* 34**,** 232-237.

GEBERT, L. F. R. & MACRAE, I. J. 2019. Regulation of microRNA function in animals. *Nature Reviews Molecular Cell Biology,* 20**,** 21-37.

GEBESHUBER, C. A., KORNAUTH, C., DONG, L., SIERIG, R., SEIBLER, J., REISS, M., TAUBER, S., BILBAN, M., WANG, S., KAIN, R., BÖHMIG, G. A., MOELLER, M. J., GRÖNE, H. J., ENGLERT, C., MARTINEZ, J. & KERJASCHKI, D. 2013. Focal segmental glomerulosclerosis is induced by microRNA-193a and its downregulation of WT1. *Nat Med,* 19**,** 481-7.

GEBHARDT, M. L., REUTER, S., MROWKA, R. & ANDRADE-NAVARRO, M. A. 2014. Similarity in targets with REST points to neural and glioblastoma related miRNAs. *Nucleic Acids Research,* 42**,** 5436-5446.

GENNADY, K., VLADIMIR, S., NIKOLAY, B., BORIS, S., MAXIM, N. A. & ALEXEY, S. 2021. Fast gene set enrichment analysis. *bioRxiv***,** 060012.

GERVASI, N. M., DIMTCHEV, A., CLARK, D. M., DINGLE, M., PISARCHIK, A. V. & NESTI, L. J. 2021. C-terminal domain small phosphatase 1 (CTDSP1) regulates growth factor expression and axonal regeneration in peripheral nerve tissue. *Scientific Reports,* 11**,** 14462.

GIBSON, W. T., HOOD, R. L., ZHAN, S. H., BULMAN, D. E., FEJES, A. P., MOORE, R., MUNGALL, A. J., EYDOUX, P., BABUL-HIRJI, R., AN, J., MARRA, M. A., CHITAYAT, D., BOYCOTT, K. M., WEAVER, D. D. & JONES, S. J. 2012. Mutations in EZH2 cause Weaver syndrome. *Am J Hum Genet,* 90**,** 110-8.

GIGEK, C. O., CHEN, E. S., OTA, V. K., MAUSSION, G., PENG, H., VAILLANCOURT, K., DIALLO, A. B., LOPEZ, J. P., CRAPPER, L., VASUTA, C., CHEN, G. G. & ERNST, C. 2015. A molecular model for neurodevelopmental disorders. *Translational Psychiatry,* 5**,** e565-e565.

GIORGI SILVEIRA, R., PERELLÓ FERRÚA, C., DO AMARAL, C. C., FERNANDEZ GARCIA, T., DE SOUZA, K. B. & NEDEL, F. 2020. MicroRNAs expressed in neuronal differentiation and their

associated pathways: Systematic review and bioinformatics analysis. *Brain Research Bulletin,* 157**,** 140-148.

GIUSTI, S. A., VOGL, A. M., BROCKMANN, M. M., VERCELLI, C. A., REIN, M. L., TRÜMBACH, D., WURST, W., CAZALLA, D., STEIN, V., DEUSSING, J. M. & REFOJO, D. 2014. MicroRNA-9 controls dendritic development by targeting REST. *Elife,* 3.

GLAROS, S., CIRRINCIONE, G. M., MUCHARDT, C., KLEER, C. G., MICHAEL, C. W. & REISMAN, D. 2007. The reversible epigenetic silencing of BRM: implications for clinical targeted therapy. *Oncogene,* 26**,** 7058-7066.

GÖTZ, M. & HUTTNER, W. B. 2005. The cell biology of neurogenesis. *Nature Reviews Molecular Cell Biology,* 6**,** 777-788.

GREGORY, R. I., YAN, K.-P., AMUTHAN, G., CHENDRIMADA, T., DORATOTAJ, B., COOCH, N. & SHIEKHATTAR, R. 2004. The Microprocessor complex mediates the genesis of microRNAs. *Nature,* 432**,** 235-240.

GRIGAITIS, P., STARKUVIENE, V., ROST, U., SERVA, A., PUCHOLT, P. & KUMMER, U. 2020. miRNA target identification and prediction as a function of time in gene expression data. *RNA Biol,* 17**,** 990-1000.

GUAJARDO, L., AGUILAR, R., BUSTOS, F. J., NARDOCCI, G., GUTIÉRREZ, R. A., VAN ZUNDERT, B. & MONTECINO, M. 2020. Downregulation of the Polycomb-Associated Methyltransferase Ezh2 during Maturation of Hippocampal Neurons Is Mediated by MicroRNAs Let-7 and miR-124. *Int J Mol Sci,* 21.

GUO, H., INGOLIA, N. T., WEISSMAN, J. S. & BARTEL, D. P. 2010. Mammalian microRNAs predominantly act to decrease target mRNA levels. *Nature,* 466**,** 835-840.

HA, M. & KIM, V. N. 2014. Regulation of microRNA biogenesis. *Nature Reviews Molecular Cell Biology,* 15**,** 509-524.

HALDER, D., LEE, C.-H., HYUN, J. Y., CHANG, G.-E., CHEONG, E. & SHIN, I. 2017. Suppression of Sin3A activity promotes differentiation of pluripotent cells into functional neurons. *Scientific Reports,* 7**,** 44818.

HAN, J., DENLI, A. M. & GAGE, F. H. 2012. The enemy within: intronic miR-26b represses its host gene, ctdsp2, to regulate neurogenesis. *Genes Dev,* 26**,** 6-10.

HAN, J., LEE, Y., YEOM, K.-H., NAM, J.-W., HEO, I., RHEE, J.-K., SOHN, S. Y., CHO, Y., ZHANG, B.-T. & KIM, V. N. 2006. Molecular basis for the recognition of primary microRNAs by the Drosha-DGCR8 complex. *cell,* 125**,** 887-901.

HAN, J., PEDERSEN, J. S., KWON, S. C., BELAIR, C. D., KIM, Y.-K., YEOM, K.-H., YANG, W.-Y., HAUSSLER, D., BLELLOCH, R. & KIM, V. N. 2009. Posttranscriptional Crossregulation between Drosha and DGCR8. *Cell,* 136**,** 75-84.

HARRIS, J. R., GAO, C. W., BRITTON, J. F., APPLEGATE, C. D., BJORNSSON, H. T. & FAHRNER, J. A. 2023. Five years of experience in the Epigenetics and Chromatin Clinic: what have we learned and where do we go from here? *Human Genetics*.

HARWOOD, J. C., KENT, N. A., ALLEN, N. D. & HARWOOD, A. J. 2019. Nucleosome dynamics of human iPSC during neural differentiation. *EMBO reports,* 20**,** e46960.

HASELEY, A., WALLIS, K. & DEBROSSE, S. 2021. Kleefstra syndrome: Impact on parents. *Disability and Health Journal,* 14**,** 101018.

HASHIMOTO, Y., AKIYAMA, Y. & YUASA, Y. 2013. Multiple-to-multiple relationships between microRNAs and target genes in gastric cancer. *PLoS One,* 8**,** e62589.

HE, H. H., MEYER, C. A., SHIN, H., BAILEY, S. T., WEI, G., WANG, Q., ZHANG, Y., XU, K., NI, M., LUPIEN, M., MIECZKOWSKI, P., LIEB, J. D., ZHAO, K., BROWN, M. & LIU, X. S. 2010. Nucleosome dynamics define transcriptional enhancers. *Nature Genetics,* 42**,** 343-347.

HE, Y., LI, H. B., LI, X., ZHOU, Y., XIA, X. B. & SONG, W. T. 2018. MiR-124 Promotes the Growth of Retinal Ganglion Cells Derived from Müller Cells. *Cell Physiol Biochem,* 45**,** 973-983.

HERGENREDER, E., MINOTTI, A. P., ZORINA, Y., OBERST, P., ZHAO, Z., MUNGUBA, H., CALDER, E. L., BAGGIOLINI, A., WALSH, R. M., LISTON, C., LEVITZ, J., GARIPPA, R., CHEN, S., CICERI, G. & STUDER, L. 2024. Combined small-molecule treatment accelerates maturation of human pluripotent stem cell-derived neurons. *Nature Biotechnology*.

HØJFELDT, J. W., LAUGESEN, A., WILLUMSEN, B. M., DAMHOFER, H., HEDEHUS, L., TVARDOVSKIY, A., MOHAMMAD, F., JENSEN, O. N. & HELIN, K. 2018. Accurate H3K27 methylation can be established de novo by SUZ12-directed PRC2. *Nature structural & molecular biology,* 25**,** 225-232.

HOURS, C., RECASENS, C. & BALEYTE, J. M. 2022. ASD and ADHD Comorbidity: What Are We Talking About? *Front Psychiatry,* 13**,** 837424.

HUANG, H. Y., LIN, Y. C., CUI, S., HUANG, Y., TANG, Y., XU, J., BAO, J., LI, Y., WEN, J., ZUO, H., WANG, W., LI, J., NI, J., RUAN, Y., LI, L., CHEN, Y., XIE, Y., ZHU, Z., CAI, X., CHEN, X., YAO, L., CHEN, Y., LUO, Y., LUXU, S., LUO, M., CHIU, C. M., MA, K., ZHU, L., CHENG, G. J., BAI, C., CHIANG, Y. C., WANG, L., WEI, F., LEE, T. Y. & HUANG, H. D. 2022a. miRTarBase update 2022: an informative resource for experimentally validated miRNA-target interactions. *Nucleic Acids Res,* 50**,** D222-d230.

HUANG, X., BASHKENOVA, N., HONG, Y., LYU, C., GUALLAR, D., HU, Z., MALIK, V., LI, D., WANG, H., SHEN, X., ZHOU, H. & WANG, J. 2022b. A TET1-PSPC1-Neat1 molecular axis modulates PRC2 functions in controlling stem cell bivalency. *Cell Rep,* 39**,** 110928.

HUANG, X. J., WANG, X., MA, X., SUN, S. C., ZHOU, X., ZHU, C. & LIU, H. 2014. EZH2 is essential for development of mouse preimplantation embryos. *Reprod Fertil Dev,* 26**,** 1166-75.

HUANG, Y.-C., SHIH, H.-Y., LIN, S.-J., CHIU, C.-C., MA, T.-L., YEH, T.-H. & CHENG, Y.-C. 2015. The epigenetic factor Kmt2a/Mll1 regulates neural progenitor proliferation and neuronal and glial differentiation. *Developmental Neurobiology,* 75**,** 452-462.

HUANG, Y., MYERS, S. J. & DINGLEDINE, R. 1999. Transcriptional repression by REST: recruitment of Sin3A and histone deacetylase to neuronal genes. *Nature Neuroscience,* 2**,** 867-872.

HUNTER, J., RIVERO-ARIAS, O., ANGELOV, A., KIM, E., FOTHERINGHAM, I. & LEAL, J. 2014. Epidemiology of fragile X syndrome: A systematic review and meta-analysis. *American Journal of Medical Genetics Part A,* 164**,** 1648-1658.

HUNTZINGER, E. & IZAURRALDE, E. 2011. Gene silencing by microRNAs: contributions of translational repression and mRNA decay. *Nature Reviews Genetics,* 12**,** 99-110.

IMAGAWA, E., HIGASHIMOTO, K., SAKAI, Y., NUMAKURA, C., OKAMOTO, N., MATSUNAGA, S., RYO, A., SATO, Y., SANEFUJI, M. & IHARA, K. 2017. Mutations in genes encoding polycomb repressive complex 2 subunits cause Weaver syndrome. *Human mutation,* 38**,** 637-648.

INAGAWA, M., NAKAJIMA, K., MAKINO, T., OGAWA, S., KOJIMA, M., ITO, S., IKENISHI, A., HAYASHI, T., SCHWARTZ, R. J., NAKAMURA, K., OBAYASHI, T., TACHIBANA, M., SHINKAI, Y., MAEDA, K., MIYAGAWA-TOMITA, S. & TAKEUCHI, T. 2013. Histone H3 lysine 9 methyltransferases, G9a and GLP are essential for cardiac morphogenesis. *Mechanisms of Development,* 130**,** 519-531.

INSEL, T. R. 2010. Rethinking schizophrenia. *Nature,* 468**,** 187-193.

INUI, M., MARTELLO, G. & PICCOLO, S. 2010. MicroRNA control of signal transduction. *Nature Reviews Molecular Cell Biology,* 11**,** 252-263.

ISHIGURO, K., KITAJIMA, H., NIINUMA, T., MARUYAMA, R., NISHIYAMA, N., OHTANI, H., SUDO, G., TOYOTA, M., SASAKI, H., YAMAMOTO, E., KAI, M., NAKASE, H. & SUZUKI, H. 2021. Dual EZH2 and G9a inhibition suppresses multiple myeloma cell proliferation by regulating the interferon signal and IRF4-MYC axis. *Cell Death Discov,* 7**,** 7.

JARRED, E. G., QU, Z., TSAI, T., OBERIN, R., PETAUTSCHNIG, S., BILDSOE, H., PEDERSON, S., ZHANG, Q.-H., STRINGER, J. M., CARROLL, J., GARDNER, D. K., VAN DEN BUUSE, M., SIMS, N. A., GIBSON, W. T., ADELSON, D. L. & WESTERN, P. S. 2022. Transient Polycomb activity represses developmental genes in growing oocytes. *Clinical Epigenetics,* 14**,** 183.

JEON, H., XIE, J., JEON, Y., JUNG, K. J., GUPTA, A., CHANG, W. & CHUNG, D. 2023. Statistical Power Analysis for Designing Bulk, Single-Cell, and Spatial Transcriptomics Experiments: Review, Tutorial, and Perspectives. *Biomolecules,* 13.

JIE, J., LIU, D., WANG, Y., WU, Q., WU, T. & FANG, R. 2022. Generation of MiRNA sponge constructs targeting multiple MiRNAs. *J Clin Lab Anal,* 36**,** e24527.

JIN, B., TAO, Q., PENG, J., SOO, H. M., WU, W., YING, J., FIELDS, C. R., DELMAS, A. L., LIU, X., QIU, J. & ROBERTSON, K. D. 2007. DNA methyltransferase 3B (DNMT3B) mutations in ICF syndrome lead to altered epigenetic modifications and aberrant expression of genes regulating development, neurogenesis and immune function. *Human Molecular Genetics,* 17**,** 690-709.

JOHNSON, R., GAMBLIN, R. J., OOI, L., BRUCE, A. W., DONALDSON, I. J., WESTHEAD, D. R., WOOD, I. C., JACKSON, R. M. & BUCKLEY, N. J. 2006. Identification of the REST regulon reveals extensive transposable element-mediated binding site duplication. *Nucleic acids research,* 34**,** 3862-3877.

JOHNSON, R., SAMUEL, J., NG, C. K. L., JAUCH, R., STANTON, L. W. & WOOD, I. C. 2009. Evolution of the Vertebrate Gene Regulatory Network Controlled by the Transcriptional Repressor REST. *Molecular Biology and Evolution,* 26**,** 1491-1507.

JOHNSON, R., TEH, C. H., KUNARSO, G., WONG, K. Y., SRINIVASAN, G., COOPER, M. L., VOLTA, M., CHAN, S. S., LIPOVICH, L., POLLARD, S. M., KARUTURI, R. K., WEI, C. L., BUCKLEY, N. J. & STANTON, L. W. 2008. REST regulates distinct transcriptional networks in embryonic and neural stem cells. *PLoS Biol,* 6**,** e256.

JONAS, S. & IZAURRALDE, E. 2015. Towards a molecular understanding of microRNA-mediated gene silencing. *Nature reviews genetics,* 16**,** 421-433.

JONES, F. S. & MEECH, R. 1999. Knockout of REST/NRSF shows that the protein is a potent repressor of neuronally expressed genes in non-neural tissues. *Bioessays,* 21**,** 372-6.

JONES, WENDY D., DAFOU, D., MCENTAGART, M., WOOLLARD, WESLEY J., ELMSLIE, FRANCES V., HOLDER-ESPINASSE, M., IRVING, M., SAGGAR, ANAND K., SMITHSON, S., TREMBATH, RICHARD C., DESHPANDE, C. & SIMPSON, MICHAEL A. 2012. De Novo Mutations in MLL Cause Wiedemann-Steiner Syndrome. *The American Journal of Human Genetics,* 91**,** 358-364.

JORDI, E., HEIMAN, M., MARION-POLL, L., GUERMONPREZ, P., CHENG, S. K., NAIRN, A. C., GREENGARD, P. & GIRAULT, J.-A. 2013. Differential effects of cocaine on histone posttranslational modifications in identified populations of striatal neurons. *Proceedings of the National Academy of Sciences,* 110**,** 9511-9516.

JUNG, J., YEOM, C., CHOI, Y. S., KIM, S., LEE, E., PARK, M. J., KANG, S. W., KIM, S. B. & CHANG, S. 2015. Simultaneous inhibition of multiple oncogenic miRNAs by a multi-potent microRNA sponge. *Oncotarget,* 6**,** 20370-87.

KABAYIZA, K. U., MASGUTOVA, G., HARRIS, A., RUCCHIN, V., JACOB, B. & CLOTMAN, F. 2017. The Onecut Transcription Factors Regulate Differentiation and Distribution of Dorsal Interneurons during Spinal Cord Development. *Front Mol Neurosci,* 10**,** 157.

KANDURI, M., SANDER, B., NTOUFA, S., PAPAKONSTANTINOU, N., SUTTON, L. A., STAMATOPOULOS, K., KANDURI, C. & ROSENQUIST, R. 2013. A key role for EZH2 in epigenetic silencing of HOX genes in mantle cell lymphoma. *Epigenetics,* 8**,** 1280-8.

KANEKO, M., ROSSER, T. & RACA, G. 2021. Dilated cardiomyopathy in a patient with autosomal dominant EEF1A2-related neurodevelopmental disorder. *European Journal of Medical Genetics,* 64**,** 104121.

KANEKO, S., BONASIO, R., SALDAÑA-MEYER, R., YOSHIDA, T., SON, J., NISHINO, K., UMEZAWA, A. & REINBERG, D. 2014. Interactions between JARID2 and noncoding RNAs regulate PRC2 recruitment to chromatin. *Molecular cell,* 53**,** 290-300.

KANG, W., WONG, L. C., SHI, S.-H. & HÉBERT, J. M. 2009. The transition from radial glial to intermediate progenitor cell is inhibited by FGF signaling during corticogenesis. *Journal of Neuroscience,* 29**,** 14571-14580.

KANTON, S., BOYLE, M. J., HE, Z., SANTEL, M., WEIGERT, A., SANCHÍS-CALLEJA, F., GUIJARRO, P., SIDOW, L., FLECK, J. S., HAN, D., QIAN, Z., HEIDE, M., HUTTNER, W. B., KHAITOVICH, P., PÄÄBO, S., TREUTLEIN, B. & CAMP, J. G. 2019. Organoid single-cell genomic atlas uncovers human-specific features of brain development. *Nature,* 574**,** 418-422.

KARAGKOUNI, D., PARASKEVOPOULOU, M. D., CHATZOPOULOS, S., VLACHOS, I. S., TASTSOGLOU, S., KANELLOS, I., PAPADIMITRIOU, D., KAVAKIOTIS, I., MANIOU, S., SKOUFOS, G., VERGOULIS, T., DALAMAGAS, T. & HATZIGEORGIOU, A. G. 2017. DIANA-TarBase v8: a decade-long collection of experimentally supported miRNA–gene interactions. *Nucleic Acids Research,* 46**,** D239-D245.

KARIUKI, D., ASAM, K., AOUIZERAT, B. E., LEWIS, K. A., FLOREZ, J. C. & FLOWERS, E. 2023. Review of databases for experimentally validated human microRNA–mRNA interactions. *Database,* 2023.

KAUFMANN, W. E., KIDD, S. A., ANDREWS, H. F., BUDIMIROVIC, D. B., ESLER, A., HAAS-GIVLER, B., STACKHOUSE, T., RILEY, C., PEACOCK, G., SHERMAN, S. L., BROWN, W. T. & BERRY-KRAVIS, E. 2017. Autism Spectrum Disorder in Fragile X Syndrome: Cooccurring Conditions and Current Treatment. *Pediatrics,* 139**,** S194-s206.

KAUR, A., CHAUDHRY, C., KAUR, P., DANIEL, R. & SRIVASTAVA, P. 2022. Pattern Recognition of Common Multiple Congenital Malformation Syndromes with Underlying Chromatinopathy. *J Pediatr Genet*.

KENIRY, A., GEARING, L. J., JANSZ, N., LIU, J., HOLIK, A. Z., HICKEY, P. F., KINKEL, S. A., MOORE, D. L., BRESLIN, K., CHEN, K., LIU, R., PHILLIPS, C., PAKUSCH, M., BIBEN, C., SHERIDAN, J. M., KILE, B. T., CARMICHAEL, C., RITCHIE, M. E., HILTON, D. J. & BLEWITT, M. E. 2016. Setdb1-mediated H3K9 methylation is enriched on the inactive X and plays a role in its epigenetic silencing. *Epigenetics Chromatin,* 9**,** 16.

KERCHNER, K. M., MOU, T.-C., SUN, Y., RUSNAC, D.-V., SPRANG, S. R. & BRIKNAROVÁ, K. 2021. The structure of the cysteine-rich region from human histone-lysine N-methyltransferase EHMT2 (G9a). *Journal of Structural Biology: X,* 5**,** 100050.

KIM, E. J., LEUNG, C. T., REED, R. R. & JOHNSON, J. E. 2007. In vivo analysis of Ascl1 defined progenitors reveals distinct developmental dynamics during adult neurogenesis and gliogenesis. *J Neurosci,* 27**,** 12764-74.

KIM, S. C., LEE, E. H., YU, J. H., KIM, S. M., NAM, B. G., CHUNG, H. Y., KIM, Y. S., CHO, S. R. & PARK, C. H. 2019. Cell Surface Antigen Display for Neuronal Differentiation-Specific Tracking. *Biomol Ther (Seoul),* 27**,** 78-84.

KIM, Y.-K., KIM, B. & KIM, V. N. 2016. Re-evaluation of the roles of DROSHA, Exportin 5, and DICER in microRNA biogenesis. *Proceedings of the National Academy of Sciences,* 113**,** E1881-E1889.

KIROV, G., POCKLINGTON, A. J., HOLMANS, P., IVANOV, D., IKEDA, M., RUDERFER, D., MORAN, J., CHAMBERT, K., TONCHEVA, D., GEORGIEVA, L., GROZEVA, D., FJODOROVA, M., WOLLERTON, R., REES, E., NIKOLOV, I., VAN DE LAGEMAAT, L. N., BAYÉS, À., FERNANDEZ,

E., OLASON, P. I., BÖTTCHER, Y., KOMIYAMA, N. H., COLLINS, M. O., CHOUDHARY, J., STEFANSSON, K., STEFANSSON, H., GRANT, S. G. N., PURCELL, S., SKLAR, P., O'DONOVAN, M. C. & OWEN, M. J. 2012. De novo CNV analysis implicates specific abnormalities of postsynaptic signalling complexes in the pathogenesis of schizophrenia. *Molecular Psychiatry,* 17**,** 142-153.

KLEEFSTRA-SYNDROME-UK 2018. Kleefstra Syndrome Survey Results 2018.

KLEEFSTRA, T., BRUNNER, H. G., AMIEL, J., OUDAKKER, A. R., NILLESEN, W. M., MAGEE, A., GENEVIÈVE, D., CORMIER-DAIRE, V., VAN ESCH, H. & FRYNS, J.-P. 2006a. Loss-of-function mutations in euchromatin histone methyl transferase 1 (EHMT1) cause the 9q34 subtelomeric deletion syndrome. *The American Journal of Human Genetics,* 79**,** 370-377.

KLEEFSTRA, T., BRUNNER, H. G., AMIEL, J., OUDAKKER, A. R., NILLESEN, W. M., MAGEE, A., GENEVIÈVE, D., CORMIER-DAIRE, V., VAN ESCH, H., FRYNS, J. P., HAMEL, B. C., SISTERMANS, E. A., DE VRIES, B. B. & VAN BOKHOVEN, H. 2006b. Loss-of-function mutations in euchromatin histone methyl transferase 1 (EHMT1) cause the 9q34 subtelomeric deletion syndrome. *Am J Hum Genet,* 79**,** 370-7.

KLEEFSTRA, T., KRAMER, J. M., NEVELING, K., WILLEMSEN, M. H., KOEMANS, T. S., VISSERS, L. E., WISSINK-LINDHOUT, W., FENCKOVA, M., VAN DEN AKKER, W. M. & KASRI, N. N. 2012. Disruption of an EHMT1-associated chromatin-modification module causes intellectual disability. *The American Journal of Human Genetics,* 91**,** 73-82.

KLEIN, M. E., LIOY, D. T., MA, L., IMPEY, S., MANDEL, G. & GOODMAN, R. H. 2007. Homeostatic regulation of MeCP2 expression by a CREB-induced microRNA. *Nature Neuroscience,* 10**,** 1513-1514.

KLUIVER, J., SLEZAK-PROCHAZKA, I., SMIGIELSKA-CZEPIEL, K., HALSEMA, N., KROESEN, B.-J. & VAN DEN BERG, A. 2012a. Generation of miRNA sponge constructs. *Methods,* 58**,** 113-117.

KLUIVER, J., SLEZAK-PROCHAZKA, I., SMIGIELSKA-CZEPIEL, K., HALSEMA, N., KROESEN, B. J. & VAN DEN BERG, A. 2012b. Generation of miRNA sponge constructs. *Methods,* 58**,** 113-7.

KOEMANS, T. S., KLEEFSTRA, T., CHUBAK, M. C., STONE, M. H., REIJNDERS, M. R. F., DE MUNNIK, S., WILLEMSEN, M. H., FENCKOVA, M., STUMPEL, C., BOK, L. A., SIFUENTES SAENZ, M., BYERLY, K. A., BAUGHN, L. B., STEGMANN, A. P. A., PFUNDT, R., ZHOU, H., VAN BOKHOVEN, H., SCHENCK, A. & KRAMER, J. M. 2017. Functional convergence of histone methyltransferases EHMT1 and KMT2C involved in intellectual disability and autism spectrum disorder. *PLoS Genet,* 13**,** e1006864.

KONG, S., LU, Y., TAN, S., LI, R., GAO, Y., LI, K. & ZHANG, Y. 2022. Nucleosome-Omics: A Perspective on the Epigenetic Code and 3D Genome Landscape. *Genes (Basel),* 13.

KOO, B., LEE, K.-H., MING, G.-L., YOON, K.-J. & SONG, H. 2023. Setting the clock of neural progenitor cells during mammalian corticogenesis. *Seminars in Cell & Developmental Biology,* 142**,** 43-53.

KREISLER, A., STRISSEL, P. L., STRICK, R., NEUMANN, S. B., SCHUMACHER, U. & BECKER, C. M. 2010. Regulation of the NRSF/REST gene by methylation and CREB affects the cellular phenotype of small-cell lung cancer. *Oncogene,* 29**,** 5828-38.

KRUTZFELDT, J., RAJEWSKY, N., BRAICH, R., RAJEEV, K., TUSCHL, T., MANOHARAN, M. & STOFFEL, M. 2005. Silencing of microRNAs in vivo with 'antagomirs' Nature. 2005; 438: 685–689. *The first of use, to our knowldege, of antisense oligonucleotides to silence miRNA expression in vivo*.

KUANG, Z., ZHAO, Y. & YANG, X. 2023. Machine learning approaches for plant miRNA prediction: Challenges, advancements, and future directions. *Agriculture Communications,* 1**,** 100014.

KUMAR, D., CINGHU, S., OLDFIELD, A. J., YANG, P. & JOTHI, R. 2021. Decoding the function of bivalent chromatin in development and cancer. *Genome Res,* 31**,** 2170-2184.

KUMAR, S., CURRAN, J. E., DELEON, E., LEANDRO, A. C., HOWARD, T. E., LEHMAN, D. M., WILLIAMS-BLANGERO, S., GLAHN, D. C. & BLANGERO, J. 2020. Role of miRNA-mRNA Interaction in Neural Stem Cell Differentiation of Induced Pluripotent Stem Cells. *International Journal of Molecular Sciences,* 21**,** 6980.

KUNDAJE, A., MEULEMAN, W., ERNST, J., BILENKY, M., YEN, A., HERAVI-MOUSSAVI, A., KHERADPOUR, P., ZHANG, Z., WANG, J., ZILLER, M. J., AMIN, V., WHITAKER, J. W., SCHULTZ, M. D., WARD, L. D., SARKAR, A., QUON, G., SANDSTROM, R. S., EATON, M. L., WU, Y.-C., PFENNING, A., WANG, X., CLAUSSNITZERYAPING LIU, M., COARFA, C., ALAN HARRIS, R., SHORESH, N., EPSTEIN, C. B., GJONESKA, E., LEUNG, D., XIE, W., DAVID HAWKINS, R., LISTER, R., HONG, C., GASCARD, P., MUNGALL, A. J., MOORE, R., CHUAH, E., TAM, A., CANFIELD, T. K., SCOTT HANSEN, R., KAUL, R., SABO, P. J., BANSAL, M. S., CARLES, A., DIXON, J. R., FARH, K.-H., FEIZI, S., KARLIC, R., KIM, A.-R., KULKARNI, A., LI, D., LOWDON, R., ELLIOTT, G., MERCER, T. R., NEPH, S. J., ONUCHIC, V., POLAK, P., RAJAGOPAL, N., RAY, P., SALLARI, R. C., SIEBENTHALL, K. T., SINNOTT-ARMSTRONG, N. A., STEVENS, M., THURMAN, R. E., WU, J., ZHANG, B., ZHOU, X., ABDENNUR, N., ADLI, M., AKERMAN, M., BARRERA, L., ANTOSIEWICZ-BOURGET, J., BALLINGER, T., BARNES, M. J., BATES, D., BELL, R. J. A., BENNETT, D. A., BIANCO, K., BOCK, C., BOYLE, P., BRINCHMANN, J., CABALLERO-CAMPO, P., CAMAHORT, R., CARRASCO-ALFONSO, M. J., CHARNECKI, T., CHEN, H., CHEN, Z., CHENG, J. B., CHO, S., CHU, A., CHUNG, W.-Y., COWAN, C., ATHENA DENG, Q., DESHPANDE, V., DIEGEL, M., DING, B., DURHAM, T., ECHIPARE, L., EDSALL, L., FLOWERS, D., GENBACEV-KRTOLICA, O., et al. 2015. Integrative analysis of 111 reference human epigenomes. *Nature,* 518**,** 317-330.

KUWAHARA, A., HIRABAYASHI, Y., KNOEPFLER, P. S., TAKETO, M. M., SAKAI, J., KODAMA, T. & GOTOH, Y. 2010. Wnt signaling and its downstream target N-myc regulate basal progenitors in the developing neocortex. *Development,* 137**,** 1035-1044.

KUZMICHEV, A., JENUWEIN, T., TEMPST, P. & REINBERG, D. 2004. Different EZH2-containing complexes target methylation of histone H1 or nucleosomal histone H3. *Molecular cell,* 14**,** 183-193.

LAGOS-QUINTANA, M., RAUHUT, R., YALCIN, A., MEYER, J., LENDECKEL, W. & TUSCHL, T. 2002. Identification of tissue-specific microRNAs from mouse. *Current biology,* 12**,** 735-739.

LAKE, B. B., CHEN, S., SOS, B. C., FAN, J., KAESER, G. E., YUNG, Y. C., DUONG, T. E., GAO, D., CHUN, J., KHARCHENKO, P. V. & ZHANG, K. 2018. Integrative single-cell analysis of transcriptional and epigenetic states in the human adult brain. *Nature Biotechnology,* 36**,** 70-80.

LAM, F. H., STEGER, D. J. & O'SHEA, E. K. 2008. Chromatin decouples promoter threshold from dynamic range. *Nature,* 453**,** 246-250.

LANDEIRA, D., SAUER, S., POOT, R., DVORKINA, M., MAZZARELLA, L., JØRGENSEN, H. F., PEREIRA, C. F., LELEU, M., PICCOLO, F. M., SPIVAKOV, M., BROOKES, E., POMBO, A., FISHER, C., SKARNES, W. C., SNOEK, T., BEZSTAROSTI, K., DEMMERS, J., KLOSE, R. J., CASANOVA, M., TAVARES, L., BROCKDORFF, N., MERKENSCHLAGER, M. & FISHER, A. G. 2010. Jarid2 is a PRC2 component in embryonic stem cells required for multi-lineage differentiation and recruitment of PRC1 and RNA Polymerase II to developmental regulators. *Nature Cell Biology,* 12**,** 618-624.

LANEVE, P., GIOIA, U., ANDRIOTTO, A., MORETTI, F., BOZZONI, I. & CAFFARELLI, E. 2010. A minicircuitry involving REST and CREB controls miR-9-2 expression during human neuronal differentiation. *Nucleic Acids Research,* 38**,** 6895-6905.

LASALLE, J. M. 2013. Autism genes keep turning up chromatin. *OA Autism,* 1**,** 14.

LAUGESEN, A., HØJFELDT, J. W. & HELIN, K. 2019. Molecular mechanisms directing PRC2 recruitment and H3K27 methylation. *Molecular cell,* 74**,** 8-18.

LAVENNIAH, A., LUU, T. D. A., LI, Y. P., LIM, T. B., JIANG, J., ACKERS-JOHNSON, M. & FOO, R. S. Y. 2020. Engineered Circular RNA Sponges Act as miRNA Inhibitors to Attenuate Pressure Overload-Induced Cardiac Hypertrophy. *Molecular Therapy,* 28**,** 1506-1517.

LEDERER, D., GRISART, B., DIGILIO, MARIA C., BENOIT, V., CRESPIN, M., GHARIANI, SOPHIE C., MAYSTADT, I., DALLAPICCOLA, B. & VERELLEN-DUMOULIN, C. 2012. Deletion of KDM6A, a Histone Demethylase Interacting with MLL2, in Three Patients with Kabuki Syndrome. *The American Journal of Human Genetics,* 90**,** 119-124.

LEE, M. G., WYNDER, C., COOCH, N. & SHIEKHATTAR, R. 2005. An essential role for CoREST in nucleosomal histone 3 lysine 4 demethylation. *Nature,* 437**,** 432-5.

LEE, S.-T., IM, W., BAN, J.-J., LEE, M., JUNG, K.-H., LEE, S. K., CHU, K. & KIM, M. 2017. Exosome-based delivery of miR-124 in a Huntington's disease model. *Journal of movement disorders,* 10**,** 45.

LEE, S. W., OH, Y. M., LU, Y. L., KIM, W. K. & YOO, A. S. 2018. MicroRNAs Overcome Cell Fate Barrier by Reducing EZH2-Controlled REST Stability during Neuronal Conversion of Human Adult Fibroblasts. *Dev Cell,* 46**,** 73-84.e7.

LEVINE, A. J. & BRIVANLOU, A. H. 2007. Proposal of a model of mammalian neural induction. *Developmental Biology,* 308**,** 247-256.

LI, G., MARGUERON, R., KU, M., CHAMBON, P., BERNSTEIN, B. E. & REINBERG, D. 2010. Jarid2 and PRC2, partners in regulating gene expression. *Genes Dev,* 24**,** 368-80.

LI, K., BRONK, G., KONDEV, J. & HABER, J. E. 2020. Yeast ATM and ATR kinases use different mechanisms to spread histone H2A phosphorylation around a DNA double-strand break. *Proceedings of the National Academy of Sciences,* 117**,** 21354-21363.

LI, X., ZHOU, W., LI, X., GAO, M., JI, S., TIAN, W., JI, G., DU, J. & HAO, A. 2019. SOX19b regulates the premature neuronal differentiation of neural stem cells through EZH2-mediated histone methylation in neural tube development of zebrafish. *Stem Cell Research & Therapy,* 10**,** 389.

LIANG, C., ZHU, H., XU, Y., HUANG, L., MA, C., DENG, W., LIU, Y. & QIN, C. 2012. MicroRNA-153 negatively regulates the expression of amyloid precursor protein and amyloid precursor-like protein 2. *Brain research,* 1455**,** 103-113.

LIENERT, F., MOHN, F., TIWARI, V. K., BAUBEC, T., ROLOFF, T. C., GAIDATZIS, D., STADLER, M. B. & SCHÜBELER, D. 2011. Genomic prevalence of heterochromatic H3K9me2 and transcription do not discriminate pluripotent from terminally differentiated cells. *PLoS Genet,* 7**,** e1002090.

LIM, L. P., LAU, N. C., GARRETT-ENGELE, P., GRIMSON, A., SCHELTER, J. M., CASTLE, J., BARTEL, D. P., LINSLEY, P. S. & JOHNSON, J. M. 2005. Microarray analysis shows that some microRNAs downregulate large numbers of target mRNAs. *Nature,* 433**,** 769-773.

LIN, X., HUANG, Y., ZOU, Y., CHEN, X. & MA, X. 2016. Depletion of G9a gene induces cell apoptosis in human gastric carcinoma. *Oncol Rep,* 35**,** 3041-3049.

LIN, Y., CHEN, F., SHEN, L., TANG, X., DU, C., SUN, Z., DING, H., CHEN, J. & SHEN, B. 2018. Biomarker microRNAs for prostate cancer metastasis: screened with a network vulnerability analysis model. *J Transl Med,* 16**,** 134.

LINARO, D., VERMAERCKE, B., IWATA, R., RAMASWAMY, A., LIBÉ-PHILIPPOT, B., BOUBAKAR, L., DAVIS, B. A., WIERDA, K., DAVIE, K., POOVATHINGAL, S., PENTTILA, P. A., BILHEU, A., DE BRUYNE, L., GALL, D., CONZELMANN, K. K., BONIN, V. & VANDERHAEGHEN, P. 2019. Xenotransplanted Human Cortical Neurons Reveal Species-Specific Development and Functional Integration into Mouse Visual Circuits. *Neuron,* 104**,** 972-986.e6.

LIU, J., GITHINJI, J., MCLAUGHLIN, B., WILCZEK, K. & NOLTA, J. 2012. Role of miRNAs in Neuronal Differentiation from Human Embryonic Stem Cell—Derived Neural Stem Cells. *Stem Cell Reviews and Reports,* 8**,** 1129-1137.

LIU, J., WU, X., ZHANG, H., PFEIFER, G. P. & LU, Q. 2017a. Dynamics of RNA Polymerase II Pausing and Bivalent Histone H3 Methylation during Neuronal Differentiation in Brain Development. *Cell Reports,* 20**,** 1307-1318.

LIU, N., ZHANG, Z., WU, H., JIANG, Y., MENG, L., XIONG, J., ZHAO, Z., ZHOU, X., LI, J., LI, H., ZHENG, Y., CHEN, S., CAI, T., GAO, S. & ZHU, B. 2015. Recognition of H3K9 methylation by GLP is required for efficient establishment of H3K9 methylation, rapid target gene repression, and mouse viability. *Genes Dev,* 29**,** 379-93.

LIU, Y., LIU, S., YUAN, S., YU, H., ZHANG, Y., YANG, X., XIE, G., CHEN, Z., LI, W., XU, B., SUN, L., SHANG, Y. & LIANG, J. 2017b. Chromodomain protein CDYL is required for transmission/restoration of repressive histone marks. *Journal of Molecular Cell Biology,* 9**,** 178-194.

LOVE, M. I., HUBER, W. & ANDERS, S. 2014. Moderated estimation of fold change and dispersion for RNA-seq data with DESeq2. *Genome Biology,* 15**,** 550.

LU, Y.-L., LIU, Y., MCCOY, M. J. & YOO, A. S. 2021. MiR-124 synergism with ELAVL3 enhances target gene expression to promote neuronal maturity. *Proceedings of the National Academy of Sciences,* 118**,** e2015454118.

MA, J., WENG, L., WANG, Z., JIA, Y., LIU, B., WU, S., CAO, Y., SUN, X., YIN, X., SHANG, M. & MAO, A. 2018. MiR-124 induces autophagy-related cell death in cholangiocarcinoma cells through direct targeting of the EZH2–STAT3 signaling axis. *Experimental Cell Research,* 366**,** 103-113.

MAGRI, L., CAMBIAGHI, M., COMINELLI, M., ALFARO-CERVELLO, C., CURSI, M., PALA, M., BULFONE, A., GARCÌA-VERDUGO, J. M., LEOCANI, L. & MINICUCCI, F. 2011. Sustained activation of mTOR pathway in embryonic neural stem cells leads to development of tuberous sclerosis complex-associated lesions. *Cell stem cell,* 9**,** 447-462.

MAIER, V. K., FEENEY, C. M., TAYLOR, J. E., CREECH, A. L., QIAO, J. W., SZANTO, A., DAS, P. P., CHEVRIER, N., CIFUENTES-ROJAS, C., ORKIN, S. H., CARR, S. A., JAFFE, J. D., MERTINS, P. & LEE, J. T. 2015. Functional Proteomic Analysis of Repressive Histone Methyltransferase Complexes Reveals ZNF518B as a G9A Regulator. *Mol Cell Proteomics,* 14**,** 1435-46.

MAIORANO, N. A. & MALLAMACI, A. 2010. The pro-differentiating role of miR-124: indicating the road to become a neuron. *RNA Biol,* 7**,** 528-33.

MAKEYEV, E. V., ZHANG, J., CARRASCO, M. A. & MANIATIS, T. 2007. The MicroRNA miR-124 promotes neuronal differentiation by triggering brain-specific alternative pre-mRNA splicing. *Molecular cell,* 27**,** 435-448.

MALMEVIK, J., PETRI, R., KLUSSENDORF, T., KNAUFF, P., ÅKERBLOM, M., JOHANSSON, J., SONEJI, S. & JAKOBSSON, J. 2015. Identification of the miRNA targetome in hippocampal neurons using RIP-seq. *Scientific Reports,* 5**,** 12609.

MANDEL, G., FIONDELLA, C. G., COVEY, M. V., LU, D. D., LOTURCO, J. J. & BALLAS, N. 2011. Repressor element 1 silencing transcription factor (REST) controls radial migration and temporal neuronal specification during neocortical development. *Proceedings of the National Academy of Sciences,* 108**,** 16789-16794.

MANDEMAKERS, W., ABUHATZIRA, L., XU, H., CAROMILE, L., HÉBERT, S., SNELLINX, A., MORAIS, V., MATTA, S., CAI, T. & NOTKINS, A. 2013. Co-regulation of intragenic microRNA miR-153 and its host gene Ia-2 β: identification of miR-153 target genes with functions related to IA-2β in pancreas and brain. *Diabetologia,* 56**,** 1547-1556.

MAO, L., DING, J., ZHA, Y., YANG, L., MCCARTHY, B. A., KING, W., CUI, H. & DING, H.-F. 2011. HOXC9 Links Cell-Cycle Exit and Neuronal Differentiation and Is a Prognostic Marker in Neuroblastoma. *Cancer Research,* 71**,** 4314-4324.

MARAGKAKIS, M., ALEXIOU, P., PAPADOPOULOS, G. L., RECZKO, M., DALAMAGAS, T., GIANNOPOULOS, G., GOUMAS, G., KOUKIS, E., KOURTIS, K. & SIMOSSIS, V. A. 2009. Accurate microRNA target prediction correlates with protein repression levels. *BMC bioinformatics,* 10**,** 1-10.

MARGUERON, R. & REINBERG, D. 2011. The Polycomb complex PRC2 and its mark in life. *Nature,* 469**,** 343-349.

MAS, G., BLANCO, E., BALLARÉ, C., SANSÓ, M., SPILL, Y. G., HU, D., AOI, Y., LE DILY, F., SHILATIFARD, A., MARTI-RENOM, M. A. & DI CROCE, L. 2018. Promoter bivalency favors an open chromatin architecture in embryonic stem cells. *Nature Genetics,* 50**,** 1452-1462.

MATHONNET, G., FABIAN, M. R., SVITKIN, Y. V., PARSYAN, A., HUCK, L., MURATA, T., BIFFO, S., MERRICK, W. C., DARZYNKIEWICZ, E., PILLAI, R. S., FILIPOWICZ, W., DUCHAINE, T. F. & SONENBERG, N. 2007. MicroRNA Inhibition of Translation Initiation in Vitro by Targeting the Cap-Binding Complex eIF4F. *Science,* 317**,** 1764-1767.

MATLIK, K., GOVEK, E. E., PAUL, M. R., ALLIS, C. D. & HATTEN, M. E. 2023. Histone bivalency regulates the timing of cerebellar granule cell development. *Genes Dev,* 37**,** 570-589.

MATSUDA, M., HAYASHI, H., GARCIA-OJALVO, J., YOSHIOKA-KOBAYASHI, K., KAGEYAMA, R., YAMANAKA, Y., IKEYA, M., TOGUCHIDA, J., ALEV, C. & EBISUYA, M. 2020. Species-specific segmentation clock periods are due to differential biochemical reaction speeds. *Science,* 369**,** 1450-1455.

MAZE, I., COVINGTON, H. E., DIETZ, D. M., LAPLANT, Q., RENTHAL, W., RUSSO, S. J., MECHANIC, M., MOUZON, E., NEVE, R. L., HAGGARTY, S. J., REN, Y., SAMPATH, S. C., HURD, Y. L., GREENGARD, P., TARAKHOVSKY, A., SCHAEFER, A. & NESTLER, E. J. 2010. Essential Role of the Histone Methyltransferase G9a in Cocaine-Induced Plasticity. *Science,* 327**,** 213-216.

MCDONALD, C. & MURPHY, K. C. 2003. The new genetics of schizophrenia. *Psychiatric Clinics,* 26**,** 41-63.

MCGANN, J. C., OYER, J. A., GARG, S., YAO, H., LIU, J., FENG, X., LIAO, L., YATES, J. R., 3RD & MANDEL, G. 2014. Polycomb- and REST-associated histone deacetylases are independent pathways toward a mature neuronal phenotype. *Elife,* 3**,** e04235.

MCGANN, J. C., SPINNER, M. A., GARG, S. K., MULLENDORFF, K. A., WOLTJER, R. L. & MANDEL, G. 2021. The Genome-Wide Binding Profile for Human RE1 Silencing Transcription Factor Unveils a Unique Genetic Circuitry in Hippocampus. *The Journal of Neuroscience,* 41**,** 6582-6595.

MCGEARY, S. E., LIN, K. S., SHI, C. Y., PHAM, T. M., BISARIA, N., KELLEY, G. M. & BARTEL, D. P. 2019. The biochemical basis of microRNA targeting efficacy. *Science,* 366.

MCPARTLAND, J. C., REICHOW, B. & VOLKMAR, F. R. 2012. Sensitivity and Specificity of Proposed DSM-5 Diagnostic Criteria for Autism Spectrum Disorder. *Journal of the American Academy of Child & Adolescent Psychiatry,* 51**,** 368-383.

MEDLEY, J. C., PANZADE, G. & ZINOVYEVA, A. Y. 2021. microRNA strand selection: Unwinding the rules. *WIREs RNA,* 12**,** e1627.

MENG, T.-G., ZHOU, Q., MA, X.-S., LIU, X.-Y., MENG, Q.-R., HUANG, X.-J., LIU, H.-L., LEI, W.-L., ZHAO, Z.-H., OUYANG, Y.-C., HOU, Y., SCHATTEN, H., OU, X.-H., WANG, Z.-B., GAO, S.-R. & SUN, Q.-Y. 2020. PRC2 and EHMT1 regulate H3K27me2 and H3K27me3 establishment across the zygote genome. *Nature Communications,* 11**,** 6354.

MILLER, D. J., DUKA, T., STIMPSON, C. D., SCHAPIRO, S. J., BAZE, W. B., MCARTHUR, M. J., FOBBS, A. J., SOUSA, A. M., ŠESTAN, N. & WILDMAN, D. E. 2012. Prolonged myelination in human

neocortical evolution. *Proceedings of the National Academy of Sciences,* 109**,** 16480-16485.

MIN, H. & YOON, S. 2010. Got target?: computational methods for microRNA target prediction and their extension. *Experimental & Molecular Medicine,* 42**,** 233-244.

MITTAL, P. & ROBERTS, C. W. M. 2020. The SWI/SNF complex in cancer — biology, biomarkers and therapy. *Nature Reviews Clinical Oncology,* 17**,** 435-448.

MIYOSHI, K., MIYOSHI, T. & SIOMI, H. 2010. Many ways to generate microRNA-like small RNAs: non-canonical pathways for microRNA production. *Molecular Genetics and Genomics,* 284**,** 95-103.

MOCHIZUKI-KASHIO, M., AOYAMA, K., SASHIDA, G., OSHIMA, M., TOMIOKA, T., MUTO, T., WANG, C. & IWAMA, A. 2015. Ezh2 loss in hematopoietic stem cells predisposes mice to develop heterogeneous malignancies in an Ezh1-dependent manner. *Blood,* 126**,** 1172-1183.

MONAGHAN, C. E., NECHIPORUK, T., JENG, S., MCWEENEY, S. K., WANG, J., ROSENFELD, M. G. & MANDEL, G. 2017. REST corepressors RCOR1 and RCOR2 and the repressor INSM1 regulate the proliferation–differentiation balance in the developing brain. *Proceedings of the National Academy of Sciences,* 114**,** E406-E415.

MOYSES-OLIVEIRA, M., YADAV, R., ERDIN, S. & TALKOWSKI, M. E. 2020. New gene discoveries highlight functional convergence in autism and related neurodevelopmental disorders. *Current Opinion in Genetics & Development,* 65**,** 195-206.

MOZZETTA, C., PONTIS, J., FRITSCH, L., ROBIN, P., PORTOSO, M., PROUX, C., MARGUERON, R. & AIT-SI-ALI, S. 2014. The Histone H3 Lysine 9 Methyltransferases G9a and GLP Regulate Polycomb Repressive Complex 2-Mediated Gene Silencing. *Molecular Cell,* 53**,** 277-289.

MOZZI, A., GUERINI, F. R., FORNI, D., COSTA, A. S., NEMNI, R., BAGLIO, F., CABINIO, M., RIVA, S., PONTREMOLI, C., CLERICI, M., SIRONI, M. & CAGLIANI, R. 2017. REST, a master regulator of neurogenesis, evolved under strong positive selection in humans and in non human primates. *Scientific Reports,* 7**,** 9530.

MUKHERJEE, S., BRULET, R., ZHANG, L. & HSIEH, J. 2016. REST regulation of gene networks in adult neural stem cells. *Nature Communications,* 7**,** 13360.

MUTCH, C. A., SCHULTE, J. D., OLSON, E. & CHENN, A. 2010. Beta-catenin signaling negatively regulates intermediate progenitor population numbers in the developing cortex. *PloS one,* 5**,** e12376.

NAGARAJAN, S. & JOHNSEN, S. A. 2016. Chapter 12 - Crosstalk Between Histone Modifications Integrates Various Signaling Inputs to Fine-Tune Transcriptional Output. *In:* BINDA, O. & FERNANDEZ-ZAPICO, M. E. (eds.) *Chromatin Signaling and Diseases.* Boston: Academic Press.

NAGARAJAN, V. K., JONES, C. I., NEWBURY, S. F. & GREEN, P. J. 2013. XRN 5'→3' exoribonucleases: structure, mechanisms and functions. *Biochim Biophys Acta,* 1829**,** 590-603.

NAGY, J., KOBOLÁK, J., BERZSENYI, S., ÁBRAHÁM, Z., AVCI, H. X., BOCK, I., BEKES, Z., HODOSCSEK, B., CHANDRASEKARAN, A., TÉGLÁSI, A., DEZSŐ, P., KOVÁNYI, B., VÖRÖS, E. T., FODOR, L., SZÉL, T., NÉMETH, K., BALÁZS, A., DINNYÉS, A., LENDVAI, B., LÉVAY, G. & ROMÁN, V. 2017. Altered neurite morphology and cholinergic function of induced pluripotent stem cell-derived neurons from a patient with Kleefstra syndrome and autism. *Transl Psychiatry,* 7**,** e1179.

NARDELLO, R., MANGANO, G. D., FONTANA, A., GAGLIARDO, C., MIDIRI, F., BORGIA, P., BRIGHINA, F., RAIELI, V., MANGANO, S. & SALPIETRO, V. 2021. Broad neurodevelopmental features and cortical anomalies associated with a novel de novo

KMT2A variant in Wiedemann−Steiner syndrome. *European Journal of Medical Genetics,* 64**,** 104133.

NARUSE, C., ABE, K., YOSHIHARA, T., KATO, T., NISHIUCHI, T. & ASANO, M. 2020. Heterochromatin protein 1γ deficiency decreases histone H3K27 methylation in mouse neurosphere neuronal genes. *The FASEB Journal,* 34**,** 3956-3968.

NARUSE, Y., AOKI, T., KOJIMA, T. & MORI, N. 1999. Neural restrictive silencer factor recruits mSin3 and histone deacetylase complex to repress neuron-specific target genes. *Proc Natl Acad Sci U S A,* 96**,** 13691-6.

NAVA, A. A. & ARBOLEDA, V. A. 2023. The omics era: a nexus of untapped potential for Mendelian chromatinopathies. *Human Genetics*.

NAZIR, F. H., BECKER, B., BRINKMALM, A., HÖGLUND, K., SANDELIUS, Å., BERGSTRÖM, P., SATIR, T. M., ÖHRFELT, A., BLENNOW, K., AGHOLME, L. & ZETTERBERG, H. 2018. Expression and secretion of synaptic proteins during stem cell differentiation to cortical neurons. *Neurochemistry International,* 121**,** 38-49.

NEO, W. H., YAP, K., LEE, S. H., LOOI, L. S., KHANDELIA, P., NEO, S. X., MAKEYEV, E. V. & SU, I. H. 2014. MicroRNA miR-124 Controls the Choice between Neuronal and Astrocyte Differentiation by Fine-tuning Ezh2 Expression *. *Journal of Biological Chemistry,* 289**,** 20788-20801.

NG, S. B., BIGHAM, A. W., BUCKINGHAM, K. J., HANNIBAL, M. C., MCMILLIN, M. J., GILDERSLEEVE, H. I., BECK, A. E., TABOR, H. K., COOPER, G. M. & MEFFORD, H. C. 2010. Exome sequencing identifies MLL2 mutations as a cause of Kabuki syndrome. *Nature genetics,* 42**,** 790-793.

NGUYEN, K., DAS, B., DOBROWOLSKI, C. & KARN, J. 2017. Multiple Histone Lysine Methyltransferases Are Required for the Establishment and Maintenance of HIV-1 Latency. *mBio,* 8.

NGUYEN, T. A., JO, M. H., CHOI, Y.-G., PARK, J., KWON, S. C., HOHNG, S., KIM, V. N. & WOO, J.-S. 2015. Functional anatomy of the human microprocessor. *Cell,* 161**,** 1374-1387.

NISHIHARA, S., TSUDA, L. & OGURA, T. 2003. The canonical Wnt pathway directly regulates NRSF/REST expression in chick spinal cord. *Biochemical and Biophysical Research Communications,* 311**,** 55-63.

NOWAK, J. S., CHOUDHURY, N. R., DE LIMA ALVES, F., RAPPSILBER, J. & MICHLEWSKI, G. 2014. Lin28a regulates neuronal differentiation and controls miR-9 production. *Nature Communications,* 5**,** 3687.

NOWAKOWSKI, T. J., RANI, N., GOLKARAM, M., ZHOU, H. R., ALVARADO, B., HUCH, K., WEST, J. A., LEYRAT, A., POLLEN, A. A., KRIEGSTEIN, A. R., PETZOLD, L. R. & KOSIK, K. S. 2018. Regulation of cell-type-specific transcriptomes by microRNA networks during human brain development. *Nature Neuroscience,* 21**,** 1784-1792.

O'MEARA, M. M. & SIMON, J. A. 2012. Inner workings and regulatory inputs that control Polycomb repressive complex 2. *Chromosoma,* 121**,** 221-234.

O'ROAK, B. J., VIVES, L., GIRIRAJAN, S., KARAKOC, E., KRUMM, N., COE, B. P., LEVY, R., KO, A., LEE, C., SMITH, J. D., TURNER, E. H., STANAWAY, I. B., VERNOT, B., MALIG, M., BAKER, C., REILLY, B., AKEY, J. M., BORENSTEIN, E., RIEDER, M. J., NICKERSON, D. A., BERNIER, R., SHENDURE, J. & EICHLER, E. E. 2012. Sporadic autism exomes reveal a highly interconnected protein network of de novo mutations. *Nature,* 485**,** 246-250.

OHNISHI, T., SHIRANE, M. & NAKAYAMA, K. I. 2017. SRRM4-dependent neuron-specific alternative splicing of protrudin transcripts regulates neurite outgrowth. *Scientific Reports,* 7**,** 41130.

OKADA, C., YAMASHITA, E., LEE, S. J., SHIBATA, S., KATAHIRA, J., NAKAGAWA, A., YONEDA, Y. & TSUKIHARA, T. 2009. A high-resolution structure of the pre-microRNA nuclear export machinery. *Science,* 326**,** 1275-1279.

OTANI, T., MARCHETTO, MARIA C., GAGE, FRED H., SIMONS, BENJAMIN D. & LIVESEY, FREDERICK J. 2016. 2D and 3D Stem Cell Models of Primate Cortical Development Identify Species-Specific Differences in Progenitor Behavior Contributing to Brain Size. *Cell Stem Cell,* 18**,** 467-480.

OTTO, S. J., MCCORKLE, S. R., HOVER, J., CONACO, C., HAN, J.-J., IMPEY, S., YOCHUM, G. S., DUNN, J. J., GOODMAN, R. H. & MANDEL, G. 2007. A New Binding Motif for the Transcriptional Repressor REST Uncovers Large Gene Networks Devoted to Neuronal Functions. *The Journal of Neuroscience,* 27**,** 6729-6739.

OUELLET, L. & DE VILLERS-SIDANI, E. 2014. Trajectory of the main GABAergic interneuron populations from early development to old age in the rat primary auditory cortex. *Front Neuroanat,* 8**,** 40.

PACKER, A. N., XING, Y., HARPER, S. Q., JONES, L. & DAVIDSON, B. L. 2008. The bifunctional microRNA miR-9/miR-9* regulates REST and CoREST and is downregulated in Huntington's disease. *The Journal of neuroscience : the official journal of the Society for Neuroscience,* 28**,** 14341-14346.

PAN, G., TIAN, S., NIE, J., YANG, C., RUOTTI, V., WEI, H., JONSDOTTIR, G. A., STEWART, R. & THOMSON, J. A. 2007. Whole-genome analysis of histone H3 lysine 4 and lysine 27 methylation in human embryonic stem cells. *Cell stem cell,* 1**,** 299-312.

PAN, M.-R., HSU, M.-C., CHEN, L.-T. & HUNG, W.-C. 2015. G9a orchestrates PCL3 and KDM7A to promote histone H3K27 methylation. *Scientific Reports,* 5**,** 18709.

PANDEY, A., SINGH, P., JAUHARI, A., SINGH, T., KHAN, F., PANT, A. B., PARMAR, D. & YADAV, S. 2015. Critical role of the miR-200 family in regulating differentiation and proliferation of neurons. *J Neurochem,* 133**,** 640-52.

PANG, A. L. Y., TITLE, A. C. & RENNERT, O. M. 2014. Modulation of microRNA expression in human lung cancer cells by the G9a histone methyltransferase inhibitor BIX01294. *Oncol Lett,* 7**,** 1819-1825.

PANG, Z. P., YANG, N., VIERBUCHEN, T., OSTERMEIER, A., FUENTES, D. R., YANG, T. Q., CITRI, A., SEBASTIANO, V., MARRO, S., SÜDHOF, T. C. & WERNIG, M. 2011. Induction of human neuronal cells by defined transcription factors. *Nature,* 476**,** 220-223.

PANTIER, R., CHHATBAR, K., QUANTE, T., SKOURTI-STATHAKI, K., CHOLEWA-WACLAW, J., ALSTON, G., ALEXANDER-HOWDEN, B., LEE, H. Y., COOK, A. G., SPRUIJT, C. G., VERMEULEN, M., SELFRIDGE, J. & BIRD, A. 2021. SALL4 controls cell fate in response to DNA base composition. *Molecular Cell,* 81**,** 845-858.e8.

PAPAIT, R., SERIO, S., PAGIATAKIS, C., RUSCONI, F., CARULLO, P., MAZZOLA, M., SALVARANI, N., MIRAGOLI, M. & CONDORELLI, G. 2017. Histone Methyltransferase G9a Is Required for Cardiomyocyte Homeostasis and Hypertrophy. *Circulation,* 136**,** 1233-1246.

PARIDAEN, J. T. & HUTTNER, W. B. 2014. Neurogenesis during development of the vertebrate central nervous system. *EMBO Rep,* 15**,** 351-64.

PARTIN, A. C., NGO, T. D., HERRELL, E., JEONG, B.-C., HON, G. & NAM, Y. 2017. Heme enables proper positioning of Drosha and DGCR8 on primary microRNAs. *Nature Communications,* 8**,** 1737.

PASINI, D., BRACKEN, A. P., HANSEN, J. B., CAPILLO, M. & HELIN, K. 2007. The polycomb group protein Suz12 is required for embryonic stem cell differentiation. *Molecular and cellular biology,* 27**,** 3769-3779.

PASINI, D., BRACKEN, A. P., JENSEN, M. R., LAZZERINI DENCHI, E. & HELIN, K. 2004. Suz12 is essential for mouse development and for EZH2 histone methyltransferase activity. *Embo j,* 23**,** 4061-71.

PASINI, D., CLOOS, P. A., WALFRIDSSON, J., OLSSON, L., BUKOWSKI, J.-P., JOHANSEN, J. V., BAK, M., TOMMERUP, N., RAPPSILBER, J. & HELIN, K. 2010. JARID2 regulates binding of the Polycomb repressive complex 2 to target genes in ES cells. *Nature,* 464**,** 306-310.

PATRIZI, A., AWAD, P. N., CHATTOPADHYAYA, B., LI, C., DI CRISTO, G. & FAGIOLINI, M. 2019. Accelerated Hyper-Maturation of Parvalbumin Circuits in the Absence of MeCP2. *Cerebral Cortex,* 30**,** 256-268.

PAUKLIN, S., MADRIGAL, P., BERTERO, A. & VALLIER, L. 2016. Initiation of stem cell differentiation involves cell cycle-dependent regulation of developmental genes by Cyclin D. *Genes Dev,* 30**,** 421-33.

PENG, C., LI, N., NG, Y.-K., ZHANG, J., MEIER, F., THEIS, F. J., MERKENSCHLAGER, M., CHEN, W., WURST, W. & PRAKASH, N. 2012. A Unilateral Negative Feedback Loop Between miR-200 microRNAs and Sox2/E2F3 Controls Neural Progenitor Cell-Cycle Exit and Differentiation. *The Journal of Neuroscience,* 32**,** 13292-13308.

PEREIRA, J. D., SANSOM, S. N., SMITH, J., DOBENECKER, M.-W., TARAKHOVSKY, A. & LIVESEY, F. J. 2010. Ezh2, the histone methyltransferase of PRC2, regulates the balance between self-renewal and differentiation in the cerebral cortex. *Proceedings of the National Academy of Sciences,* 107**,** 15957-15962.

PEREIRA, R. M., MARTINEZ, G. J., ENGEL, I., CRUZ-GUILLOTY, F., BARBOZA, B. A., TSAGARATOU, A., LIO, C.-W. J., BERG, L. J., LEE, Y., KRONENBERG, M., BANDUKWALA, H. S. & RAO, A. 2014. Jarid2 is induced by TCR signalling and controls iNKT cell maturation. *Nature Communications,* 5**,** 4540.

PERERA, A., EISEN, D., WAGNER, M., LAUBE, S. K., KÜNZEL, A. F., KOCH, S., STEINBACHER, J., SCHULZE, E., SPLITH, V., MITTERMEIER, N., MÜLLER, M., BIEL, M., CARELL, T. & MICHALAKIS, S. 2015. TET3 is recruited by REST for context-specific hydroxymethylation and induction of gene expression. *Cell Rep,* 11**,** 283-94.

PETANJEK, Z., SEDMAK, D., DŽAJA, D., HLADNIK, A., RAŠIN, M. R. & JOVANOV-MILOSEVIC, N. 2019. The Protracted Maturation of Associative Layer IIIC Pyramidal Neurons in the Human Prefrontal Cortex During Childhood: A Major Role in Cognitive Development and Selective Alteration in Autism. *Front Psychiatry,* 10**,** 122.

PHAM, V., PITTI, R., TINDELL, C. A., CHEUNG, T. K., MASSELOT, A., STEPHAN, J.-P., GULER, G. D., WILSON, C., LILL, J., ARNOTT, D. & CLASSON, M. 2020. Proteomic Analyses Identify a Novel Role for EZH2 in the Initiation of Cancer Cell Drug Tolerance. *Journal of Proteome Research,* 19**,** 1533-1547.

PIAO, X., ZHANG, X., WU, L. & BELASCO, J. G. 2010. CCR4-NOT deadenylates mRNA associated with RNA-induced silencing complexes in human cells. *Molecular and cellular biology,* 30**,** 1486-1494.

PIÑERO, J., BRAVO, À., QUERALT-ROSINACH, N., GUTIÉRREZ-SACRISTÁN, A., DEU-PONS, J., CENTENO, E., GARCÍA-GARCÍA, J., SANZ, F. & FURLONG, L. I. 2017. DisGeNET: a comprehensive platform integrating information on human disease-associated genes and variants. *Nucleic Acids Research,* 45**,** D833-D839.

PIÑERO, J., SAÜCH, J., SANZ, F. & FURLONG, L. I. 2021. The DisGeNET cytoscape app: Exploring and visualizing disease genomics data. *Computational and Structural Biotechnology Journal,* 19**,** 2960-2967.

PLANA-RIPOLL, O., PEDERSEN, C. B., HOLTZ, Y., BENROS, M. E., DALSGAARD, S., DE JONGE, P., FAN, C. C., DEGENHARDT, L., GANNA, A., GREVE, A. N., GUNN, J., IBURG, K. M., KESSING,

L. V., LEE, B. K., LIM, C. C. W., MORS, O., NORDENTOFT, M., PRIOR, A., ROEST, A. M., SAHA, S., SCHORK, A., SCOTT, J. G., SCOTT, K. M., STEDMAN, T., SØRENSEN, H. J., WERGE, T., WHITEFORD, H. A., LAURSEN, T. M., AGERBO, E., KESSLER, R. C., MORTENSEN, P. B. & MCGRATH, J. J. 2019. Exploring Comorbidity Within Mental Disorders Among a Danish National Population. *JAMA Psychiatry,* 76**,** 259-270.

PLOTNIKOVA, O. M. & SKOBLOV, M. Y. 2018. [Efficiency of the miRNA- mRNA Interaction Prediction Programs]. *Mol Biol (Mosk),* 52**,** 543-554.

POEPSEL, S., KASINATH, V. & NOGALES, E. 2018. Cryo-EM structures of PRC2 simultaneously engaged with two functionally distinct nucleosomes. *Nature Structural & Molecular Biology,* 25**,** 154-162.

POLESHKO, A., SMITH, C. L., NGUYEN, S. C., SIVARAMAKRISHNAN, P., WONG, K. G., MURRAY, J. I., LAKADAMYALI, M., JOYCE, E. F., JAIN, R. & EPSTEIN, J. A. 2019. H3K9me2 orchestrates inheritance of spatial positioning of peripheral heterochromatin through mitosis. *Elife,* 8.

PONS-ESPINAL, M., DE LUCA, E., MARZI, M. J., BECKERVORDERSANDFORTH, R., ARMIROTTI, A., NICASSIO, F., FABEL, K., KEMPERMANN, G. & TONELLI, D. D. P. 2017. Synergic functions of miRNAs determine neuronal fate of adult neural stem cells. *Stem Cell Reports,* 8**,** 1046-1061.

PÖSTYÉNI, E., KOVÁCS-VALASEK, A., URBÁN, P., CZUNI, L., SÉTÁLÓ, G., JR., FEKETE, C. & GABRIEL, R. 2021. Analysis of mir-9 Expression Pattern in Rat Retina during Postnatal Development. *Int J Mol Sci,* 22.

PRZYBORSKI, S. A. & CAMBRAY-DEAKIN, M. A. 1995. Developmental regulation of MAP2 variants during neuronal differentiation in vitro. *Developmental Brain Research,* 89**,** 187-201.

QI, C., LIU, S., QIN, R., ZHANG, Y., WANG, G., SHANG, Y., WANG, Y. & LIANG, J. 2014. Coordinated Regulation of Dendrite Arborization by Epigenetic Factors CDYL and EZH2. *The Journal of Neuroscience,* 34**,** 4494-4508.

QI, R., CAO, J., SUN, Y., LI, Y., HUANG, Z., JIANG, D., JIANG, X. H., SNUTCH, T. P., ZHANG, Y. & TAO, J. 2022. Histone methylation-mediated microRNA-32-5p down-regulation in sensory neurons regulates pain behaviors via targeting Cav3.2 channels. *Proc Natl Acad Sci U S A,* 119**,** e2117209119.

QIANG, M., DENNY, A., LIEU, M., CARREON, S. & LI, J. 2011. Histone H3K9 modifications are a local chromatin event involved in ethanol-induced neuroadaptation of the NR2B gene. *Epigenetics,* 6**,** 1095-1104.

QIAO, J., ZHAO, J., CHANG, S., SUN, Q., LIU, N., DONG, J., CHEN, Y., YANG, D., YE, D., LIU, X., YU, Y., CHEN, W., ZHU, S., WANG, G., JIA, W., XI, J. & KANG, J. 2020. MicroRNA-153 improves the neurogenesis of neural stem cells and enhances the cognitive ability of aged mice through the notch signaling pathway. *Cell Death Differ,* 27**,** 808-825.

QU, Q., SUN, G., LI, W., YANG, S., YE, P., ZHAO, C., YU, R. T., GAGE, F. H., EVANS, R. M. & SHI, Y. 2010. Orphan nuclear receptor TLX activates Wnt/β-catenin signalling to stimulate neural stem cell proliferation and self-renewal. *Nature Cell Biology,* 12**,** 31-40.

QUARTIER, A., COURRAUD, J., THI HA, T., MCGILLIVRAY, G., ISIDOR, B., ROSE, K., DROUOT, N., SAVIDAN, M.-A., FEGER, C., JAGLINE, H., CHELLY, J., SHAW, M., LAUMONNIER, F., GECZ, J., MANDEL, J.-L. & PITON, A. 2019. Novel mutations in NLGN3 causing autism spectrum disorder and cognitive impairment. *Human Mutation,* 40**,** 2021-2032.

RADWITZ, J., HAUSRAT, T. J., HEISLER, F. F., JANIESCH, P. C., PECHMANN, Y., RÜBHAUSEN, M. & KNEUSSEL, M. 2022. Tubb3 expression levels are sensitive to neuronal activity changes and determine microtubule growth and kinesin-mediated transport. *Cell Mol Life Sci,* 79**,** 575.

RAHMAN, K. U., YANG, S., AZAM, N., YUAN, Z., YU, J., ZHAO, C. & FENG, B. 2023. Mir-153-3p Modulates the Breast Cancer Cells' Chemosensitivity to Doxorubicin by Targeting KIF20A. *Cancers (Basel),* 15.

RAHMAN, M. R., PETRALIA, M. C., CIURLEO, R., BRAMANTI, A., FAGONE, P., SHAHJAMAN, M., WU, L., SUN, Y., TURANLI, B., ARGA, K. Y., ISLAM, M. R., ISLAM, T. & NICOLETTI, F. 2020. Comprehensive Analysis of RNA-Seq Gene Expression Profiling of Brain Transcriptomes Reveals Novel Genes, Regulators, and Pathways in Autism Spectrum Disorder. *Brain Sci,* 10.

RAJ, B., O'HANLON, D., VESSEY, J. P., PAN, Q., RAY, D., BUCKLEY, N. J., MILLER, F. D. & BLENCOWE, B. J. 2011. Cross-regulation between an alternative splicing activator and a transcription repressor controls neurogenesis. *Mol Cell,* 43**,** 843-50.

RAJAN, A., ANHEZINI, L., RIVES-QUINTO, N., CHHABRA, J. Y., NEVILLE, M. C., LARSON, E. D., GOODWIN, S. F., HARRISON, M. M. & LEE, C.-Y. 2023. Low-level repressive histone marks fine-tune gene transcription in neural stem cells. *eLife,* 12**,** e86127.

RAKOTOMAMONJY, J., RYLAARSDAM, L., FARES-TAIE, L., MCDERMOTT, S., DAVIES, D., YANG, G., FAGBEMI, F., EPSTEIN, M., FAIRBANKS-SANTANA, M., ROZET, J. M. & GUEMEZ-GAMBOA, A. 2023. PCDH12 loss results in premature neuronal differentiation and impeded migration in a cortical organoid model. *Cell Rep,* 42**,** 112845.

RAMALINGAM, P., PALANICHAMY, J. K., SINGH, A., DAS, P., BHAGAT, M., KASSAB, M. A., SINHA, S. & CHATTOPADHYAY, P. 2014. Biogenesis of intronic miRNAs located in clusters by independent transcription and alternative splicing. *Rna,* 20**,** 76-87.

RAO, Z., WANG, R., LI, S., SHI, Y., MO, L., HAN, S., YUAN, J., JING, N. & CHENG, L. 2021. Molecular Mechanisms Underlying Ascl1-Mediated Astrocyte-to-Neuron Conversion. *Stem Cell Reports,* 16**,** 534-547.

RAU, A., MAROT, G. & JAFFRÉZIC, F. 2014. Differential meta-analysis of RNA-seq data from multiple studies. *BMC Bioinformatics,* 15**,** 91.

REED, E. R., LATOURELLE, J. C., BOCKHOLT, J. H., BREGU, J., SMOCK, J., PAULSEN, J. S., MYERS, R. H., INVESTIGATORS, P.-H. C. A. S., INVESTIGATORS, P.-H. C. A. S., DE SORIANO, I., HOBART, C., MILLER, A., GESCHWIND, M. D., SHA, S., WINER, J., SATRIS, G., PANEGYRES, P., LEE, J., TEDESCO, M., MAXWELL, B., PERLMUTTER, J., BARTON, S., SMITH, S., WHEELOCK, V., KJER, L., MARTIN, A., FARIAS, S., CRAUFURD, D., BEK, J., HOWARD, E., RAYMOND, L., DECOLONGON, J., FAN, M., COLEMAN, A., PAULSEN, J. S., LONG, J. D., JOHNSON, H. J., KAMHOLTZ, J., DANZER, P., MILLER, A., BOCKHOLT, H. J. & MONTROSS, K. 2018. MicroRNAs in CSF as prodromal biomarkers for Huntington disease in the PREDICT-HD study. *Neurology,* 90**,** e264-e272.

REHWINKEL, J., BEHM-ANSMANT, I., GATFIELD, D. & IZAURRALDE, E. 2005. A crucial role for GW182 and the DCP1: DCP2 decapping complex in miRNA-mediated gene silencing. *Rna,* 11**,** 1640-1647.

RICHNER, M., VICTOR, M. B., LIU, Y., ABERNATHY, D. & YOO, A. S. 2015. MicroRNA-based conversion of human fibroblasts into striatal medium spiny neurons. *Nature Protocols,* 10**,** 1543-1555.

RINCK, A., PREUSSE, M., LAGGERBAUER, B., LICKERT, H., ENGELHARDT, S. & THEIS, F. J. 2013. The human transcriptome is enriched for miRNA-binding sites located in cooperativity-permitting distance. *RNA Biol,* 10**,** 1125-35.

RINGROSE, L., EHRET, H. & PARO, R. 2004. Distinct contributions of histone H3 lysine 9 and 27 methylation to locus-specific stability of polycomb complexes. *Mol Cell,* 16**,** 641-53.

RIZAVI, H. S., CHASE, K. A., LIU, C., GAVIN, H., ROSEN, C., XIA, C., GUIDOTTI, A. & SHARMA, R. P. 2022. Differential H3K9me2 heterochromatin levels and concordant mRNA expression in

postmortem brain tissue of individuals with schizophrenia, bipolar, and controls. *Frontiers in Psychiatry,* 13.

ROBEY, R. W., CHAKRABORTY, A. R., BASSEVILLE, A., LUCHENKO, V., BAHR, J., ZHAN, Z. & BATES, S. E. 2011. Histone deacetylase inhibitors: emerging mechanisms of resistance. *Molecular pharmaceutics,* 8**,** 2021-2031.

ROCKOWITZ, S. & ZHENG, D. 2015. Significant expansion of the REST/NRSF cistrome in human versus mouse embryonic stem cells: potential implications for neural development. *Nucleic Acids Research,* 43**,** 5730-5743.

RODENAS-RUANO, A., CHÁVEZ, A. E., COSSIO, M. J., CASTILLO, P. E. & ZUKIN, R. S. 2012. REST-dependent epigenetic remodeling promotes the developmental switch in synaptic NMDA receptors. *Nature Neuroscience,* 15**,** 1382-1390.

ROIDL, D. & HACKER, C. 2014. Histone methylation during neural development. *Cell and Tissue Research,* 356**,** 539-552.

ROOPRA, A., QAZI, R., SCHOENIKE, B., DALEY, T. J. & MORRISON, J. F. 2004. Localized domains of G9a-mediated histone methylation are required for silencing of neuronal genes. *Molecular cell,* 14**,** 727-738.

ROTTIERS, V. & NÄÄR, A. M. 2012. MicroRNAs in metabolism and metabolic disorders. *Nature Reviews Molecular Cell Biology,* 13**,** 239-250.

ROWITCH, D. H. & KRIEGSTEIN, A. R. 2010. Developmental genetics of vertebrate glial–cell specification. *Nature,* 468**,** 214-222.

RYU, H.-Y. & HOCHSTRASSER, M. 2021. Histone sumoylation and chromatin dynamics. *Nucleic Acids Research,* 49**,** 6043-6052.

SAHARA, S. & O'LEARY, D. D. 2009. Fgf10 regulates transition period of cortical stem cell differentiation to radial glia controlling generation of neurons and basal progenitors. *Neuron,* 63**,** 48-62.

SAMARA, A., SPILDREJORDE, M., SHARMA, A., FALCK, M., LEITHAUG, M., MODAFFERI, S., BJØRNSTAD, P. M., ACHARYA, G., GERVIN, K., LYLE, R. & ESKELAND, R. 2022. A multi-omics approach to visualize early neuronal differentiation from hESCs in 4D. *iScience,* 25**,** 105279.

SAMPATH, S. C., MARAZZI, I., YAP, K. L., SAMPATH, S. C., KRUTCHINSKY, A. N., MECKLENBRÄUKER, I., VIALE, A., RUDENSKY, E., ZHOU, M.-M., CHAIT, B. T. & TARAKHOVSKY, A. 2007. Methylation of a Histone Mimic within the Histone Methyltransferase G9a Regulates Protein Complex Assembly. *Molecular Cell,* 27**,** 596-608.

SANCHEZ, N. A., KALLWEIT, L. M., TRNKA, M. J., CLEMMER, C. L. & AL-SADY, B. 2021. Heterodimerization of H3K9 histone methyltransferases G9a and GLP activates methyl reading and writing capabilities. *J Biol Chem,* 297**,** 101276.

SANUKI, R., ONISHI, A., KOIKE, C., MURAMATSU, R., WATANABE, S., MURANISHI, Y., IRIE, S., UNEO, S., KOYASU, T., MATSUI, R., CHÉRASSE, Y., URADE, Y., WATANABE, D., KONDO, M., YAMASHITA, T. & FURUKAWA, T. 2011. miR-124a is required for hippocampal axogenesis and retinal cone survival through Lhx2 suppression. *Nat Neurosci,* 14**,** 1125-34.

SAPKOTA, D., CHINTALA, H., WU, F., FLIESLER, S. J., HU, Z. & MU, X. 2014. Onecut1 and Onecut2 redundantly regulate early retinal cell fates during development. *Proceedings of the National Academy of Sciences,* 111**,** E4086-E4095.

SATTERSTROM, F. K., KOSMICKI, J. A., WANG, J., BREEN, M. S., DE RUBEIS, S., AN, J. Y., PENG, M., COLLINS, R., GROVE, J., KLEI, L., STEVENS, C., REICHERT, J., MULHERN, M. S., ARTOMOV, M., GERGES, S., SHEPPARD, B., XU, X., BHADURI, A., NORMAN, U., BRAND, H., SCHWARTZ, G., NGUYEN, R., GUERRERO, E. E., DIAS, C., BETANCUR, C., COOK, E. H., GALLAGHER, L., GILL, M., SUTCLIFFE, J. S., THURM, A., ZWICK, M. E., BØRGLUM, A. D., STATE, M. W., CICEK,

A. E., TALKOWSKI, M. E., CUTLER, D. J., DEVLIN, B., SANDERS, S. J., ROEDER, K., DALY, M. J. & BUXBAUM, J. D. 2020. Large-Scale Exome Sequencing Study Implicates Both Developmental and Functional Changes in the Neurobiology of Autism. *Cell,* 180**,** 568-584.e23.

SAUER, M., WAS, N., ZIEGENHALS, T., WANG, X., HAFNER, M., BECKER, M. & FISCHER, U. 2021. The miR-26 family regulates neural differentiation-associated microRNAs and mRNAs by directly targeting REST. *J Cell Sci,* 134.

SAWADA, T., CHATER, T. E., SASAGAWA, Y., YOSHIMURA, M., FUJIMORI-TONOU, N., TANAKA, K., BENJAMIN, K. J. M., PAQUOLA, A. C. M., ERWIN, J. A., GODA, Y., NIKAIDO, I. & KATO, T. 2020. Developmental excitation-inhibition imbalance underlying psychoses revealed by single-cell analyses of discordant twins-derived cerebral organoids. *Molecular Psychiatry,* 25**,** 2695-2711.

SCHAEFER, A., SAMPATH, S. C., INTRATOR, A., MIN, A., GERTLER, T. S., SURMEIER, D. J., TARAKHOVSKY, A. & GREENGARD, P. 2009. Control of cognition and adaptive behavior by the GLP/G9a epigenetic suppressor complex. *Neuron,* 64**,** 678-91.

SCHMID, R. S. & ANTON, E. 2003. Role of integrins in the development of the cerebral cortex. *Cerebral Cortex,* 13**,** 219-224.

SCHMITGES, F. W., PRUSTY, A. B., FATY, M., STÜTZER, A., LINGARAJU, G. M., AIWAZIAN, J., SACK, R., HESS, D., LI, L. & ZHOU, S. 2011. Histone methylation by PRC2 is inhibited by active chromatin marks. *Molecular cell,* 42**,** 330-341.

SCHWAIBOLD, E. M. C., SMOGAVEC, M., HOBBIEBRUNKEN, E., WINTER, L., ZOLL, B., BURFEIND, P., BROCKMANN, K. & PAULI, S. 2014. Intragenic duplication of EHMT1 gene results in Kleefstra syndrome. *Molecular Cytogenetics,* 7**,** 74.

SELBACH, M., SCHWANHÄUSSER, B., THIERFELDER, N., FANG, Z., KHANIN, R. & RAJEWSKY, N. 2008. Widespread changes in protein synthesis induced by microRNAs. *nature,* 455**,** 58-63.

SEMPERE, L. F., FREEMANTLE, S., PITHA-ROWE, I., MOSS, E., DMITROVSKY, E. & AMBROS, V. 2004. Expression profiling of mammalian microRNAs uncovers a subset of brain-expressed microRNAs with possible roles in murine and human neuronal differentiation. *Genome biology,* 5**,** 1-11.

SENTURIA, R., FALLER, M., YIN, S., LOO, J. A., CASCIO, D., SAWAYA, M. R., HWANG, D., CLUBB, R. T. & GUO, F. 2010. Structure of the dimerization domain of DiGeorge critical region 8. *Protein Science,* 19**,** 1354-1365.

SHARMA, R. P., FEINER, B. & CHASE, K. A. 2015. Histone H3 phosphorylation is upregulated in PBMCs of schizophrenia patients in comparison to healthy controls. *Schizophr Res,* 169**,** 498-499.

SHEN, L., LIN, Y., SUN, Z., YUAN, X., CHEN, L. & SHEN, B. 2016. Knowledge-Guided Bioinformatics Model for Identifying Autism Spectrum Disorder Diagnostic MicroRNA Biomarkers. *Scientific Reports,* 6**,** 39663.

SHENG, J., GANG LV, Z., WANG, L., ZHOU, Y. & HUI, B. 2011. Histone H3 phosphoacetylation is critical for heroin-induced place preference. *Neuroreport,* 22**,** 575-580.

SHIBATA, M., KUROKAWA, D., NAKAO, H., OHMURA, T. & AIZAWA, S. 2008. MicroRNA-9 modulates Cajal–Retzius cell differentiation by suppressing Foxg1 expression in mouse medial pallium. *Journal of Neuroscience,* 28**,** 10415-10421.

SHIMOJO, M., LEE, J.-H. & HERSH, L. B. 2001. Role of zinc finger domains of the transcription factor neuron-restrictive silencer factor/repressor element-1 silencing transcription factor in DNA binding and nuclear localization. *Journal of Biological Chemistry,* 276**,** 13121-13126.

SHIMOZAKI, K., CLEMENSON, G. D., JR. & GAGE, F. H. 2013. Paired related homeobox protein 1 is a regulator of stemness in adult neural stem/progenitor cells. *J Neurosci,* 33**,** 4066-75.

SHIN, M. H., LEE, E.-G., LEE, S.-H., LEE, Y. S. & SON, H. 2002a. Neural cell adhesion molecule (NCAM) promotes the differentiation of hippocampal precursor cells to a neuronal lineage, especially to a glutamatergic neural cell type. *Experimental & Molecular Medicine,* 34**,** 401-410.

SHIN, M. H., LEE, E. G., LEE, S. H., LEE, Y. S. & SON, H. 2002b. Neural cell adhesion molecule (NCAM) promotes the differentiation of hippocampal precursor cells to a neuronal lineage, especially to a glutamatergic neural cell type. *Exp Mol Med,* 34**,** 401-10.

SHIRATO, H., OGAWA, S., NAKAJIMA, K., INAGAWA, M., KOJIMA, M., TACHIBANA, M., SHINKAI, Y. & TAKEUCHI, T. 2009. A jumonji (Jarid2) protein complex represses cyclin D1 expression by methylation of histone H3-K9. *Journal of Biological Chemistry,* 284**,** 733-739.

SHIVASWAMY, S., BHINGE, A., ZHAO, Y., JONES, S., HIRST, M. & IYER, V. R. 2008. Dynamic remodeling of individual nucleosomes across a eukaryotic genome in response to transcriptional perturbation. *PLoS biology,* 6**,** e65.

SHRESTHA, P., JAGANATHAN, A., HUILGOL, D., BALLON, C., HWANGBO, Y. & MILLS, A. A. 2023. Chd5 Regulates the Transcription Factor Six3 to Promote Neuronal Differentiation. *Stem Cells,* 41**,** 242-251.

SHVEDUNOVA, M. & AKHTAR, A. 2022. Modulation of cellular processes by histone and non-histone protein acetylation. *Nature Reviews Molecular Cell Biology,* 23**,** 329-349.

SIANO, M. A., DE MAGGIO, I., PETILLO, R., COCCIADIFERRO, D., AGOLINI, E., MAJOLO, M., NOVELLI, A., DELLA MONICA, M. & PISCOPO, C. 2022. De Novo Mutation in KMT2C Manifesting as Kleefstra Syndrome 2: Case Report and Literature Review. *Pediatr Rep,* 14**,** 131-139.

SIMON, J. A. & LANGE, C. A. 2008. Roles of the EZH2 histone methyltransferase in cancer epigenetics. *Mutation Research/Fundamental and Molecular Mechanisms of Mutagenesis,* 647**,** 21-29.

SINGH, A., ROKES, C., GIREUD, M., FLETCHER, S., BAUMGARTNER, J., FULLER, G., STEWART, J., ZAGE, P. & GOPALAKRISHNAN, V. 2011. Retinoic acid induces REST degradation and neuronal differentiation by modulating the expression of SCFβ-TRCP in neuroblastoma cells. *Cancer,* 117**,** 5189-5202.

SINGH, T., KURKI, M. I., CURTIS, D., PURCELL, S. M., CROOKS, L., MCRAE, J., SUVISAARI, J., CHHEDA, H., BLACKWOOD, D. & BREEN, G. 2016. Rare loss-of-function variants in SETD1A are associated with schizophrenia and developmental disorders. *Nature neuroscience,* 19**,** 571-577.

SIOUDA, M., DUJARDIN, A. D., BARBOLLAT-BOUTRAND, L., MENDOZA-PARRA, M. A., GIBERT, B., OUZOUNOVA, M., BOUAOUD, J., TONON, L., ROBERT, M., FOY, J. P., LAVERGNE, V., MANIE, S. N., VIARI, A., PUISIEUX, A., ICHIM, G., GRONEMEYER, H., SAINTIGNY, P. & MULLIGAN, P. 2020. CDYL2 Epigenetically Regulates MIR124 to Control NF-κB/STAT3-Dependent Breast Cancer Cell Plasticity. *iScience,* 23**,** 101141.

SMIRNOVA, L., GRÄFE, A., SEILER, A., SCHUMACHER, S., NITSCH, R. & WULCZYN, F. G. 2005. Regulation of miRNA expression during neural cell specification. *European Journal of Neuroscience,* 21**,** 1469-1477.

SOLMI, M., SONG, M., YON, D. K., LEE, S. W., FOMBONNE, E., KIM, M. S., PARK, S., LEE, M. H., HWANG, J., KELLER, R., KOYANAGI, A., JACOB, L., DRAGIOTI, E., SMITH, L., CORRELL, C. U., FUSAR-POLI, P., CROATTO, G., CARVALHO, A. F., OH, J. W., LEE, S., GOSLING, C. J., CHEON, K.-A., MAVRIDIS, D., CHU, C.-S., LIANG, C.-S., RADUA, J., BOYER, L., FOND, G., SHIN, J. I. &

CORTESE, S. 2022. Incidence, prevalence, and global burden of autism spectrum disorder from 1990 to 2019 across 204 countries. *Molecular Psychiatry,* 27**,** 4172-4180.

SONG, B.-F., XU, L.-Z., JIANG, K. & CHENG, F. 2023. MiR-124-3p inhibits tumor progression in prostate cancer by targeting EZH2. *Functional & Integrative Genomics,* 23**,** 80.

SREESHMA, B. & DEVI, A. 2023. JARID2 and EZH2, the eminent epigenetic drivers in human cancer. *Gene,* 879**,** 147584.

STAPPERT, L., BORGHESE, L., ROESE-KOERNER, B., WEINHOLD, S., KOCH, P., TERSTEGGE, S., UHRBERG, M., WERNET, P. & BRÜSTLE, O. 2013. MicroRNA-based promotion of human neuronal differentiation and subtype specification. *PloS one,* 8**,** e59011.

STARK, K. L., XU, B., BAGCHI, A., LAI, W.-S., LIU, H., HSU, R., WAN, X., PAVLIDIS, P., MILLS, A. A. & KARAYIORGOU, M. 2008. Altered brain microRNA biogenesis contributes to phenotypic deficits in a 22q11-deletion mouse model. *Nature genetics,* 40**,** 751-760.

STEWART, D. R. & KLEEFSTRA, T. 2007. The chromosome 9q subtelomere deletion syndrome. *American Journal of Medical Genetics Part C: Seminars in Medical Genetics,* 145C**,** 383-392.

STEWART, S. A., DYKXHOORN, D. M., PALLISER, D., MIZUNO, H., YU, E. Y., AN, D. S., SABATINI, D. M., CHEN, I. S., HAHN, W. C., SHARP, P. A., WEINBERG, R. A. & NOVINA, C. D. 2003. Lentivirus-delivered stable gene silencing by RNAi in primary cells. *Rna,* 9**,** 493-501.

STOCK, J. K., GIADROSSI, S., CASANOVA, M., BROOKES, E., VIDAL, M., KOSEKI, H., BROCKDORFF, N., FISHER, A. G. & POMBO, A. 2007. Ring1-mediated ubiquitination of H2A restrains poised RNA polymerase II at bivalent genes in mouse ES cells. *Nat Cell Biol,* 9**,** 1428-35.

SU, L. N., SONG, X. Q., WEI, H. P. & YIN, H. F. 2017. Identification of neuron-related genes for cell therapy of neurological disorders by network analysis. *J Zhejiang Univ Sci B,* 18**,** 172-182.

SU, X., KAMEOKA, S., LENTZ, S. & MAJUMDER, S. 2004. Activation of REST/NRSF target genes in neural stem cells is sufficient to cause neuronal differentiation. *Mol Cell Biol,* 24**,** 8018-25.

SUBBANNA, S., NAGRE, N. N., SHIVAKUMAR, M., UMAPATHY, N. S., PSYCHOYOS, D. & BASAVARAJAPPA, B. S. 2014. Ethanol induced acetylation of histone at G9a exon1 and G9a-mediated histone H3 dimethylation leads to neurodegeneration in neonatal mice. *Neuroscience,* 258**,** 422-432.

SULLIVAN, P. F., KENDLER, K. S. & NEALE, M. C. 2003. Schizophrenia as a Complex Trait: Evidence From a Meta-analysis of Twin Studies. *Archives of General Psychiatry,* 60**,** 1187-1192.

SUN, G., YE, P., MURAI, K., LANG, M.-F., LI, S., ZHANG, H., LI, W., FU, C., YIN, J., WANG, A., MA, X. & SHI, Y. 2011. miR-137 forms a regulatory loop with nuclear receptor TLX and LSD1 in neural stem cells. *Nature Communications,* 2**,** 529.

SUN, Y.-M., COOPER, M., FINCH, S., LIN, H.-H., CHEN, Z.-F., WILLIAMS, B. P. & BUCKLEY, N. J. 2008. Rest-mediated regulation of extracellular matrix is crucial for neural development. *PloS one,* 3**,** e3656-e3656.

SUN, Y.-M., GREENWAY, D. J., JOHNSON, R., STREET, M., BELYAEV, N. D., DEUCHARS, J., BEE, T., WILDE, S. & BUCKLEY, N. J. 2005. Distinct Profiles of REST Interactions with Its Target Genes at Different Stages of Neuronal Development. *Molecular Biology of the Cell,* 16**,** 5630-5638.

SUZUKI, F., OKUNO, M., TANAKA, T. & SANUKI, R. 2020. Overexpression of neural miRNAs miR-9/9* and miR-124 suppresses differentiation to Müller glia and promotes differentiation to neurons in mouse retina in vivo. *Genes Cells,* 25**,** 741-752.

SYDNOR, V. J., LARSEN, B., BASSETT, D. S., ALEXANDER-BLOCH, A., FAIR, D. A., LISTON, C., MACKEY, A. P., MILHAM, M. P., PINES, A. & ROALF, D. R. 2021. Neurodevelopment of the

association cortices: Patterns, mechanisms, and implications for psychopathology. *Neuron,* 109**,** 2820-2846.

SZULWACH, K. E., LI, X., SMRT, R. D., LI, Y., LUO, Y., LIN, L., SANTISTEVAN, N. J., LI, W., ZHAO, X. & JIN, P. 2010. Cross talk between microRNA and epigenetic regulation in adult neurogenesis. *J Cell Biol,* 189**,** 127-41.

TACHIBANA, M., NOZAKI, M., TAKEDA, N. & SHINKAI, Y. 2007. Functional dynamics of H3K9 methylation during meiotic prophase progression. *Embo j,* 26**,** 3346-59.

TACHIBANA, M., SUGIMOTO, K., FUKUSHIMA, T. & SHINKAI, Y. 2001. Set domain-containing protein, G9a, is a novel lysine-preferring mammalian histone methyltransferase with hyperactivity and specific selectivity to lysines 9 and 27 of histone H3. *Journal of Biological Chemistry,* 276**,** 25309-25317.

TACHIBANA, M., SUGIMOTO, K., NOZAKI, M., UEDA, J., OHTA, T., OHKI, M., FUKUDA, M., TAKEDA, N., NIIDA, H. & KATO, H. 2002a. G9a histone methyltransferase plays a dominant role in euchromatic histone H3 lysine 9 methylation and is essential for early embryogenesis. *Genes & development,* 16**,** 1779-1791.

TACHIBANA, M., SUGIMOTO, K., NOZAKI, M., UEDA, J., OHTA, T., OHKI, M., FUKUDA, M., TAKEDA, N., NIIDA, H., KATO, H. & SHINKAI, Y. 2002b. G9a histone methyltransferase plays a dominant role in euchromatic histone H3 lysine 9 methylation and is essential for early embryogenesis. *Genes Dev,* 16**,** 1779-91.

TACHIBANA, M., UEDA, J., FUKUDA, M., TAKEDA, N., OHTA, T., IWANARI, H., SAKIHAMA, T., KODAMA, T., HAMAKUBO, T. & SHINKAI, Y. 2005. Histone methyltransferases G9a and GLP form heteromeric complexes and are both crucial for methylation of euchromatin at H3-K9. *Genes Dev,* 19**,** 815-26.

TAHILIANI, M., MEI, P., FANG, R., LEONOR, T., RUTENBERG, M., SHIMIZU, F., LI, J., RAO, A. & SHI, Y. 2007. The histone H3K4 demethylase SMCX links REST target genes to X-linked mental retardation. *Nature,* 447**,** 601-605.

TAJIMA, K., YAE, T., JAVAID, S., TAM, O., COMAILLS, V., MORRIS, R., WITTNER, B. S., LIU, M., ENGSTROM, A., TAKAHASHI, F., BLACK, J. C., RAMASWAMY, S., SHIODA, T., HAMMELL, M., HABER, D. A., WHETSTINE, J. R. & MAHESWARAN, S. 2015. SETD1A modulates cell cycle progression through a miRNA network that regulates p53 target genes. *Nature Communications,* 6**,** 8257.

TALKOWSKI, M. E., ROSENFELD, J. A., BLUMENTHAL, I., PILLALAMARRI, V., CHIANG, C., HEILBUT, A., ERNST, C., HANSCOM, C., ROSSIN, E., LINDGREN, A. M., PEREIRA, S., RUDERFER, D., KIRBY, A., RIPKE, S., HARRIS, D. J., LEE, J. H., HA, K., KIM, H. G., SOLOMON, B. D., GROPMAN, A. L., LUCENTE, D., SIMS, K., OHSUMI, T. K., BOROWSKY, M. L., LORANGER, S., QUADE, B., LAGE, K., MILES, J., WU, B. L., SHEN, Y., NEALE, B., SHAFFER, L. G., DALY, M. J., MORTON, C. C. & GUSELLA, J. F. 2012. Sequencing chromosomal abnormalities reveals neurodevelopmental loci that confer risk across diagnostic boundaries. *Cell,* 149**,** 525-37.

TATTON-BROWN, K., HANKS, S., RUARK, E., ZACHARIOU, A., DUARTE, S. D. V., RAMSAY, E., SNAPE, K., MURRAY, A., PERDEAUX, E. R. & SEAL, S. 2011. Germline mutations in the oncogene EZH2 cause Weaver syndrome and increased human height. *Oncotarget,* 2**,** 1127.

TATTON-BROWN, K., LOVEDAY, C., YOST, S., CLARKE, M., RAMSAY, E., ZACHARIOU, A., ELLIOTT, A., WYLIE, H., ARDISSONE, A. & RITTINGER, O. 2017. Mutations in epigenetic regulation genes are a major cause of overgrowth with intellectual disability. *The American Journal of Human Genetics,* 100**,** 725-736.

TAY, Y., ZHANG, J., THOMSON, A. M., LIM, B. & RIGOUTSOS, I. 2008. MicroRNAs to Nanog, Oct4 and Sox2 coding regions modulate embryonic stem cell differentiation. *Nature,* 455**,** 1124-1128.

TELLEY, L., AGIRMAN, G., PRADOS, J., AMBERG, N., FIÈVRE, S., OBERST, P., BARTOLINI, G., VITALI, I., CADILHAC, C. & HIPPENMEYER, S. 2019. Temporal patterning of apical progenitors and their daughter neurons in the developing neocortex. *Science,* 364**,** eaav2522.

TELLEY, L., GOVINDAN, S., PRADOS, J., STEVANT, I., NEF, S., DERMITZAKIS, E., DAYER, A. & JABAUDON, D. 2016. Sequential transcriptional waves direct the differentiation of newborn neurons in the mouse neocortex. *Science,* 351**,** 1443-1446.

THIENPONT, B., ARONSEN, J. M., ROBINSON, E. L., OKKENHAUG, H., LOCHE, E., FERRINI, A., BRIEN, P., ALKASS, K., TOMASSO, A., AGRAWAL, A., BERGMANN, O., SJAASTAD, I., REIK, W. & RODERICK, H. L. 2017. The H3K9 dimethyltransferases EHMT1/2 protect against pathological cardiac hypertrophy. *J Clin Invest,* 127**,** 335-348.

TICK, B., BOLTON, P., HAPPÉ, F., RUTTER, M. & RIJSDIJK, F. 2016. Heritability of autism spectrum disorders: a meta-analysis of twin studies. *Journal of Child Psychology and Psychiatry,* 57**,** 585-595.

TOMASELLI, P. J., ROSSOR, A. M., HORGA, A., LAURA, M., BLAKE, J. C., HOULDEN, H. & REILLY, M. M. 2017. A de novo dominant mutation in KIF1A associated with axonal neuropathy, spasticity and autism spectrum disorder. *Journal of the Peripheral Nervous System,* 22**,** 460-463.

TOMASSI, S., ROMANELLI, A., ZWERGEL, C., VALENTE, S. & MAI, A. 2021. Polycomb Repressive Complex 2 Modulation through the Development of EZH2-EED Interaction Inhibitors and EED Binders. *J Med Chem,* 64**,** 11774-11797.

TRIPATHY, R., LECA, I., VAN DIJK, T., WEISS, J., VAN BON, B. W., SERGAKI, M. C., GSTREIN, T., BREUSS, M., TIAN, G., BAHI-BUISSON, N., PACIORKOWSKI, A. R., PAGNAMENTA, A. T., WENNINGER-WEINZIERL, A., MARTINEZ-REZA, M. F., LANDLER, L., LISE, S., TAYLOR, J. C., TERRONE, G., VITIELLO, G., DEL GIUDICE, E., BRUNETTI-PIERRI, N., D'AMICO, A., REYMOND, A., VOISIN, N., BERNSTEIN, J. A., FARRELLY, E., KINI, U., LEONARD, T. A., VALENCE, S., BURGLEN, L., ARMSTRONG, L., HIATT, S. M., COOPER, G. M., ALDINGER, K. A., DOBYNS, W. B., MIRZAA, G., PIERSON, T. M., BAAS, F., CHELLY, J., COWAN, N. J. & KEAYS, D. A. 2018. Mutations in MAST1 Cause Mega-Corpus-Callosum Syndrome with Cerebellar Hypoplasia and Cortical Malformations. *Neuron,* 100**,** 1354-1368.e5.

TRIVEDI, P., PANDEY, M., KUMAR RAI, P., SINGH, P. & SRIVASTAVA, P. 2023. A meta-analysis of differentially expressed and regulatory genes with their functional enrichment analysis for brain transcriptome data in autism spectrum disorder. *Journal of Biomolecular Structure and Dynamics,* 41**,** 9382-9388.

TROPEPE, V., HITOSHI, S., SIRARD, C., MAK, T. W., ROSSANT, J. & VAN DER KOOY, D. 2001. Direct Neural Fate Specification from Embryonic Stem Cells: A Primitive Mammalian Neural Stem Cell Stage Acquired through a Default Mechanism. *Neuron,* 30**,** 65-78.

TSUNEKAWA, Y., BRITTO, J. M., TAKAHASHI, M., POLLEUX, F., TAN, S. S. & OSUMI, N. 2012. Cyclin D2 in the basal process of neural progenitors is linked to non-equivalent cell fates. *Embo j,* 31**,** 1879-92.

TSUTSUMI, A., KAWAMATA, T., IZUMI, N., SEITZ, H. & TOMARI, Y. 2011. Recognition of the pre-miRNA structure by Drosophila Dicer-1. *Nat Struct Mol Biol,* 18**,** 1153-8.

UEDA, H., KURITA, J.-I., NEYAMA, H., HIRAO, Y., KOUJI, H., MISHINA, T., KASAI, M., NAKANO, H., YOSHIMORI, A. & NISHIMURA, Y. 2017. A mimetic of the mSin3-binding helix of NRSF/REST ameliorates abnormal pain behavior in chronic pain models. *Bioorganic & Medicinal Chemistry Letters,* 27**,** 4705-4709.

UEDA, J., TACHIBANA, M., IKURA, T. & SHINKAI, Y. 2006. Zinc finger protein Wiz links G9a/GLP histone methyltransferases to the co-repressor molecule CtBP. *J Biol Chem,* 281**,** 20120-8.

VALOUEV, A., JOHNSON, S. M., BOYD, S. D., SMITH, C. L., FIRE, A. Z. & SIDOW, A. 2011. Determinants of nucleosome organization in primary human cells. *Nature,* 474**,** 516-520.

VAN DEN AMEELE, J., TIBERI, L., VANDERHAEGHEN, P. & ESPUNY-CAMACHO, I. 2014. Thinking out of the dish: what to learn about cortical development using pluripotent stem cells. *Trends in neurosciences,* 37**,** 334-342.

VAN DER RAADT, J., VAN GESTEL, S. H. C., NADIF KASRI, N. & ALBERS, C. A. 2019. ONECUT transcription factors induce neuronal characteristics and remodel chromatin accessibility. *Nucleic Acids Res,* 47**,** 5587-5602.

VEDADI, M., BARSYTE-LOVEJOY, D., LIU, F., RIVAL-GERVIER, S., ALLALI-HASSANI, A., LABRIE, V., WIGLE, T. J., DIMAGGIO, P. A., WASNEY, G. A., SIARHEYEVA, A., DONG, A., TEMPEL, W., WANG, S. C., CHEN, X., CHAU, I., MANGANO, T. J., HUANG, X. P., SIMPSON, C. D., PATTENDEN, S. G., NORRIS, J. L., KIREEV, D. B., TRIPATHY, A., EDWARDS, A., ROTH, B. L., JANZEN, W. P., GARCIA, B. A., PETRONIS, A., ELLIS, J., BROWN, P. J., FRYE, S. V., ARROWSMITH, C. H. & JIN, J. 2011. A chemical probe selectively inhibits G9a and GLP methyltransferase activity in cells. *Nat Chem Biol,* 7**,** 566-74.

VISVANATHAN, J., LEE, S., LEE, B., LEE, J. W. & LEE, S.-K. 2007. The microRNA miR-124 antagonizes the anti-neural REST/SCP1 pathway during embryonic CNS development. *Genes & development,* 21**,** 744-749.

VOIGT, P., LEROY, G., DRURY, WILLIAM J., III, ZEE, BARRY M., SON, J., BECK, DAVID B., YOUNG, NICOLAS L., GARCIA, BENJAMIN A. & REINBERG, D. 2012. Asymmetrically Modified Nucleosomes. *Cell,* 151**,** 181-193.

VOIGT, P., TEE, W. W. & REINBERG, D. 2013. A double take on bivalent promoters. *Genes Dev,* 27**,** 1318-38.

VUE, T. Y., KOLLIPARA, R. K., BORROMEO, M. D., SMITH, T., MASHIMO, T., BURNS, D. K., BACHOO, R. M. & JOHNSON, J. E. 2020. ASCL1 regulates neurodevelopmental transcription factors and cell cycle genes in brain tumors of glioma mouse models. *Glia,* 68**,** 2613-2630.

WALKER, E., MANIAS, J. L., CHANG, W. Y. & STANFORD, W. L. 2011. PCL2 modulates gene regulatory networks controlling self-renewal and commitment in embryonic stem cells. *Cell Cycle,* 10**,** 45-51.

WALKER, M. P., LAFERLA, F. M., ODDO, S. S. & BREWER, G. J. 2013. Reversible epigenetic histone modifications and Bdnf expression in neurons with aging and from a mouse model of Alzheimer's disease. *AGE,* 35**,** 519-531.

WALLOIS, F., ROUTIER, L. & BOUREL-PONCHEL, E. 2020. Chapter 25 - Impact of prematurity on neurodevelopment. *In:* GALLAGHER, A., BULTEAU, C., COHEN, D. & MICHAUD, J. L. (eds.) *Handbook of Clinical Neurology.* Elsevier.

WANG, D.-Y., KOSOWAN, J., SAMSOM, J., LEUNG, L., ZHANG, K.-L., LI, Y.-X., XIONG, Y., JIN, J., PETRONIS, A., OH, G. & WONG, A. H. C. 2018a. Inhibition of the G9a/GLP histone methyltransferase complex modulates anxiety-related behavior in mice. *Acta Pharmacologica Sinica,* 39**,** 866-874.

WANG, F., SONG, W., ZHAO, H., MA, Y., LI, Y., ZHAI, D., PI, J., SI, Y., XU, J., DONG, L., SU, R., ZHANG, M., ZHU, Y., REN, X., MIAO, F., LIU, W., LI, F., ZHANG, J., HE, A., SHAN, G., HUI, J., WANG, L. & YU, J. 2017. The RNA-binding protein QKI5 regulates primary miR-124-1 processing via a distal RNA motif during erythropoiesis. *Cell Research,* 27**,** 416-439.

WANG, Y., ZHANG, D., TANG, Z., ZHANG, Y., GAO, H., NI, N., SHEN, B., SUN, H. & GU, P. 2018b. REST, regulated by RA through miR-29a and the proteasome pathway, plays a crucial role in RPC proliferation and differentiation. *Cell Death & Disease,* 9**,** 444.

WANG, Z.-J., ZHONG, P., MA, K., SEO, J.-S., YANG, F., HU, Z., ZHANG, F., LIN, L., WANG, J., LIU, T., MATAS, E., GREENGARD, P. & YAN, Z. 2020. Amelioration of autism-like social deficits by

targeting histone methyltransferases EHMT1/2 in Shank3-deficient mice. *Molecular Psychiatry,* 25**,** 2517-2533.

WAPINSKI, O. L., VIERBUCHEN, T., QU, K., LEE, Q. Y., CHANDA, S., FUENTES, D. R., GIRESI, P. G., NG, Y. H., MARRO, S., NEFF, N. F., DRECHSEL, D., MARTYNOGA, B., CASTRO, D. S., WEBB, A. E., SÜDHOF, T. C., BRUNET, A., GUILLEMOT, F., CHANG, H. Y. & WERNIG, M. 2013. Hierarchical mechanisms for direct reprogramming of fibroblasts to neurons. *Cell,* 155**,** 621-35.

WEITZ, S. H., GONG, M., BARR, I., WEISS, S. & GUO, F. 2014. Processing of microRNA primary transcripts requires heme in mammalian cells. *Proceedings of the National Academy of Sciences,* 111**,** 1861-1866.

WEN, B., WU, H., SHINKAI, Y., IRIZARRY, R. A. & FEINBERG, A. P. 2009. Large histone H3 lysine 9 dimethylated chromatin blocks distinguish differentiated from embryonic stem cells. *Nature Genetics,* 41**,** 246-250.

WESTBROOK, T. F., HU, G., ANG, X. L., MULLIGAN, P., PAVLOVA, N. N., LIANG, A., LENG, Y., MAEHR, R., SHI, Y., HARPER, J. W. & ELLEDGE, S. J. 2008. SCFbeta-TRCP controls oncogenic transformation and neural differentiation through REST degradation. *Nature,* 452**,** 370-4.

WESTPHAL, D. S., ANDRES, S., MAKOWSKI, C., MEITINGER, T. & HOEFELE, J. 2018. MAP2 – A Candidate Gene for Epilepsy, Developmental Delay and Behavioral Abnormalities in a Patient With Microdeletion 2q34. *Frontiers in Genetics,* 9.

WILES, E. T. & SELKER, E. U. 2017. H3K27 methylation: a promiscuous repressive chromatin mark. *Curr Opin Genet Dev,* 43**,** 31-37.

WOHL, S. G. & REH, T. A. 2016. miR-124-9-9* potentiates Ascl1-induced reprogramming of cultured Müller glia. *Glia,* 64**,** 743-62.

WU, H., CHEN, X., XIONG, J., LI, Y., LI, H., DING, X., LIU, S., CHEN, S., GAO, S. & ZHU, B. 2011. Histone methyltransferase G9a contributes to H3K27 methylation in vivo. *Cell Res,* 21**,** 365-7.

WU, J. & XIE, X. 2006. Comparative sequence analysis reveals an intricate network among REST, CREBand miRNA in mediating neuronal gene expression. *Genome biology,* 7**,** 1-14.

WU, S., HUANG, S., DING, J., ZHAO, Y., LIANG, L., LIU, T., ZHAN, R. & HE, X. 2010. Multiple microRNAs modulate p21Cip1/Waf1 expression by directly targeting its 3' untranslated region. *Oncogene,* 29**,** 2302-2308.

XIAO, Z., XIE, Y., HUANG, F., YANG, J., LIU, X., LIN, X., ZHU, P. & ZHENG, S. 2022. MicroRNA-205-5p plays a suppressive role in the high-fat diet-induced atrial fibrosis through regulation of the EHMT2/IGFBP3 axis. *Genes & Nutrition,* 17**,** 11.

XIE, L., ZHANG, Z., TAN, Z., HE, R., ZENG, X., XIE, Y., LI, S., TANG, G., TANG, H. & HE, X. 2014. microRNA-124 inhibits proliferation and induces apoptosis by directly repressing EZH2 in gastric cancer. *Molecular and Cellular Biochemistry,* 392**,** 153-159.

XU, C., WANG, C., MENG, Q., GU, Y., WANG, Q., XU, W., HAN, Y., QIN, Y., LI, J., JIA, S., XU, J. & ZHOU, Y. 2019. miR-153 promotes neural differentiation in the mouse hippocampal HT-22 cell line and increases the expression of neuron-specific enolase. *Mol Med Rep,* 20**,** 1725-1735.

XU, J., WATTS, J. A., POPE, S. D., GADUE, P., KAMPS, M., PLATH, K., ZARET, K. S. & SMALE, S. T. 2009. Transcriptional competence and the active marking of tissue-specific enhancers by defined transcription factors in embryonic and induced pluripotent stem cells. *Genes & development,* 23**,** 2824-2838.

XUE, Q., YU, C., WANG, Y., LIU, L., ZHANG, K., FANG, C., LIU, F., BIAN, G., SONG, B., YANG, A., JU, G. & WANG, J. 2016. miR-9 and miR-124 synergistically affect regulation of dendritic branching via the AKT/GSK3β pathway by targeting Rap2a. *Scientific Reports,* 6**,** 26781.

YAMADA, A., HIRASAWA, T., NISHIMURA, K., SHIMURA, C., KOGO, N., FUKUDA, K., KATO, M., YOKOMORI, M., HAYASHI, T., UMEDA, M., YOSHIMURA, M., IWAKURA, Y., NIKAIDO, I., ITOHARA, S. & SHINKAI, Y. 2021. Derepression of inflammation-related genes link to microglia activation and neural maturation defect in a mouse model of Kleefstra syndrome. *iScience,* 24**,** 102741.

YAMADA, A., SHIMURA, C. & SHINKAI, Y. 2018. Biochemical validation of EHMT1 missense mutations in Kleefstra syndrome. *Journal of Human Genetics,* 63**,** 555-562.

YAO, X., GLESSNER, J. T., LI, J., QI, X., HOU, X., ZHU, C., LI, X., MARCH, M. E., YANG, L., MENTCH, F. D., HAIN, H. S., MENG, X., XIA, Q., HAKONARSON, H. & LI, J. 2021. Integrative analysis of genome-wide association studies identifies novel loci associated with neuropsychiatric disorders. *Translational Psychiatry,* 11**,** 69.

YAP, K., XIAO, Y., FRIEDMAN, B. A., JE, H. S. & MAKEYEV, E. V. 2016. Polarizing the Neuron through Sustained Co-expression of Alternatively Spliced Isoforms. *Cell Rep,* 15**,** 1316-28.

YE, F., ALVAREZ-CARBONELL, D., NGUYEN, K., LESKOV, K., GARCIA-MESA, Y., SREERAM, S., VALADKHAN, S. & KARN, J. 2022. Recruitment of the CoREST transcription repressor complexes by Nerve Growth factor IB-like receptor (Nurr1/NR4A2) mediates silencing of HIV in microglial cells. *PLOS Pathogens,* 18**,** e1010110.

YEH, E., DAO, D. Q., WU, Z. Y., KANDALAM, S. M., CAMACHO, F. M., TOM, C., ZHANG, W., KRENCIK, R., RAUEN, K. A., ULLIAN, E. M. & WEISS, L. A. 2018. Patient-derived iPSCs show premature neural differentiation and neuron type-specific phenotypes relevant to neurodevelopment. *Mol Psychiatry,* 23**,** 1687-1698.

YEKTA, S., SHIH, I.-H. & BARTEL, D. P. 2004. MicroRNA-Directed Cleavage of HOXB8 mRNA. *Science,* 304**,** 594-596.

YOKOYAMA, A., TAKEZAWA, S., SCHÜLE, R., KITAGAWA, H. & KATO, S. 2008. Transrepressive function of TLX requires the histone demethylase LSD1. *Molecular and cellular biology*.

YOO, A. S., SUN, A. X., LI, L., SHCHEGLOVITOV, A., PORTMANN, T., LI, Y., LEE-MESSER, C., DOLMETSCH, R. E., TSIEN, R. W. & CRABTREE, G. R. 2011. MicroRNA-mediated conversion of human fibroblasts to neurons. *Nature,* 476**,** 228-231.

YOSHIDA, K., MÜLLER, D. J. & DESARKAR, P. 2023. Psychiatric manifestations of Kleefstra syndrome: a case report. *Front Psychiatry,* 14**,** 1174195.

YUAN, A., RAO, M. V. & NIXON, R. A. 2017. Neurofilaments and neurofilament proteins in health and disease. *Cold Spring Harbor perspectives in biology,* 9**,** a018309.

YUAN, L.-T., LEE, W.-J., YANG, Y.-C., CHEN, B.-R., YANG, C.-Y., CHEN, M.-W., CHEN, J.-Q., HSIAO, M., CHIEN, M.-H. & HUA, K.-T. 2021a. Histone Methyltransferase G9a-Promoted Progression of Hepatocellular Carcinoma Is Targeted by Liver-Specific Hsa-miR-122. *Cancers,* 13**,** 2376.

YUAN, P., DING, L., CHEN, H., WANG, Y., LI, C., ZHAO, S., YANG, X., MA, Y., ZHU, J. & QI, X. 2021b. Neural stem cell-derived exosomes regulate neural stem cell differentiation through miR-9-Hes1 axis. *Frontiers in Cell and Developmental Biology,* 9**,** 601600.

YUAN, P., HAN, J., GUO, G., ORLOV, Y. L., HUSS, M., LOH, Y. H., YAW, L. P., ROBSON, P., LIM, B. & NG, H. H. 2009. Eset partners with Oct4 to restrict extraembryonic trophoblast lineage potential in embryonic stem cells. *Genes Dev,* 23**,** 2507-20.

YUAN, W., XU, M., HUANG, C., LIU, N., CHEN, S. & ZHU, B. 2011. H3K36 Methylation Antagonizes PRC2-mediated H3K27 Methylation *. *Journal of Biological Chemistry,* 286**,** 7983-7989.

ZANGARI, J., ILIE, M., ROUAUD, F., SIGNETTI, L., OHANNA, M., DIDIER, R., ROMÉO, B., GOLDONI, D., NOTTET, N., STAEDEL, C., GAL, J., MARI, B., MOGRABI, B., HOFMAN, P. & BREST, P.

2017. Rapid decay of engulfed extracellular miRNA by XRN1 exonuclease promotes transient epithelial-mesenchymal transition. *Nucleic acids research,* 45**,** 4131-4141.

ZDANOWICZ, A., THERMANN, R., KOWALSKA, J., JEMIELITY, J., DUNCAN, K., PREISS, T., DARZYNKIEWICZ, E. & HENTZE, M. W. 2009. Drosophila miR2 primarily targets the m7GpppN cap structure for translational repression. *Mol Cell,* 35**,** 881-8.

ZENG, T. B., PIERCE, N., LIAO, J. & SZABÓ, P. E. 2021. H3K9 methyltransferase EHMT2/G9a controls ERVK-driven noncanonical imprinted genes. *Epigenomics,* 13**,** 1299-1314.

ZENG, Y., YI, R. & CULLEN, B. R. 2005. Recognition and cleavage of primary microRNA precursors by the nuclear processing enzyme Drosha. *The EMBO journal,* 24**,** 138-148.

ZHANG, J., JI, F., LIU, Y., LEI, X., LI, H., JI, G., YUAN, Z. & JIAO, J. 2014a. Ezh2 Regulates Adult Hippocampal Neurogenesis and Memory. *The Journal of Neuroscience,* 34**,** 5184-5199.

ZHANG, J., ZHANG, Y., YOU, Q., HUANG, C., ZHANG, T., WANG, M., ZHANG, T., YANG, X., XIONG, J., LI, Y., LIU, C.-P., ZHANG, Z., XU, R.-M. & ZHU, B. 2022. Highly enriched BEND3 prevents the premature activation of bivalent genes during differentiation. *Science,* 375**,** 1053-1058.

ZHANG, Q., AGIUS, S. C., FLANIGAN, S. F., UCKELMANN, M., LEVINA, V., OWEN, B. M. & DAVIDOVICH, C. 2021a. PALI1 facilitates DNA and nucleosome binding by PRC2 and triggers an allosteric activation of catalysis. *Nature Communications,* 12**,** 4592.

ZHANG, W., ZANG, J., JING, X., SUN, Z., YAN, W., YANG, D., SHEN, B. & GUO, F. 2014b. Identification of candidate miRNA biomarkers from miRNA regulatory network with application to prostate cancer. *J Transl Med,* 12**,** 66.

ZHANG, X., HUANG, C. T., CHEN, J., PANKRATZ, M. T., XI, J., LI, J., YANG, Y., LAVAUTE, T. M., LI, X. J., AYALA, M., BONDARENKO, G. I., DU, Z. W., JIN, Y., GOLOS, T. G. & ZHANG, S. C. 2010. Pax6 is a human neuroectoderm cell fate determinant. *Cell Stem Cell,* 7**,** 90-100.

ZHANG, X., LIU, F., YANG, F., MENG, Z. & ZENG, Y. 2021b. Selectivity of Exportin 5 binding to human precursor microRNAs. *RNA Biol,* 18**,** 730-737.

ZHAO, C., SUN, G., LI, S. & SHI, Y. 2009. A feedback regulatory loop involving microRNA-9 and nuclear receptor TLX in neural stem cell fate determination. *Nature structural & molecular biology,* 16**,** 365-371.

ZHAO, J., SHEN, J., WANG, Z., BAI, M., FAN, Y., ZHU, Y. & BAI, W. 2022. CircRNA-0100 positively regulates the differentiation of cashmere goat SHF-SCs into hair follicle lineage via sequestering miR-153-3p to heighten the KLF5 expression. *Arch. Anim. Breed.,* 65**,** 55-67.

ZHAO, X. D., HAN, X., CHEW, J. L., LIU, J., CHIU, K. P., CHOO, A., ORLOV, Y. L., SUNG, W.-K., SHAHAB, A. & KUZNETSOV, V. A. 2007. Whole-genome mapping of histone H3 Lys4 and 27 trimethylations reveals distinct genomic compartments in human embryonic stem cells. *Cell stem cell,* 1**,** 286-298.

ZHU, Y., PENG, Q., LIN, Y., ZOU, L., SHEN, P., CHEN, F., MIN, M., SHEN, L., CHEN, J. & SHEN, B. 2017. Identification of biomarker microRNAs for predicting the response of colorectal cancer to neoadjuvant chemoradiotherapy based on microRNA regulatory network. *Oncotarget,* 8**,** 2233-2248.

ZYLICZ, J. J., DIETMANN, S., GÜNESDOGAN, U., HACKETT, J. A., COUGOT, D., LEE, C. & SURANI, M. A. 2015. Chromatin dynamics and the role of G9a in gene regulation and enhancer silencing during early mouse development. *Elife,* 4.